CHARACTERIZATION OF THE ROLE OF STRA6 IN TUMOR SUPPRESSION MECHANISMS

Thesis submitted for the degree of

Doctor of Philosophy in Biochemistry

At the University of Leicester

By

Marwah Suliman Maashi

Department of Molecular and cell Biology

College of Medicine, Biological Science, and Psychology

University of Leicester, UK

July 2017

Declaration

I, Marwah Suliman Maashi, hereby declare that this project report entitled "Characterization of the role of Stra6 in tumor suppression mechanisms" is based on work carried out by the author in the Department of Molecular and Cell Biology, the University of Leicester during the period April 2013 and September 2016. All of the work recorded in this thesis is original unless otherwise acknowledged in the text or references. None of the work has been submitted for another degree in this or any other university. Please refer to any information will be used from this thesis that should be fully cited.

Marwah Suliman Maashi

Dedication

I dedicate this work to the memory of my father, who would have been happy to see me finish this thesis for obtaining my PhD degree, I wish you were here!!

Abstract

Characterization Of The Role Of Stra6 In Tumor Suppression Mechanisms

Marwah Suliman Maashi

Stra6 is a protein that is upregulated in response to retinoids. Interestingly, we have found that Stra6 can induces p53 independently of DNA damage through ROS generation. Stra6 have shown a great induction of p53 protein levels with high stability as well. p53 stabilisation through Stra6 leads to stimulate downstream proapoptotic events such as increase the activation of caspase-3, caspase-9 and PARP cleavage. Stra6 have shown the capability of driving tumour cell to apoptosis after cell sensitized with ATRA and stimulated with DNA damaging agents. However, both Stra6 and p53 were important to achieve maximum percentage of cell death, as this was observed by detecting a positive feedback loop between Stra6 and p53. Pull-down assay of Stra6 protein have shown truncated forms of the Stra6 protein with molecular weights of 25 and 15 kDa. Basically, we have found that the small form of Stra6 with 25 kDa was translocated from cell membrane to cytosol in the absence of DNA damage and it was found to be located within the nucleus in response to DNA damage. Furthermore, this shorter form of Stra6 was capable of generating ROS and enhancing p53 dependent apoptotic cell death via the upregulation mechanism of the downstream cascade of p53 signalling pathway. Additionally, mass spectrometry data have identified some of cytosolic and nuclear proteins as Stra6's protein binding partners. Remarkably, several of these identified proteins were related to apoptosis, as well were associated in the regulation of important cellular mechanisms. We propose that Stra6 can sensitize tumor cells to DNA damaging agents and function as an apoptotic protein in a p53-dependent manner.

Acknowledgment

First of all, I would like to thank God almighty who has given me everything to accomplish this thesis: patience, health, wisdom, and blessing.

I would like to thank my project supervisor Dr. Salvador Macip for his support, guidance and continuous monitoring. His office door was always open for me when I ever had a difficulty or a question about my research or writing. He steered me in the right direction whenever I was needed help all this 4 years period. I am so grateful for his exceptional supervision and help particularly during the thesis evaluation.

I would also like to acknowledge my sponsor scholarship provided by King Abdulaziz University in Saudi Arabia. Thank you for giving me this opportunity to expand my knowledge in science. I would also like to acknowledge my committee members at University of Leicester Dr. Raj Patel and Dr Nickolai Barlev for their guidance and support in evaluating this project at its beginning phase. I would like to thank, Dr Jesvin Samuel, Dr. Mohammad Althubiti, Sandra Germano, Dr Yishang Chen, Akang Ekpenyong-Akiba and Kostas Polymeros. I must also acknowledge all the lab members in 3/37.

Special thanks to who this work is dedicated for, the most two important persons in my life, my mother Aishah Al-Abdali and my father Suliman Maashi (may he rest in peace after a year suffering from brain tumor) providing me with unfailing support continuous encouragements and prayers all my way. I will never forget the waiting times you had spent dad and mom, for my late working nights at lab, and you had all the love to share a meal with me. Without their love and wonderful blessing, I wouldn't be able to make this thesis possible at all.

I would also like to thank my brother and sisters, Abdulaziz, Safa'a, Mervet, Manal, Khlood for their support, and special thanks for my sister Mashael who known a lot of being alone and away from home, thank you for being stayed in my Phd journey even with all separate distance, your helped was very appreciated.

My deepest and most honest appreciation for the unconditional support received goes to my husband, Mettab Al-Ameri, for his support have seen me through many ups and downs. None of this would have been possible without his love, encouragement, wisdom and understanding.

Finally, I would also like take this opportunity to thank my friends and sisters Shatha Felmban and Reham Balahmar. Thank you for being part of my life along this way, thank you for sharing my happiness and sadness moments and being my second family in UK.

Table of Contents

The list of tables

List of figures

Abbreviations

9-cRA	9-cis retinoic acid
AIP-1	Apoptosis-inducing protein 1
ALDH4	Aldehyde dehydrogenase 4
APAF-1	Apoptotic protease activating factor- 1
APL	Acute promyelocytic leukemia
ATM	Ataxia-telangiectasia mutated
ATR	Ataxia telangiectasia and Rad3-related protein
ATRA	All-trans retinoic acid
BAD	Bcl-2-associated death promoter
BAK	BcL-2 antagonist/killer 1
BAX	Bcl-2-associated X protein
Bcl-2	B-cell lymphoma 2
BID	BH3-interacting domain death agonist)
CaM	Calmodulin
c-FLIP	Cellular-FADD-like IL-1β-converting enzyme -inhibitory protein
CRBP-I	Cellular retinol binding protein-I
CRBP-II	Cellular retinol binding protein-II
CT	The C-terminus domain
DBD	The DNA-binding domain
DIABLO proteins	Direct IAP binding proteins
DISC	Death-inducing signaling complex
Dox	Doxorubicin
FADD	Fas-associated death domain
GFP	Green fluorescent protein
GLUT4	Glucose transporter type 4
GPX1	Glutathione peroxidase
Jak2	Janus kinase 2
JNK	c-Jun N-terminal kinase
LRAT	Lecithin retinol acyl transferase
MAPK	The mitogen activated protein kinase
MCL1 protein	Myeloid Cell Leukemia 1
MnSOD	Manganese superoxide dismutase
NLS	Nuclear localisation sequence
OD	The oligomerisation domain
PIDD	p53-induced protein-death domain
PLZF	The promyelocytic leukemia zinc finger gene
PPARγ	Peroxisome proliferator actuated receptor gamma
PRO	Proline-rich region
PTMs	Post-translational modifications
RA	Retinoic acid
RAR	Retinoic acid receptor
RARE	Retinoic acid response elements
RBP	Retinol binding protein

RD	The regulatory domain
RNS	Reactive nitrogen species
ROS	Reactive oxygen species
RPE	Retinal pigment epithelium
RXR	Retinoid X receptor
SESN1/2	SESN1 and SESN2 Sestrins
SMAC	Second mitochondria-derived activator of caspases
SOCS3	Suppressor of cytokine signaling 3
Stat5	Signal transducer and activator of transcription 5
Stra6	Stimulated by retinoic acid 6
TAD	Transactivation domain
TIGAR	TP53 Induced Glycolysis Regulatory Phosphatase
TNF	Tumor necrosis factor
TTR	Transthyretin
VLDL	Very low-density lipoprotein

1 Introduction

1.1 DNA damage responses through p53

There are a wide range of cell stresses, including DNA damage, heat shock, genotoxicity, oncogene activation, oxidative stress and hypoxia (Vousden & Prives, 2009). When cells are subjected to these stresses, they experience complicated mechanisms of DNA repair, with the specific end goal to keep the genome stable. One of these essential pathways includes the involvement of p53 to achieve cell-cycle arrest, which permits the DNA to be repaired and rectified. When the harm is excessively broad, making it impossible to be repaired, it induces cell senescence or cell apoptosis (Feng et al., 2005; Tasdemir et al., 2008; Kibe et al., 2012; Marouco et al., 2013).

The p53 protein has diverse functions, including the activation of cell-cycle arrest, senescence, differentiation and apoptosis (Vousden, 2002). p53 is a tumour suppressor that converts stress signals into cellular responses by means of activation or repression of many gene promoters (Eliyahu et al., 1989), and any loss of p53 function could lead to carcinogenesis. Because of this, p53 is considered the 'Guardian of the Genome' (Lane, 1992).

Furthermore, the extracellular elements assume a critical part in cell fate, and a greater understanding of how these elements influence the way cells react to harm could allow us to plan the best procedures for cancer prevention and treatment. These elements include DNA damaging agents and supplements (nutrients) that may shift the DNA damage response towards cell death instead of cell cycle arrest or DNA repair.

1.1.1 p53 is the guardian of the genome

The p53 protein earned its name as the 'Guardian of the Genome' because its function is to maintain the genome's integrity (Long & Ryan, 2012). It essentially serves as a transcription factor that manages a system of more than 300 gene promoters through activation or repression of an extensive variety of gene functions that would, in the long run, result in cell-cycle arrest,

senescence or apoptosis, among other responses (Eliyahu et al., 1989). Transcription-independent roles have likewise been illustrated, such as regulating metabolism, apoptosis and autophagy (Green & Kroemer, 2009).

There are numerous studies of p53 in the existing literature; however, after 30 years of research, they have not yet influenced directly cancer management and therapy. p53 was first identified in 1979 by Arnold Levine, David Lane and William Old; identifying it as a protein bound to the simian virus 40 (SV40) T antigen (Deleo et al., 1979). Strikingly, at the outset, it was hypothesised that p53 had an oncogenic function, as a consequence of its accumulation in tumour cells, that advanced malignant transformation and proliferation (Dippold et al., 1981). However, after 10 years, the understanding of p53's action changed, and it was determined that p53 gained oncogenic trademarks due to mutations (Baker et al., 1989). In 1992, the development of knockout mice experiments highlighted the function of wild-type p53 as a tumour suppressor (Donehower et al., 1992).

The p53 multitasking functions are key for tumour suppression and for preventing the accumulation of malignant cells (Vousden & Prives, 2009). The loss of p53 function happens independently of the cell type or fundamental underlying oncogenic mechanism in almost all cancers (Junttila & Evan, 2009). It has been shown that TP53-null mice develop sarcomas and lymphomas (Donehower et al., 1992), and they appear to be highly susceptible to have spontaneous tumourigenesis (Kemp et al., 1994). Inactivation of only one copy of the TP53 gene in mice made them profoundly susceptible to developing a malignancy at an early stage (Lozano & Zambetti, 2005). It has been proposed that all tumour cells somehow escape TP53 control, either by changing TP53 itself or by transforming or disturbing basic upstream and downstream proteins from the p53 pathways (Vousden, 2002). Consistently, mutant p53 has been implicated in more than 50% of a wide range of cancers (Kruse & Gu, 2009a).

1.1.2 p53 protein structure

The human TP53 gene is located at chromosome 17p13.1, and it has 19,200 base pairs across 11 exons, and contains about 10 introns (Kobayashi & Kawashima, 1996). The p53 is a nuclear protein of 53 kDa composed of 393 amino acids. As a monomer (Figure 1.1), p53 is a multi-domain protein subdivided into three main structural domains, each corresponding to specific functions: 1) The N Terminus/Transactivation domain (TAD, residues 1-100), including the proline-rich region (PRO, residues 67-100); 2) The DNA-binding domain (DBD, residues 101-300); and 3) The C-terminus domain (CT, residues 301-393), including the nuclear localisation sequence (NLS, residues 303-322), the oligomerisation domain (OD, residues 323-362) and the regulatory domain (RD, residues 363-393; Bai & Zhu, 2006). The p53 protein is active as a homotetramer, a dimer of two dimers (Cho et al., 1994; Weinberg et al., 2004). Most of the p53 domains and their subdomains/regions are important for a specific tumour-suppressor function (Kim et al., 2012). In this section, these p53 components, from N-terminus to C-terminus, will be discussed in brief to show how they specifically function and how they give p53 protein its unique characteristics.

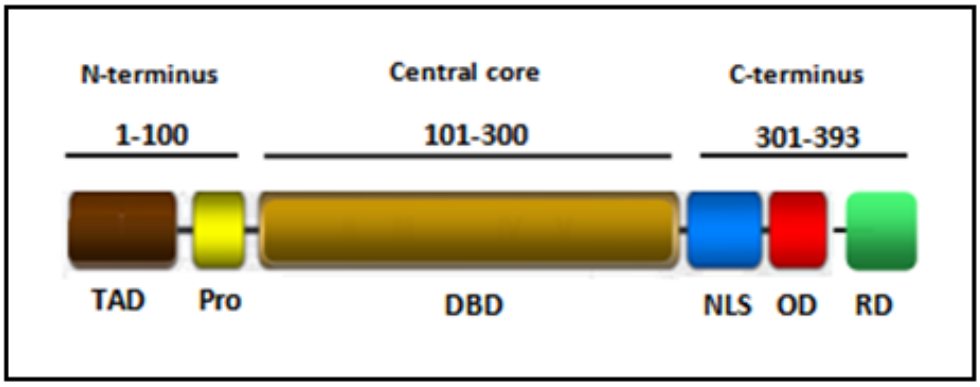

Figure 1.1: p53 protein structure. The p53 protein is a monomer consisting of 393 amino acids and three main functional structural domains: N-terminus region, containing the transactivation domain (TAD) and proline-rich domain (PD); the central core, including the sequence-specific DNA-binding domain, which is crucial for p53-binding activity; and a complex C-terminus domain, consisting of nuclear localisation sequence (NLS), oligomerisation domain (OD) and regulatory domain (RD). (Adapted from Kim et al., 2012)

The N-terminus domain plays a vital role in p53 transcriptional activity and stability (Lin et al., 1994; Venot et al., 1999; Espinosa et al., 2001); it contains the TAD I and TAD II domains, which undergo post-translational modifications (PTMs) that modulate their biological function (Jenkins et al., 2012). At this region, the interaction with MDM2 (Mouse double minute 2 homolog) masks the transactivation domain, resulting in the inhibition of p53 transcriptional activity (Oliner et al., 1993). MDM2 protein regulates the activity of p53 protein by blocking its transcriptional activity, through the mechanism of exporting p53 protein into the cytoplasm, and/or by the mechanism of promoting the degradation of the p53 protein (Alarcon-Vargas & Ronai, 2002). Some researchers have reported that p53 attains its stability by interrupting p53-MDM2 interactions and by binding to other proteins when serine (15 & 20) and threonine 18 are phosphorylated by both the ATM and ATR protein kinases (Rajagopalan et al., 2009; Ji et al., 2014). Furthermore, the phosphorylation of S46 boosts apoptosis by p53, which is mediated by the apoptosis-inducing protein 1 (AIP-1); this protein is one of the proteins that localises within mitochondria and induces apoptosis when the mitochondrial membrane is permeabilised (Oda et al., 2000; Smeenk et al., 2011).

The proline-rich domain (PD), which is next to the TAD domain in the N-terminus, works as an essential part of the p53 structure by inducing growth repression (Zhu et al., 1999); this is achieved through recruiting and modulating the promoter of genes responsible for p53-mediated cell cycle arrest or apoptosis (Edwards et al., 2003).

In 1997, scientists reported that PD is a crucial element in p53 stability, as the PD-null p53 model showed p53 was more prone to be targeted for degradation by MDM2 (Sakamuro et al., 1997). Knockout studies have shown that deletion of the PD domain has an adverse effect on the expression of some genes, such as p21 and MDM2; however, other genes have shown little response to this deletion, such as BAX and death receptor 5 (DR5) (Zhu et al., 1999).

DNA binding domain (DBD) mutations have been reported in approximately 90% of most observed p53 mutations in human cancers, which reflects how this domain is significant in conserving p53's tumour-suppressor function (Olivier et al., 2010; Freed-Pastor & Prives, 2012).

The C-terminus domain of the p53 structure contributes to the transcriptional activity and DNA binding of p53; this function was determined when studies demonstrated that the deletion of this region weakened p53 DNA binding and transactivation capabilities (Kim et al., 2012; Hamard et al., 2012). Nuclear localisation sequence (NLS) and nuclear export signals (NES) are both inside the C-terminus, and they control p53 transport between the nucleus and the cytoplasm (Liang & Clarke, 1999). The next domain is the oligomerisation domain (OD), also referred to as the tetramerisation domain, which permits formation of the p53 dynamic homotetramer that is fundamental for p53 transcriptional activity (Clore et al., 1995). The C-terminus is known to be a site for many PTMs; therefore, many PTMs are found in the regulatory domain (RD), and this could affect p53 stability and control p53 activity (McKinney et al., 2004). S392 phosphorylation has been shown to induce p53 stabilisation by allowing p53 oligomerisation, in addition to enhancing p53-DNA binding activity (Matsumoto et al., 2006). Furthermore, acetylation of K373 attenuates the binding of the MDM2 to p53 (Kruse & Gu, 2009a).

1.1.3 p53 activation and regulation

Activation upregulates specific target genes with defined cellular action, such as DNA repair, cell-cycle arrest, senescence and apoptosis. Furthermore, all of these different cellular stresses prompt a p53 protein accumulation in the cell (Vousden & Prives, 2009).Generally, outcomes of p53 activation towards mild or extensive stress strongly promote the activation of cell-cycle arrest by means of activating p53 target genes, such as the cyclin-dependent kinase inhibitor p21 CIP1/WAF1 (Cyclin-dependent kinase inhibitor 1) and GADD45α (Growth arrest and DNA-damage-inducible protein), although extreme stress signals induce apoptosis through the stimulation of p53 target genes like BAX, PUMA, NOXA, DR5, p53AIP, PIG3, FAS and APAF1, or they induce cell

senescence through the stimulation of CDKN1A (Cyclin Dependent Kinase Inhibitor 1A) , PML (Progressive multifocal leukoencephalopathy) and PAI1 (Plasminogen activator inhibitor-1).

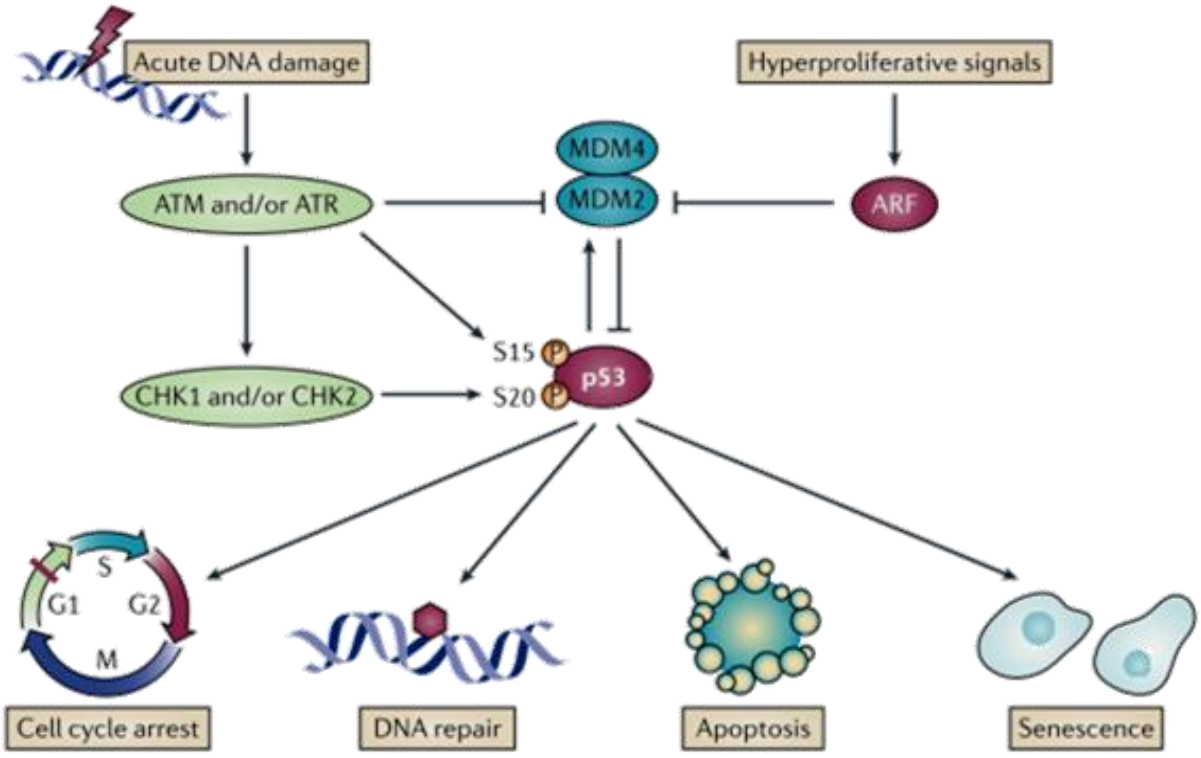

Figure 1. 2: The classical representation of p53 activation and response. DNA damage, genotoxic stress, oncogene activation, hypoxia and other stress signals introduced through the p53 pathway result in various cellular response such as DNA damage, which begins when the DNA double-strand breaks and elicits the activation of Ataxia-telangiectasia mutated (ATM) — a kinase that phosphorylates the Chk2 kinase — or DNA replication ataxia telangiectasia and Rad3-related protein (ATR) that phosphorylates Chk1 that would phosphorylate p53 on Ser 15 and Ser 20. PTMs interrupt the interaction between p53 and its negative regulators. Furthermore, PTMs permit the interaction of p53 with its target transcriptional genes for inducing responses such as DNA repair, cell-cycle arrest, senescence and apoptosis. Hyper-proliferative signals also activate p53 through disturbing the MDM2–p53 interaction that is capable of stimulating the ARF tumour-suppressor transcription. As a result, ARF activation boosts p53 activity and stability, inducing different p53 responses, such as apoptosis or cellular senescence (Bieging et al., 2014).

Other cellular stress signals encourage cell differentiation and DNA repair via repair proteins for example, DDB2 and p53r2 (Stiewe, 2007; Michalak et al., 2010; Spike & Wahl, 2011; Li et al., 2012; Abdelalim & Tooyama, 2014; Bieging et al., 2014).

As mentioned before, once the cell is under stress, a wide variety of complicated post-translational modification mechanisms regulate p53, determining its stabilisation, sub-cellular localisation and protein-protein interaction (Scoumanne & Chen, 2008; Vousden & Ryan, 2009; Smeenk et al., 2011; Muller & Vousden, 2013).

The p53 upstream modulators, ATM, ATR, Chk1, Chk2 and DNA-dependent protein kinase (DNA-PK), are engaged and activated after DNA damage; this, in turn, switches on a series of PTMs, such as phosphorylation or acetylation (Bieging et al., 2014; Figure 1.2).

One of the primary and essential conformational changes that p53 exhibits after stress is phosphorylation. Phosphorylation of serine residues (Ser15) is involved in the accummulation of p53 within the nucleus. Furthermore, phosphorylation of serine residues (Ser20) in the N-terminal domain of p53 demonstrates its effect on disrupting the p53-MDM2 interaction and preventing ubquitination-dependent degradation; all of these PTMs elevate p53 levels and leads to its accumulation inside the cell (Shieh et al., 1997).

The MDM2-MDMX heterodimer is formed, thus working as an E3 ubiquitin ligase that adds ubiquitin molecules to lysine residues. This biological action mediates the proteasomal degradation of p53 protein; accordingly, p53 protein is maintained low in normal conditions (Appella & Anderson, 2001). Moreover, MDM2 is not only a p53-negative regulator but also one of the important p53 transcriptional target genes. In this manner, this biological activity forms a negative feedback loop.

Another way to maintain the p53 protein inactive in normal situations is the folding of the C-terminal tail against the N-terminus of p53 protein, which

shields the DNA-binding domain. The phosphorylation of the C-terminus interrupts this folded conformation and increases the p53-DNA binding ability (Hupp et al., 1992). A further PTM in the C-terminus domain, the acetylation of lysine residues, would also enhance the activation of p53-DNA binding (Gu & Roeder, 1997).

Therefore, each different stress stimuli affecting the cell induces the p53 protein to act specifically, depending on the strength of the stress signals received, among other things. All of the p53 protein's biological functions are determined by three main regulatiory mechanisms: PTMs, sub-cellular localisation and protein-protein interaction. The latter two regulatory mechanisms will be discussed in the next section.

1.1.4 p53's role in apoptosis

Apoptosis is an energy-dependent mechanism that is defined as a programmed cell death, and it is involved in both physiological and pathological processes (Norbury & Hickson, 2001). Two main pathways determine the apoptotic events: the extrinsic and intrinsic pathways (Figure 1.3). These pathways share the latest component of apoptotic machinery: effector caspases 3, 6 and 7 (Igney & Krammer, 2002). Caspase-3 is an essential proteolytic enzyme related to the cysteine protease family that has an equally important role in both Extrinsic and Intrinsic apoptotic pathways as primary regulator of apoptotic DNA fragmentation (Gown & Willingham, 2002).

Basically, in the extrinsic pathway, an extracellular ligand is associated to cell surface death receptors; for example, p53 can activate the extrinsic apoptotic pathway by regulating the expression of the tumour necrosis factor (TNF) family, including FAS, TNF-α and TRAIL, as well as the death receptor DR5/killer and the p53-induced protein-death domain (PIDD) (Chicheportiche et al., 1997; Wu et al., 1997). When their specific binding ligands activate these receptors, Fas-associated death domain (FADD) is recruited and associates with the receptor's death domain (Wajant, 2002). The Death-

inducing signalling complex (DISC) is then formed and stimulates the activation of initiator caspases 8 and 10; in consequence, the effector caspases 3, 6 and 7 will also be activated (Kischkel et al., 1995). In order to control the cellular responses toward the extrinsic pathway, FLICE-like inhibitory protein (c-FLIP) binds to the FADD and caspase-8; thus, apoptotic signals will be repressed (Kataoka et al., 1998).

The intrinsic pathway is a non-receptor cell death pathway. DNA damage, oncogene activation, free radicals and hypoxia trigger this pathway (Elmore, 2007). p53 activates the BCL2 family members, BAX (Bcl-2-associated X protein), BAK (BcL-2 antagonist/killer 1) were both considered as multi-domain pro-apoptotic proteins. While these proteins were considered as BH-3 only domain, for instance; NOXA (Latin for damage), PUMA (p53 upregulated modulator of apoptosis), BAD (Bcl-2-associated death promoter), BID (BH3 interacting domain death agonist) and BIM (BCL2 interacting protein BIM) (Miyashita & Reed, 1995; Oda et al., 2000). The Bcl-2 family proteins are key elements that participate in deciding if the cell will undergo apoptosis or survive (Elmore, 2007).

After direct activation of BAX by p53 following DNA damage, oxidative stress or nutrient deprivation, BAX is localised into the outer membrane of the mitochondria, and this facilitates the formation of a mitochondrial pore that leads to cytochrome-C release (Chipuk et al., 2004); this action also promotes BAX to oligomerise with BAK to form a BAX/BAK dimer. This is formed when the cytoplasmic p53 binds to BAD, a pro-apoptotic BCL2 family member. This interaction between p53 and BAD diassociates BAD from its negative regulator, the anti-apoptotic MCL1 protein (Myeloid Cell Leukaemia 1), a member of the Bcl-2 family (B-cell lymphoma 2) (Jiang, 2001), which results in localization of the p53/BAD complex to the mitochondria outer membrane (Jiang, 2001). Conversely, members of the Bcl-2 and Bcl-XL family proteins regulate the prevention of cytochrome-C release from the mitochondria by keeping the mitochondrial permeability transition pore closed (Cory & Adams, 2002).

Once the mitochondrial permeability transition pores are opened and cytochrome-C is released the SMAC/DIABLO (second mitochondria-derived activator of caspases/direct IAP binding proteins) in order to inhibits the anti-apoptotic proteins (IAP's) that allow activation of caspases.

At that point, cytochrome-C reacts with APAF-1 (apoptotic protease activating factor 1) to form an apoptosome complex that facilitates activation of pro-caspase-9 into the active caspase-9 that is activates pro-caspase-3 into the effector caspase-3 and in initiating downstream apoptotic events such as cell shrinkage, chromatin condensation, formation of cytoplasmic blebs as well as apoptotic bodies. Finally, the apoptotic bodies are phagocytosed by parenchymal cells and macrophages (Weinberg, 2007; Elmore, 2007).

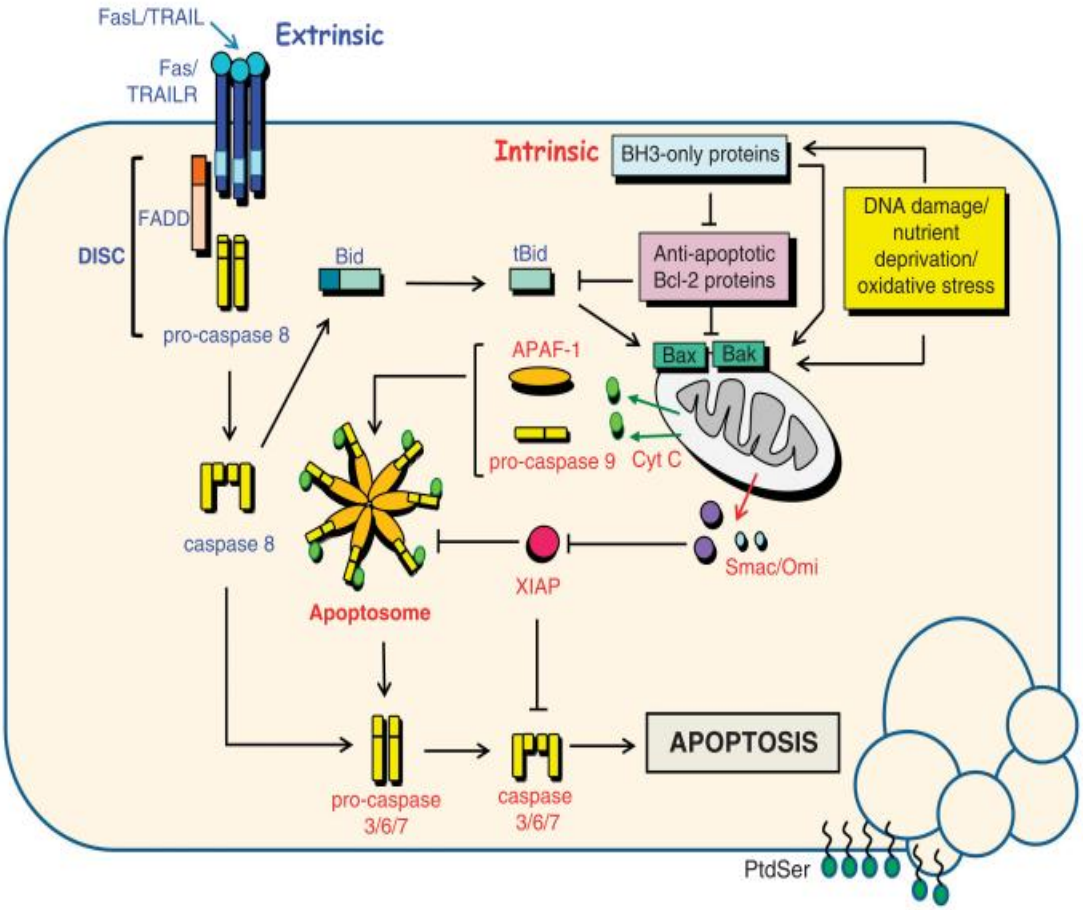

Figure 1. 3: Schematic representation of extrinsic and intrinsic apoptotic pathways. Each pathway needs specific stimuli to provoke molecular events that induce caspase activation towards apoptosis. External death signal (for instance, cytokines) activate the extrinsic pathway via members of the TNFa receptor family and stimulate apoptosis by death-inducing signalling complex (DISC) and involvement of the caspase cascade starting by caspase-8 activation. Whereas the intrinsic pathway is stimulated by internal stress signals (for instance, DNA damage /oxidative stress). The intrinsic pathway is initiated by the mitochondrial outer membrane permeabilization (MOMP) and release of the cytochrome c and Smac (also known as DIABLO). Cytochrome c release triggers the formation of the cytochrome c/Apaf-1/caspase-9 apoptosome, which subsequently activates the executioner caspases-3, 6 and/or 7 that results in apoptosis and the formation of cellular breakdown. (Adapted from Long & Ryan, 2012).

1.1.4.1 Oxidative stress, p53 and its role in apoptosis

Apoptosis activated by p53 is accompanied by an increase in the levels of intracellular reactive oxygen species (ROS). Some of the p53 target genes, such as the PIG3 and FDXR genes, are part of the ROS-related pathways (Polyak et al., 1997). ROS and reactive nitrogen species (RNS) work as key elements in numerous cell mechanisms, including apoptosis, cell development, cell signalling and inflammation. Exogenous components, such as ionising or non-ionising radiation, medications and/or drugs (Simon et al., 2000; Boonstra, 2004; Valko et al., 2007; Kryston et al., 2011; Yang et al., 2013), generate these free radicals, helping the cells develop antioxidant protection mechanisms in the process.

p53 has a significant impact in deciding cell survival through the modulation of intracellular ROS. p53 can work as both a negative and a positive regulator of ROS (Macip et al., 2003). Numerous recent studies have proposed that under low levels of stress, p53 switches on an anti-oxidative stress transcriptional program, which prompts proteins such as sestrins (SESN1 and SESN2), glutathione peroxidase (GPX1), manganese superoxide dismutase (MnSOD) and aldehyde dehydrogenase 4 (ALDH4) to reduce ROS levels. (Tan, et al., 1999; Hussain et al., 2004; Yoon et al., 2004). Additionally, p53-triggered glycolysis and apoptosis controller TIGAR known as (TP53 Induced Glycolysis Regulatory Phosphatase). TIGAR and the antioxidant glutathione, are produced to maintain low ROS levels (Bensaad et al., 2006).

In p53 knockout mouse models, scientists have noticed that the absence of these anti-oxidative stress proteins is associated with increased intracellular ROS levels, bringing about more oxidative DNA damage and tumourigenesis (Sablina et al., 2005).

The p53 protein accomplishes its tumour-suppressing function and controls cell metabolism through different pathways and an array of mechanisms; however, exactly how this regulates apoptosis by oxidative stress and, to a limited extent, ROS generation to maintain cellular redox is poorly

understood. For instance, ROS generates a positive feedback loop by enabling p53 upregulation and stabilisation to induce apoptosis (Vigneron & Vousden, 2010).

In summary, p53 brings about apoptosis through three distinct stages: (I) the transcriptional enlistment of redox-related genes; (II) the initiation of reactive oxygen species and (III) the oxidative degradation of mitochondria; that resulted in full circle of cell death (Polyak et al., 1997).

1.1.5 p53 subcellular localisation

The previous section mentioned how the p53 protein was modulated and controlled by specific mechanisms that determine its biological function. One of these regulatory mechanisms is the subcellular localisation of p53. This section will explore how this essential regulatory mechanism possibly influences p53 activity.

Studies have explored the importance of some factors on p53's nuclear and cytoplasmic localisation, as well as its nuclear import and export (O'Brate & Giannakakou, 2003; Laine & Ronai, 2007; Kruse & Gu, 2009b; Liu et al., 2010; Yuan et al., 2010). All of these factors are necessary in determining the distribution of p53 inside the cell. Furthermore, the two domains of the p53 C-terminus region, the nuclear localisation signal (NLS) and the nuclear export signal (NES), are crucial for p53 transport between nucleus and cytoplasm and vice-versa (Liang & Clarke, 2001).

Many PTMs (such as phosphorylation, ubiquitination and acetylation), along with p53's protein-binding partners, in each specified condition of cellular stress that affect the p53 pathway, influence the p53 subcellular localisation (Appella & Anderson, 2001).

MDM2 is a dominant factor in defining the p53 localisation within the cell. MDM2 manages p53's transport from the nucleus to the cytoplasm by its own nuclear export signal (NES) and mono-ubiquitination (O'Brate & Giannakakou, 2003; Dai & Gu, 2010).

In addition, p53 has been implicated in mitochondrial localisation that leads to triggering a direct mitochondrial cell death. This mechanism is observed when DNA damage or genotoxic stresses initiate it or as a consequence of cytoplasmic p53 being stimulated and accumulated in the mitochondrial compartment (Kruse & Gu, 2009b).

1.1.6 Molecular interaction of p53 with other proteins

The upstream positive and negative regulators of p53, besides PTMs and protein-protein interactions, are considered key elements in determining p53 activity, stability, oligomerization and subcellular localisation (Kruse & Gu, 2009a; Vousden & Prives, 2009; Fernandez-Fernandez & Sot, 2011b; Murray-Zmijewski et al., 2008).

Studies have shown that human p53 can interact with approximately 360 proteins, based on public protein–protein interaction databases (Figure 1.4; Lin et al., 2014).

The proteins that bind to p53 can have a wide range of consequences on p53 functionality and stability, and understanding these interactions are critical for finding relevant therapeutic approaches.

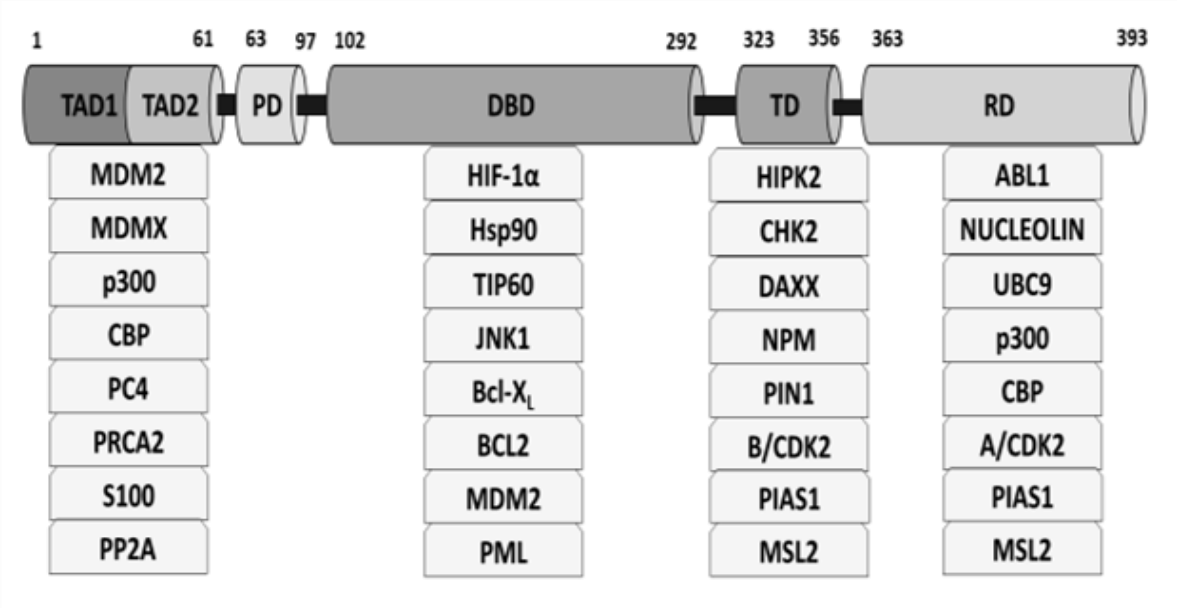

Figure 1. 4: Summary diagram of the most relevant p53-binding protein partners.

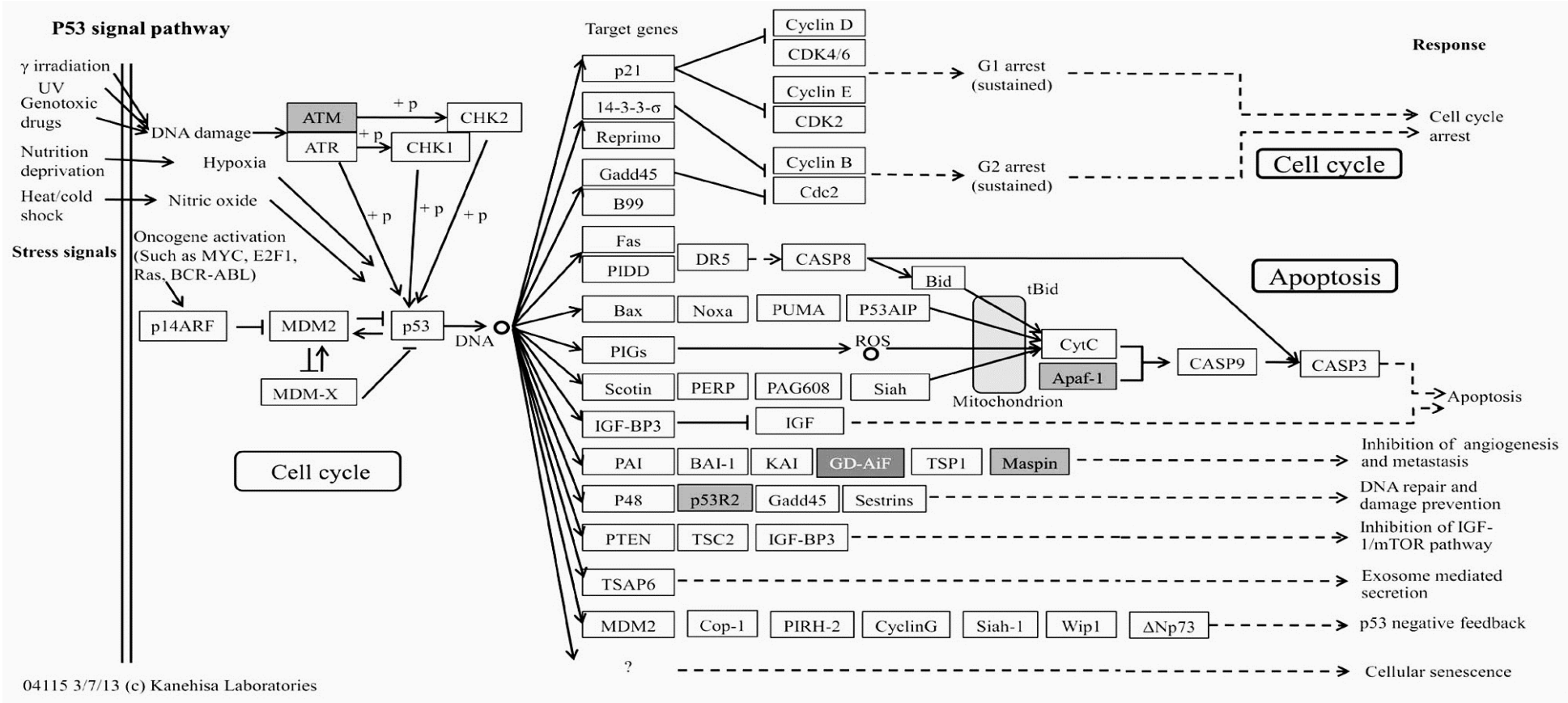

Figure 1. 5: The p53-signalling pathway and its target genes from the KEGG database. Here is a diagram shows p53 signalling pathway following different stress signals that resulted in activating of various target genes each of them responsible of producing specific cellular response (Adapted from Lin et al., 2014).

1.2 The retinoic acid pathway

In 1916, vitamin A was one of the first vitamins discovered (Wolf, 1996). In 1930, Moore demonstrated that beta-carotene, a yellow plant pigment, is transformed in the mammalian body to produce a colourless retinol also known as Vitamin A that is found in food and used as a dietary supplement to replace its deficiency in the mammalian body. In 1931, Karrer solved the D beta-carotene and retinol molecular structures (Figure 1.6 A-B; Wolf, 1996).

These days, the term vitamin A is utilised as the nonexclusive descriptor for retinoids showing the natural biological activity of retinol. Retinoids are a class of molecules comprised of four isoprene (2-methyl-1,3-butadiene) units organised in a head-to-tail structure (Olson, 1996). Vitamin A is classified as a fat-soluble vitamin that plays an important role in vision, maintaining epithelial surfaces, immunity, reproduction, cell differentiation and embryonic development and growth (Blomhoff & Blomhoff, 2006).

Furthermore, vitamin A's various bio-activities are identified with its antioxidant characteristics. For example, lycopene and β-carotene are powerful antioxidant prevention agents (Hix, 2004; Paiva, 1999), while retinol, retinyl esters and retinoic acid (RA) have been identified in the D-lipid peroxidation prevention mechanism *in vitro* (Samokyszyn & Marnett, 1990). Another outstanding function of vitamin A is its involvement in the visual cycle via a process known as photo isomerisation.

In 1933, Wald and his colleagues discovered the underlying molecular mechanism of vitamin A, and they identified how vitamin A had a role in vision; the rod photo receptor cell has a visual pigment known as Rhodopsin, which has 11-cis retinal as its cofactor for light sensitivity. Following the activation of this receptor by light, the 11-cis retinal is converted to all-trans by isomerisation, which results in the release of all-trans retinaldehyde (Ritter et al., 2008).

Vitamin A dietary sources are mainly plant sources, which contain the pro-vitamin A carotenoids (mostly β-carotene), and some animal sources, which have retinyl esters and retinol as vitamin A precursors (Blomhoff & Blomhoff, 2006).

The recommended daily intake of vitamin A varies between 400 to 1300 µg daily, depending on gender and age (IARC-Carotenoids, 1998; IARC- Vitamin A, 1998). There are many major health problems related to vitamin A deficiency, such as vision loss (blindness) and abnormalities related to the heart, brain, eyes, respiratory system and urogenital system, as well as severe infections that can lead to death (Goodman, 1984**;** Ross et al., 2000). Vitamin A deficiency is an important issue in several developing countries.

Vitamin A acts as positive and negative moderator of numerous pathological situations, such as visual disorders, cancer, infectious diseases, diabetes and skin diseases (Chivot, 2005; Love & Gudas, 1994; Niles, 2004; Stephensen, 2001; Travis et al., 2007; Yang et al., 2005; Zouboulis, 2001). Most of these physiological and/or pathological functions can be attributed to vitamin A's main biologically dynamic metabolites: all-trans retinoic acid (ATRA) and 9-cis retinoic acid (9cRA). (Figure 1.6). These metabolites control gene transcription by means of nuclear retinoic acid receptor (RAR) and retinoid X receptor (RXR) regulatory mechanisms (Chambon, 1996). These nuclear receptors and their biological functions will be discussed in section 1.2.3.2. Furthermore, Stra6's (Stimulated by retinoic acid 6) characteristics, functions and unique features enable it to act as a cell membrane receptor/RBP receptor; (RBP will be discussed in section 1.2.3.1) and vitamin A transporter that mediates its cell uptake. The various biological roles of Stra6 will be highlighted in later sections.

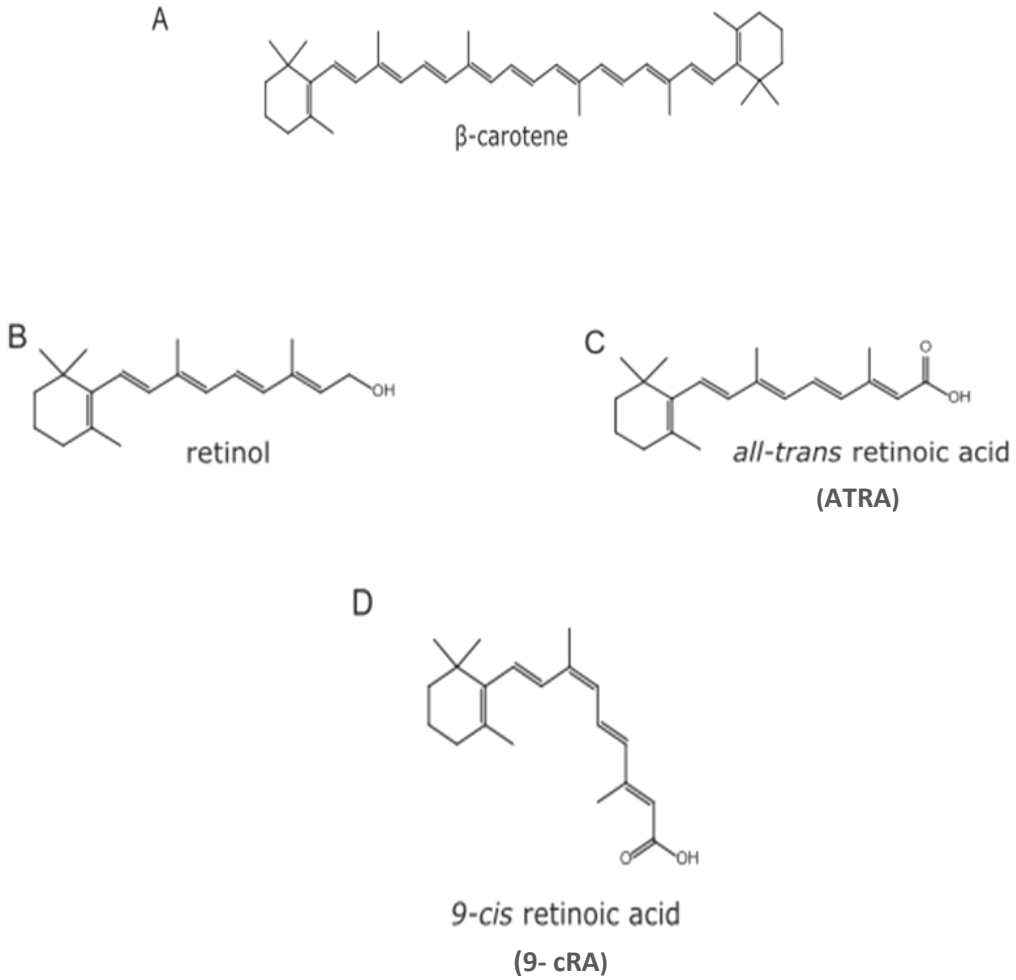

Figure 1.6: **Chemical structures for vitamin A's main source, precursor and active metabolites.** The main source of vitamin A in plants is β-carotene **(A)**; the major transport and storage form of vitamin A is Retinol **(B)**; the two most important forms of vitamin A's biologically active compounds are ATRA and 9-cRA **(C and D)**. (Adapted from Lidén and Eriksson, 2006).

1.2.1 Vitamin A digestion and absorption

As previously mentioned, one of vitamin A's precursors are carotenoids (pro-vitamin A). There are more than 600 types of carotenoids; however, not all of them demonstrate vitamin A bioactivity. β-carotene, α-carotene and β-cryptoxanthin are three forms of carotenoids that are mostly conserved and converted to the all-trans retinol form (Bender et al., 2003). Carotenoids share the similar structure of an extra carbon chain with double bonds, which have a mostly but not predominantly conjugated structure of β-ionone ring on both or only one end of the chain. Carotenoid compounds are present in a wide range of vegetables and fruits, such as tomatoes, carrots, spinach, kale, sweet potatoes, apricots and mangoes. Preformed vitamin A can also be found in eggs, milk, butter, fish and liver. Approximately 70% of pro-vitamin A and preformed vitamin A precursor from plant and animal sources, respectively, is absorbed, depending on the way that the food is prepared (Bender, 2003; Straub & Pfander, 1987; Dietary Reference Intakes, 2001). The retinol conjugates with other food particles, particularly fatty acid esters such as retinyl palmitate or even small protein components. In the stomach, a pepsin enzyme mode of action hydrolyses the carotenoids and retinyl esters from proteins. Because vitamin A is a fat-soluble vitamin, it forms fat globules in the stomach (Ong, 1993).

Bile salts in the duodenum work to emulsify and degrade these fat globules into small droplet molecules. In addition, the pancreatic juices and lipases hydrolyse these small droplets several times. Later, the end product of this soluble solution is absorbed across the duodenum membrane (microvilli border) and the enterocyte (Harrison & Hussain, 2001).

1.2.2 Vitamin A transport, metabolism and storage

All of the different sources of Vitamin A, including preformed vitamin A (retinyl esters) and pro-vitamin A carotenoids (like β-carotene and retinol), are metabolised and hydrolysed in the intestine to form retinaldehyde, or retinal, under the action of the 15,15'-carotene dioxygenase enzyme. Retinal can be reversed to its precursor form, retinol, by retinal reductase, or it can be

further oxidised to its retinoic acid form, which is a non-reversible metabolite form of vitamin A.

In the intestinal mucosal cell, cellular retinol binding protein-II (CRBP-II) is conjugated with retinol to form the esterified version of retinol (retinyl palmitate). Furthermore, phophatidylcholine acts as a fatty acid donor molecule to form retinyl estearate and retinyl oleate compounds via the action of the lecithin retinol acyl transferase (LRAT) enzyme. The action of acyl CoA retinol acyltranferase (ARAT) can perform another esterification mechanism to further esterify the free retinol, involving an LRAT mechanism of action (Ong, 1993).

Retinal esters and carotenoids enter the blood after they are conjugated to chylomicron and lipoproteins, such as (VLDLs) very low-density lipoproteins, and those compounds transport vitamin A through lymphatic circulation or via blood. Later, carotenoids are cleaved into retinol to be transported to other cells and tissues (for example bone marrow, blood, muscles, adipose tissues, spleen, kidneys and lungs) by means of endocytosis (Schmitz et al., 1991) or to be stored in the parenchymal cells of the liver, mostly in the form of retinyl esters. The hydrolysis mode of action cleaves retinyl esters into retinol, which binds to cellular retinol-binding protein-I (CRBP-I) in the liver, facilitating the release of retinol from its storage as required. Furthermore, CRBP-I contributes to regulating the plasma physiological level of vitamin A in the form of free retinol in the cell by preventing a further oxidation processes in the case of high vitamin A intakes due to diet or supplements (Napoli, 1993; Ong, 1994; Ross & Ternus, 1993), as well as to maintain an adequate concentration of retinol in the blood, approximately 2 µM (Dietary Reference Intakes, 2001).

Contrary to the other previously identified forms of vitamin A transportation, retinoic acid (RA) is directly transported by passing through portal circulation

from the duodenum to the liver, and it is found in the plasma incorporated with albumin (Senoo, 2004; Figure 1.7)

Vitamin A hypervitaminosis and toxicity occur when all of the regulatory mechanisms fail or when the hepatic storage thresholds reach capacity and cannot accept any more retinol.

Toxicity mainly results from an extremely large quantity of retinyl esters leaking from the liver and being allocated into the cell membrane in cooperation with plasma lipoproteins, such as low-density lipoprotein (LDL). Therefore, high retinyl ester levels in the blood are widely used in humans as a universal marker for persistent hypervitaminosis A (Krasinski et al., 1989; Croquet et al., 2000; Ukleja et al., 2002). However, the underlying mechanisms of vitamin A toxicity remain elusive.

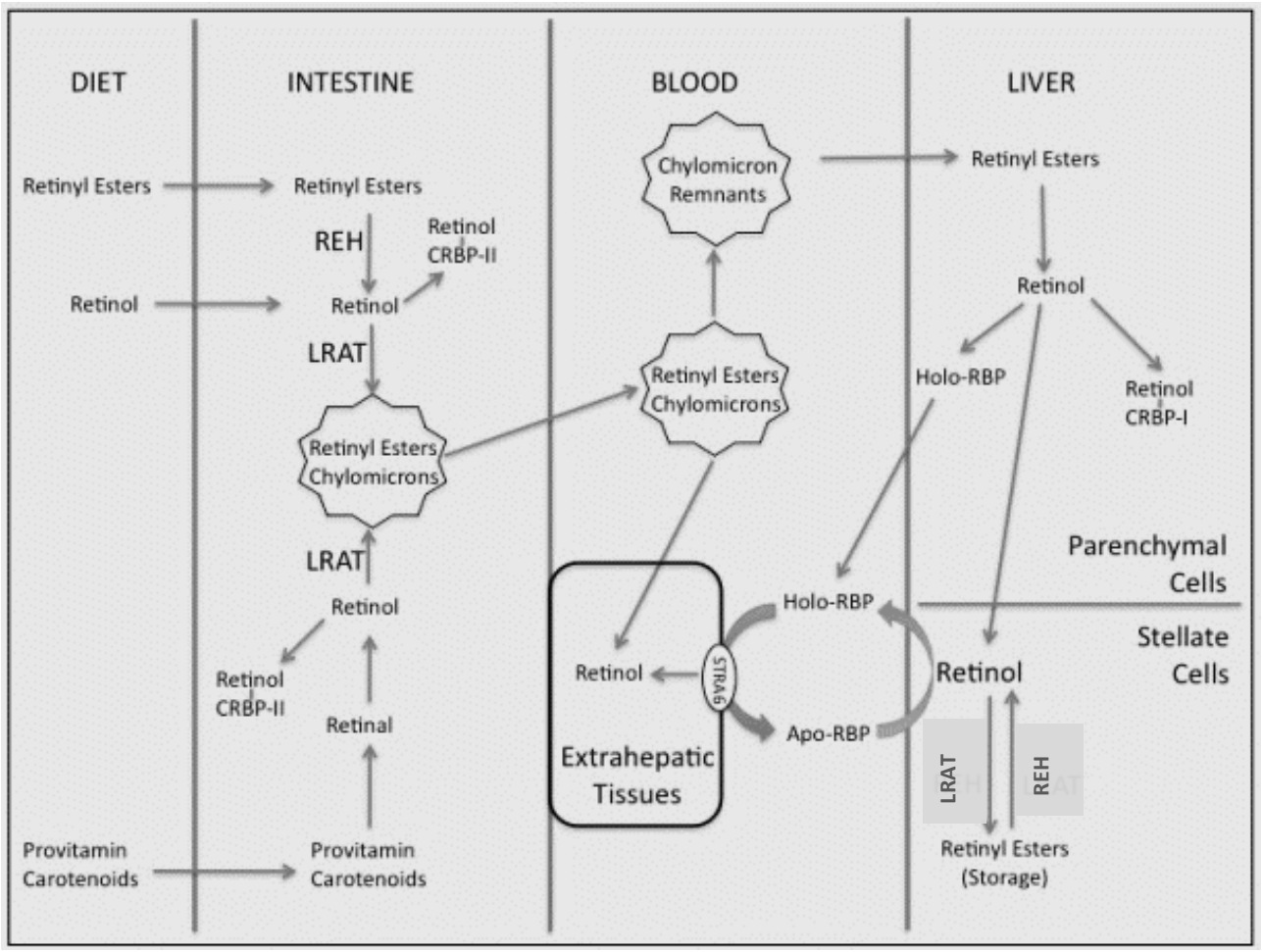

Figure 1.7: **Vitamin A transport, metabolism and storage**. This is a summarised schematic diagram overview of vitamin A transportation and metabolism via the regulation of various enzymatic reactions under the control of the cellular retinol-binding protein process. For more details, please refer to section 1.2.2. (Adapted from Ong, 1994).

1.2.3 Retinoid signalling in target cells

Vitamin A, particularly its main signalling active form, all-trans retinoic acid (ATRA), has vital cellular functions. Small amounts of retinol are metabolised to ATRA (Napoli, 1996), mainly via CRABP I, to convert it to 4-oxo-retinoic acid and to maintain low levels of intracellular ATRA concentration. CRABP II works by transporting ATRA to the nucleus for subsequent interactions with retinoic acid receptors (RAR; Fiorella et al., 1993; Figure 1.8).

Retinoid receptors play a crucial role in adapting various cellular responses, and their cellular importance will be discussed in more detail in section 1.2.3.2.

RA is an essential metabolite that promotes the regulation, proliferation and differentiation of several cell types, including the development of normal embryonic growth, immune systems and liver function, while also maintaining the appropriate structure and function of the skin and epithelial cells in the lungs, urogenital organs and gastrointestinal tract (Ross & Ternus, 1993). For instance, RA induces the differentiation of keratinocytes and transforms them from immature to mature epidermal cells (Wolf, 1984; Creek et al., 1993). Furthermore, RA can induce cellular arrest in the G1 phase of the cell cycle and a reduction in the S-phase (Lotan et al., 1981). For example, RA upregulates p21 and can induce apoptosis through the stimulation of death receptors like FAS, DR4 and DR5; accordingly, RA can inhibit tumour cell growth (Altucci & Gronemeyer, 2001).

In addition, ATRA has shown its role in myeloid cell differentiation, and many studies have previously reported this effect. Wolbach and Howe (1978) and Hodges et al. (1978) showed that *in vivo* vitamin A deficiency resulted in a significant reduction in haematopoiesis. Generally, RA works in producing granulopoiesis from normal bone marrow storage and multipotent hematopoietic cells (Gratas et al., 1993; Tocci et al., 1996). ATRA has also shown an effective cell-cycle arrest in several myeloid cell lines and in human

cancerous cell lines, including lung squamous carcinoma, breast cancer, ovarian cancer and bladder cancer cell lines. This was achieved through regulating CDKs and cell-cycle inhibitors by means of direct or indirect cell-cycle arrest (Bocchia et al., 1997; Hsu et al., 2001; Sueoka et al., 1999; Zhu et al., 1997). Furthermore, successful ATRA treatment has been reported in promyelocytic leukaemia patients (Altucci & Gronemeyer, 2001), and this will be discussed in section 1.3.4

1.2.3.1 Retinoid-binding protein

Free retinol is chemically unstable and needs a carrier protein to protect it from oxidation and to deliver it to the target tissues. The retinol-binding protein (RBP) performs this function. RBP and transthyretin (TTR) bind to retinol and facilitate its transport, as well as its release (Bellovino et al., 1996). Also, TTR is a protein produced in the liver for the purpose of carrying chemical compounds used in cell metabolism throughout the body, another compound that TTR is binding to is a thyroid hormone called thyroxine. However, while RA can diffuse throughout the cell membrane, retinol is rarely present in its free form because it is unstable, insoluble and toxic to cells (Naylor & Newcomer, 1999). The retinoid transportation process from plasma to cytoplasm is still in question.

A 1:1:1 ratio of RBP, TTR and retinol is known as the holo-RBP-TTR complex (Bender et al., 2003), and it is called apo-RBP when no retinol is present. This combination of RBP and TTR molecules is critical to RBP because it increases its molecular weight, and it is essential to prevent RBP's chances of being lost via glomerular filtration in the kidneys. RBP increases the concentration of plasma retinol to more than 1000-fold in comparison to free plasma retinol (Goodman, 1984).

RBP can be found in, and produced by, many other organs and tissues apart from the liver, which was originally believed to be the one and only source that would produce RBP (Zheng et al., 1999). However, the underlying actions on RBP functions in these tissues that produce RBP remains elusive.

For instance, it was recently identified that adipose tissue produces RBP as adipocytokine, which is a cell-signalling protein that promotes insulin resistance (Yang et al., 2005). Although, there are different sub-classes of RBP including RBP1 (also known as CRBP-I) and RBP2 (also known as CRBP-II). Both RBP1 and RBP2 are cellular, whereas RBP3 is detected within the Interstitial lumen and RBP4 is predominately detected within plasma (Fierce et al., 2008).

The infusion of RBP4 into mice has confirmed this result, creating insulin resistance and glucose intolerance. This proposes a conceivable option regarding insulin resistance (Yang et al., 2005).

Regarding vitamin A homeostasis, about 20% of the vitamin A (retinyl esters) in the adipose tissue is made from chylomicrons through lipoprotein lipases; thus, this explains why RBP could exist in the adipocyte, offering a return mechanism of extra retinol (Blaner et al., 1994).

RBP knockout mice have shown a severe defect in metabolising vitamin A from its liver storage, as well as an intense sensitivity to vitamin A deficiency; thus, even with a dietary supplement of vitamin A, it was clearly shown their vitamin A serum level was reduced. Furthermore, typical symptoms of vitamin A deficiency were observed, such as weakening of normal immune function by having low levels of immunoglobulin, heart abnormalities and vision difficulties. However, visual ability was able to be reversed based on a vitamin A supplementary diet (Quadro et al., 1999).

All of the above studies, as well as the current existing knowledge, highlight RBP's critical role in many pathophysiological diseases and its significant function in retinol transfer.

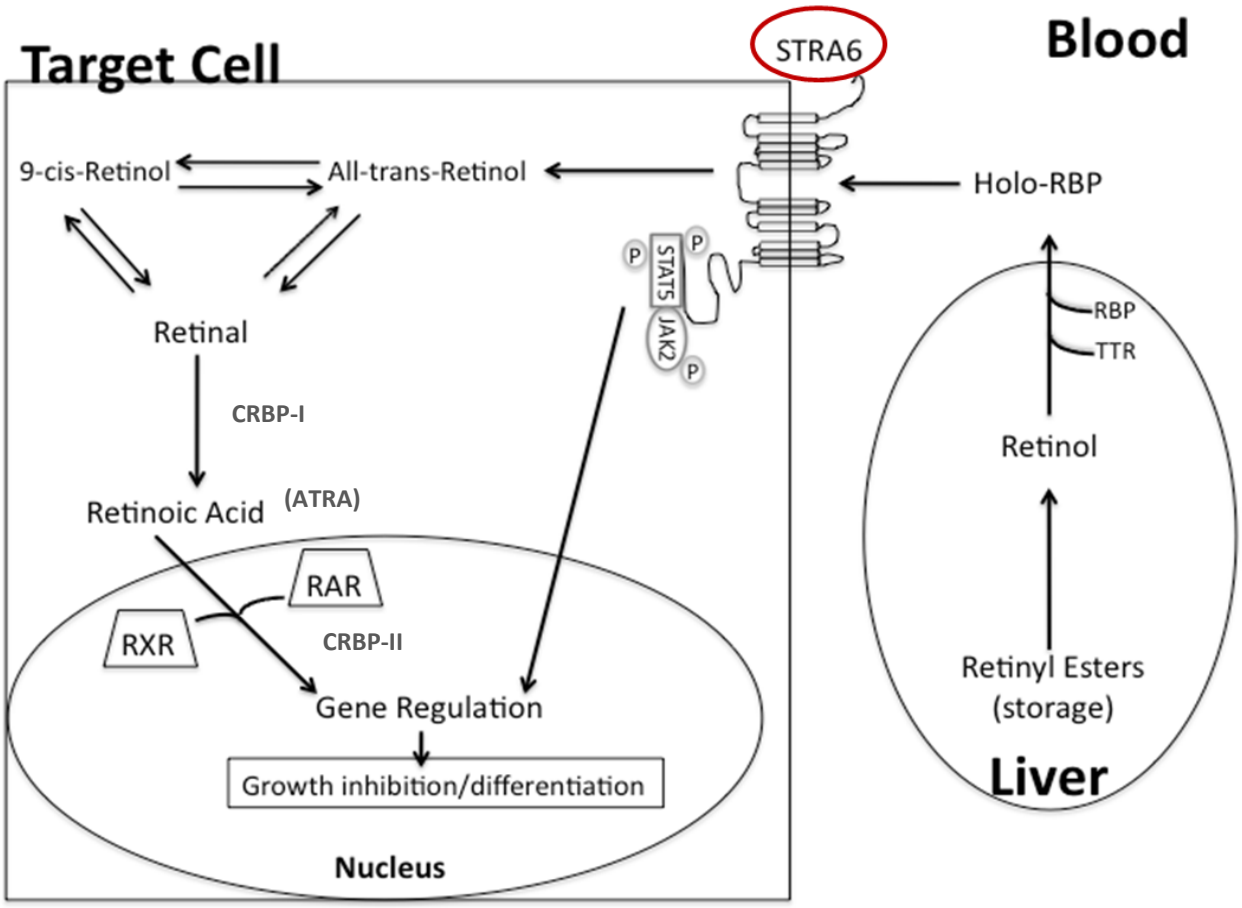

Figure 1.8: **Retinoid signalling in target cell.** Stra6 intervenes in the uptake of retinol from RBP into the cell. Once in the target cell, the retinol is metabolised to ATRA and/or 9-cRA, which is translocated into the nucleus and then binds to homo- or heterodimers of retinoic receptors RARs and RXRs to trigger the activation of target genes. Holo-RBP binding to its receptor Stra6 trigger the tyrosine phosphorylation of Stra6 protein in C-terminus domain. Phosphorylated Stra6 causes Jak2 recruitment, which phosphorylates Stat5 and translocates it to the nucleus to modulate multiple cellular functions through the regulation of various downstream target genes.

1.2.3.2 Retinoid receptors

Once inside the target cell, retinol is converted under the action of alcohol dehydrogenase and retinaldehyde dehydrogenase to retinaldehyde and retinoic acid (RA), in the form of ATRA and/or 9-cRA, respectively. After that, RA is bound to CRBP-I for transportation to the nucleus in order to trigger a series of cellular responses via retinoic acid receptors that initiate gene expression. RA mediates its physiological function through its two classes of nuclear receptors: retinoic acid receptors (RARs) and retinoid X receptors (RXRs) (Gropper et al., 2005; Resendes & Rosmarin, 2006; Gillespie & Gudas, 2007). Both of these receptors are known to have several isotypes, including RAR α, β and γ, that would be activated mostly via ATRA and 9-cRA; however, RARs bind to 9-cRA with low affinity compared to ATRA (Allenby et al., 1994; Repa et al., 1993) and RXR α, β and γ are activated mainly through 9-cRA (Petkovich et al., 1987; Krust et al., 1989; Heyman et al., 1992; Allenby et al., 1993).

ATRA mediates cell growth and differentiation by binding to RARs (Tang & Gudas, 2011). Through alternative splicing mechanisms, both RARs and RXRs possess many isoforms, such as RAR α1 and α2, RAR γ1 and γ2 and RAR β1-β4, which have various regulatory properties and functions (Swift et al., 2006). They can be further homodimerised or heterodimerised towards the regulation of particular promoter regions of specific genes through binding with retinoic acid response elements (RARE), which are specific DNA nucleotide sequences (Gillespie & Gudas, 2007). In addition, RAR/RXR heterodimeris can be ATP-dependent for the recruitment of chromatin remodelling complexes (Tang & Gudas, 2011).

Examples of RAR target genes include genes that participate in ATRA activation, like RBP2 and RBP4 (Mangelsdorf et al., 1991). In general, all of these responses allow retinoid-dependent transcriptional activity to occur (Panariello et al., 1996).

There has been extensive investigation into RAR expression and its physiological importance. RARα is the predominantly expressed isoform; however, RARβ and RARγ demonstrate a particular distribution based on cell type and tissue origin (Dolle, 2009).

From previous experimental studies, data has shown that both RARα and RARγ play important roles in cell-cycle arrest and growth inhibition (Boyle et al., 1999). However, RARβ has shown the tendency to support cell proliferation, differentiation and survival (Zhuang et al., 2003; Boyle et al., 1999) following ATRA stimulation.

At some stage in carcinogenesis, the loss or silencing of RARβ 2 expression is common in human breast cancer cells and hepatoma cancerous cells. RARβ 2 defects will generally induce cell-cycle inhibitors, including p21 and p27 (Suzui et al., 2004; Li et al., 2004). This supports the importance of the RARβ2-RA signalling pathway in cellular proliferation and differentiation (Faria et al., 1999; Chen et al., 2007).

Retinoid (ATRA) resistance has been reported due to a defect in RAR α, β or γ that happens along with cancer development, such as in colon cancer (Freemantle et al., 2003; Lee et al., 2000). The mutant receptor is mostly associated with RARβ as a result of RARE methylation at the RARβ promoter region (Sonneveld et al., 1998; Gudas & Wagner, 2011).

1.3 Stra6

1.3.1 Background

In 1970, RBP was characterised to have a specific cell membrane receptor in the retinal pigment epithelium (RPE) (Bok & Heller, 1976; Chen & Heller, 1977; Maraini & Gozzoli**,** 1975). Since then, this evidence has also been found in many other tissues, such as placenta, macrophages, undifferentiated keratinocytes, bone marrow and choroid plexus. These tissues express the RBP receptor, which is important for the diverse functions of vitamin A in

foetal development, immune response, cell differentiation, cell proliferation and brain development (Bhat & Cama, 1997; Hagen et al., 1999; MacDonald et al., 1990; Sivaprasadarao et al., 1994; Smeland et al., 1995). In general, the RBP receptors show a predominant distribution in the blood-organ barriers (MacDonald et al., 1990) of the brain, RPE and placenta, as well as in both genders' reproductive systems, CNS, skin, heart, kidneys and lungs (Stephensen et al., 2001; Baybutt et al., 2000; Ikeda et al., 2005; Livera et al., 2002; Varani et al., 2000; Weiler et al., 2001; Xu et al., 2001).

Recently, the RBP cell surface receptor was discovered to be the stimulated by retinoic acid 6 (Stra6), first described in P19 embryonic carcinoma cells (Bouillet et al., 1995).

Beside Stra6's function in facilitating retinol uptake from RBP as its own receptor, it was also classified as a transporter for vitamin A and as a unique protein with no similar homology to any known ion channels, receptors, transporters and cell signalling proteins (Bouille et al., 1997; Kawaguchi et al., 2010; Chen et al., 2016).

A recent study has established that Stra6 contributes to p53-induced cell death after DNA damage and, thus, was independent to RA induction (Carrera et al., 2013). In addition, Stra6 was involved in lipid metabolism and insulin resistance in obesity and type 2 diabetes (Berry et al., 2012; Kawaguchi et al., 2012; Muenzner et al., 2013; Marwarha et al., 2014). Furthermore, it was recently suggested that holo-RBP and its receptor Stra6 have a role in driving oncogenic transformation (Berry et al., 2014). All of these various functions have been related to Stra6, and its involvement in many different pathways will be discussed in greater detail in section 1.3.3.1

In 2015, the Stra6 gene was identified to encode two different mRNAs that were transcribed by two different promoters, which resulted in producing the long and short isoforms of Stra6 (Laursen et al., 2015).

Stra6's mutations have been identified in humans. For instance, the Matthew-Wood syndrome occurs due to truncating mutations in Stra6. Matthew-Wood syndrome results in severe microphthalmia/anophthalmia, which is characterised by the loss of one or both eyes, and it is also associated with severe pathological defects such as mental retardation, lung hypoplasia, congenital heart defects, intrauterine growth impairment, pancreatic malformations and duodenal stenosis (Golzio et al., 2007; Pasutto et al., 2007; Wang et al., 2010; Chassaing et al., 2009; Chitayat et al., 2007).

Stra6 molecular analysis in humans has demonstrated either a homozygous insertion or deletion in *exon-2* or a homozygous insertion in *exon-7* of the Stra6 gene; this study was done on two foetuses of related families that had been diagnosed with Matthew-Wood syndrome (Golzio et al., 2007). Thus, a study was carried out on three foetuses plus one child, and all of them acquired Matthew-Wood syndrome with anophthalmia and mental retardation (Chassaing et al., 2009).

The loss of retinoid uptake in the eye as a result of knocked down Stra6 has been studied in zebrafish models, and the results demonstrated vitamin A inadequacy and developmental deformities due to the loss of Stra6 (Isken et al., 2008). Furthermore, Stra6-null mice models have revealed prominent ocular defects (Ruiz et al., 2012; Berry et al., 2013). Hence, the hypothesis is that Stra6 is vital for retinol homeostasis in the eye.

The Stra6-null mice models have inspired debate regarding the existence of another protein/receptor in relation to retinol transport to the target cells, since this function of retinol uptake from RBP seems to not be limited to Stra6 (Ruiz et al., 2012; Berry et al., 2013). RBP4 receptor-2 (RBPR2) is a newly identified protein that shares 40% homology with Stra6- and it could have a role in retinol metabolism and transport independent of Stra6 function (Alapatt et al., 2013; Berry et al., 2013).

The number of Stra6-related papers has increased in recent years. However, there is still a lack of important information related to Stra6 subcellular localisation upon retinoid induction, as well as characterising Stra6's interacting partners. Hence, there is a necessary need for more cellular, biological and structural models to be investigated.

1.3.2 Stra6 structure

Stra6 protein/receptor has a fragile nature in addition to its transient binding to RBP, thus making the structural study of this receptor protein a challenging task. In 2007, Kawaguchi's group was one of the first to characterise the Stra6 structure by stabilising the interaction of RBP-Stra6 via a well-planned approach that allows a high purification affinity to the RBP-Stra6 complex molecule (Kawaguchi et al., 2007). In consequence to its previous purification method, Stra6's structure was described as a multi-transmembrane protein of no known function to any earlier identified protein. Stra6 is a 74-kDa protein (Kawaguchi et al., 2008). Stra6's topology model includes 19 distinguishing domains: five of these domains are outside the cell and represented as extracellular domains, nine domains are across cell membranes and identified as transmembrane domains, and the final five domains are inside the cellular matrix and considered intracellular domains (Figure 1.9).

In identifying the potential binding sites of RBP4 in the Stra6 protein in order to mediate the retinol uptake and to facilitate its transport across the plasma membrane, a significant number of mutational studies have been done to identify some amino acids as possible sites for RBP4 binding in bovine Stra6, including Tyr^{336}, Gly^{340} and $Gly^{342.}$ (Kawaguchi et al., 2008). However, human Stra6 shows a polymorphism (G339S) in correlation to the above bovine Stra6 mutations that reflects pathological defects due to the probable deterioration of RBP4's ability to bind to its receptor (Stra6) and its failure to perform its functions (Pasutto et al., 2007).

Breen and his colleagues were the first group of scientists to explore the Stra6 crystal structure. They have expressed Stra6 in Pichia pastoris as a fusion protein with green fluorescent protein (GFP) and have revealed that the 1 mole-RBP:1 mole-Stra6 complex transient interaction was retinol independent (Breen et al., 2015).

Another group has recently studied Stra6 structure by purifying Stra6 from a zebrafish model, and it found a natural unpredicted link between Stra6 and calmodulin (CaM), which forms a 180 kDa complex molecule; CaM is known as a binding partner and a functional controller for various membrane protein members (Tidow & Nisse, 2013), such as transporters, ion channels and enzymes. Furthermore, researchers have illustrated a possible idea of retinol's release mechanism from the Stra6 hydrophobic pocket that facilitates the diffusion of retinol across the cellular plasma membrane (Chen et al., 2016).

From the literature, regardless of the clear significance of Stra6 protein, there is little evidence regarding its structure. The existing data is limited to the Stra6 primary structure, and no records exist on the secondary, tertiary or quaternary structure of Stra6 receptor. In addition, Stra6 crystal structure investigational studies will be an extraordinarily significant measure in enlightening, as well as highlighting, its mechanism of action; however, for this information to be fully understood, it must be added to studies identifying Stra6 protein-binding partners.

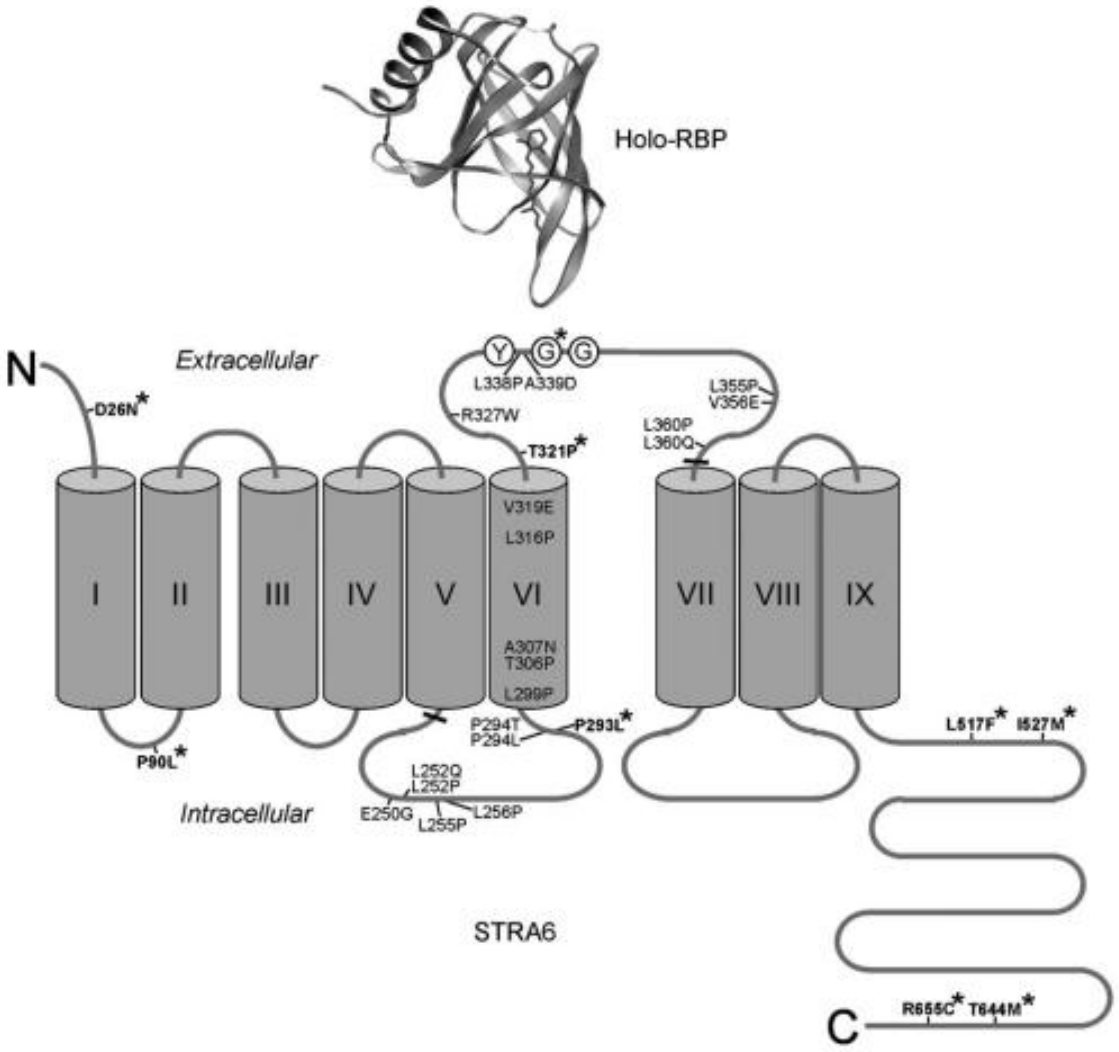

Figure 1.9: **A model of Stra6 receptor protein and possible sites of Stra6 mutations and polymorphisms.** The Roman numerals from I to IX represent Stra6 transmembrane domains. That includes 19 distinguishing domains: five of these domains are outside the cell and represented as extracellular domains, nine domains are across cell membranes and identified as transmembrane domains, and the final five domains are inside the cellular matrix and considered intracellular domains. Thickened lines mark the region of Stra6 subjected to random mutagenesis. (Adapted from Kawaguchi et al., 2008).

1.3.3 Stra6 activation

On a target cell, Stra6 binds to the holo-RBP-TTR complex and thus allows Stra6 to mediate retinol uptake by catalysing the release of retinol, mainly via the action of LRAT and CRBP-I (Kawaguchi et al., 2008). LRAT enhances retinol uptake from Stra6 and converts retinol to its storage form (retinyl esters). CRBP-I further stimulates the retinol uptake mechanism from the holo-RBP complex via Stra6. Furthermore, LRAT and CRBP-I maintain the total level of vitamin A in order to avoid vitamin A toxicity by means of monitoring the Stra6 retinol uptake, inhibiting Stra6 from loading retinol back to RBP, helping Stra6 to uncouple from holo-RBP complex and permitting apo-RBP to experience further kidney filtration (Kawaguchi et al., 2008).

ATRA has been shown to increase the Stra6 mRNA levels, dependent on the concentrations, as Stra6 is identified as an RA-inducible gene that is mainly mediated by the retinoid receptors' heterodimerisation of RXRα/RARY. However, other retinoid receptors were in some cases induced by Stra6, such as in RARα and RARβ (Bouillet et al., 1997).

It has been found that Stra6 is necessary for vitamin A homeostasis in the eye but not in other organs. A study has been done on Stra6 knockout mice models to evaluate the importance of Stra6. The results showed vitamin A levels dropped significantly when compared to the other model of Stra6 WT mice (Terra et al., 2013). In 2014, Skazik and his colleagues determined that the depleted status of Stra6 in the HaCaT cells, a spontaneously transformed aneuploid keratinocyte cell line from adult human skin, does not affect the target cells' retinol uptake. However, this resulted in a significant thickness of the epidermal layer, which was associated with an elevation of epidermal markers, including Krt6, Krt10 and Krt16, and an observed expansion of Ki67 expression. The same results have also been observed using an *in vivo* model (Laursen & Gudas, 2014). This supports the hypothesis that there are other undiscovered mechanisms related to retinol uptake other than Stra6.

The Stra6 cell surface receptor performs numerous vital roles in human health and disease, and we will discuss some of them in the following section, particularly in respect to Stra6's involvement in triggering various signalling cascades. However, other signalling pathways that explain Stra6's observed functions are still elusive.

1.3.3.1 Involvement of Stra6 in other pathways

Researchers have recently found that Stra6 does more than serve as a mechanism for retinol uptake from RBP and reloading it back to RBP. Stra6 has a role as a cell surface signalling receptor after it binds to holo-RBP by recruitment and activation of Janus kinase 2 (Jak2) and signal transducer and activator of transcription 5 (Stat5).

Basically, the Stra6 SH2-binding motif in the cytosolic domain of the receptor undergoes tyrosine phosphorylation following a direct binding to the holo-RBP complex; hence, a specific tyrosine residue is phosphorylated, and JAK2/Stat5 is activated, thus facilitating Stat5 translocation to the nucleus where downstream regulation and expression of target genes takes place, including regulation of the cell differentiation and proliferation process (Berry et al., 2012).

Investigations have been done *in vivo* using mouse models to determine the role of Stat5 in the carcinogenesis mechanism. They have reported the activity of Stat5 mostly as a proto-oncogene molecule involved in many cancers, including breast tumours (Wagner & Rui, 2008). In particular, Stat5a is activated after it is phosphorylated, with 75% of breast malignancies demonstrating a nuclear localisation of Stat5a (Cotarla et al., 2004).

ERα and Cyclin D1 are highly expressed after the overexpression of Stat5a, which results in cell differentiation and proliferation (Li et al., 2006; Park et al., 2002). Furthermore, Stat5a's expression has been revealed to endorse the occurrence of sporadic cancers in mice (Iavnilovitch et al., 2004). Additionally,

mouse models of Stat5a's expression have demonstrated a high tendency to develop adenocarcinomas after one year.

Related to stress signalling in the cell, the mitogen activated protein kinase (MAPK) pathway is the primary invoked pathway in such cellular events. The MAPK pathway induces cell death, inflammatory cellular responses and kidney fibrosis, mainly under the stimulatory effect of the cAMP that provoked MAPK family members, including p38 and c-Jun N-terminal kinase (JNK), (Kyriakis & Avruch, 2001**;** Tian et al., 2000).

Several studies have reported that the activation of JNK and p38 leads to RAR depletion, and they also participate in the regulation of apoptotic events (Tian et al., 2000). Jak2-Stat5 signalling cascades exert their actions indirectly via a series of events that trigger the JNK-p38 cascade activation and leads to apoptosis (Lejeune et al., 2002; Fuster et al., 2011).

Recently, a model has suggested that Stra6 is a signalling transduction molecule (Chen et al., 2012; Berry et al., 2011). Chen et al. have shown enhanced phosphorylation of Jak2 and Stat5 upon holo-RBP and Stra6 binding, thus promoting the production of more AC6 that will in turn catalyse more cAMP, where all of these cellular cascade events promote apoptosis by means of CRBP-I and RARα suppression and via JNK and p38 activation as an outcome (Chen et al., 2012).

In 2001, Szeto et al. performed a screening study to evaluate genes related to the Wnt-1 regulatory response. They found that Stra6 mRNA is greatly expressed; thus, suggesting Stra6 to be a critical key regulator in cancer. The researchers also determined a synergistic effect between the Wnt-1 and RA pathways following a combined treatment of ATRA and Wnt-1 overexpressed active constructs, which results in high expression levels of Stra6. The Stra6 induction by Wnt-1 is mediated mainly via the activation of RAR nuclear receptors (Szeto et al., 2001).

Recent findings have linked Stra6 to the cellular responses to DNA damage events (Carrera et al., 2013). The researchers found that Stra6 played a part in the mechanism of p53-induced cell death (Carrera et al., 2013). In addition, Stra6 induction after DNA damage was shown to be RA independent, and did not activate RARs target genes. Generally, these findings have proposed that Stra6 is a new member of the p53 pathway (Carrera et al., 2013).

Retinoids induce an assortment of metabolic activities in the fat tissue, including lipolysis (Bonet et al., 2012). However, most studies in adipocytes have recognized ATRA as a potent inhibitor of adipogenesis when present at early phases of cellular differentiation (Ziouzenkova et al., 2007; Kamei et al., 1994). These inhibitory impacts were observed to be mediated by aberrant mechanisms, including RARα (Kamei et al., 1994; Xue et al., 1996), and by inhibition of the pro-adipogenic transcription component CCAAT/enhancer-binding protein (C/EBP), (Schwarz et al., 1997).

ATRA stimulates the expression of the transforming development variable β effector protein SMAD3 to activate RARα, which lowers C/EBPβ DNA binding by collaborating with C/EBPβ through its Mad homology 1 domain (Choy & Derynck, 2003). Other than RARα, RARγ has likewise been implicated in the inhibitory impacts of ATRA on adipocyte differentiation by enhancing the expression of the strong inhibitor of adipogenesis, which is known as delta-like 1 homolog/pre-adipocyte factor PREF-1. However, Stra6's role as a mediator for retinol transfer via RBP4 to adipocyte progenitor cells is not entirely clear (Berry et al., 2012).

Although cell retinoid homeostasis via RBP signalling has been associated with insulin resistance, it has not been clearly identified. RBP phosphorylates Stra6, which works as a signal transducer and activator for translating Stat5 in hepatocytes, adding to the progression of insulin resistance by inducing cytokine signalling 3 (SOCS3), as well as by suppressing the expression of

peroxisome proliferator actuated receptor gamma (PPARγ) (Berry et al., 2011; Berry et al., 2012).

Taking everything together, GLUT4-RBP4-Stra6, may also be assumed to be an essential part in the pathogenesis of type 2 diabetes, where a particular glucose transporter type 4 (GLUT4) is suppressed in the adipocyte. GLUT4 is the insulin-managed glucose transporter discovered principally in fat tissues and striated muscle (skeletal and cardiovascular), and it prompts an increased expression of RBP4 that creates more insulin resistance through Stra6 (Nair et al., 2010).

Past studies have also demonstrated that Stra6 can influence the immune response. In most reactive T-cells, Stra6 was upregulated via mesenteric lymph node-dendritic cells in a blended lymphocyte pool (Kang et al., 2007). Retinoids are well known to regulate T-cell sub-classes, including Th1, Th2, Th17 and T-regulatory cell development and function (Cantorna et al., 1994; Stephensen et al., 2002; Mucida et al., 2007; Benson et al., 2007).

1.3.4 Retinoids, Stra6 and cancer

Investigations have been done to determine the role of vitamin A in carcinogenesis, particularly on the retinoic acid capability on cancer pathogenesis. Results have shown that it could, to some degree, decrease the incidence of tumours in mammals (Muto et al., 1998; McCormick et al., 1999; Anzano et al., 1994). Epidemiological studies exploring the relationship between a vitamin A supplementary diet and human tumours raised the theory that low vitamin A intake may have an additive role on cancer development and that people who consume three or more servings of leafy foods every day, especially those rich in carotenoids, have lower risks of a few types of malignancies (Stähelin et al., 1991). The reports originated from case control and cohort studies have indicated a reverse relationship between the utilization of pro-vitamin A (β-carotene) and the risk of tumours, such as lung and stomach tumours (Wakai et al., 2011; Larsson et al., 2007).

Studies from a number of human cancers, including kidney, skin, kidney, breast and bladder, have revealed an abnormal reduction of intracellular retinyl ester levels and diminished LRAT expression (Liu & Gudas, 2005; Guo et al., 2002; Sheren-Manoff et al., 2006). In renal cancer, investigations have found that low levels of LRAT expression are correlated with low retinol concentration in the target cell, as a consequence of diminishing retinol uptake from the holo-RBP complex (Guo et al., 2001).

Another important fact that has a significant impact on disturbing the RA signalling pathway in cancer cells is the RARβ2 silencing due to gene methylation processes (Hu et al., 1991). Furthermore, some studies have revealed that RARβ-RARE is epigenetically silenced in various types of cancers (Sirchia et al., 2002; Hoque et al., 2004; Fazi et al., 2007).

ATRA has been reported to be engaged in inducing cellular differentiation and regulation of numerous cell types. Indeed, ATRA's observed biological functions have indicated a possible drug for many cancer treatments (Altucci & Gronemeyer, 2001).

Furthermore, some studies have proposed that retinoids have a strong antiproliferative impact on colon cellular growth *in vitro,* and they could have potential for the chemoprevention of colon cancer. *In vivo* studies using rat models have revealed a similar concept regarding retinoids' ability to inhibit the transformation of colon progenitor cells to be a cancerous colon cells (Delage et al., 2004; Wargovich et al., 2000; Zheng et al., 1999).

Retinoids trigger apoptosis in numerous types of cancer cells, for instance, in acute promyelocytic leukaemia (APL). ATRA has turned out to be a critical agent in the treatment of leukaemia, and it is the most preferred drug for the treatment of APL (Chomienne et al., 1996).

APL mostly shows a chromosomal translocation t (15; 17) between the RARα gene on chromosome 17 and the PML gene on chromosome 15, resulting in

the formation of the RARα-PML fusion protein. However, a few APL cases show an association between the RARα gene combined with the promyelocytic leukaemia zinc finger gene (PLZF), which shows more resistance to retinoid treatment due to additional HDAC-containing complexes. Therefore, a combined treatment of ATRA and HDAC inhibitor, such as sodium butyrate, has been suggested (Zhang et al., 2000; Marks et al., 2000). APL was characterised to have improper retinoic acid signalling via excessive repression and oligomerization of RARE target genes by the action of HDAC, which hinders PML signalling and permanently arrests only promyelocytic cells (Breems-de Ridder et al., 2000; de Thé & Chen, 2010). Pharmacological doses of ATRA are used as treatment for APL to get its advantages of promoting cell differentiation and of restoring the defective cell signalling (Zhang et al., 2000; Breems-de Ridder et al., 2000). Conversely, treatment with ATRA alone is linked with a high rate of relapse, mainly because of ATRA resistance. In 10-15% of cases, patients treated with ATRA have suffered serious symptoms of retinoic acid disorder, which is characterized by expanding counts of leukocytes, fever, respiratory problems, weight gain, pericardial effusions, low blood pressure and sometimes impermanent renal functions (Altucci & Gronemeyer, 2001).

Recently, the treatment of APL has not only been based on retinoids alone but also on introducing the concept of combined treatment with chemotherapy agents. In 2014, Ablain and colleagues performed an experimental study that provided the first knowledge of the APL treatment mechanism involving p53 as a principle key element in PML-RARA fusion protein deterioration via direct p53 response to DNA damage by means of deacetylation of p53. Thus, showed that activating the PML-dependent regulation of p53 target genes shows post-transitional modification (PTM) of p53 protein and p53 stabilisation and activation (Ablain et al., 2014).

In light of previous experimental results, particularly these studies by Carrera et al. (2013) and Ablain et al. (2014), our main purpose is to define Stra6

functions in the p53 signalling pathway, as little research has been done in regards to this aspect of Stra6. Furthermore, the recent results of Ablain's group could provide a reasonable justification for retinoids (ATRA) treatment via a combined treatment with DNA-damaging agents dependent on p53 status to treat cancers other than PML. Since Stra6's involvement in such cancer models has not been investigated, our research will be important in revealing the mechanisms that link ATRA-Stra6-p53 together and in providing a comprehensive understanding of the underlying mechanism of potential combination therapies.

1.4 Aims of the project

Based on the previous findings:

(I) Stra6 enhances p53-induced apoptosis following DNA damage and

(II) Stra6 is induced by retinoids (vitamin A)

Our aims are as follows:

1. To further characterize the involvement of Stra6 in the p53-dependent DNA damage response inducing apoptosis.

2. To study the potential of Stra6 as a novel target for cancer treatment.

1.4.1 Hypothesis

Stra6 induction by All-trans retinoic acid (ATRA) may sensitize tumour cells to p53-induced apoptosis after treatment with DNA-damaging agents.

1.4.2 Specific objectives

(I) Evaluation of the up-regulation of Stra6 by ATRA to study retinoid mediated enhancement of cancer cell sensitivity to DNA damaging agents in response to Stra6 induction.

(II) Identification of proteins that bind to Stra6.

(III) Determination of Stra6 sub-cellular localisation.

2 Materials and Methods

2.1 Cell culture

Different cancer cells (Table 2.1) were cultured in DMEM (Dulbecco's Modified Eagle Medium) GIBCO supplemented with 10% v/v FBS Foetal Bovine Serum (FBS) (GIBCO) as well as 50 units/ml of Penicillin-Streptomycin (GIBCO) (Table 2.2). A 5% CO_2 incubator was used to culture the cells, Phosphate buffered saline (PBS) was used to wash the cells two times before being incubated in 2 ml of 0.05% v/v Trypsin-EDTA for 3 minutes at 37 °C, until the cells detached from the plate. Upon detaching the cells, the trypsin was inactivated by adding 6 ml of DMEM, then pelleting the cells at 1200 g for 5 minutes. After washing the cells once in PBS, they were re-suspended in 5 ml of media, and re-plated at the desired cell density.

2.1.1 Long-term storage of human cell lines

For long-term storage of cell lines, freezing of the cells was done upon being 100% confluent in culture plates. After aspirating the old medium, the cells were washed and trypsinised using 5 ml of PBS and 2 ml of 0.05% v/v trypsin respectively, and incubated for 3 minutes. After being collected in 6 ml of media, the cells were centrifuged at a rate of 1200 g for 5 minutes. Cells were Suspended in 3 ml DMEM (as previously described) supplemented with 10% v/v DMSO (Sigma-Aldrich, #D5879). Freezing was done after transferring 1 ml aliquots to cryovials. For the cells to survive, a controlled decrease in temperature was performed by having the vials inserted in an isopropanol chamber and maintained at -80°C overnight, with the vials being transferred and stored in liquid nitrogen storage racks 24 hours later. A water bath at 37 °C was used for thawing the cells by inserting the frozen cryovials in the water bath for 2 minutes, and later transferring the cells to a plate with 9 ml of warm media. The old medium was aspirated 24 hours later and fresh medium was added.

Table 2.1: Cancer cell lines used

Name	Type	p53 status
EJp53	human bladder cancer cell	tetracycline (tet)-off inducible p53 expression system (Sugrue et al., 1997)
EJp53 sh-Stra6	human bladder cancer cell	tetracycline (tet)-off inducible p53 expression system (Sugrue et al., 1997)
HCT116	human colon cancer cell line	$^{+}/^{+}$
HCT116 p53-/-	human colon cancer cell line	$^{-}/^{-}$
HCT116 sh-Stra6	human colon cancer cell line	$^{+}/^{+}$
U2OS	human bone osteosarcoma epithelial cells	$^{+}/^{+}$
PA-1	human ovarian carcinoma cell line	$^{+}/^{+}$
MCF-7	human breast cancer cell line	$^{+}/^{+}$
H460	human lung cancer cell line	$^{+}/^{+}$
JVM-3	B-prolymphocytic leukaemia cell line	$^{+}/^{+}$
DOHH2	large B-cell lymphoma	$^{+}/^{+}$
KIS	large B-cell lymphoma	$^{+}/^{+}$

Table 2. 2: Reagents for cell culture

Reagent	Supplier	Product#
Dulbecco's Modified Eagle medium (DMEM) (high glucose, GlutaMAX™, pyruvate)	Gibco	61965-026
Foetal Bovine Serum (FBS)	Gibco	10500-064
Penicillin-streptomycin	Gibco	15140-122
Phosphate-buffered saline (PBS)	Gibco	20012-019
Trypsin-EDTA (0.05%, Phenol red)	Gibco	25300-054

2.1.2 Cell counting

A BIO-RAD automated machine counter) was used for counting viable cells. After mixing 10 µl of suspension cells with an equal amount of Trypan blue solution, an addition of 10 µl of the mixture to a counting slide (BIO-RAD, Cell counter Dual chamber) was performed. The slide was inserted into the machine, thereby automatically reading the quantity of the cells. Cells were counted every day. After cell counting, fresh media was added.

2.1.3 Treatment of cells

2.1.3.1 Cell treatment with DNA damaging agents: Doxorubicin

As an anthracycline antibiotic, Doxorubicin is capable of intercalating within the DNA double helix and inhibit macromolecules such as topoisomerase II (Capranco, et al. 1990). Doxorubicin hydrochloride (Sigma-Aldrich, #44583) was used in the DNA damage studies. The doxorubicin's concentration as well as the incubation duration varied depending on the cell and experiment and it ranged between 0.5 to 2 µM/ml (0.2 to 1 µg/ml). Treatment times were for 24 to 48 hours. A few experiments utilized Camptothecin (CPT) at 5 – 10 µM/ml for 24 -48 hours.

2.1.3.2 Cell treatment with Radiation

Cell irradiation was done using the Xstrahl RS320 X-Ray irradiator machine. The doses ranged between 10 and 15 grey. Upon completion, the cells were transferred back to the incubator for further conditioning for 24-48 hours, before further analysis was performed.

2.1.3.3 Cell treatment with ATRA

ATRA (Sigma-Aldrich, R2625) was used at a concentration of 1 - 2 µ M for 24 -48 hours.

2.2 Protein extraction and analysis

2.2.1 Whole cell lysate

After removing the medium, the plates were washed two times using 1x PBS and trypsinised. Pellets were collected and stored on ice then an addition of 1 µl of phosphatase Inhibitor (Sigma Aldrich), 1 µl of Protease Inhibitor Cocktail Set III (Calbiochem) and 100 µl of Radioimmunoprecipitation assay buffer (RIPA) (50 mM Tris HCl, 1% v/v NP40, 0.5% w/v SDS, 150 mM NaCl, 2 mM EDTA, 50 mM NaF, pH 7.4) was done. A 20-min incubation on ice followed. A syringe was used for rupturing the cells (5 times) followed by centrifugation at 12000 g for 5 minutes at 4°C. The supernatant was transferred to labelled tubes and 35 µl 4X loading buffer (8% w/v SDS, 20% v/v 2-mercaptoethanol, 40% v/v glycerol, 0.4% w/v bromophenol blue, 200 mM Tris HCl pH 6.8) was added to 100 µl of the sample. This was followed by boiling the sample at 95°C, and later cooling it at room temperature prior being spun and loaded into the SDS-Polyacrylamide gel. Alternatively, storing for future use was done at -80°C.

2.2.2 Cell Fractionation using sucrose gradients

Ice-cold PBS-MC (1x PBS, $MgCl_2$, 1 mM $CaCl_2$) was used to wash cells two times at 300xg for 5 min. 1 ml ice-cold Hypotonic buffer (RSB: 10 mM HEPES-KOH, 10 mM KCl, 1.5 mM, $MgCl_2$, pH 7.5) was used to re-suspend the cells, containing complete Protease Inhibitor Cocktail (EDTA), 10 mM NaF, 10 µM MG132, 1 mM activated Na_3VO_4 , 5 mM N-ethylmaleimide, for 10-minute. An ice-cold Dounce homogenizer was used for rupturing the cells. This was followed by centrifuging the homogenate at 500 x g for 10 min at 4°C. Sucrose Density Gradients (about 12 ml) for SW40 Ti Rotors were

produced by using an automated gradient maker. A 10-50% sucrose gradient was prepared. Buffer 1: 10 mM HEPES-KOH 10% (W/V) Sucrose, 1mM $MgCl_2$, pH 7.4; buffer 2: 10 mM HEPES-KOH, 1 mM $MgCl_2$, 50% (W/V) Sucrose, pH 7.4. After the sucrose gradients were incubated on ice for 10 minutes, the homogenate was loaded carefully on top of the gradient to minimize gradient disruption. This was followed by balancing and loading the tubes into SW40 Ti buckets and centrifugation them at 100,000x g for 18 hours at 4°C. This was followed by fractionating the sample into 24x 0.5 ml fractions. After transferring 50-100 µl to 96-well plate plus adding 30 µl of 4x Laemmli Sample Buffer, the sample was then loaded into a 10% polyacrylamide gel and protein detection was done as described in subsequent sections (2.2.4 – 2.2.7).

2.2.3 Handcasting polyacrylamide gels

Various percentages of polyacrylamide gels were used alongside 1.5 mm thickness Bio-Rad glass plates, depending on the target protein's size. Each gel comprised of resolving (bottom) and stacking (top) parts. To prepare the gel, 1 x 1.5 mm outer glass plate and 1 inner glass plate underwent thorough washing using ddH_2O and were subjected to air-drying before being washed with ethanol. A Mini-PROTEAN PAGE (polyacrylamide gel electrophoresis) system (Bio-Rad) with multi- casting chamber was used to assemble the glass pair. The first step involved preparing 15 ml resolving gel and instantly loading it into the mini gel unit, leaving some space for the stacking gel while being overlaid with distilled water, with solidification being achieved 30 minutes later.

After setting the gel, water was removed and an overlaying of the 3 ml stacking gel over the separating gel was done. This was instantly followed by insertion of a 1.5 mm comb gently, and given 30 minutes to set.

- This led to the preparation of 10 % 15 ml of resolving gel: 2.5 ml of 40 % Acrylamide mix, 4.8 ml of ddH_2O, 0.1 ml of 10% w/v SDS, 2.5 ml of 1.5M Tris (pH 8.8), 0.1 ml of 10% w/v Ammonium persulfate plus 4 µl of TEMED.

- Stacking gel (3 ml): 2.23 ml of ddH_2O, 380 µl of 1.0 M Tris (pH 6.8), 380 µl of 40 % Acrylamide mix, 30 µl of 10% w/v ammonium persulfate, 30 µl of SDS, plus 3 µl of TEMED.

2.2.4 SDS polyacrylamide gel electrophoresis

After placing the hand-cast gel in the electrophoresis cell, 500 ml 1x SDS-running buffer was added. Samples heated at 90-100°C were directly loaded using a pipette, together with µl protein ladder added to the first lane of the gel. A 1-hour electrophoresis was conducted to ensure that the proteins reached the gel's bottom section, primarily at 120 V, and later increased to 160 V after the samples reached the resolving gel. The electrophoresis process was terminated prior to the dye front leaving the gel.

- 10X Running buffer: 0.25 M Tris, 1.92 M Glycine, 1% w/v SDS

2.2.5 Western blot (WB)

A wet transfer system was used for Western blotting. A piece of nitrocellulose membrane (GE Healthcare Whatman, #11375334) was cut at the desired size. Assembling the transfer chamber was achieved in a tray using the appropriate quantity of 1X transfer buffer. The preparation of gel and membrane sandwich was achieved by placing one foam pad on the cassette holder's given side and one filter paper sheet used for covering purposes, followed by placing the gel with resolved proteins over it. This was followed by the addition of the nitrocellulose membrane on the gel while another filter paper sheet placed was over it and covered using another foam pad. Eventually, the cassette holder was secured and positioned inside the tank, thereby being immersed into 500 ml of 1x transfer buffer, with the contents of the tank being cooled by an ice block. The system was subjected to 100 V for an hour.

- 10X Transfer buffer: 0.25 M Tris, 1.92 M Glycine
- 1X Transfer buffer: 100 ml 10X transfer buffer, 700 ml ddH_2O, 200 ml Methanol

2.2.6 Protein detection

The membrane was immersed into 10 ml of blocking solution followed by 45 min incubation at room-temperature with gentle rocking.

- Washing buffer: 1X PBS, 0.1% v/v Tween (Sigma-Aldrich, # P2287)
- Blocking solution: 5% w/v Bovine Serum Albumin (Sigma-Aldrich, #A9418), 1X PBS, 0.1% v/v Tween

2.2.7 Immunological detection

This process involves primary and secondary antibodies. The initial stage was conducted with the blocked membrane using primary antibody (refer to Table 2.3), diluted to the required concentration in 10 ml blocking solution, using Sodium azide (NaN_3). The difference in incubation intervals was based on the antibody, but in general, the incubation time was 2 hours at room temperature or overnight at 4 °C on a shaker. Before addition of the secondary antibody, washing buffer was used to wash the membrane thrice for 10 minutes, rocking moderately at room temperature, to get rid of unbound antibody. The subsequent step involved incubating with 10 ml of matching secondary antibody (refer to Table 2.4), prepared in 3% w/v BSA, 1X PBS, and 0.1% v/v Tween. The incubation period lasted for 1 hour at room temperature while being gently rocked. For secondary fluorescence, the use of foil to cover the membrane was done to prevent light sensitivity. This was followed by washing the membrane using 10 ml of washing buffer 3X 10 minutes, rocking heavily to get rid of unbound secondary antibody. Incubating the membrane with chemiluminescent HRP Substrate (Millipore, #11556345) for 3 minutes on cling film was conducted to have the protein detected. After getting rid of the excessive reagent, a cling film was used for wrapping the membrane, which was then mounted on the upper face of the cassette. The autoradiography film (Thermo Scientific, #34099) development was used in detecting the membrane's chemiluminescent signal in the dark room. Alterantively, an Odyssey detection scanner was used in detecting the membrane upon analysing the image using Image Studio Software programme.

Table 2. 3: List of primary antibodies used

Name	Clonality	Source	Dilution	Company
p53 (DO-1)	Monoclonal	Mouse	1:1000	Santacruz
Stra6-C term (ab73490)	Polyclonal	Rabbit	1:500	Abcam
Stra6-C term (43200002)	Polyclonal	Rabbit	1:1000	NOVUS
Stra6-N term	Polyclonal	Rabbit	1:500	Abnova
Stra6 FL (D01P)	Polyclonal	Rabbit	1:500	Abnova
β-actin	Polyclonal	Rabbit	1:1000	Abcam
β-actin	Monoclonal	Mouse	1:500	Santacruz
Caspase 3	Polyclonal	Rabbit	1:1000	Cell Signaling
Caspase 9	Polyclonal	Rabbit	1:1000	Cell Signaling
PARP	Polyclonal	Rabbit	1:1000	Cell Signaling
BAX	Polyclonal	Rabbit	1:500	Abcam
JNK	Polyclonal	Rabbit	1:1000	Cell Signaling
P-JNK	Polyclonal	Rabbit	1:1000	Cell Signaling
P- γH2A.X (phospho S139)	Polyclonal	Rabbit	1:5000	Abcam
HNRNPK	Monoclonal	Mouse	1:1000	Sigma-Aldrich
PRX VI	Monoclonal	Mouse	1:1000	Santacruz
Lamin A+C	Polyclonal	Rabbit	1:500	LSBio
HMGB1	Polyclonal	Rabbit	1:500	GeneTex
Na^+/K^+ ATPase α	Polyclonal	Mouse	1:2000	Santacruz
HDAC-1	Polyclonal	Rabbit	1:1000	Abcam
MAPK	Polyclonal	Rabbit	1:2000	Cell Signaling
IgG	Monoclonal	Mouse	1:1000	Santacruz
GFP	Polyclonal	Rabbit	1:1000	Abcam

Table 2. 4: List of secondary antibodies used

Name	Dilution	Company
HRP-Mouse	1:5000	Bio-Rad
HRP-Rabbit	1:5000	Bio-Rad
IRDye-Anti-Mouse IgG (H+L)	1:5000	LI-COR
IRDye-Anti-Rabbit IgG (H+L)	1:5000	LI-COR

2.3 RNA isolation and qRT-PCR

2.3.1 RNA isolation

After seeding the cells into 6-well plates, transfection was done 24 hours later (as explained in 2.11.5) with some being treated using doxorubicin (as explained in 2.1.3.1) or ATRA (as explained in 2.1.3.2) or a combination of the two. Harvesting of the cells was done through trypsinization. Pellets were transferred to 1.5 ml microcentrifuge tubes. After being washed twice using 1X cold PBS, the cells were centrifuged at 3000 g at 4 °C for 5-minute. Besides being of RNA grade, all the equipment and chemicals during the RNA extraction were equally maintained free of RNAase. To have RNA extracted from the harvested cells, 1 ml of TRIzol Reagent (Sigma-Aldrich, #T9424) was used to re-suspend the pellet and later homogenized through pipetting. Before adding 200 µl (20 % of the starting TRIzol) of chloroform (Sigma-Aldrich, #C2432) an incubation period of 10 minutes was done at room temperature. After a vigorous shaking of the samples, they were subjected to 5-minute incubation at room temperature and 15-minutes centrifuging at 13000 g and 4 °C. Afterwards, transfer of the aqueous supernatant into a freshly clean microcentrifuge tube (RNase free) was done. RNA precipitation involved addition of 500 µl Isopropanol (half of the starting volume of TRIzol), (Sigma-Aldrich, # I9516) followed by centrifugation at 1300 g and 4 °C for 15 minutes. After removing the supernatant, the

RNA pellet was washed two times using 70% v/v ethanol, followed by another centrifugation at 8000 g and 4 °C for 10 minutes. Upon getting rid of the supernatant, the pellet was subjected to air-drying for about 5-10 minutes. 30 µl of RNase-free water was used in re-dissolving the pellet. After nucleic acids were quantified using Nanodrop ND-8000 (Thermo Scientific), the samples were stored at -80 °C awaiting the subsequent phase.

2.3.2 cDNA synthesis

Preparation of cDNA was achieved from purified RNA by using a First-Strand cDNA Synthesis Kit (GE Healthcare Life Science, #27-9261-01). All samples underwent mixing of 1 µg of purified RNA with an appropriate quantity of RNase-free ddH_2O up to a volume of 30 µl, then heating the samples at 65°C for a 10-minutes in a heat-block and instantly undergoing ice cooling for 2 minutes. During the reaction involving the reverse transcription, the RNA solution was mixed with first-strand reaction fused beads (buffer, dGTP, dATP, dTTP, dCTP, reverse transcriptase, RNase/DNase-free BSA, as well as RNAguard™, mixed with RNase-free ddH_2O and 5 µg Oligo(dT) primer (Invitrogen, #18418-012) to attain a total volume of 33µl. The subsequent phase was to mix the reaction gently through vortexing and having it spun for a short duration and eventually undergoing 1-hour incubation at 37 °C in a regulated incubator. Storage of the sample for future use was then done at -20 °C.

2.3.3 Quantitative Real-time PCR (qRT-PCR)

As shown in table 2.5, the design of primers was done for the comparative quantification of gene expression. The target gene expression was normalized by using GAPDH or β-Actin as an endogenous control gene. To come up with the reaction mix, various ingredients were used, including 10 µl 2x sensimix SYBR NO-ROX master mix (Bioline, #QT650-02), 2 µl of diluted cDNA (1:10 with ddH_2O), 20X primer mix (200-400 nM), as well as ddH_2O. Each sample was done in triplicate. The subsequent phase included mixing and centrifuging the samples lightly, while the reactions were done on Corbett Life Science-Rotor-Gene 6000 by engaging these thermal cycling parameters: 10-minute enzyme activation “hold” at 95 °C, succeeded by 15-seconds 50 cycles denaturation at 95 °C as well as 60-seconds elongation/annealing at 60 °C. PCR analysis

resulted in a melting curve utilized in verifying the primers' specificity. Analysis of the data was done through viewing the amplification plots, while setting both baseline and threshold values. The final procedure involved a manual comparative quantification analysis, in addition to a relative expression value founded on the comparative C_t calculations as shown below.

[delta] $C_{t,\ sample} = C_{t,\ sample} - C_{t,\ GAPDH}$

[delta][delta] C_t = [delta] $C_{t,\ sample}$ - [delta] $C_{t,\ reference}$

Table 2. 5: List of primers used for qRT-PCR

Gene	Forward 5' - 3'	Reverse 5' - 3'	Supplier
Stra6	TCCTGCCTACCATCCTCCT	AGACAGACCTCCACCCAAC	Eurofins
RARα	GGGCAAATACACTACGAACAAC	GGCGAACTCCACAGTCTTAAT	Primer Design
RARβ	GCCTTACCCTAAATCGAACTCA	GCCTGTTTCTGTGTCATCCAT	Primer Design
β-actin	GCGGGAAATCGTGCGTGACA	AAGGAAGGCTGGAAGAGTGC	Primer Design
GAPDH	TCTCTGCTCCTCCTGTTC	GCCCAATACGACCAAATGC	Eurofins

2.4 Flow Cytometry

Being a laser-based technology, flow cytometry enables the detection of diverse features of singles particles within a fluid as it flows via the laser beam one by one. Flow cytometry is able to identify various cell qualities like its relative size, internal granularity, or complexity as well as fluorescence intensity, which are established through recording the cell's scattering of incident laser light to emit fluorescence. Its extensive application lies within the identification and definition of various cell populations and equally expression of cell surface and intracellular molecules. Cells passing via the beam will have the light detected scattered as either side scatter which

is proportionate to cellular density or forward scatter which associates with size or inner complexity, that is, nucleus shape, granularity, etc. Flow cytometry is equally capable of detecting the DNA fluorescence (via PI staining) and apoptosis (via annexin V staining).

2.4.1 Propidium Iodide

Propidium Iodide (PI) is a fluorescent molecule capable of intercalating into nucleic acids. Upon binding to DNA and excited with a wavelength light of 488 nm, it is able to fluoresce red. To examine the cell death percentage, a Propidium Iodide staining followed by a FACS analysis was typically conducted in this study. After splitting the cells into 6-well plates, a timeframe of 24 hours was given prior commencing the treatment. The samples were equally duplicated while each sample's media was aspirated and gathered in 15-ml labelled falcon tubes. An amount of 2 ml of 1x PBS was used for washing the cells and was retained in the media tube. The process of collecting the cells in media tubes and 1x PBS was initiated after adding 1 ml of trypsin. This was followed by centrifuging the tubes at 200g for 5 min and eventually washing of the pellet two times, using 1x PBS. A mixture of the pellet and 1 ml of 70 % ethanol was prepared and placed at -20 °C at minimum 30 minutes. After taking the cells out of the freezer, they were centrifuged at 200g for duration of 5 minutes. This was followed by washing the cells once using 1 ml of 1x PBS. The pellet was again suspended in 300 µl of PI buffer: 10 µg/ml RNase A, 50 µg/ml of Propidium Iodide, 1× PBS, and shifted to polystyrene round-bottom tubes. This was followed by incubating the tubes at 37 °C in the dark for half an hour. Beckton Dickinson FACSCanto II and FACSDiva 6.0 software were used for recording 10,000 events for each sample for analysis and acquisition purposes.

2.4.2 Annexin V

Floating and adherent cells were gathered and washed using 1x binding buffer without fixation. This was followed by the re-suspension of cells at $1x10^6$ cells/ml in 1x binding buffer. On average, an addition of 0.5 µl of annexin V- FITC was considered for each 1 ml of 1x binding buffer (1:2000). After that, incubation of the mixture was done for 15

minutes at room temperature in dark. This prepared the samples ready for reading with FACS.

- Annexin binding buffer 5x: 50 mM HEPES, 750 mM NaCl, 5 mM $MgCl_2$, 9 mM $CaCl_2$, pH 7.4.

2.5 Measurement of intracellular oxidation

Cell permeable fluorescent dyes are among the extensively used methods for assessing oxidative stress, with 2'-7'-dichlorodihydrofluorescein diacetate (H_2DCFDA) being considered a significant fluoregenic reagent to establish reactive oxygen intermediates in cells. When subjected to oxygen presence, H_2DCFDA changes to heavily green fluorescent 2'-7'-dichlorodihydrofluorescein.

2.5.1 DCF Staining

DMSO was used to dilute 10 mg/ml stocks of H_2DCFDA (Biotium) initially prepared afresh prior utilizing it with minimal exposure to the air. This was followed by directly adding H_2DCFDA to the plate, by taking into consideration 0.5 µl of diluted H_2DCFDA per ml of the eventual medium (H_2DCFDA concentration 5 mg/ml). After that, all the samples underwent 30-minutes incubation in the dark at 37 °C, 5% CO_2. After being trypsinised, the cells were collected. After re-suspending the cell pellet in 500 µl sterile PBS, the cell pellet was moved to FACS tubes and shielded from light. ROS levels were examined instantly by flow cytometry for stimulation and emission wavelengths for the green (FITC) channel as well as ensuring the samples are maintained at 4 °C until analysis. Finally, a diagram of MFI (mean fluorescence intensity) values was plotted.

2.5.2 Using NAC and GSH to inhibit ROS generation

Treatment with antioxidants involved exposing the cells to 2 µM Glutathione (GSH) or 10 mM of N-acetyl-L-cysteine (NAC) for 16 hours. After that, DCF staining was used to estimate ROS as explained in section (2.5.1) or protein was extracted, followed by the analysis of protein lysate via western blot as explained in section 2.2.

2.6 MTS cell viability assay

CellTiter-Glo Reagent (Promega, #G7571) was used to estimate cell viability. After seeding cells into 96-well plates (with each well's density being 25 X 10^4), a growth period of 24 hours was allowed. A number of wells containing medium without cells

were used as a negative control. Subsequent to 24 hours of growth, cells were treated and allowed to grow for 24 hours within a humidified 5% CO_2 atmosphere at 37°C. On the next day, 20 µl of CellTiter-Glo Reagent was added to each well, with the plate being covered firmly using an aluminium foil and later undergoing a 2-6-hour incubation at 37°C. Subsequent to incubation, an Infinite F50 Robotic Absorbance microplate reader (Tecan) was used to measure absorbance at 490 nm.

2.7 Immunoprecipitation (IP)

After blocking 25 µl of protein A Sepharose beads (GE Healthcare) with 40 µl of 5% w/v BSA, incubation was done overnight at 4 °C in the rotator. Later, the extract solution (protein lysate) was mixed with 1 µg of the appropriate antibody followed by an overnight incubation in the rotator at 4 °C. The next blocked beads were incubated with the extract (Ab with protein lysate) with a 3-hours incubation following at 4 °C while in a rotary state. This was followed by spinning the tubes down for 3 minutes at 2000 g and 4 °C. After that, the supernatant (SN, equally identified as FT (flow through)) was removed and stored in a different tube at -80 °C. Resuspension of the antibody-beads complex was done using 500 µl of washing buffer followed by 5-minutes incubation at 4 °C on the rotary wheel, and later spinning it for 3 minutes at 2000 g and 4 °C. Resuspension of the antibody-beads complex was done once more in 500 µl of washing buffer two times. This was followed by IP elution through addition of 4x SDS loading buffer (Laemmli). After that, the samples were boiled for 5 minutes to achieve boiling point at 95 °C. This made the samples ready for loading as well as being run on 10 % SDS-PAGE electrophoresis. The next step included staining the gel with Instant Commasiee Blue stain while excising the bands from the gel to transfer it for mass spectrometry analysis. The PNACL (protein and nucleic acid lab) at the University of Leicester provided the protein identification process. The gel issued at PNACL was trypsin digested while the peptides were established by the use of LC-MS/MS.

- Wash buffer: 20 mM Tris-HCl pH 8.0, 120 mM NaCl, 0.5% w/v NP40 (Sigma-Aldrich, #NP40S)
- IP buffer: 20 mM Tris-HCl pH 8.0, 120 mM NaCl, 0.5% v/v NP40 (Sigma-Aldrich, #NP40S), 1 % v/v protease inhibitor (Sigma-Aldrich, #S8820) ,1 mM PMSF.

2.8 Mass spectrometry

After cutting the gel lanes into slices of about 1.5 mm, they were transferred to a 96 well low binding PCR plate. After washing each slice using ammonia bicarbonate (80 µl, 50 mM) for 30 minutes, buffer aspiration was done. Before getting rid of the solvent, acetonitrile (80 µl) was used to de-stain each slice for 30 mins. After the aspiration of acetonitrile, an addition of trypsin (Promega, sequencing grade modified trypsin V5111, 20 µg / 1.8 ml 25 mM ammonium bicarbonate, 15 µl) was done to each of the dehydrated pieces of gel. After sealing the plate, it was heated overnight at 30 °C. Once the sealing film was removed, the extraction buffer was added to each well (80 µl, 97% TFA (0.2 %) 3% v/v acetonitrile). Extraction of the samples was done for 1 hour at room temperature. After extraction, the samples were moved into low-binding Eppendorf tubes and dried in a speed vac. An injection of solvent (40 µl, 5% v/v Trifluoroacetic acid - TFA) was used in re-dissolving the samples and then samples were analysed through mass spectrometry (Shevchenko et al., 2006). Separation of complex peptide fusions was achieved through Nanoscale LC by the use of Waters nanoACQUITY UPLC. Chromatography was conducted using a 50-mins reversed-phase gradient (formic acid (0.1 %) / acetonitrile) as well as a 75 µm x 25 cm C-18 column (Waters, BE130) functioning at 300 nL/min. A SYNAPT G2S (Waters Manchester UK) was used in performing Mass spectrometry analysis operating in a data-independent (MSE) manner. The chosen analysis method allowed a simultaneous analysis of the precursor and fragment ions from the tryptic digest peptides. Processing and acquisition of the resulting data was done with ProteinLynx Global Server (Waters) while Scaffold (Proteome Software, Oregon, USA) was used in the visualization and re-analysis.

2.9 Protein-Protein Interactions (PPI) using Co-immunoprecipitation (Co-IP)

After splitting the cells into 100 mm plates, cells were treated and/or transfected as described. Washing of the cells was done twice using 2 ml of 1X PBS, upon aspirating the media and eventually cells were collected by scraping and stored in 15 ml tubes. Upon centrifuging the tubes for 5 minutes at 1100 g and 4 °C, the pellet was stored at -

80 °C for immunoprecipitation. Before immunoprecipitation, re-suspension of the pellet in 1 ml of binding buffer 1 was done through pipetting and later undergoing ice-incubation for 30 minutes while gently mixing occasionally. An hour prior use, pre-chilling of the Diagenode Bioruptor 2000 water bath was done using ice to prevent water from heating too fast as a result of thermal inertia, while keeping the water bath cold using ice during the process of sonication.

Upon setting the sonicator at optimum power (30 seconds on and 30 seconds off), it was operated for half an hour, with three intervals (3x) with each running 10 minutes. This was followed by spinning the samples at 13000 g at 4 °C for 15 minutes after being transferred to a new tube. Transferring the supernatant to another microcentrifuge tube was the next step with a 10 % aliquot at -80°C being considered for input. Dilution of the residue extract was done using 300 µl Buffer 2. After diluting the extract, it was sub-divided into two microcentrifuge tubes; with one being utilized for IP by having 1 µg of antibody added against the protein of interest. The other tube was utilized as a negative control by having 1 µg of normal mouse IgG added. Preparation and washing of 2 tubes having 20 µl of packed beads (GE Healthcare) was done using 1 ml of Buffer 3 for three times, and 40 µl of 5% w/v BSA was added to have the beads pre-blocked. Finally, incubation of the tubes was done at 4 °C overnight on the rotating wheel.

On the following day, the mixture of beads and BSA underwent incubation using the supernatant/antibody, and later rotated at 4 °C for 3 hours. This was followed by having the beads centrifuged at 2000 g and 4 °C for 3 mins, while the supernatant was aspirated off. After having the beads washed three times using 1 ml Buffer 1, with each wash lasting for 5 minutes at 4 °C and being rotated, they were later subjected to a spinning phase at 2000 g and 4 °C for 3 minutes and eventually the supernatant removed. The inputs were thawed after re-suspending the beads in 40 µl of 1X PBS. This was followed by an addition of an appropriate amount of 4X SDS (Laemmli) to IP, input samples and negative control, while having the samples denatured through exposing them to 95 °C of heat for 5 minutes. Subsequent to that, protein analysis was done, as explained in 2.2.5.

- Buffer 1: PBS, 50 mM NaCl, 1 % v/v NP-40 (Sigma-Aldrich, #NP40S), 1 mM PMSF.
- Buffer 2: PBS, 50 mM NaCl, 1 mM PMSF, 1 % v/v Protease Inhibitors (Sigma-Aldrich, #S8820).
- Buffer 3: PBS, 50 mM NaCl, 0.2 % v/v NP-40, 1 mM PMSF.

2.10 Immunofluorescence imaging and confocal microscopy

Cells were split into 6-well plates with sterile glass coverslips (Thermo Scientific Nunc, #EW-48510-10) and they were let to grow in humidified 5 % CO_2 atmosphere at 37 °C incubator. Transfection of the cells was done in accordance with the above description using 4 µg of plasmids. 24 hours after treatment, aspiration of media from the plates was done with the cells being washed thrice using ice-cold Ca_2^+ and Mg_2^+ free 1x PBS. Fixing of the cells was done using either 1 ml of 3.7 % (v/v) formaldehyde at room temperature for 20 mins or ice-cold 100 % methanol for 30 minutes at 4 °C while shaking them lightly. Subsequent to fixing, washing of the cells was done thrice using ice-cold Ca_2^+ and Mg_2^+ free 1x PBS and permeabilized with ice-cold 1 ml 0.1 % Triton X-100 for 12 minutes. Furthermore, ice-cold Ca_2^+ and Mg_2^+ free 1x PBS was used for washing the cells 3 times and blocked using 3 % (w/v) BSA for 20 minutes. Incubation of the coverslips was done using 100 µl of 1:100 primary antibodies overnight at 4 °C. the next day entailed washing the coverslips thrice using ice-cold Ca_2^+ and Mg_2^+ free 1 x PBS with incubation being done using 100 µl of 1:400 secondary anti-rabbit (Alexa Fluor 488, Invitrogen) for 45 mins in the dark. Subsequent to incubation, washing of the coverslips was done using ice-cold Ca_2^+ and Mg_2^+ free 1x PBS. Cell nuclei were stained using 1 ml diluted to 1:1000 of 40, 6-diamidino-2-phenylindole, dihydrochloride (DAPI, Invitrogen) for 10 mins at room temperature in dark. Labelling of the slides (Thermo Scientific, #EW-01839-08) was done while adding 6 µl of Fluoromount TM aqueous mounting medium (Sigma Aldrich, #F4680) on each slide. After having the slides labelled, mounting of the coverslips was done, followed by sealing using transparent nail varnish. The reason behind letting the slides dry in the dark was to have the coverslip secured in place besides having them stored at 4 °C until examination. Confocal microscopy was used in the analysis of the slides.

A Leica TCS SP5 confocal laser-scanning microscope (63X oil objective) was used for viewing the slides for confocal microscopy, while LAS-AF software was considered in the analysis. The z-axis images were captured every 0.4 µm to entirely cover the cell's thickness. An argon laser line 488 nm was considered in exciting the DyLight 488 while the emissions were gathered between 500 and 590 nm. The diode laser line 405 nm was utilized in exciting DAPI with the emissions being gathered between 415-480 nm. Furthermore, 594 nm laser line was used in exciting Red mCherry while the emissions collected between 605-700nm.

2.11 Plasmids preparation and transfection

2.11.1 Bacterial transformation

As described in Table 2.6, bacterial transformation with different plasmids was done for either overexpression of the anticipated protein or DNA preparation by mini- and midiprep. For the purposes of obtaining sufficient plasmids for cell transfection, the plasmids growth was done using Stellar Competent Cells (Clontech) typically considered an E. coli-HST08 strain with the capacity to offer high transformation efficacy. After placing bacterial cells (50 µl of in an Eppendorf) on ice to thaw, an addition of 1 µl of plasmid was done. After incubating the mixture on ice for about 15-30 minutes, a heat block was used to achieve a heat shock at 42°C for 1-2 minutes to induce the plasmid DNA uptake. The subsequent step involved immediately returning the mixture on ice while incubating it for 5 minutes and adding 100 µl of S.O.C media to each tube under sterile conditions. With the transformation mix being left for 30 minutes at 37 °C, shaking was equally done at 200 g. Spreading of the cells onto LB agar plates supplemented using the appropriate antibiotic was done at a concentration of 100 µg/ml in agar plate and under sterile condition. After inverting these plates, they were left overnight approximately for 16 hours at 37 °C in a regulated incubator for growth purposes.

2.11.2 Isolation of plasmid DNA by DNA midiprep

Midipreps were considered due to the requirement of large quantity of ultrapure plasmid DNA for the cell transfection. Just as mentioned earlier, an addition of Plasmid

DNA (1 µl) was done on top of efficient competent cells (50 µl). On the following day, one colony from the plate was taken and mixed with 3 ml of LB broth (Sigma-Aldrich, #L3022) complemented with the preferred antibiotic (100 µg/ml) and eventually undergoing a 6 hours incubation at 37 °C while shaking at 200 g. This was followed by inoculating 100 ml of LB in a conical flask supplemented with 100 µg/ml of the preferred antibiotic with 100 µl of the bacterial colony, later incubated 37 °C and agitated at 200 g. Harvesting procedure included centrifuging the cells at 6000g and 4 °C for 20 minutes. A QIAGEN plasmid midi kit (Qiagen, #12143) was used to isolate the plasmid DNA in accordance with the manufacturer's directions. This was followed by eluting the DNA using 500 µl of sterile ddH_2O while nano-drop spectrophotometer being used in the quantification process. Plasmids were stored at -20 °C until further use.

2.11.3 Primer design for plasmid

Primer design was done for various with tags on N terminus or C terminus region. Table 2.6 summarizes the vectors and primers utilized.

Upon preparation of the plasmids, sequencing was performed to guarantee the readiness and efficacy of the plasmids for future use. The University of Leicester was the venue for all vectors cloning work, done by PROTEX group, particularly thanks to Dr. Xiaowen Yang's efforts, support and advice concerning vector selection and primer design.

2.11.4 PCR amplification from plasmid

After preparing the PCR mix including 10 µl 2x sensimix SYBR NO-ROX master mix (Bioline, #QT650-02), 2 µl of diluted cDNA (1:10 with ddH_2O), 20X primer mix (200-400 nM), as well as ddH_2O, proof reading DNA-no Taq, also known as Velocity DNA Polymerase, was used. In accordance with PCR cycling and manufacturer protocol, we loaded the samples' end products on 1.0 % gel electrophoresis.

Preparation method for the gel involved combining 1 g of agarose powder with 100 mL of 1X TAE buffer followed by storing it in the tank with the required amount of 1X TAE buffer. The first well was fed with 5µl DNA marker (1kb Gene Ruler DNA ladder plus,

Biolab) and 25 µl from each DNA sample being loaded to each well using 6X DNA-loading dye (Fermentaz). Eventually, the gel was run at 105 V for 1 hour. This was followed by extraction of DNA from agarose gel through Qiaquick gel extraction kit while the quantification of the concentration done by the use of a nano-drop spectrophotometer. The needed DNA template from (PCR) to be delivered to PROTEX was 50 ng/µl.

- 50X TAE: 242 g Tris, 57.1 mL glacial acetic acid, and 20.81 g EDTA dissolved in 1L ddH_2O

2.11.5 Plasmid transfection

Turbofect^{TM} transfection reagent (Thermo Scientific, # R0531) was used in the cells' transfection using various plasmids. A day prior transfection, cell seeding was done to ensure about 70 % confluence during the transfection day. 6.0 µg of DNA plasmid were diluted in 600 µl of Opti-MEM low serum medium (Gibco, #31985-047) for each 60 mm plate, using a sterile tube with the solution being mixed lightly and incubated for minutes. After adding 12.0 µl of Turbofect^{TM} transfection reagent to the DNA/Opti-MEM mixture, pipetting was done upon mixing and later subjected to 20 minutes incubation at room temperature for the purposes of complexes formation. The next phase involved adding the mixture gently drop by drop to the plated cells. After shaking, the cells were stored within a humidified 5 % CO_2 atmosphere at 37 °C. The plates considered varied in size while volume of plasmid and Turbofect^{TM} transfection reagent were scaled down as expected.

Table 2.6: Plasmids used in experiments

Name	**Insert name**	**Vector**	**primer**
Stra6	Stra6 (FL)	pLEICS-12	F-5'-ACCCAAGCTTGGTACCATGTCGTCCCAGCCAGCA-3' R-5'-GACGGAGCTCGAATTTCATCAGGGCTGGGCACCATT-3'
Stra6-C-EGFP	Stra6 (FL)	pLEICS-29	F-5'-TAGCGCTACCGGACTCAGATCTCGAGATGTCGTCCCAGCCAGCA-3' R-5'-CTGAAAATACAGGTTCTCGAGGGGCTGGGCACCATT-3'
Stra6-Sm Sm=Small-C	C term	pLEICS-12	F-5'-ACCCAAGCTTGGTACCAGTCCTCGTGGCCCTTCT-3' R-5'-GACGGAGCTCGAATTTCACTGAGGCTGTCCTGG-3'
Stra6-Sm-C-EGFP	C term	pLEICS-29	F-5'- TAGCGCTACCGGACTCAGATCTCGAGATGAGTCCTCGTGGCCCTTCT-3' R-5'-CTGAAAATACAGGTTCTCGAGCTGAGGCTGTCCTGG-3'
Stra6-N-EGFP	Stra6 (FL)	pLEICS-21	F-5'-AAAACCTGTATTTTCAGGGCGCCTCGTCCCAGCCAGCA-3' R-5'-TACCGTCGACTGCAGAATTTCAGGGCTGGGCACCATT-3'
Stra6-N-mcherry	Stra6 (FL)	pLEICS-23	F-5'-AAAACCTGTATTTTCAGGGCGCCTCGTCCCAGCCAGCA-3' R-5'-TACCGTCGACTGCAGAATTTCAGGGCTGGGCACCATT-3'

2.12 Software programme

2.12.1 Phosphorylation prediction of Stra6

Potential phosphorylation sites of Stra6 with advanced bioinformatics software tools, using the NetPhos 2.0 software.

http://www.cbs.dtu.dk/services/NetPhos/

Sequence- and structure-based prediction of eukaryotic protein phosphorylation sites. Blom, N., Gammeltoft, S., and Brunak, S. Journal of Molecular Biology: 294(5): 1351-1362, 1999.

2.12.2 Proteases cleavage prediction of Stra6

Expected proteases that would play a role in Stra6 cleavage was analysed using the MEROPS database and this work was done kindly by Dr. J. Villa (Universitat de Vic, Spain).

http://merops.sanger.ac.uk

Rawlings, N.D., Barrett, A.J. & Finn, R.D. (2016) Twenty years of the MEROPS database of proteolytic enzymes, their substrates and inhibitors. Nucleic Acids Res 44, D343-D350.

2.13 Statistical analysis

All the trials were replicated in a triplicate or more, with the resulting data being conveyed as means ± standard deviations. Prism software (GraphPad 6 version 6, California, USA) was used in Statistical analysis procedure. One-way ANOVA (breakdown of variance of means) was used to determine statistical significance by comparing more than 3 data sets, with comparison of the two data sets being done through unpaired t-test analysis. The significant variations between multiple sets of data were further achieved with Tukey's multiple comparison post analysis ($p < 0.05$ was regarded statistically significant and underscored with an asterix (*).

3 Characterising the novel function of Stra6

3.1 Introduction

Stra6's function is to facilitate retinol uptake from RBP as its specific receptor. Stra6 has been classified not only as a transporter for vitamin A, but also as a unique protein with no similar homology to any known ion channels, receptors, transporters and cell signalling proteins that have been identified. However, Carrera et al. in (2013) proposes that Stra6 has an additional, novel function as a new member in the p53 cell death signalling pathway.

Though Carrera et al. (2013) proposed a new function of Stra6, research has not yet fully addressed the role of Stra6 in the p53 signalling pathway. Therefore, the purpose of the current study is to address this research gap and to investigate how retinoid treatment, via the induction of Stra6, would have impact on the p53 signalling pathway towards cell death. In particular, this study aims to define the link between retinoid signalling and p53 signalling pathways through Stra6. Moreover, this study investigates how retinoids can be used in combination with DNA damaging agents, which should upregulate Stra6 at both transcriptional and transitional levels. This study also considers the role of Stra6 in such treatments, thus determining how ATRA-Stra6-p53 operate together and provides a comprehensive understanding of the underlying mechanism of combinational therapy for successfully treating cancer.

3.2 *In vitro* up regulation of Stra6 by ATRA to sensitise cancer cells to DNA damaging agents

3.2.1 Determining the mRNA levels of Stra6 and retinoic acid receptors in response to different stimuli

To evaluate the levels of induction of Stra6 and the nuclear retinoic acid receptors (RARα & RARβ) upon ATRA stimulation compared to DNA damage agents, the mRNA expression was quantified using qRT-PCR. This experiment was conducted on several different cell lines that all have WT p53. EJp53, a

human bladder cancer cell line that comprises a tetracycline (tet)-off inducible p53 expression system (Sugrue et al., 1997), was used to control the expression of p53 by removal of the tet from the culture media. EJp53 cells were cultured with tet with or without an ATRA treatment of 1 μM for 24 hours. Alternatively, tet was removed from the media for two days to get a sufficient induction of p53, and cells were treated with a similar concentration of ATRA 1 μM for 24 hours. Cells were then collected and RNA was isolated to be used for cDNA synthesis. The qRT-PCR analysis was performed with specified designed primers for Stra6, RARα and RARβ. The obtained C_t values were normalised against GAPDH and against the C_t value of the control to calculate the mRNA fold change.

Following p53 induction by tet removal and ATRA treatment, a significant increase in the Stra6 mRNA levels was observed. These levels were one hundred times the Stra6 mRNA levels of induction through ATRA treated cells with a similar dose and by p53 expression alone, which had previously demonstrated a low level of Stra6 mRNA upregulation (Figure 3.1). Moreover, cells treated with ATRA alone demonstrated a greater tendency to upregulate RARβ than the cells treated with ATRA after p53 induction, which produce more RARα than RARβ upregulation. These results suggest that the combined ATRA treatment with p53 dependent induction produces more significant Stra6 upregulation compared to each treatment on its own, but this does not correlate with RAR induction.

The study continued by examining a more physiological induction of p53 expression, i.e. after DNA damage using doxorubicin (Dox). The cell lines used were the human colon cancer cell line (HCT116), the human bone osteosarcoma epithelial cells (U2OS) and human chronic B cell leukaemia, also known as B-prolymphocytic leukaemia cell line (JVM-3). Each of these cell lines was treated in similar experimental conditions. As shown in Figure 3.2 A, B and C, Stra6 mRNA levels increased significantly after the cells were pre-sensitised with 1 μM of ATRA and incubated with 1.4 μM of Dox for 24 hours,

compared to other treatments. RARs upregulation showed that the arrangement of different RARs depends on the treatment protocol pattern similar to that presented in Figure 3.1.

3.2.2 Determining the protein levels of Stra6 and p53

Next, we determined Stra6 and p53 protein levels in response to ATRA and DNA damage in a wide range of cell lines. This information was then used to correlate the upregulation status of Stra6 to its transcriptional level. p53 induction by tet removal, p53 physiological induction using Dox or radiation or treatment of cells with ATRA were used. Prior to WB analysis, each cell line was classified into two groups based on its origin. The first group was comprised of solid tumour cell lines including EJp53 (human bladder cancer cell line), HCT116 (human colon cancer cell line), U2OS (human bone osteosarcoma epithelial cells), MCF-7 (human breast cancer cell line), PA-1 (human ovarian carcinoma cell line), and H460 (human lung cancer cell line). The other group included blood leukaemia and lymphoma cell lines including JVM-3 (B-prolymphocytic leukaemia cell line) as well as KIS and D0HH2 (large B-cell lymphoma) cell lines.

EJp53 cells constituted the experimental model cell line for this study. Tet was removed from the media for 48 hours to induce p53 expression or tet was kept in the media to suppress p53 induction. Additionally, cells were treated with 1 µM of ATRA for 24 hours with or without tet regulation. Total protein lysates were prepared to perform WB. Figure 3.3A confirms a previous result found by Carrera et al. (2013), which demonstrates that under DNA damage, which is comparable to tet removal to induce p53 expression, that Stra6 induction was combined by p53 induction and it was only dependent on WT-p53 cell status. We observed that p53 protein levels after tet is removed is upregulated significantly after ATRA treatment (Figure 3.3B).

EJp53

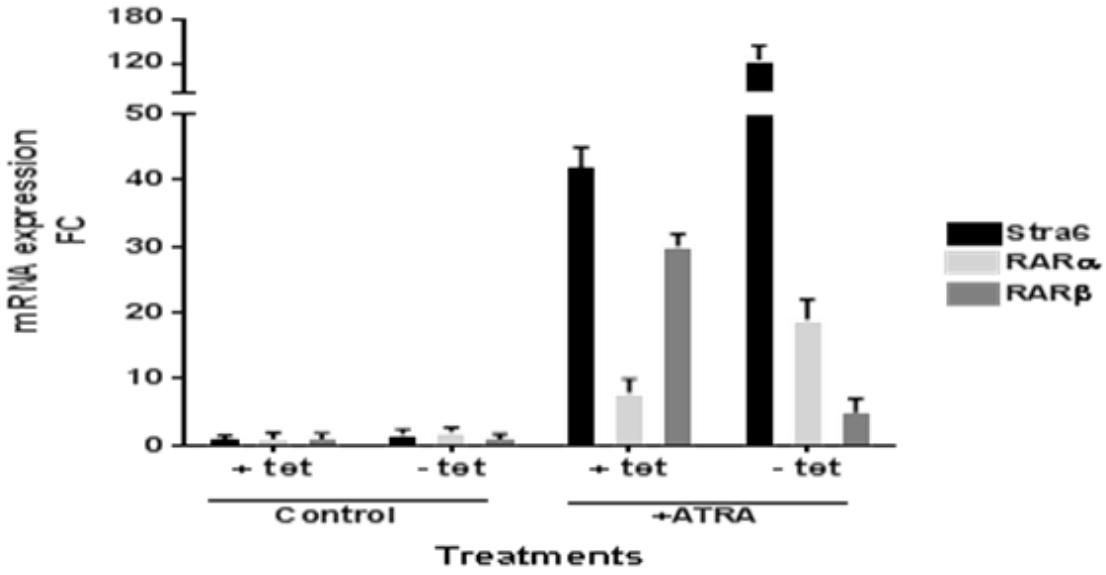

Figure 3.1: **Up-regulation of Stra6 and retinoic acid receptors (α and β) mRNA levels in EJp53 cells.** RNA was isolated from EJp53 cells under the control of tet and after tet removal to induce p53 expression for 48 hours. 1 µM of ATRA for 24-hr was also used. Data are expressed as a fold change compared to the control, are normalised to GAPDH as a loading control and represent the mean ± SD of three independent experiments.

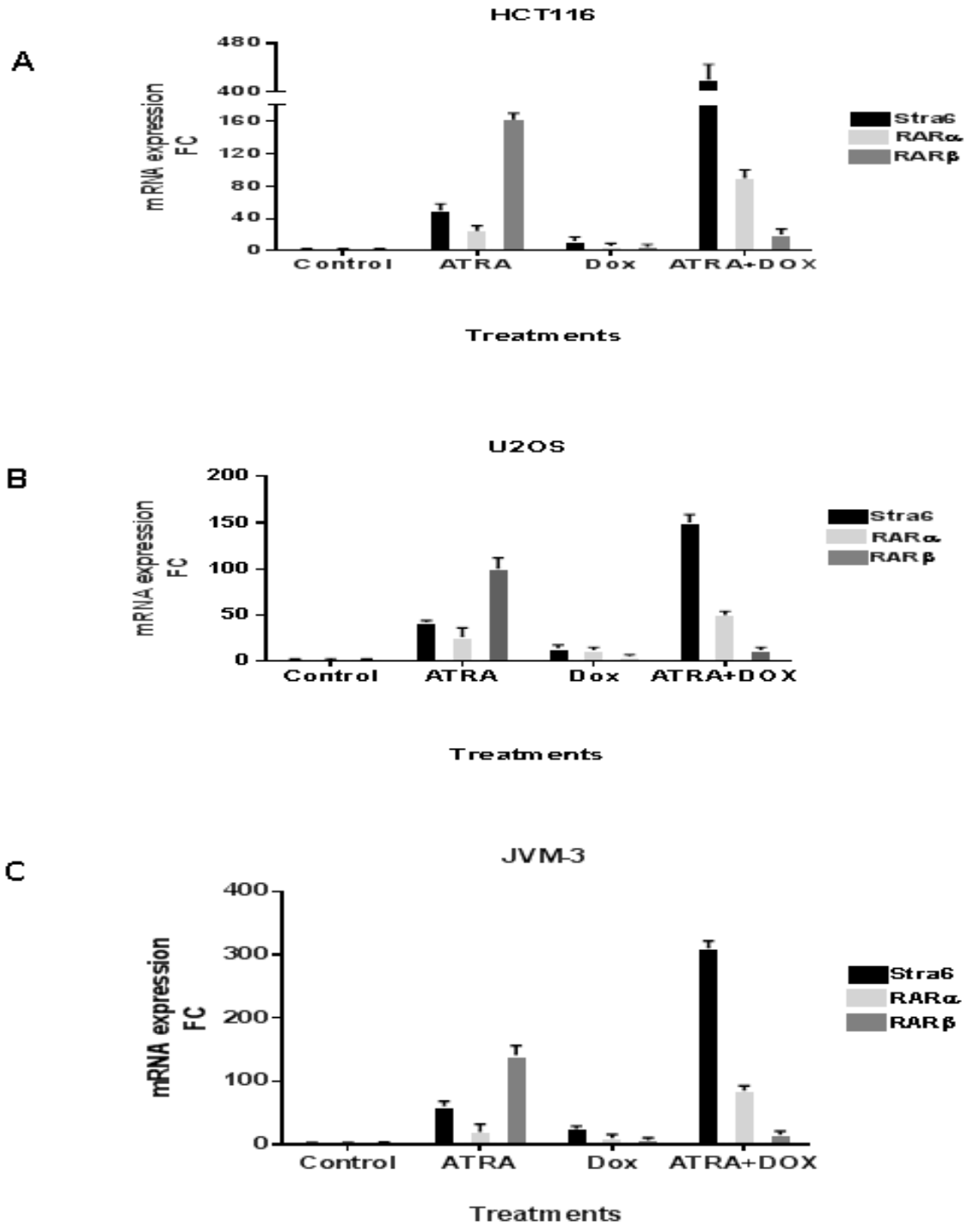

Figure 3.2: **Up-regulation of Stra6 and retinoic acid receptors (α and β) mRNA levels.** RNA was isolated from **(A)** HCT116 WT p53 cells, **(B)** U2OS WT p53 cells and **(C)** JVM-3 cells treated with 1 µM of ATRA and/or 1.4 µM of Dox for 24-hr. Data are expressed as a fold change compared to the control, are normalised to GAPDH as a loading control and represent the mean ± SD of three independent experiments.

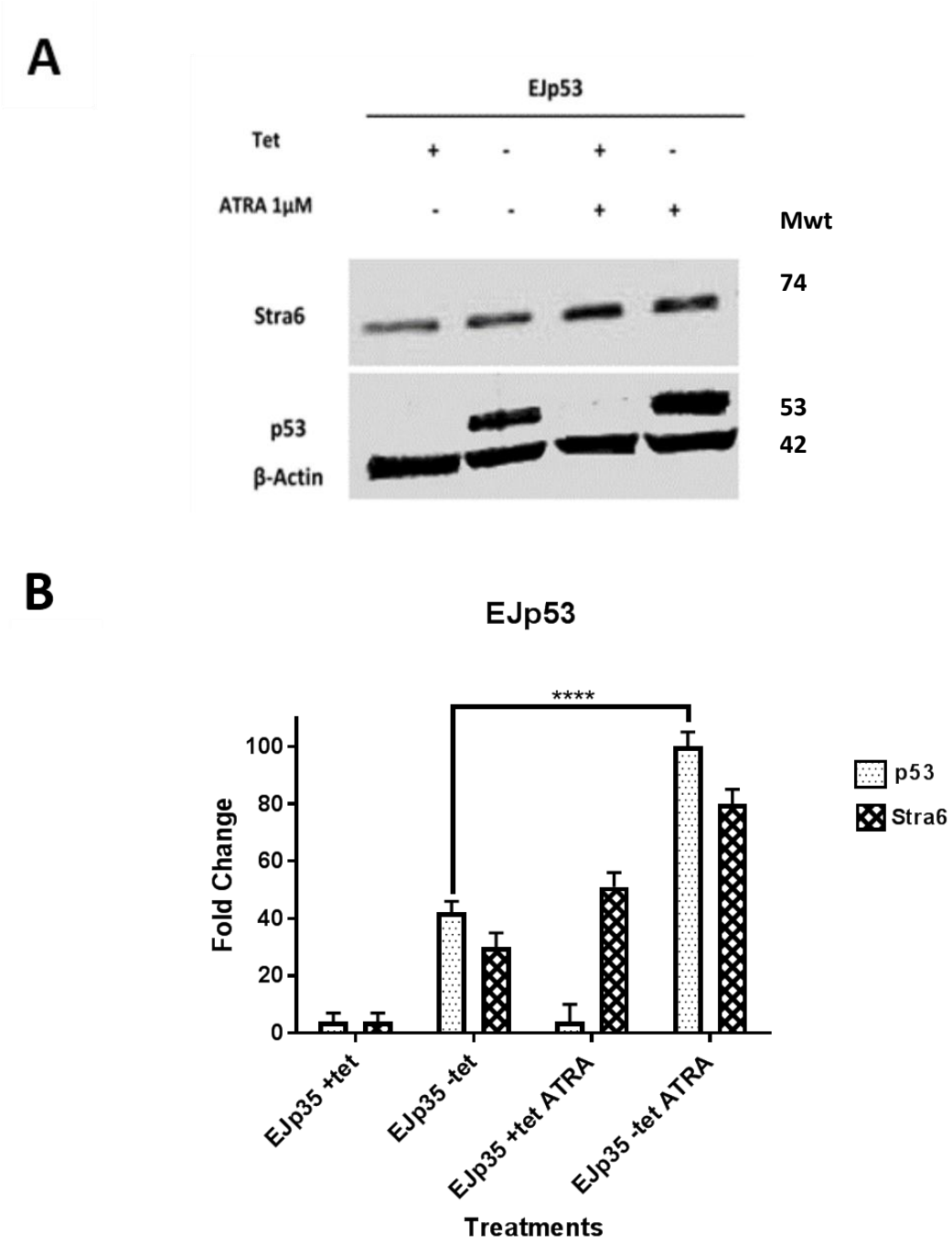

Figure 3.3: **Stra6 and p53 protein levels are upregulated after p53 induction and ATRA treatment in EJp53 cells**. **(A)** Tet was removed from the media for 48 hrs to induce p53 expression or it was kept in the media to suppress p53 induction. Additionally, cells were treated with 1 µM of ATRA for 24 hrs. β-Actin was used as a loading control. **(B)** Western blot fold change indicated that Stra6 upregulation is associated with a significant increase in p53 protein levels, specifically in ATRA treatment after p53 induction by tet removal (****$p<0.0001$). Data are expressed as a fold change compared to the control and represent the mean ± SD of three independent experiments. Mwt was indicated (kDa).

Moreover, the Stra6 was upregulated by both p53 and ATRA, and even more when both were combined.

In addition to these results, we wanted to confirm the role of DNA damage in Stra6 expression after ATRA treatment and to confirm the role of ATRA in p53 expression after using DNA damaging agents. Cells (HCT116, U2OS, MCF-7, PA-1, H460, KIS, D0HH2 and JVM-3) were treated with 1.4 to 2 µM of Dox for 24 hours or irradiated with a dose of 10 gray with or without previous ATRA sensitisation (1 µM, 24 hrs). Alternatively, cells were treated only with 1 µM of ATRA for 24 hours. Protein lysates were collected, and Stra6 and p53 protein levels were assessed by WB. As shown in Figures 3.4 – 3.11, consistent with Stra6 mRNA results, levels of Stra6 increased after treatment with ATRA and DNA damaging agents, compared to induction by DNA damaging agents or ATRA alone.

Moreover, this finding was similar to that obtained inducing p53 using a tet regulatable expression system and DNA damaging agents. This showed that p53 is upregulated more in response to a combined treatment of ATRA with Dox or radiation for 24 hours, compared to treatment involving DNA damaging agents alone. However, ATRA treatment was not able to induce p53 expression on its own (Figures 3.4 – 3.11).

These findings suggest that combined therapy using ATRA and DNA damaging agents can induce high levels of Stra6 and can also induce p53 significantly. This is also the case of the levels of Stra6 and p53 (Figure 3.4 – 3.11), which suggests that the upregulation of both Stra6 and p53 may be under the effect of a positive feedback loop.

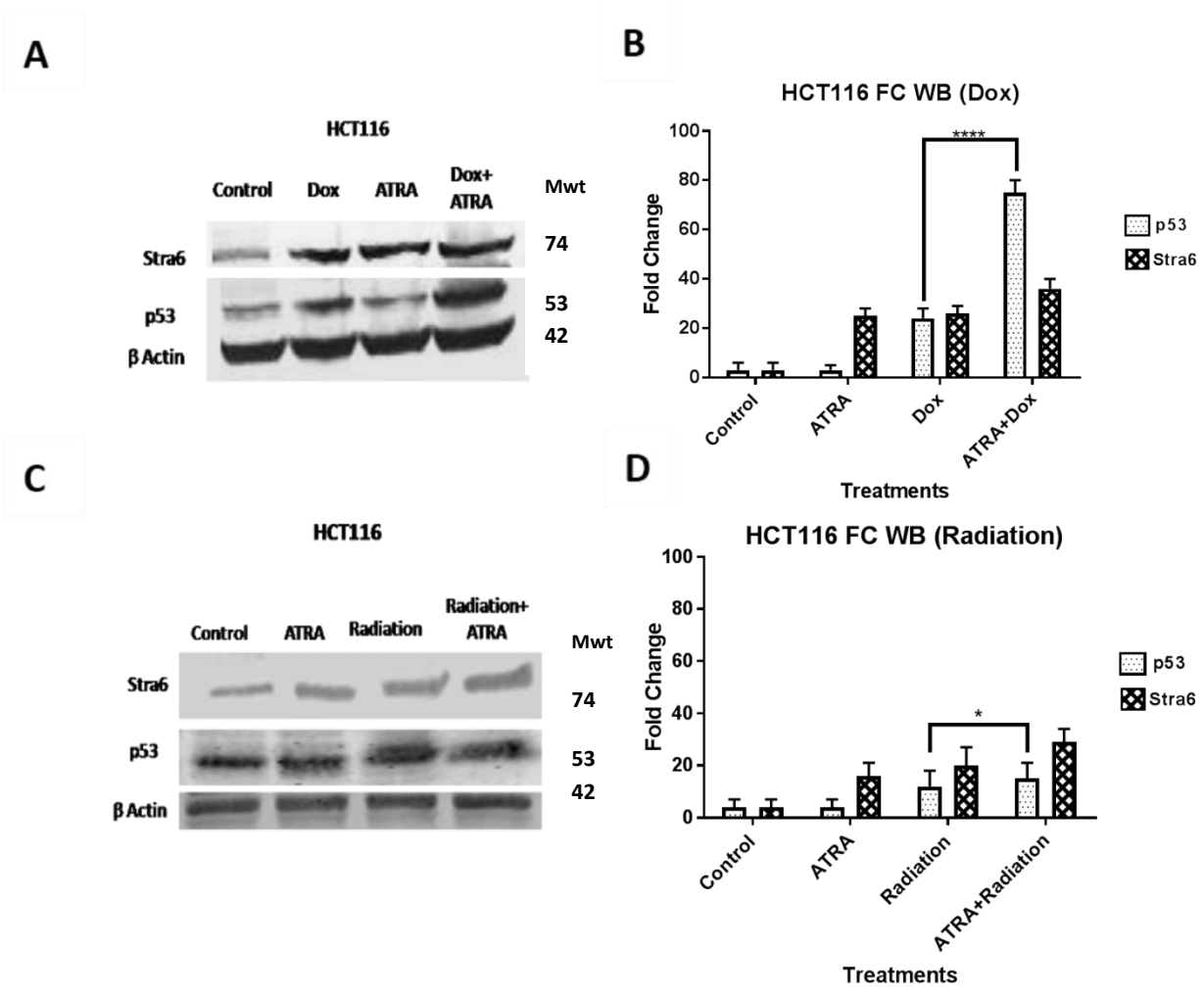

Figure 3.4: **Stra6 and p53 protein levels after DNA damage and ATRA treatment in HCT116 WT p53 cells**. (**A & C**) Western blots of HCT116 cells WT p53 after 24 hrs of Dox 1.4 µM, irradiated with 10 grays, treated with 1 µM of ATRA or a combined treatment of ATRA with Dox or ATRA with radiation. β-Actin was used as a loading control. (**B & D**) Quantitation of the Western blots. Stra6 upregulation is associated with a significant increase in p53 protein levels, specifically in ATRA treatment after p53 induction by Dox (****p<0.0001) compared top53 induction by radiation (*<p0.05). Data are expressed as a fold change compared to the control and represent the mean ± SD of three independent experiments. Mwt was indicated (kDa).

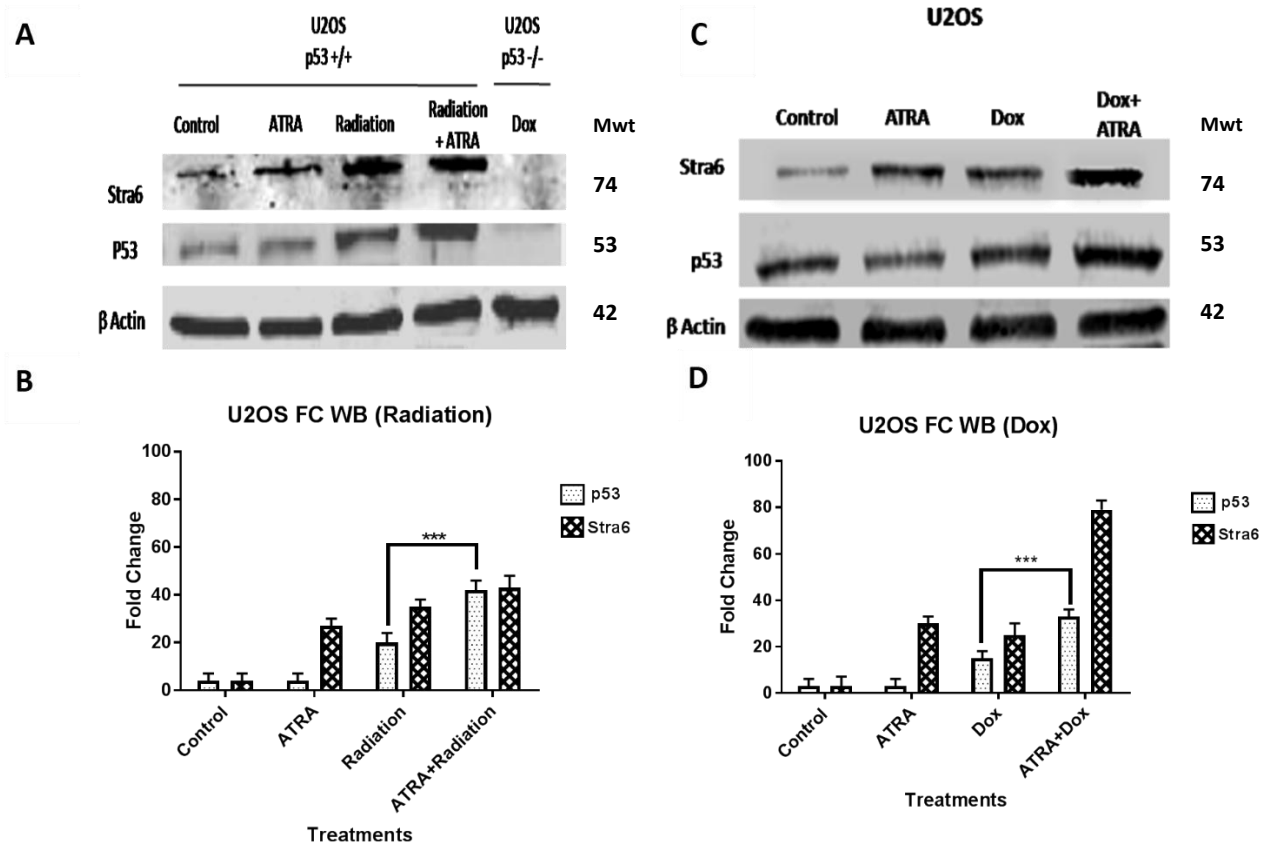

Figure 3.5: Stra6 and p53 protein levels after p53 induction and ATRA treatment in U2OS cells. **(A & C)** Western blots of U2OS cells after 24 hrs of Dox 1.4 µM, irradiated with 10 grays, treated with 1 µM of ATRA, or a combined treatment of ATRA with Dox or ATRA with radiation. β-Actin was used as a loading control. **(B & D)** Quantitation of the Western blots. Stra6 upregulation is associated with a significant increase in p53 protein levels, specifically in ATRA treatment after p53 induction either by Dox or radiation (***p<0.001). Data are expressed as a fold change compared to the control and represent the mean ± SD of three independent experiments. Mwt was indicated (kDa).

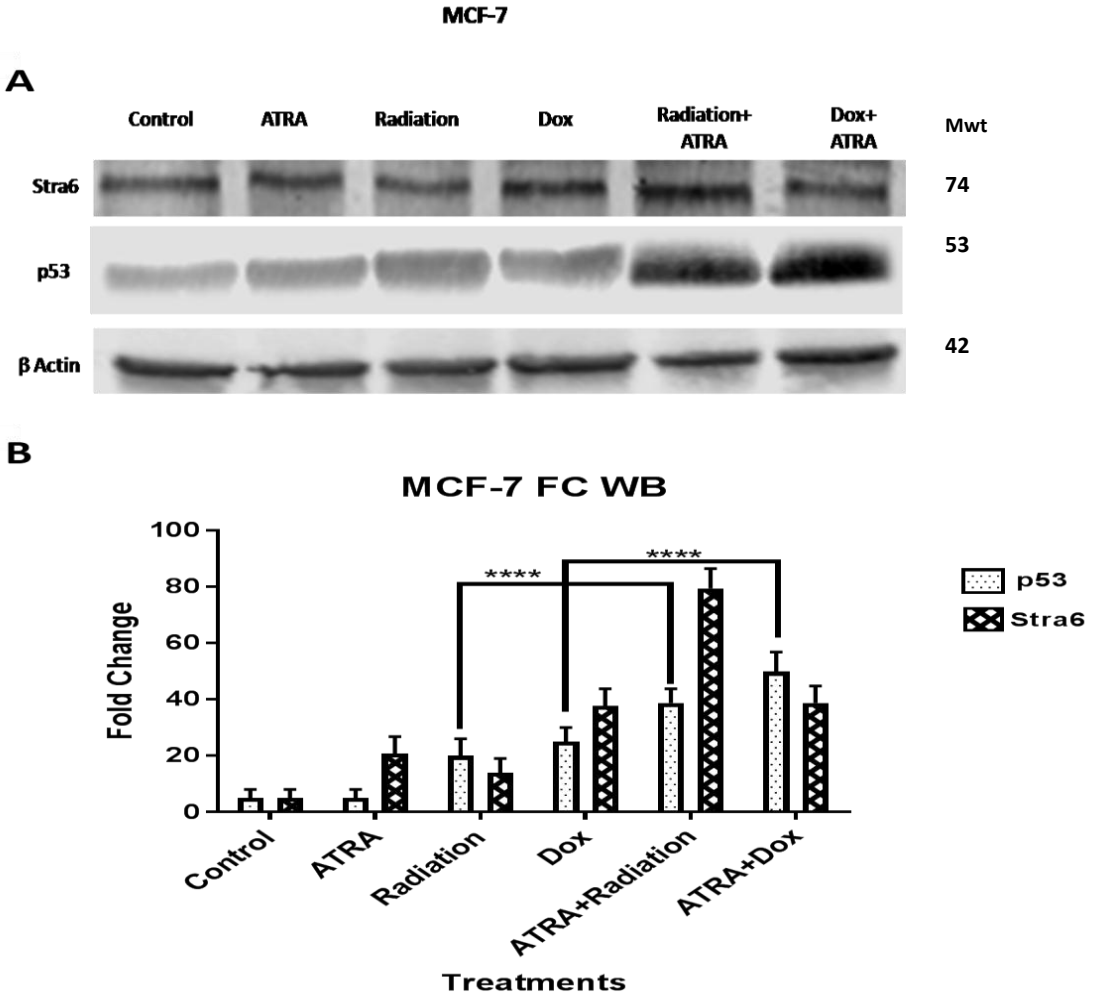

Figure 3.6: Stra6 and p53 protein levels after p53 induction and ATRA treatment in MCF-7 cells. (A) Western blot of MCF-7 cells showing Stra6 up-regulation after 24 hrs of Dox 1.4 µM, irradiation with 10 grays, treatment with1 µM of ATRA, or combined treatment of ATRA with Dox or ATRA with radiation. β-Actin was used as a loading control. **(B)** Quantitation of the Western blot indicates that Stra6 upregulation is associated with a significant increase in p53 protein levels, specifically in ATRA treatment after p53 induction either by Dox or radiation (****p<0.0001). Data are expressed as a fold change compared to the control and represent the mean ± SD of three independent experiments. Mwt was indicated in (kDa).

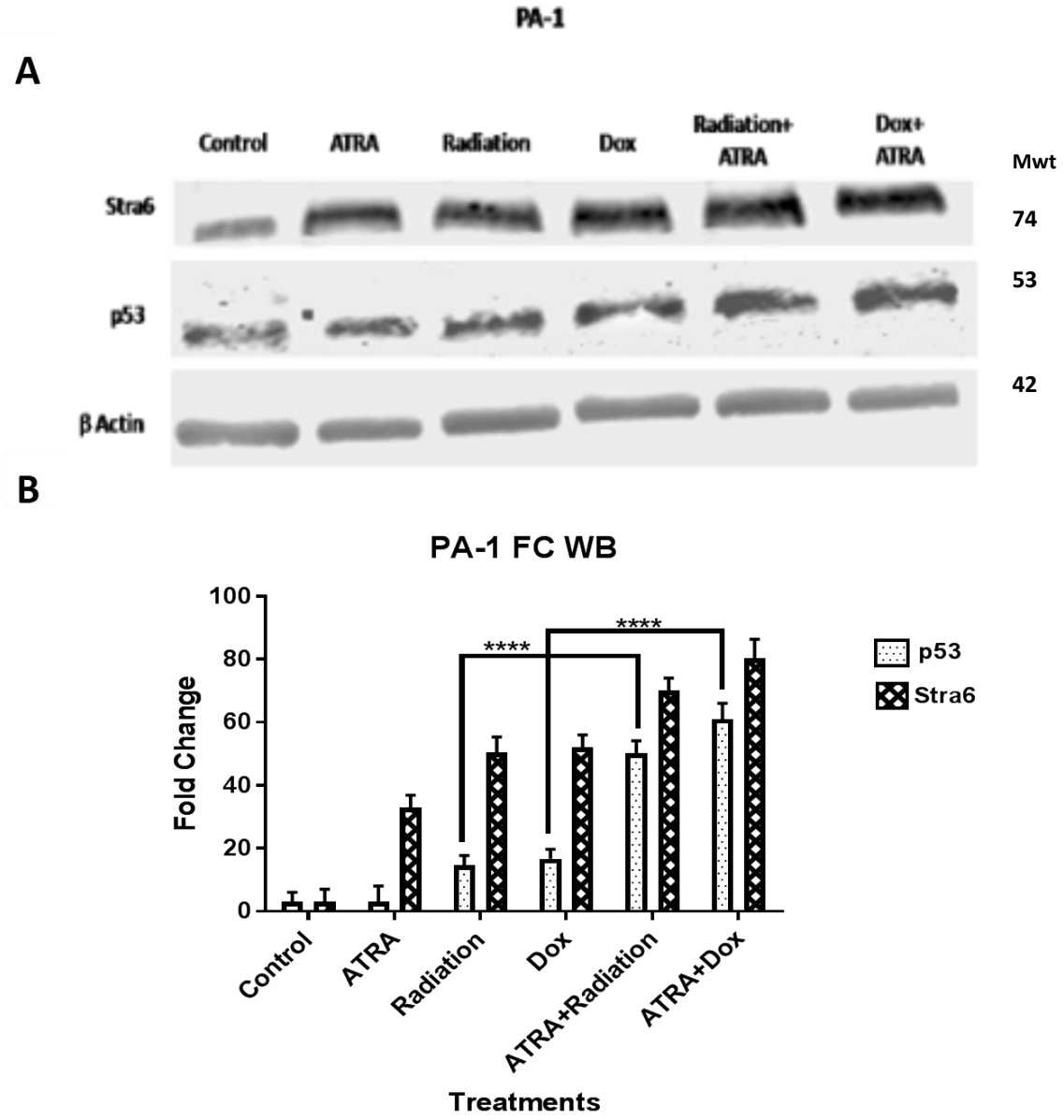

Figure 3.7: Stra6 and p53 protein levels after p53 induction and ATRA treatment in PA-1 cells. **(A)** Western blot of PA-1 cells showing Stra6 up-regulation after 24 hrs of Dox 1.4 µM or radiated with 10 grays, treatment with 1 µM of ATRA, or combined treatment of ATRA with Dox or ATRA with radiation. β-Actin was used as a loading control. **(B)** Quantitation of the Western blot indicates that Stra6 upregulation is associated with a significant increase in p53 protein levels, specifically in ATRA treatment after p53 induction either by Dox or radiation (****p<0.0001). Data are expressed as a fold change compared to the control and represent the mean ± SD of three independent experiments. Mwt was indicated in (kDa).

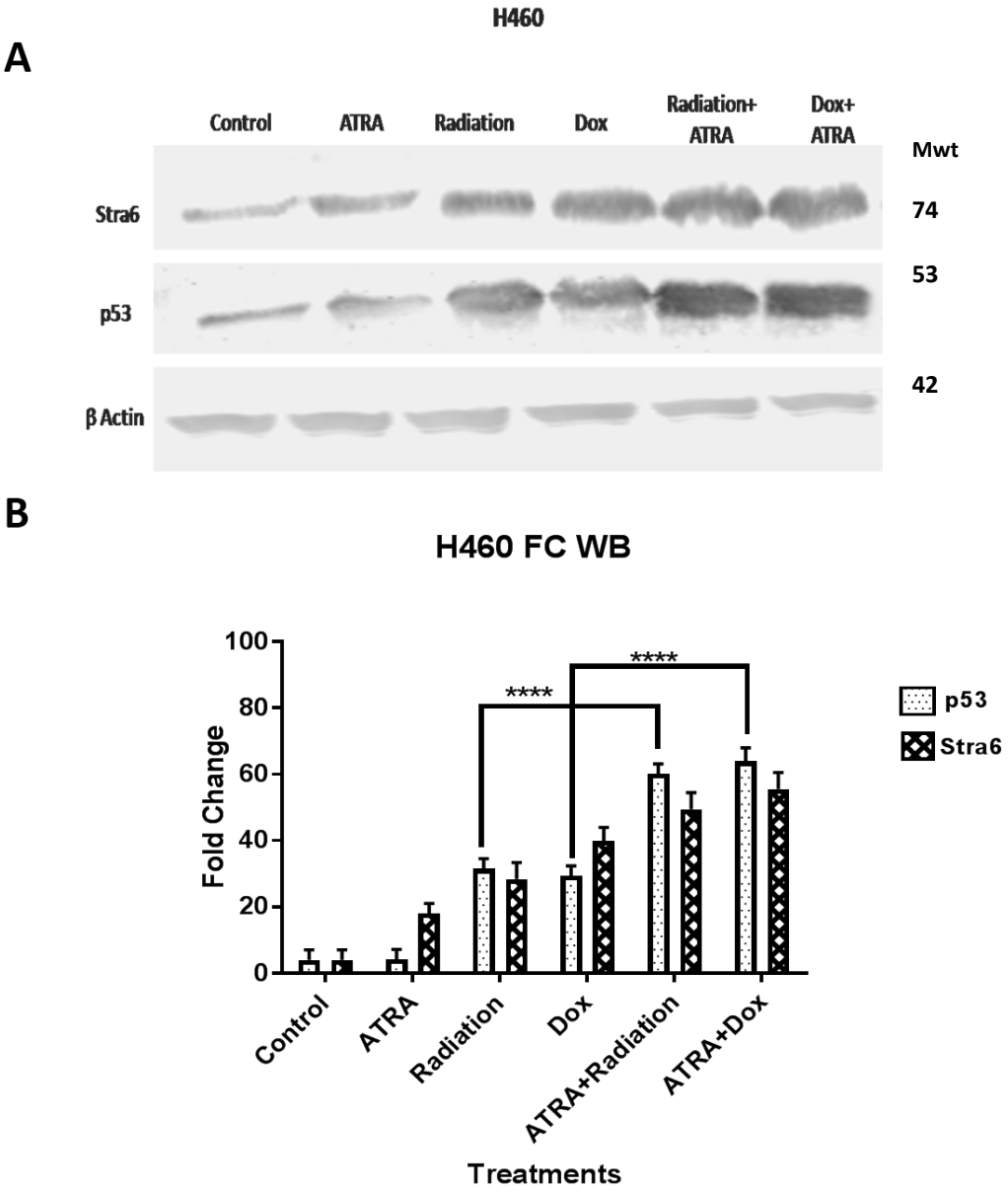

Figure 3.8: Stra6 and p53 protein levels after p53 induction and ATRA treatment in H460 cells. (A) Western blot of H460 cells showing Stra6 up-regulation after 24 hrs of Dox 1.4 µM or radiated with 10 grays, treatment with 1 µM of ATRA, or combined treatment of ATRA with Dox or ATRA with radiation. β-Actin was used as a loading control. **(B)** Quantitation of the Western blot indicates that Stra6 upregulation is associated with a significant increase in p53 protein levels, specifically in ATRA treatment after p53 induction either by Dox or radiation (****p<0.0001). Data are expressed as a fold change compared to the control and represent the mean ± SD of three independent experiments. Mwt was indicated in (kDa).

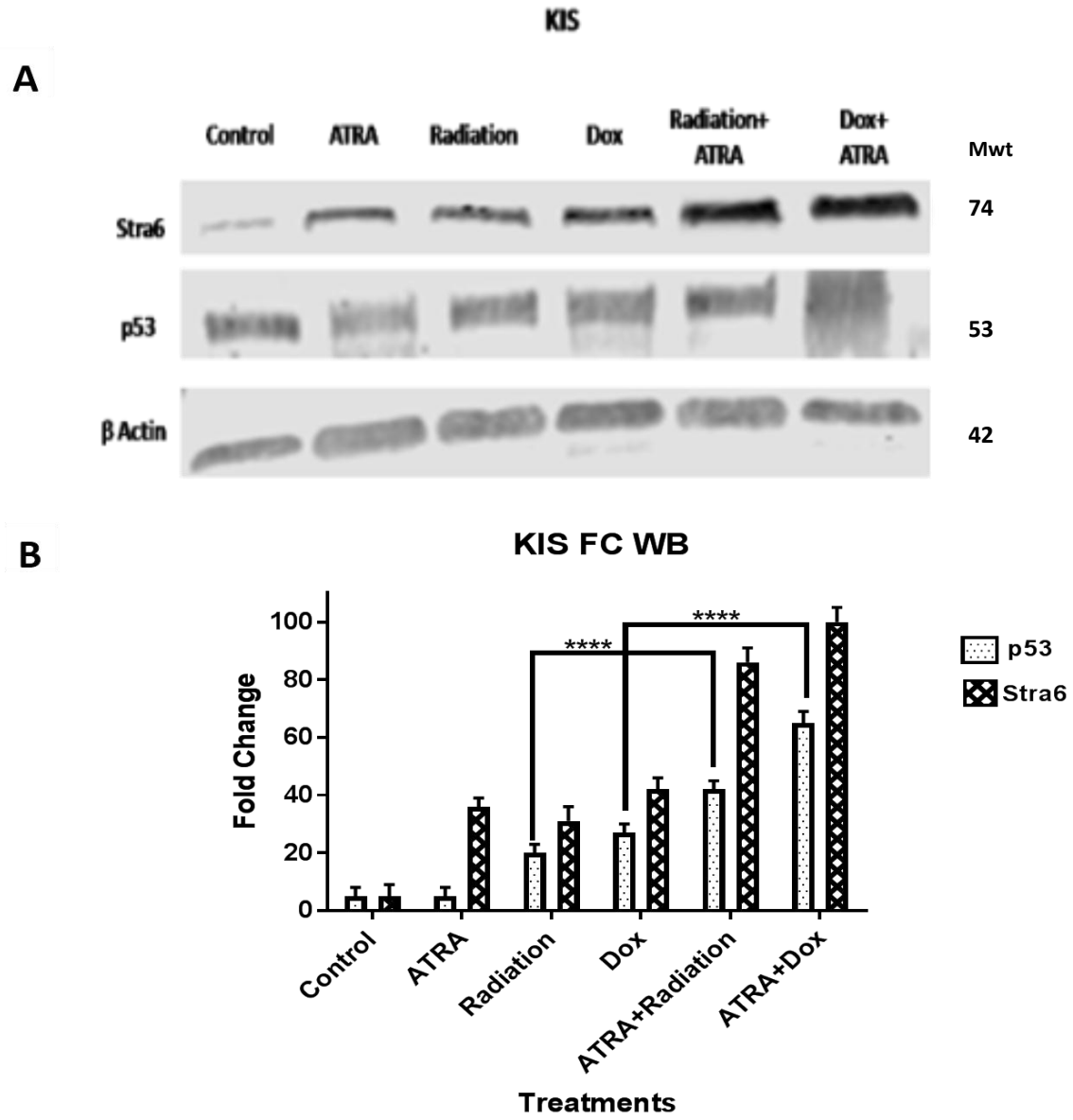

Figure 3.9: Stra6 and p53 protein levels after p53 induction and ATRA treatment in KIS cells. **(A)** Western blot of KIS cells showing Stra6 up-regulation after 24 hrs of Dox 1.4 µM or radiated with 10 grays, treatment with 1 µM of ATRA, or combined treatment of ATRA with Dox or ATRA with radiation. β-Actin was used as a loading control. **(B)** Quantitation of the Western blot indicates that Stra6 upregulation is associated with a significant increase in p53 protein levels, specifically in ATRA treatment after p53 induction either by Dox or radiation (****p<0.0001). Data are expressed as a fold change compared to the control and represent the mean ± SD of three independent experiments. Mwt was indicated in (kDa).

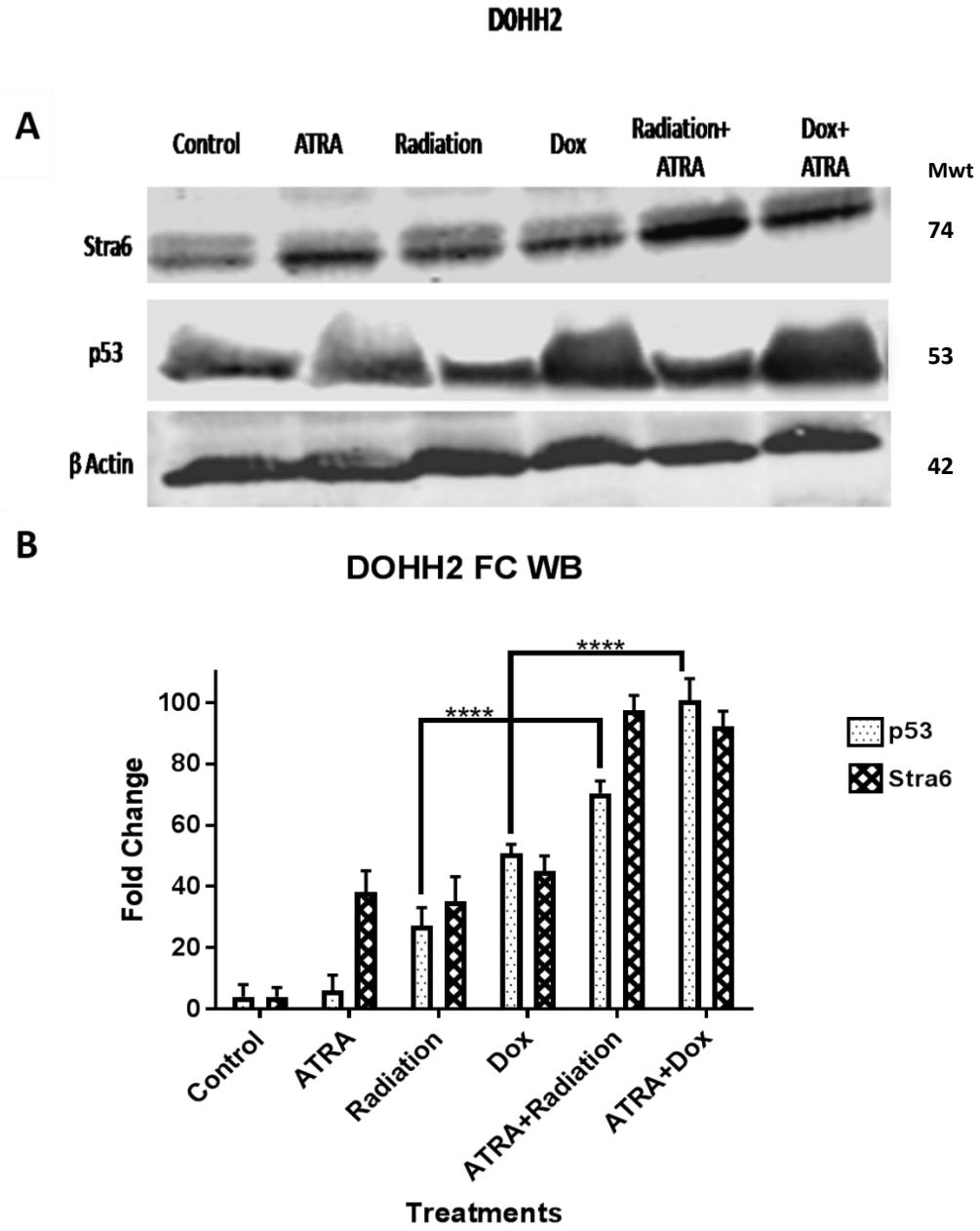

Figure 3.10: **Stra6 and p53 protein levels after p53 induction and ATRA treatment in DOHH2 cells. (A)** Western blot of D0HH2 cells showing Stra6 up-regulation after 24 hrs of Dox 1.4 µM or radiated with 10 grays, treatment with 1 µM of ATRA, or combined treatment of ATRA with Dox or ATRA with radiation. β-Actin was used as a loading control. **(B)** Quantitation of the Western blot indicates that Stra6 upregulation is associated with a significant increase in p53 protein levels, specifically in ATRA treatment after p53 induction either by Dox or radiation (****p<0.0001). Data are expressed as a fold change compared to the control and represent the mean ± SD of three independent experiments. Mwt was indicated in (kDa).

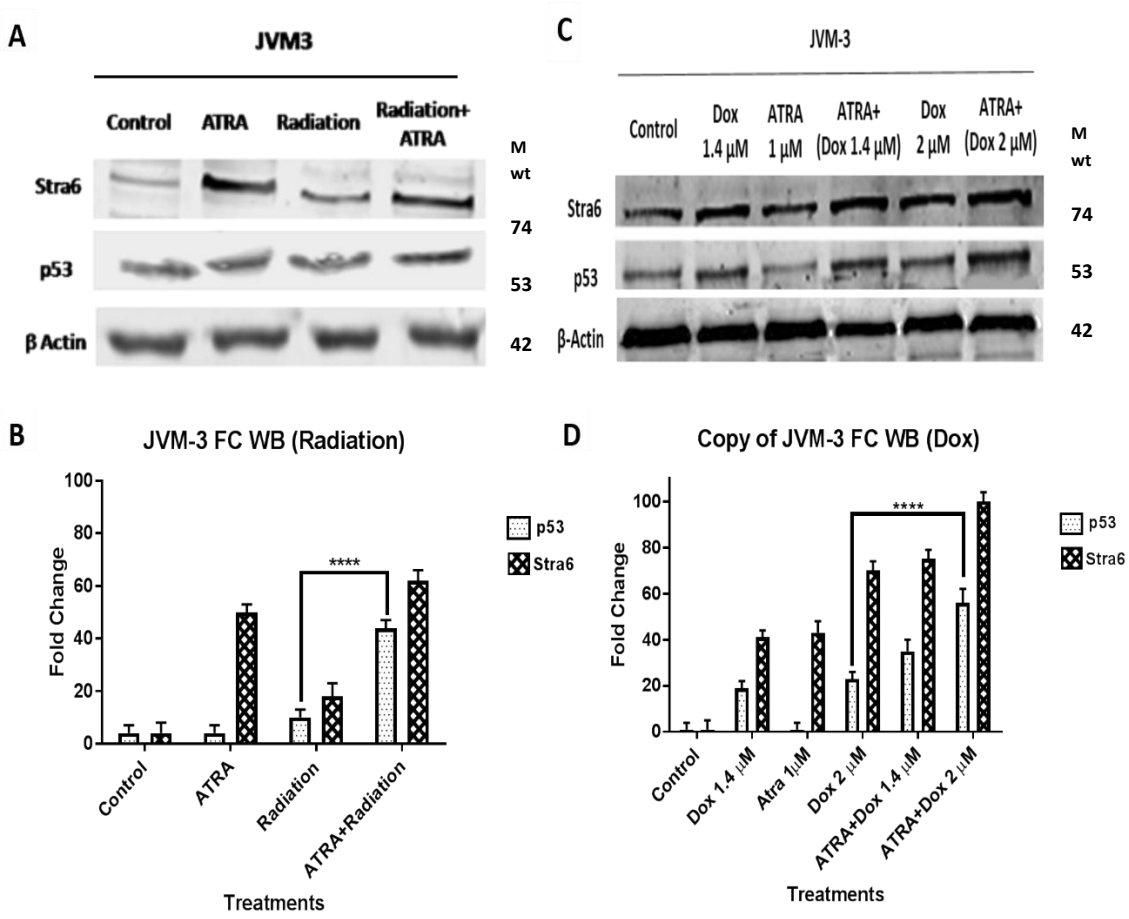

Figure 3.11: **Stra6 and p53 protein levels after p53 induction and ATRA treatment in JVM-3 cells. (A & C)** Western blot of JVM-3 cells Showing Stra6 and p53 protein levels after 24 hrs of cells treated with Dox (1.4 or 2 μM), radiated with 10 grays or treated with 1 μM of ATRA and treated with a combination of ATRA with Dox or ATRA with radiated cells. β-Actin was used as a loading control. **(B & D)** Quantitation of the Western blot indicates that Stra6 upregulation is associated with a significant increase in p53 protein levels, specifically in ATRA treatment after p53 induction either by Dox or radiation (****p<0.0001). Data are expressed as a fold change compared to the control and represent the mean ± SD of three independent experiments. Mwt was indicated in (kDa).

3.2.3 Exploring the effect of ATRA and DNA damaging agents on both cellular metabolism and morphological changes

3.2.3.1 Determining cell viability counts in JVM-3 cells

We next attempted to determine whether there is any influence on cell viability after a combined treatment of ATRA (1 µM) and Dox (2 µM). This analysis was performed using a JVM-3 cell line. Cells were placed into six well-plates in equal amounts; the next day and for the following three days, cells were stained with trypan blue and counted using an automated cell counting machine. Figure 3.12 shows that a combined treatment of ATRA and Dox on JVM-3 cells significantly reduces cell viability (*$p < 0.05$), compared to treatment using Dox only. Contrary to these results, an ATRA treatment using a similar concentration (1 µM) shows a slight, sustained increase in cell viability counts within three days of continuous cell viability assessment. This suggests that ATRA alone at 1 µM concentration does not induces cell death but it enhances DNA damaging agents.

Additional investigations were conducted to confirm the effects of the combined treatment of ATRA and DNA damaging agents on cell viability. An MTS is a cell proliferation colorimetric assay which is considered one of the most commonly used screening methods to estimate cell viability. MTS was performed in JVM-3 cells 24 and 48 hours after treatments. Similar to the result obtained in Figure 3.12, cell proliferation was reduced significantly upon ATRA and Dox treatments for 48 hours ($p<0.0001$). This reduction in cellular metabolic activity could be associated with cell death or cell cycle arrest. Unlike combined treatment of ATRA and Dox, the level of cell proliferation significantly increased over the first 24 hours of cells treated with ATRA compared to the control.

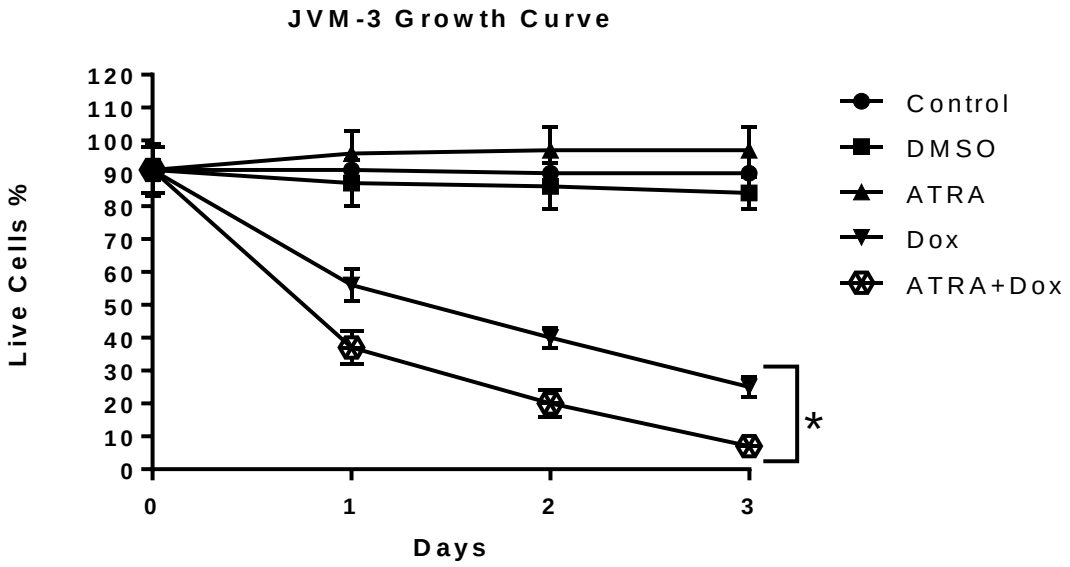

Figure 3.12: Decreasing of cell viability counts following combined treatment of ATRA and Dox in JVM-3 cells. Cells were split into six well-plate in equal amounts; the next day and for the following three days, cells were stained with trypan blue and counted using an automated cell counting machine. Data are expressed as the mean ± SD of three independent experiments. Cells treated with combined treatments of ATRA and Dox yielded a significance of *p,0.05 compared to Dox treated cells.

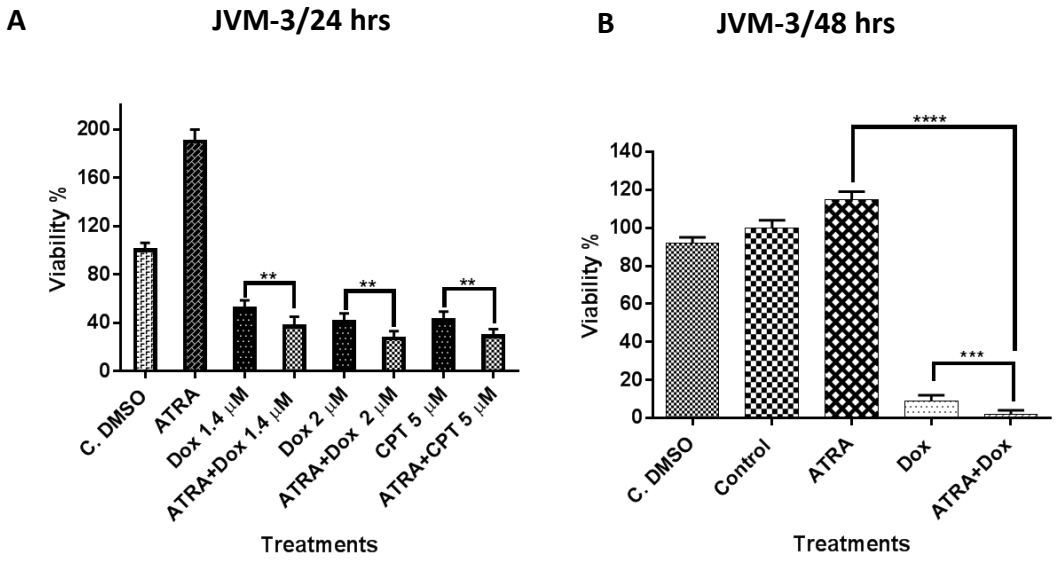

Figure 3.13: Reduced cell proliferation in JVM-3 cells using MTS Cell Proliferation Colorimetric Assay. (A) JVM-3 cells were treated with different concentrations of DNA damaging agents for 24 hrs: Dox (1.4 µM and 2 µM) or with 5 µM CPT, all with or without 1 µM of ATRA treatment. **(B)** JVM-3 cells were treated for 48 hrs with 1 µM of ATRA, 2 µM of Dox or with similar concentrations of ATRA and Dox. **(A & B)** indicate colorimetric quantification and calculation of cell viability. Data are expressed as the mean ± SD of three independent experiments. **p<0.01, ***p<0.001 and ****p<0.0001.

3.2.3.2 Determining the morphological changes in EJp53 and JVM-3 cell lines

We then performed microscopic experiments to further assess the effect of ATRA in response to p53 induction by studying the morphological changes in EJp53 and JVM-3 cells. In general, results showed variation in the size and shape of the cells according to the type of treatment used, and the degree of cell deterioration ranged from slightly moderate (in the case of using a DNA damaging agent only) to highly severe (in response to a combined treatment of ATRA and Dox).

EJp53 cells were split into equal cell numbers to begin different treatment protocols. In Figure 3.14, 1 µM of ATRA in the presence of tet to supress p53 was shown to have no effect on the morphology of the cells. By contrast, induction of p53 by tet removal for 48 hours yielded elongated cells with a slight tendency to lose cell membrane, as shown in Figure 3.14B. Moreover, in Figure 3.14D cells were treated with 1 µM of ATRA for 24 hours and p53 induced by tet removal from media for 48 hours have shown many cells lost membrane and some cells even degraded completely (Figure 3.14).

Similar results determining the effect of ATRA on the DNA damage response of using Dox were observed in JVM-3 as shown in Figure 3.15. JVM-3 cells were split into equal cell numbers in six well-plates. Figure 3.15A represents cells before any treatment. After 48 hours, the control cells demonstrated typical rounded cells, suggestive of normal cell growth (Figure 3.15B). However, when cells were incubated with 1 µM of ATRA for 48 hours, the cells became more enlarged (Figure 3.15C). Figures 3.15 D and E display ruptured cells with characteristic apoptotic cells that exhibit common properties of apoptotic bodies and cellular membrane blebs as well as nuclei with a horse-shoe like appearance. This was detected more after ATRA treatment (1 µM, 48 hours) in response to DNA damage induction by Dox (2 µM, 48 hours) than in Dox treatment alone of similar concentration and incubation time (Figure 3.15).

Overall, these results were consistent with previous results of cell viability counts and cell proliferation assays that showed a significant reduction in cell metabolic activity and viability after a combined treatment of ATRA and Dox. Therefore, further studies are necessary to investigate the effects of ATRA on enhancing DNA damage cellular response and to correlate these detected morphological changes of the cells with the previously obtained results of p53 protein upregulation, that was associated with Stra6 upregulation after the cell was treated with ATRA and exposed to DNA damaging agents.

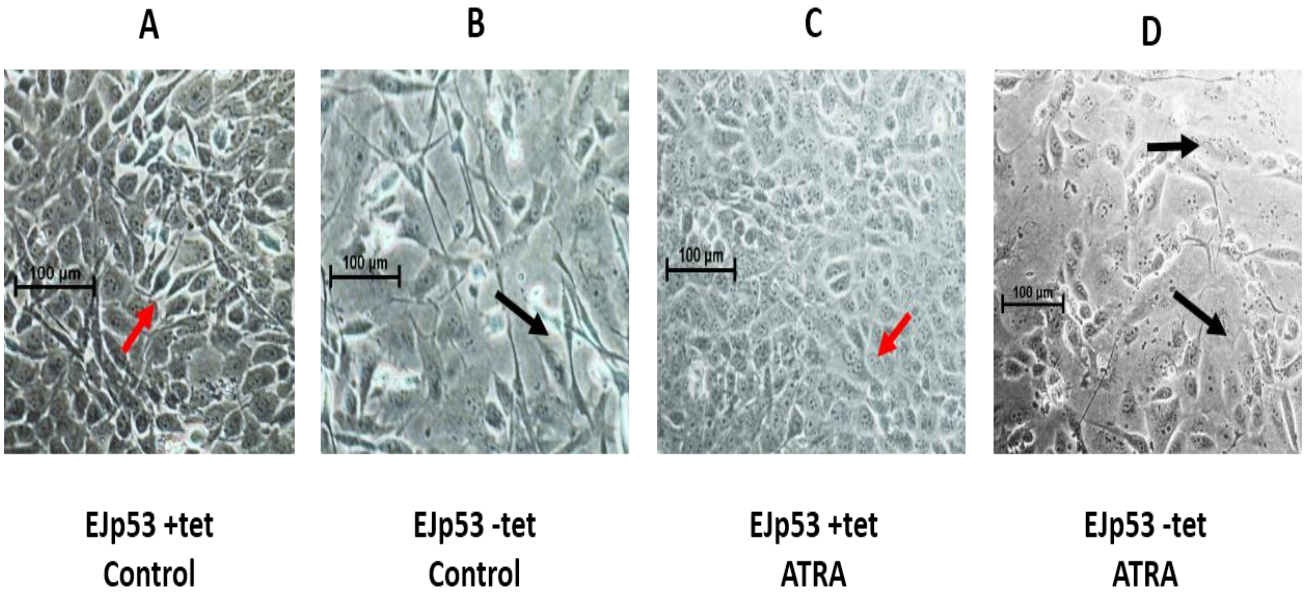

Figure 3.14: p53 induction following ATRA treatment induced changes on the cellular morphology of EJp53 cells. (A) EJp53 cells were put under the control of tet for 48 hrs so that p53 would not be expressed. **(B)** Tetracycline (tet) was removed from the media for 48 hrs to induce p53 expression. **(C)** Here, the EJp53 cells under tet control are incubated with 1 µM of ATRA for 24 hrs. **(D)** Tet is removed for 48 hrs with 1 µM of ATRA treatment for 24 hrs. Captured images are visualised using light microscopy (10x objective lens). In **(A & C),** the red arrows indicate typical spindle shape and compact cells with no cellular changes have been detected after ATRA treatment. In (B & D), the black arrows indicate elongated cells with more tendency to lose cell membranes after ATRA treatment in response to p53 induction. Images presented are from one experiment and characteristic of three independent experiments. Scale bar = 100 µm.

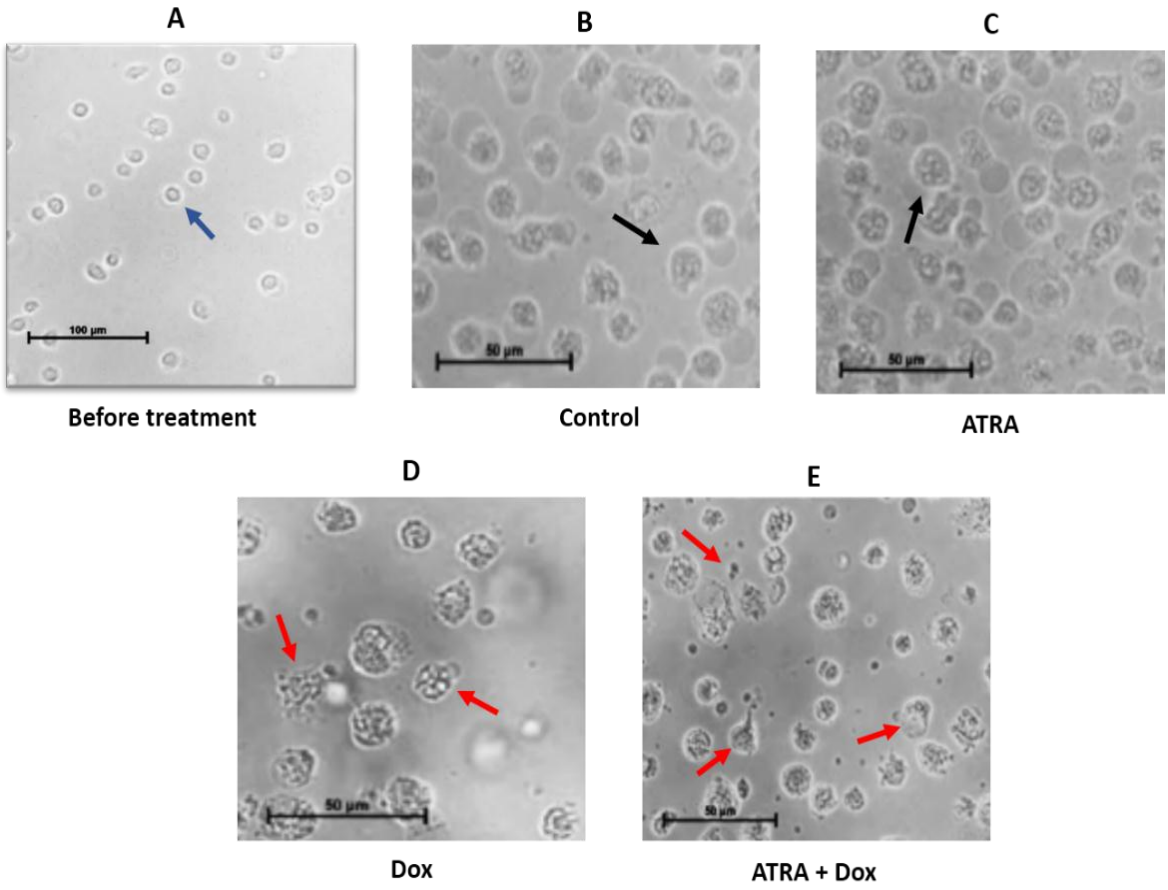

Figure 3.15: **Characterised apoptotic cellular morphology is observed after ATRA treatment and p53 induction in the JVM-3 cells. (A)** JVM-3 cells were split into equal cell numbers in six well-plates; this image represents the cells before any treatment is received. Figure 3.15 **(B)** represents the JVM-3 control cells after 48 hrs. **(C)** Here, the JVM-3 cells were incubated with 1 µM of ATRA for 48 hrs. Figure 3.15 **(D)** shows the JVM-3 cells after 48 hrs with 2 µM of Dox treatment. Figure 3.15 **(E)** represents the JVM-3 cells after ATRA and Dox combined treatment after 48 hrs. Captured images were visualised using light microscopy (20x objective lens). In **(A),** the blue arrow indicates zero time of cell cultured. In **(B)**, the black arrow indicates typical rounded cells. In **(C)**, the black arrow indicates more enlarged cells after ATRA treatment with no cellular changes. In **(D & E)**, the red arrows indicate ruptured cells with characteristic apoptotic cells, which observed showed common properties of apoptotic bodies and membrane blebs as well as nuclei with a horse-shoe like appearance. These features are detected more highly after ATRA treatment in response to p53 induction compared to Dox treatment alone. Images presented are from one experiment and representative of three independent experiments. Scale bar = 100 µm in **(A)** and = 50 µm in **(B-E).**

3.3 Determining the effect of ATRA and DNA damaging agents on cell death:

3.3.1 Measurement of cell death by PI staining

The results of this study suggest that both Stra6 and p53 are upregulated on the translational level in a positive feed-back loop after ATRA treatment and induction of DNA damage. We were interested in determining whether this effect would increase the induction of cell death. In seven different cell lines (JVM-3, U2OS, HCT116, PA-1, MCF-7, D0HH2 and KIS), cell death was measured using PI staining. Cells were treated with 1 µM ATRA, treated with 2 µM Dox, irradiated with a dose of 10 gray, received a combined treatment of ATRA and Dox or received ATRA and radiation for 24 hours. Results showed that ATRA did not induce Sub-G1 cell death compared to the control (Figure 3.16). However, the results did reveal the ability of ATRA to determine cell fate by shifting the status of a cell from cell cycle arrest to cell death in response to DNA damaging agents (Dox and radiation) in the majority of our tested cells (Figure 3.16). This confirms that ATRA treatment can enhance DNA damage responses, which we hypothesized is a Stra6-mediated effect.

3.3.2 Apoptotic cell death profile

Based on the obtained results, we then wanted to use Annexin V staining and FACS analysis to determine whether apoptotic cell death occurs in the combined treatment of ATRA and Dox. The results confirmed that ATRA did not induce cell death but did significantly enhance apoptotic cell death after DNA damage using Dox by an approximately four-fold increase, compared to the result of using Dox alone in JVM-3 cells (Figure 3.17). Similar results were observed in U2OS, H460, MCF-7 and HCT116 cell lines, as shown in Figures 3.18, 3.19, 3.20 and 3.21, respectively.

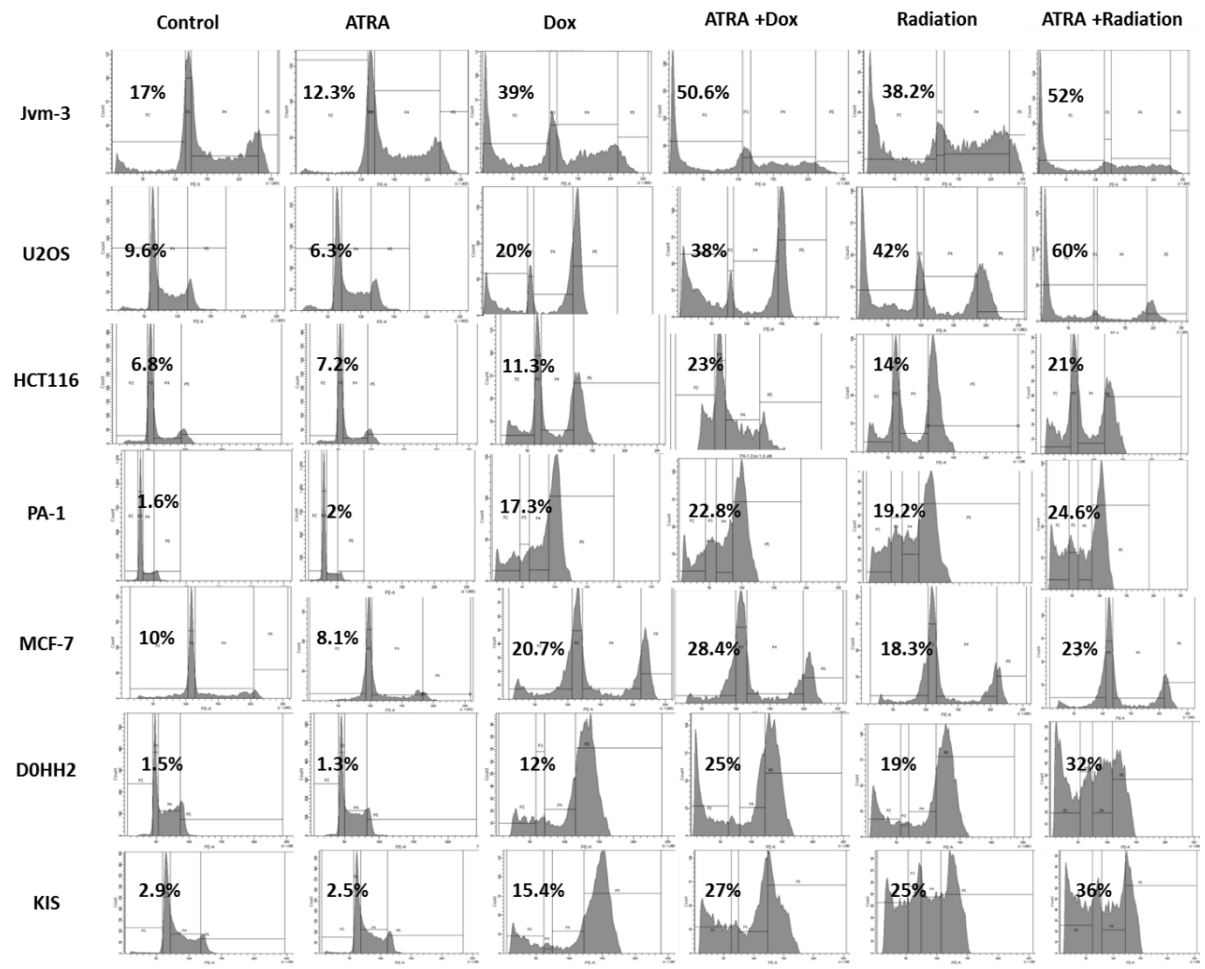

Figure 3.16.1: **ATRA increases cell death in response to p53 after using DNA damaging agents**. In seven different cell lines (JVM-3, U2OS, HCT116, PA-1, MCF-7, D0HH2 and KIS). Cell death was measured by PI staining. Cells were treated with 1 µM ATRA, treated with 2 µM Dox, irradiated with a dose of 10 gray, received a combined treatment of ATRA and Dox or received ATRA and radiation for 24 hrs. The cells were then stained with PI for FACS analysis. The graphs depict representative PI staining. The numbers indicate percentages of Sub-G1 events of cell death.

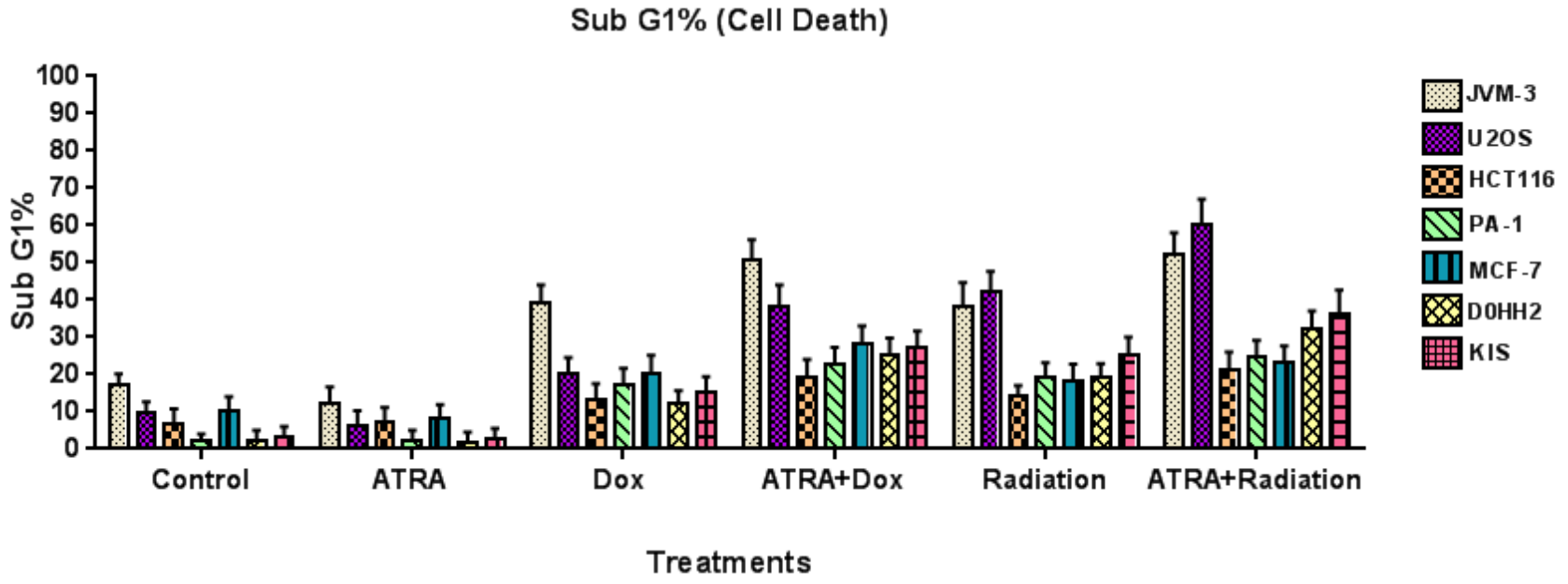

Figure 3.16.2: A summary of cell death measured by PI staining in seven different cell lines. Cells were treated with 1 µM ATRA, treated with 2 µM Dox, irradiated with a dose of 10 gray, received a combined treatment of ATRA and Dox or received ATRA and radiation for 24 hrs. The cells were then stained with PI for FACS analysis. The graphs depict representative PI staining. The numbers indicate percentages of Sub-G1 events of cell death. Data are expressed as the mean ± SD of three independent experiments.

A

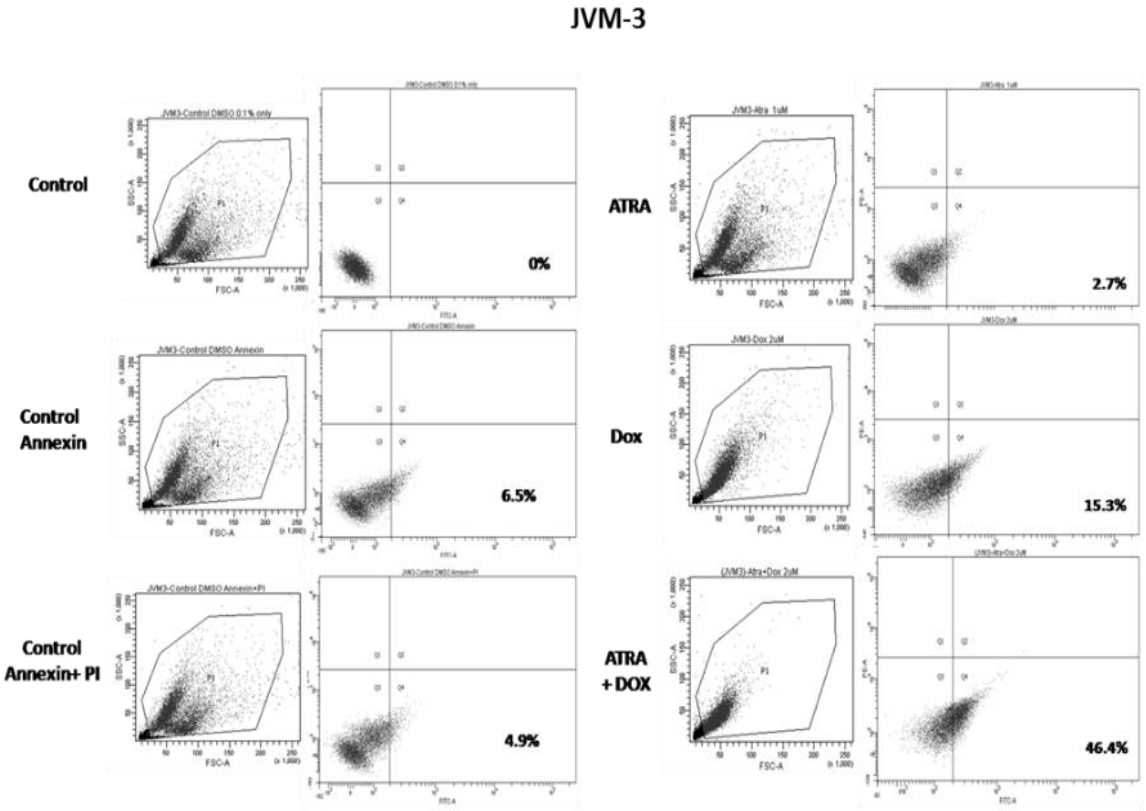

B

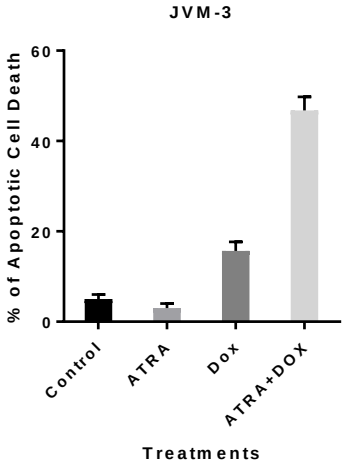

Figure 3.17: ATRA enhances apoptotic cell death in combination with chemotherapeutic agent in JVM-3 cells. **(A)** Representative FACS analysis of Annexin V/PI-stained cells. Apoptosis was assessed using Annexin V staining and FACS analysis. Cells were treated with 1 µM ATRA, treated with 2 µM Dox or received a combined treatment of ATRA and Dox of similar concentrations, 1 µM and 2 µM respectively, for 48 hrs. **(B)** Summary of the data shown in A. The numbers indicate percentage of positive apoptotic cells compared to control. Data are expressed as the mean ± SD of three independent experiments.

A

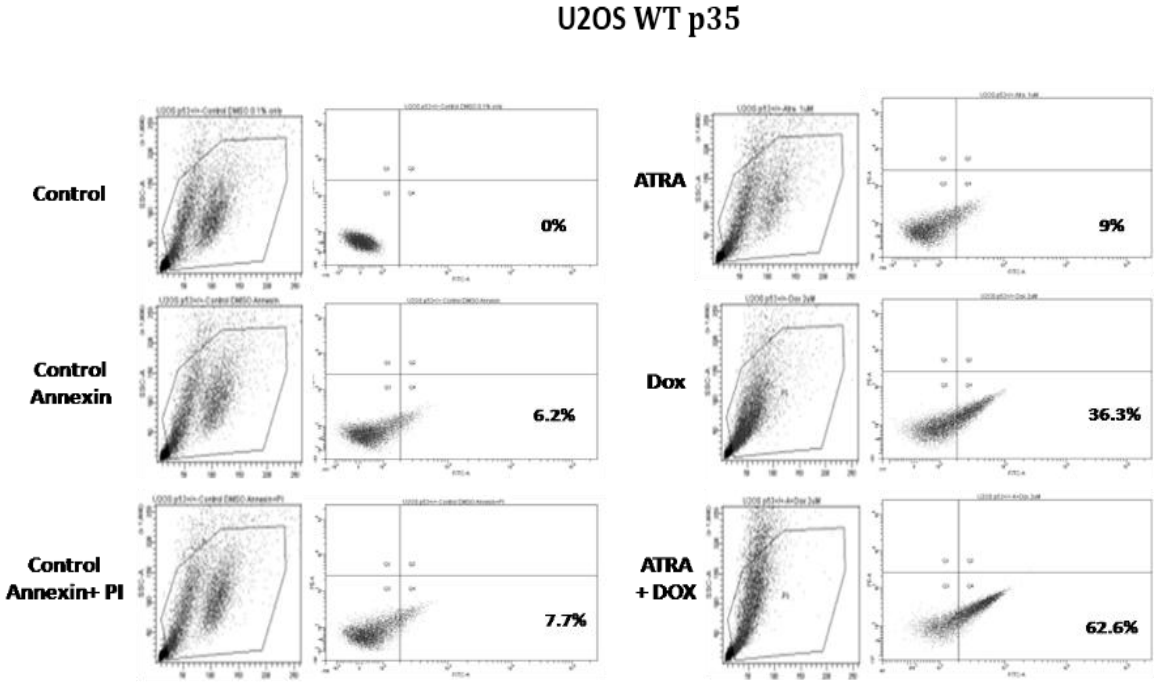

B

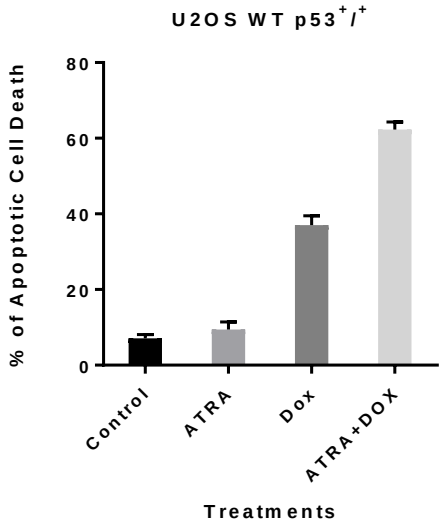

Figure 3.18: ATRA enhances apoptotic cell death in combination with chemotherapeutic agent in U2OS cells. (A) Representative FACS analysis of Annexin V/PI-stained cells. Apoptosis was assessed using Annexin V staining and FACS analysis. Cells were treated with 1 µM ATRA, treated with 2 µM Dox or received a combined treatment of ATRA and Dox of similar concentrations, 1 µM and 2 µM respectively, for 48 hrs. **(B)** Summary of the data shown in A. The numbers indicate percentage of positive apoptotic cells compared to control. Data are expressed as the mean ± SD of three independent experiments.

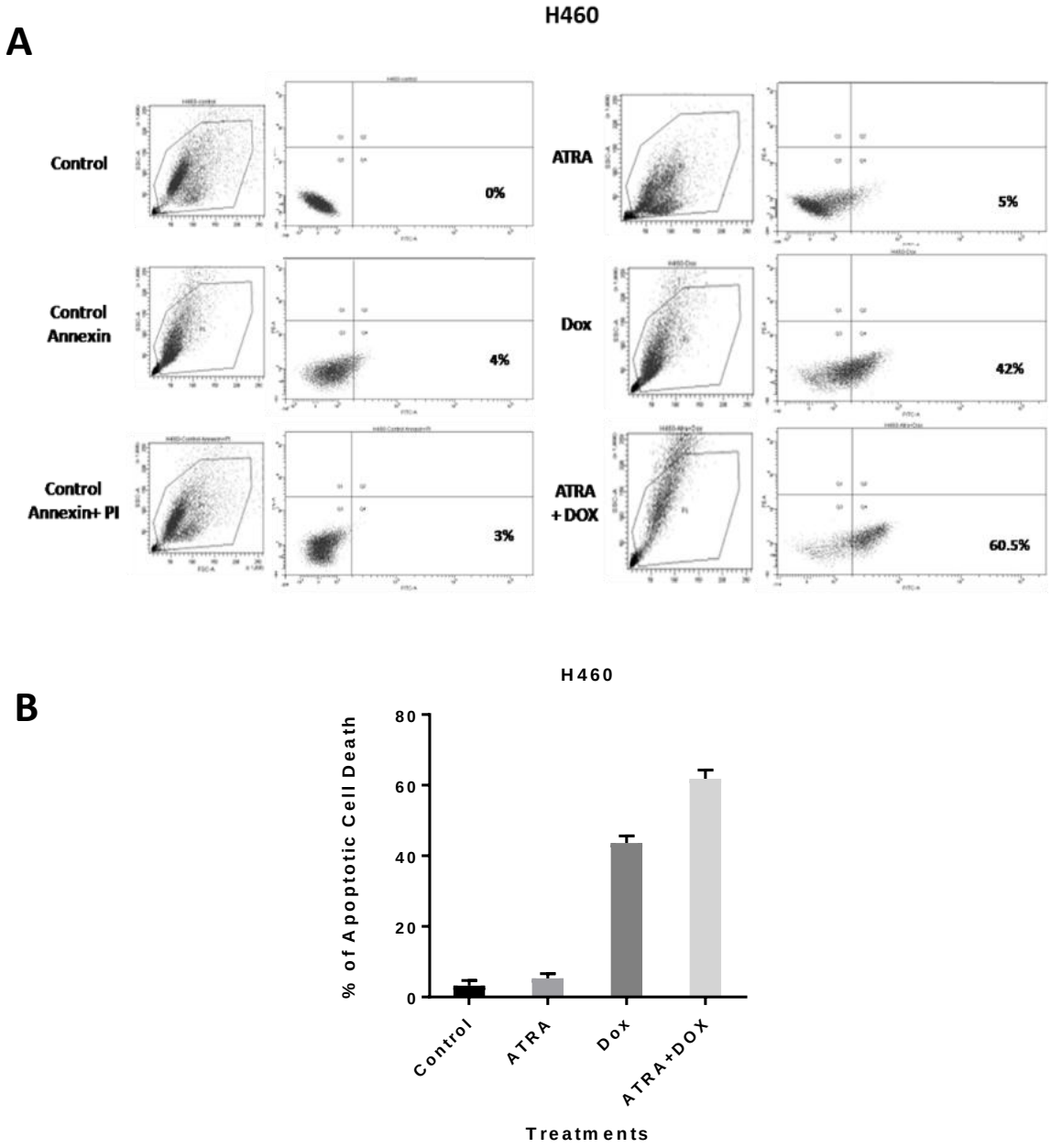

Figure 3.19: ATRA enhances apoptotic cell death in combination with chemotherapeutic agent in H460 cells. (A) Representative FACS analysis of Annexin V/PI-stained cells. Apoptosis was assessed using Annexin V staining and FACS analysis. Cells were treated with 1 µM ATRA, treated with 2 µM Dox or received a combined treatment of ATRA and Dox of similar concentrations, 1 µM and 2 µM respectively, for 48 hrs. **(B)** Summary of the data shown in **(A).** The numbers indicate percentage of positive apoptotic cells compared to control. Data are expressed as the mean ± SD of three independent experiments.

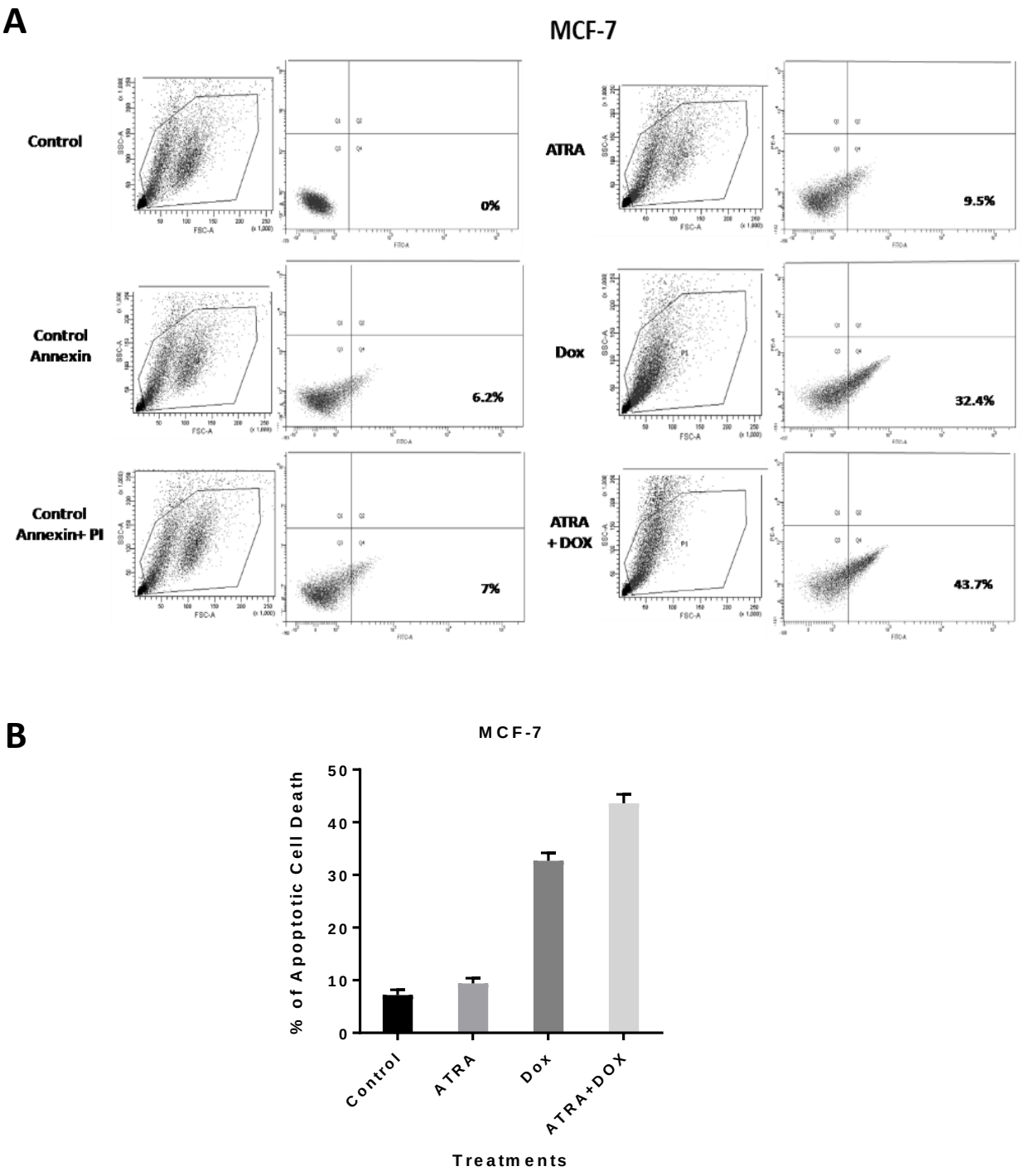

Figure 3.20: **ATRA enhances apoptotic cell death in combination with chemotherapeutic agent in MCF-7 cells.** (A) Representative FACS analysis of Annexin V/PI-stained cells. Apoptosis was assessed using Annexin V staining and FACS analysis. Cells were treated with 1 µM ATRA, treated with 2 µM Dox or received a combined treatment of ATRA and Dox of similar concentrations, 1 µM and 2 µM respectively, for 48 hrs. (B) Summary of the data shown in A. The numbers indicate percentage of positive apoptotic cells compared to control. Data are expressed as the mean ± SD of three independent experiments.

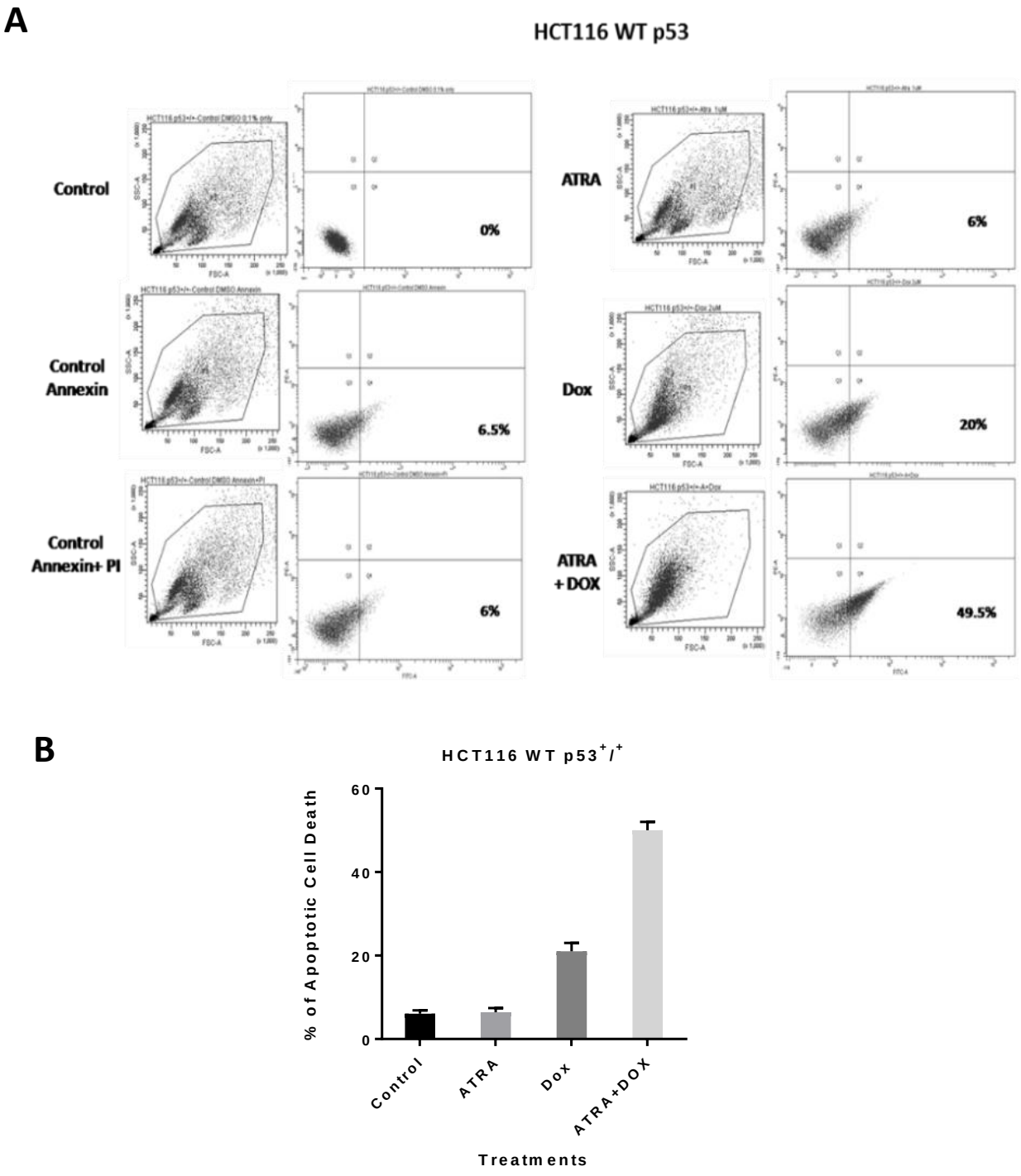

Figure 3.21: ATRA enhances apoptotic cell death in combination with chemotherapeutic agent in HCT116 cells. (A) Representative FACS analysis of Annexin V/PI-stained cells. Apoptosis was assessed using Annexin V staining and FACS analysis. Cells were treated with 1 µM ATRA, treated with 2 µM Dox or received a combined treatment of ATRA and Dox of similar concentrations, 1 µM and 2 µM respectively, for 48 hrs. **(B)** Summary of the data shown in A The numbers indicate percentage of positive apoptotic cells compared to control. Data are expressed as the mean ± SD of three independent experiments.

3.4 The positive feed-back loop between Stra6 and p53:

3.4.1 ATRA increases the expression of p53 through Stra6

The results obtained by the study so far have verified that ATRA is not able to induce cell death or upregulate p53 protein level without a DNA damage response provoked by DNA damaging agents. Therefore, to understand whether this effect is mediated by Stra6 (as it is one component of the retinoic signalling pathway), the HTC116 (p53 +/+) shStra6 was used as the experimental cell line model. To evaluate whether this cell line has indeed a suppressed expression of the Stra6 gene, the cells were treated with 2 µM of ATRA for 24 hrs. The Stra6 mRNA levels were assessed with qPCR and the Stra6 protein expression levels were assessed by immunoblotting. Results obtained from both qPCR and WB analysis demonstrated no increase in Stra6 at the transcriptional and transitional levels, respectively, as expected (Figure 3.22 A and B).

Once the efficiency of the ShStra6 was confirmed, the impact of Stra6 absence on p53 upregulation in response to DNA damage and ATRA was evaluated. WB was performed in HCT116 ShStra6 and EJp53 shStra6 cells, as shown in Figures 3.22 C and D. It was observed that p53 protein levels are depleted significantly in cells that lack Stra6 after a combined treatment of ATRA (1 µM) and Dox (2 µM) for 24 hours compared to a wild type cell model that possesses Stra6. Moreover, a similar observation was observed in EJp53 cell lines, where p53 induction was regulated by removal of tet from media for 48 hours and incubated with 1 µM of ATRA for 24 hours on both cell lines of EJp53 sh-Luciferace and sh-Stra6. There was a noticeable depletion in p53 protein levels in the absence of Stra6 compared to control cells, which suggested that p53 upregulation in response to DNA damage is enhanced by the presence of Stra6 (Figure 3.22). This is consistent with the fact that ATRA, which induces Stra6, enhances p53 responses.

Further investigations were necessary to determine the role of p53 on Stra6 upregulation in response to DNA damage and ATRA, since our earlier results that were presented in section 3.2.2 have shown a synergistic effect regarding Stra6 upregulation when Stra6 was induced by p53 after DNA damage and when Stra6 was induced after ATRA treatment. The combined treatment of ATRA and DNA damaging agents demonstrated the synergy of both treatments in producing more Stra6 mRNA and protein levels than solo treatments. We conducted western blot and qPCR in U2OS p53 null cells and in HCT116 p53 null cells, as shown in Figure 3.23. While ATRA could induce Stra6 expression, DNA damaging agents did not in the absence of p53. Our results demonstrated the importance of p53 after DNA damage for upregulating Stra6 on both transcriptional and transitional levels.

Both p53 and Stra6 have shown to be involved in inducing cell death after ATRA and DNA damage response induction by DNA damaging agents. Hence, the absence of p53 and Stra6 had a great impact on cell fate, as shown in Figure 3.24, which was determined by PI Staining and FACS analysis on EJp53 sh-Stra6 and HCT116 sh-Stra6 as well as on U2OS p53 null cells. The cells that lacked p53 or Stra6 tended to be arrested or in other means they tended to show less cell death compared to their counterpart's wild type cells after ATRA and DNA damage response.

These results were extended by assessing apoptotic cell death using Annexin V staining and FACS analysis in HCT116 WT p53 sh-Stra6 and HCT116 p53 null cells. In Figure 3.25, the results demonstrated that both Stra6 and p53 cooperate in the induction of apoptotic cell death after a combined therapy of ATRA and DNA damage agents. The results indicate a reduction in apoptotic cell death, regardless of if the cells did not have p53 or Stra6 genes when compared to their counterpart WT cells.

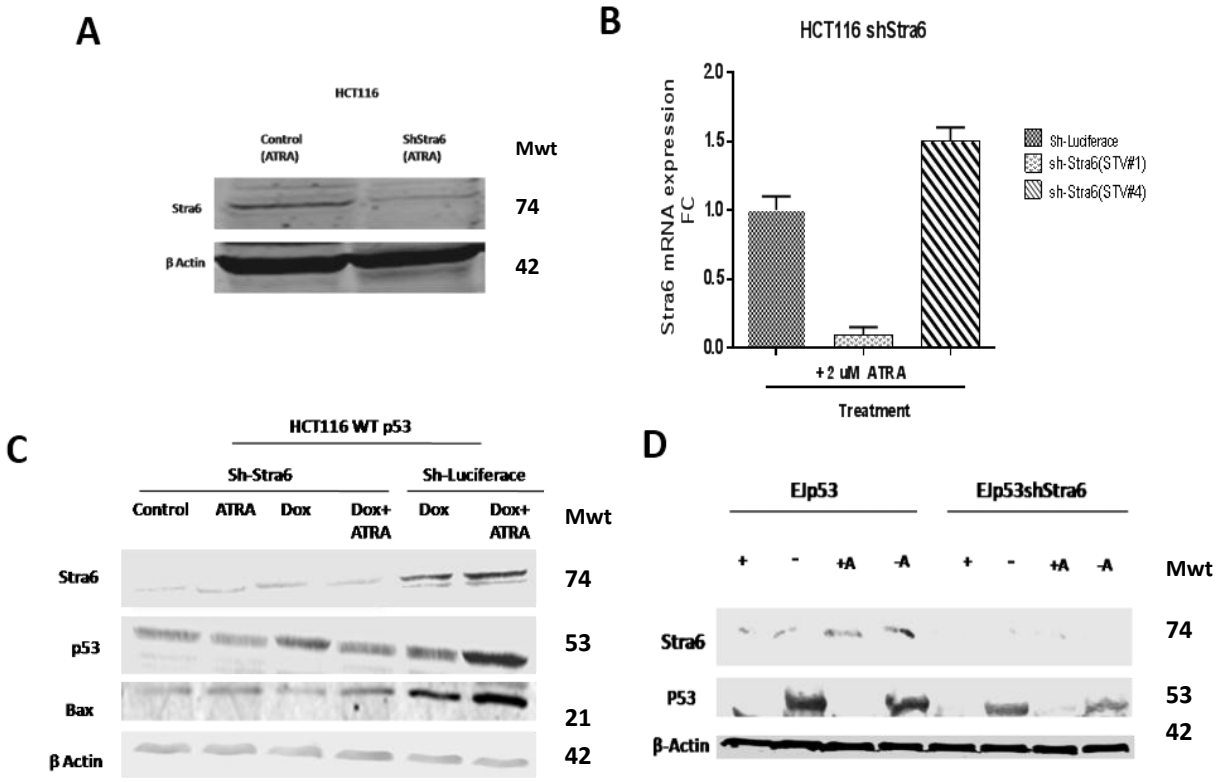

Figure 3.22: ATRA increases the expression of p53 through Stra6. **(A)** A WB of HCT116 WT p53 sh-Luciferase to assess the Stra6 protein levels in Stra6 knock down mode (sh-Stra6) under the stimulation of 2 µM of ATRA for 24 hrs incubation time was conducted. **(B)** RNA was isolated from HCT116 sh-Stra6 cells with two different ShRNA against Stra6 (numbers 1 and 4) to silence Stra6 gene expression. These were prepared previously in the laboratory. To determine which cell line would be used for later experiments, cells were treated with 2 µM of ATRA for 24 hrs. Stra6 mRNA levels are expressed as a fold change compared to the HCT116 sh-Luciferace control and is normalised to β-actin as loading control. Data represent the mean ± SD of three independent experiments **(C)** p53 protein levels are depleted significantly in cells that lack Stra6 after a combined treatment of ATRA (1 µM) and Dox (2 µM) for 24 hrs compared to the wild type cells that possess Stra6. **(D)** A similar observation is can be seen in EJp53 cell lines, where p53 induction was regulated by removal of tet from media for 48 hrs and incubated with 1 µM of ATRA for 24 hrs for both cell lines of EJp53 sh-Luciferace and sh-Stra6 cells. Mwt was indicated in (kDa).

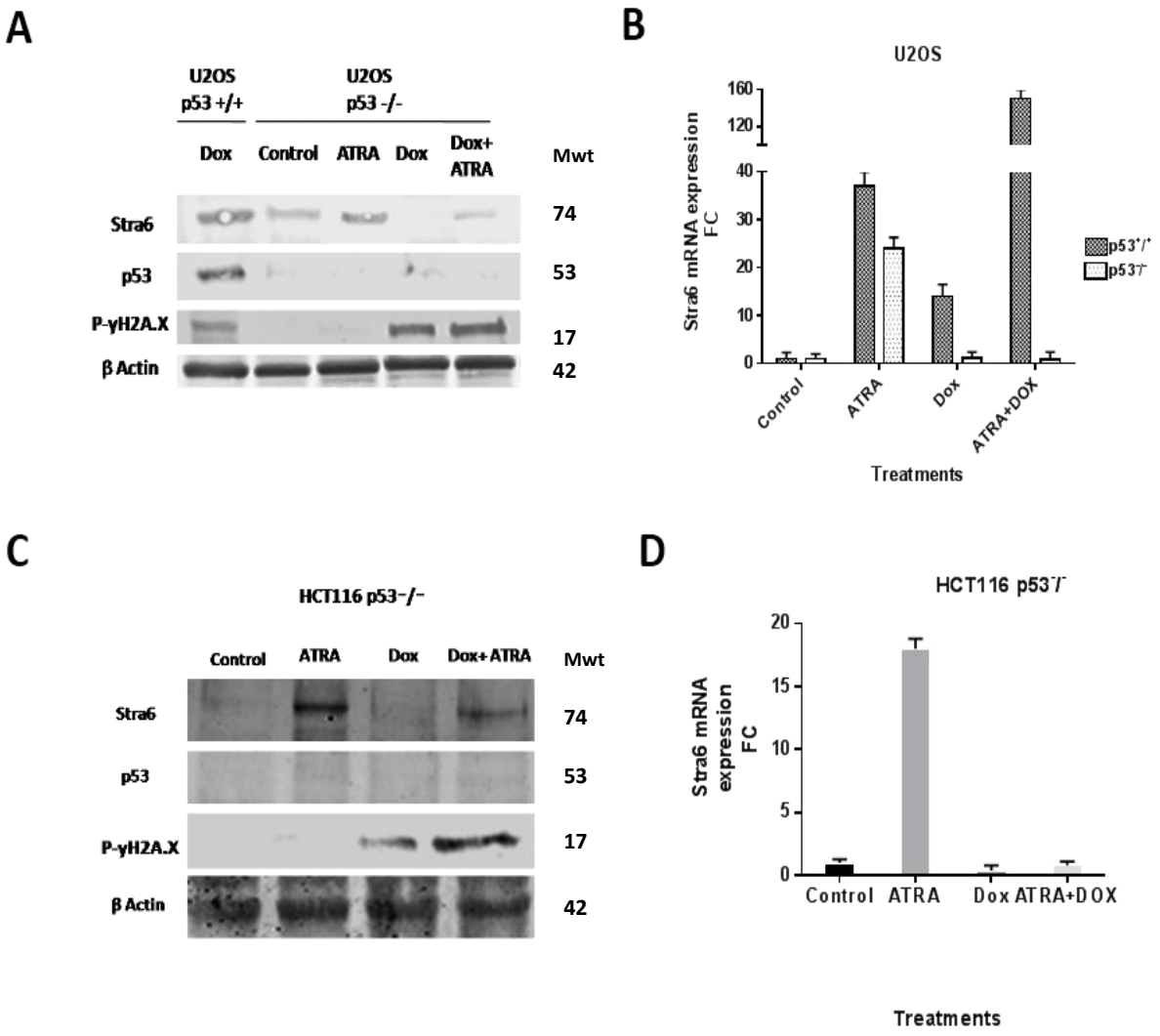

Figure 3.23: p53 control the transcriptional and transitional activity of Stra6 after DNA damage and not ATRA. (**A &C)** Western blots of U2OS and HCT116 (p53 null) cell lines demonstrated that Stra6 protein levels are down-regulated significantly after 24 hrs in cells treated with 1 µM of ATRA and 2 µM of Dox. P-ϒH2A.X is used as a control for DNA damage response and β- Actin is used as a loading control. WB results are representative of similar results of three independent experiments. (**B & D)** RNA was isolated from U2OS and HCT116 (p53 null) cells. Stra6 mRNA levels cannot upregulate under 1 µM of ATRA stimulation compared to WT p53 counterparts. Stra6 mRNA levels are significantly suppressed in the p53 null cell models where cells are treated with a combination of 1 µM of ATRA and 2 µM of Dox for 24 hrs. Stra6 mRNA levels are expressed as a fold change compared to the control and are normalised to β-actin as loading control. Data represent the mean ± SD of three independent experiments. Mwt was indicated in (kDa).

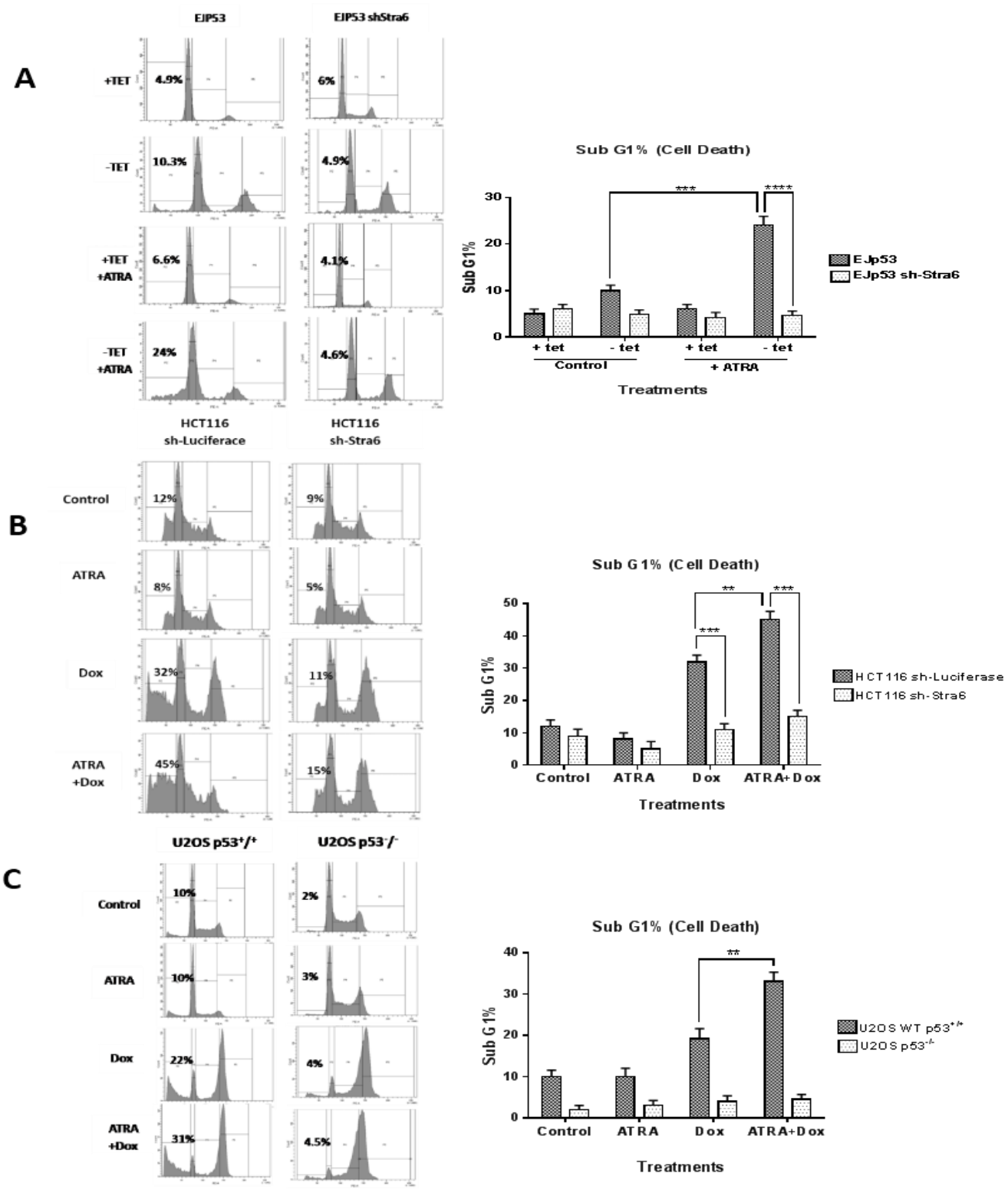

Figure 3.24: **Cells that possess Stra6 favour cell death rather than cell cycle arrest dependent on p53. (A, B and C)** The graphs show representative cell death profiles that were measured by PI staining using FACS analysis. ATRA increases cell death in response to p53 after using DNA damaging agents through Stra6 in a p53 dependent manner. Cells were treated with 1 µM ATRA, 2 µM Dox or received a combined treatment of ATRA and Dox for 24 hrs. The numbers indicate percentages of Sub-G1 events of cell death. Data are expressed as a mean of three independent experiments. **p<0.01, ***p<0.001 and ****p<0.0001.

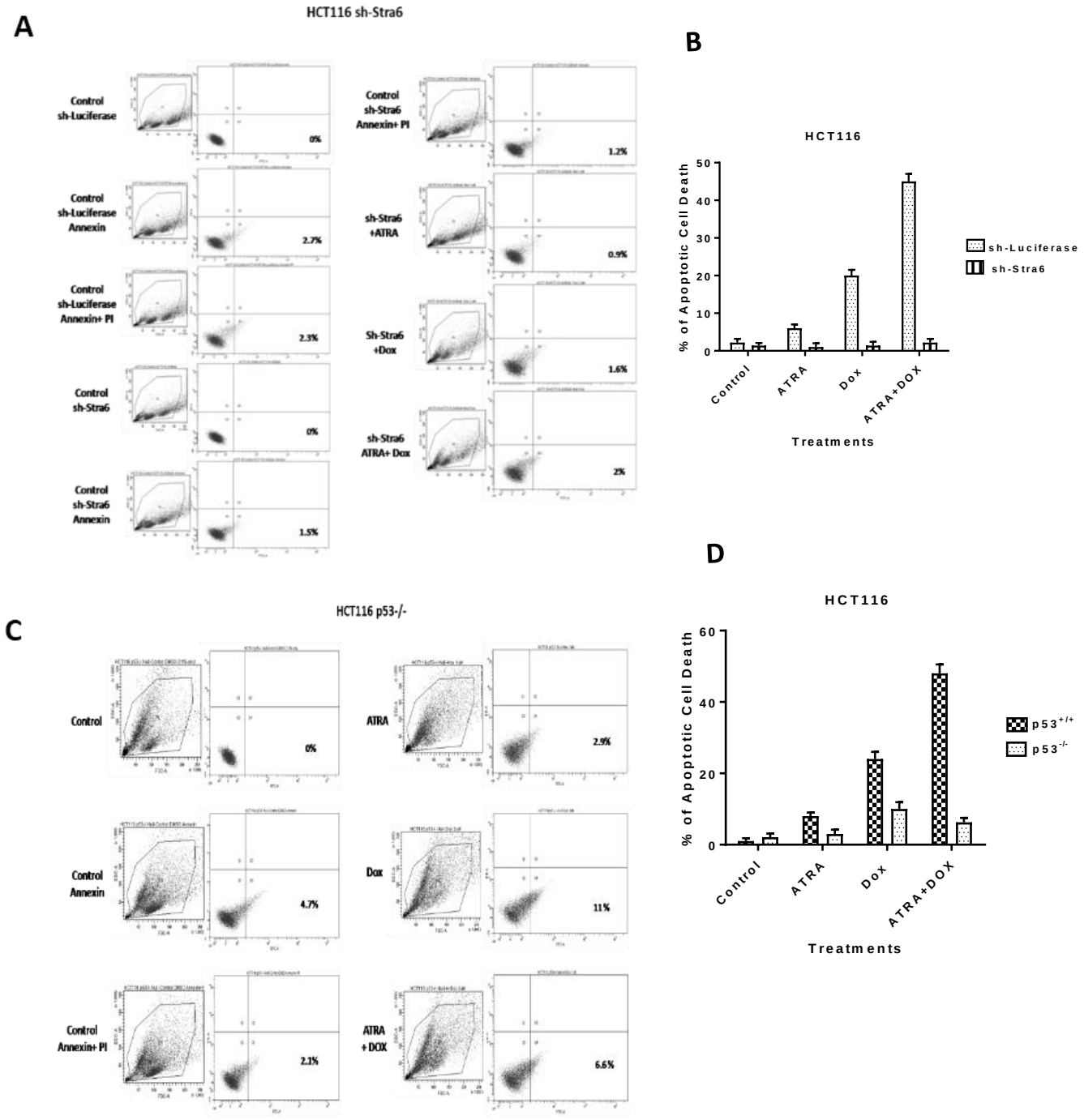

Figure 3.25: Both Stra6 and p53 genes are equally important for apoptotic cell death induction. (A & C) Apoptosis was assessed using Annexin V staining and FACS analysis in HCT116 WT p53 sh-Stra6 and HCT116 p53 null cells. Cells were treated with 1 µM ATRA, treated with 2 µM Dox or received a combined treatment of ATRA and Dox of similar concentrations, 1 µM and 2 µM respectively, for 48 hrs. **(B & D)** The graphs represent cell death as a percentage in positive apoptotic cells. Data are expressed as the mean ± SD of three independent experiments.

3.4.2 Stra6 induces p53

Given the previously obtained results (Figure 3.22), which showed that responses to p53 expression increases after DNA damage via Stra6, we wanted to explore the possibility of whether Stra6 itself could induce p53, as suggested by our results, and upregulate the retinoic acid receptors (RARα and RARβ).

As seen in Figure 3.26A, EJp53 cells under the regulatory effect of tet do not express p53. Stra6, RARα and RARβ mRNA levels were quantified in cells treated with 1 μM ATRA for 24 hours or transfected with 4 μg of Stra6 for 24 hours. Stra6 mRNA levels were up-regulated much higher than the physiological levels of Stra6 induced by ATRA, with an approximately ten-fold increase. However, the retinoic acid receptors (α and β) mRNA levels were upregulated in cells treated with ATRA only and not in Stra6 transfection.

Next, EJp53 cells after tet was removed for 48 hours to permit p53 expression were treated with 1 μM of ATRA for 24 hours or transfected with 4 μg of Stra6 for 24 hours. There was a clear and significant upregulation in p53 protein level after Stra6 transfection (Figure 3.26B). To test whether this induction of p53 by Stra6 is dependent on the DNA damage response to take place, WB was performed on HCT116 $p53^{+}/^{+}$ cells treated with 1 μM ATRA for 24 hours, treated with 1.4 μM Dox for 24 hours or transfected with 4 μg of Stra6 without using any DNA damaging agents for 24 hours.

The results suggest that Stra6 induces p53 independent of DNA damage, as seen in Figure 3.26C. Moreover, it was clear that p53 protein levels depended on the received treatment. In cells treated with Dox, p53 was induced and was clearly associated with a moderate increase in Stra6 protein level. More importantly, in the cells transfected with Stra6 without using any DNA damaging agents, RARα and RARβ were not induced at all. Stra6 could induce p53 with a more potent expression level and stability compared to the p53 protein level induced after DNA damage response occurred (Figure 3.26).

3.4.3 Stra6 induces apoptotic cell death

Because Stra6 was found to induce p53 independently of DNA damage, we wanted to test whether Stra6 could also induce apoptotic cell death independently of p53.

To determine this, Annexin V staining and FACS analysis were conducted on HCT116 WT p53 ($p53^{+/+}$) and HCT116 p53 null ($p53^{-/-}$) cells after both cell types were transfected with 4 µg of Stra6. Cells were treated with 1 µM ATRA, treated with 2 µM Dox or received a combined treatment of ATRA and Dox of similar concentrations (1 µM and 2 µM, respectively) for 24 hours after 4 µg of Stra6 transfection for 48 hours. As shown in Figure 3.27, Stra6 had no influence to enhance the induction of apoptotic cell death in cells that lack TP53. In addition, Stra6 itself showed an apoptotic cell death percentage similar to those cells after using DNA damage (Dox) to induce apoptotic cell death (Figure 3.21). Overall, this shows that Stra6 overexpression induces apoptotic cell death depending on p53 and shows additive apoptotic cell death after a combined treatment of ATRA and Dox (Figure 3.27).

3.4.4 Stra6 enhances the induction of pro-apoptotic and apoptotic proteins

As shown earlier, Stra6 induces p53-independent cell death; thus, we were interested in investigating the pro-apoptotic genes such as Bax and caspases (3 and 9) after Stra6 induction by ATRA and Dox or Stra6 transfection. Furthermore, a WB was conducted to investigate whether enhancement of Stra6 induction of pro-apoptotic and apoptotic genes is dependent on p53. As shown in Figure 3.28, caspase 9, cleaved caspase 9 and Bax were all up-regulated in the JVM-3 cells treated with 1 µM of ATRA and 10 gray of radiation for 24 hours (Figure 3.28A). Moreover, caspase 3 and cleaved caspase 3 were also up-regulated in HCT116 WT p53 cells but not in HCT116 p53 null cells after transfection with 8 µg of Stra6 for 48 hours with a panel of varying treatments (Figure 3.28B and C). This shows that Stra6 enhances the induction of pro-apoptotic and apoptotic proteins dependent on p53.

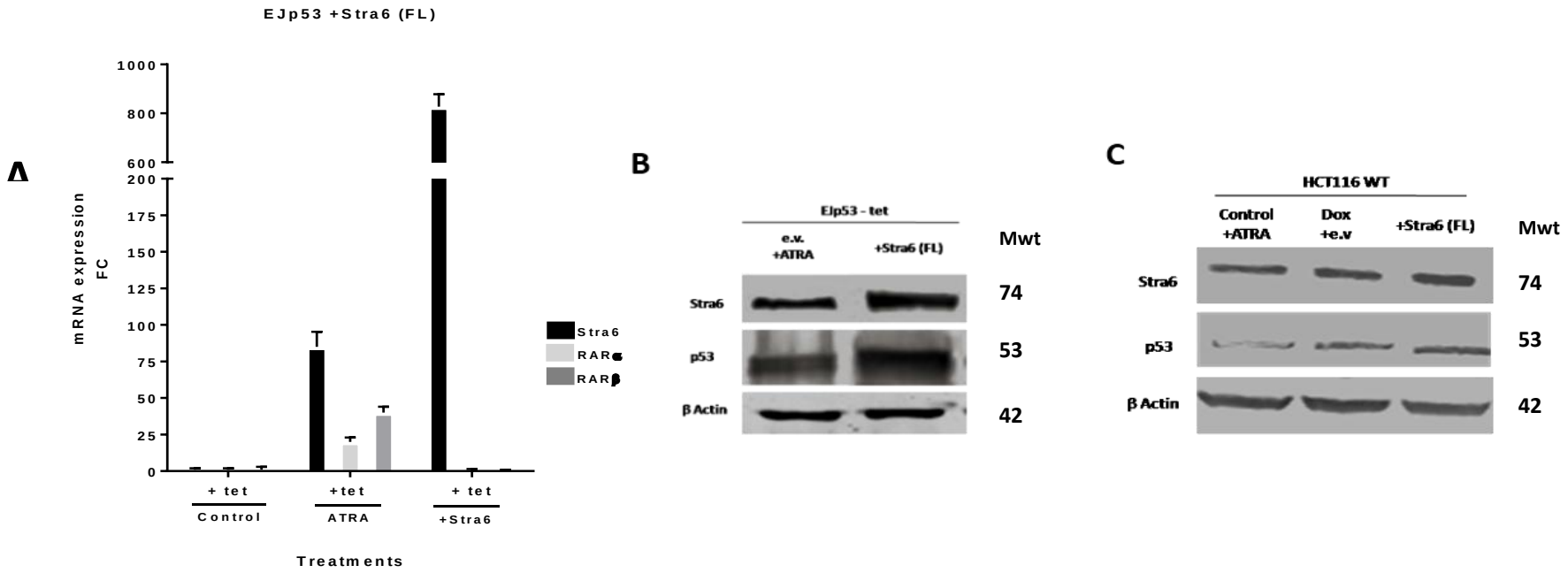

Figure 3.26: **Stra6 induces p53. (A)** EJp53 cells under the control of tet were either treated with ATRA (1 µM, 24 hrs) or transfected with 4 µM of Stra6 for 24 hrs. Stra6 mRNA levels were up-regulated in a 10-fold increase after Stra6 transfection, and the retinoic acid receptors (α and β) mRNA levels were upregulated only in ATRA treated cells but not in Stra6 transfection. Data are expressed as fold changes compared to the control and are normalised to GAPDH as a loading control and represent the mean ± SD of three independent experiments. **(B)** EJp53 cells express p53 induction after 48 hrs of tet removal. Cells were transfected with an empty vector (e.v.) and treated with 1 µM of ATRA for 24 hrs or transfected with 4 µg of Stra6 for 24 hrs. There was a clear upregulation in p53 expression after Stra6 transfection. β-actin was used as a loading control. **(C)** Similar to the previous experimental conditions in **(B),** to induce p53, the HCT116 WT p53 cells were treated with 1.4 µM of Dox for 24 hrs. The levels of p53 protein were determined and its up-regulation was clearly associated with Stra6 and not related to ATRA or to the downstream retinoic acid receptor as shown in (A) after the cells were transfected with 4 µg of Stra6 (FL) for 24 hrs without using any DNA damaging agents.

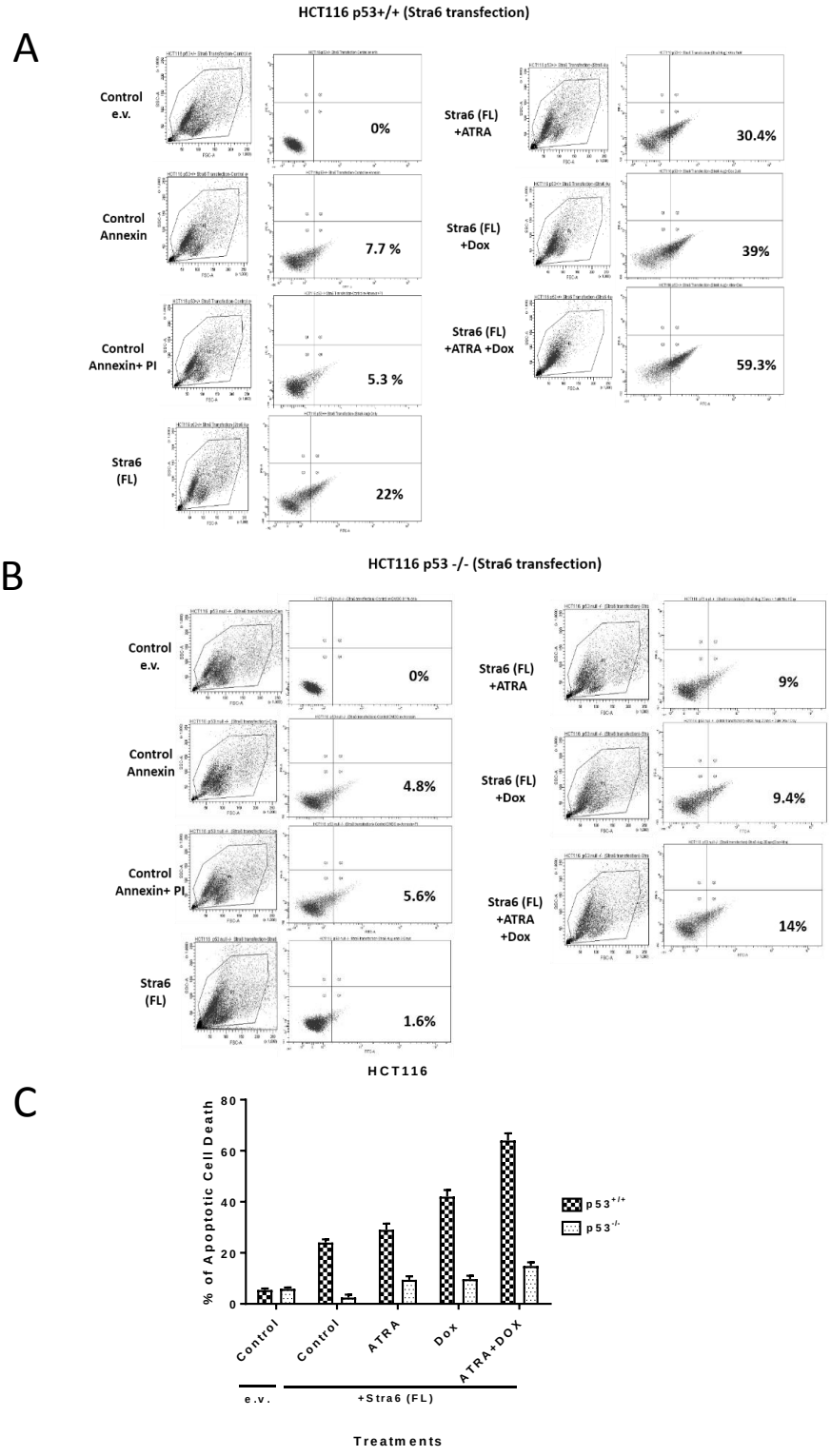

Figure 3.27: **Stra6 induces apoptotic cell death dependent on p53**. **(A)** Apoptosis was assessed using Annexin V staining and FACS analysis in HCT116 WT p53 or HCT116 p53 null cells. Split cells were treated with 1 µM ATRA, treated with 2 µM Dox or received a combined treatment of ATRA and Dox of similar concentrations (1 µM and 2 µM, respectively) for 24 hrs after 4 µg of Stra6 transfection for 48 hrs. **(B)** Stra6 has no influence to enhance the induction of apoptotic cell death in cells that lack TP53. The numbers indicated in percentages of positive apoptotic cells in the same conditions, expressed as the mean ± SD of three independent experiments.

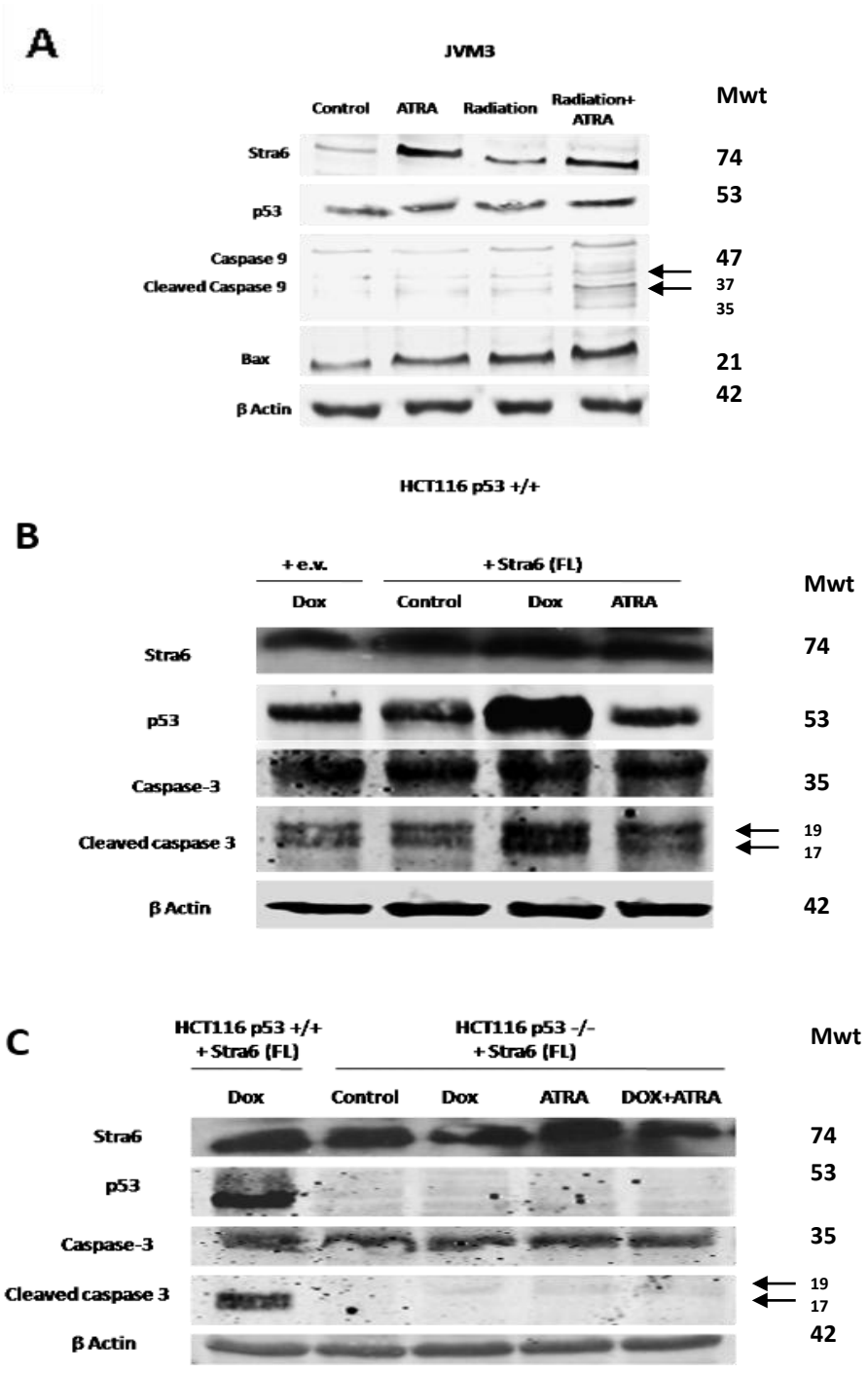

Figure 3.228: **Stra6 enhances the induction of pro-apoptotic and apoptotic proteins dependent on p53. (A)** Caspase 9, cleaved caspase 9 and Bax were all up-regulated in the JVM-3 treated cells with combined treatment of 1 µM of ATRA and 10 gray of radiation for 24 hrs. **(B)** Caspase 3 and cleaved caspase 3 were also up-regulated in HCT116 WT p53 cells after transfection with Stra6 (8 µg, 48 hrs) and treated with Dox 2 µM, ATRA 1 µM for 24 hrs or transfection with an empty vector (e.v.) and treated with Dox 2 µM for 24 hrs. **(C)** HCT116 p53 null cells after Stra6 transfection and treatments in a similar condition to (B) did not detect cleaved caspase 3. β-actin is used as a loading control.

3.5 Stra6 and Reactive Oxygen Species (ROS)

3.5.1 Determining the effect of ATRA and DNA damage on ROS generation

We have previously shown that Stra6 can induce ROS and this has an impact on p53 cell function (Carrera et al., 2013). We next studied whether Reactive Oxygen Species (ROS) levels correlated with the observed synergistic effect of ATRA and DNA damage on upregulation of p53 and p53 target genes in response to the induction of apoptosis in JVM-3, U2OS and HCT116 cells.

As shown in Figure 3.29, measurements of ROS mean fluorescence intensity (MFI) indicated a significant increase in stimulated cells that received combined treatments of ATRA and Dox, compared to ROS levels in cells treated with ATRA or Dox alone. Of note, JVM-3 cells showed much higher ROS levels than U2OS and HCT116 cells. This is consistent with our previous results.

3.5.2 Stra6 induces ROS

Further, we also studied whether Stra6 induces ROS by measuring ROS levels in HCT116 (p53 $^{+}/^{+}$) sh-Stra6 and transfecting HCT116 (p53 $^{+}/^{+}$) with Stra6 to assess Stra6 role towards ROS generation.

Figure 3.30A depicts the ROS measurements in the HCT116 WT p53 sh-Stra6 model, which is accompanied by a strong overall reduction in MFI fold change compared to the result of HCT116 WT p53 shown in Figure 3.29C. Moreover, the HCT116 WT p53 cells after transfection with 4 µg of Stra6 for 48 hrs with or without using an ATRA and Dox combined treatment indicated a significant increase of ROS in the presence of both stimuli (Figure 3.30B). Our results suggest the importance of endogenous Stra6 to mediate ROS generation and confirmed that Stra6 induces ROS accumulation within the cells. Moreover, Stra6 transfected cells demonstrate ROS induction similar to that yielded by Dox alone, as shown in Figure 3.29C.

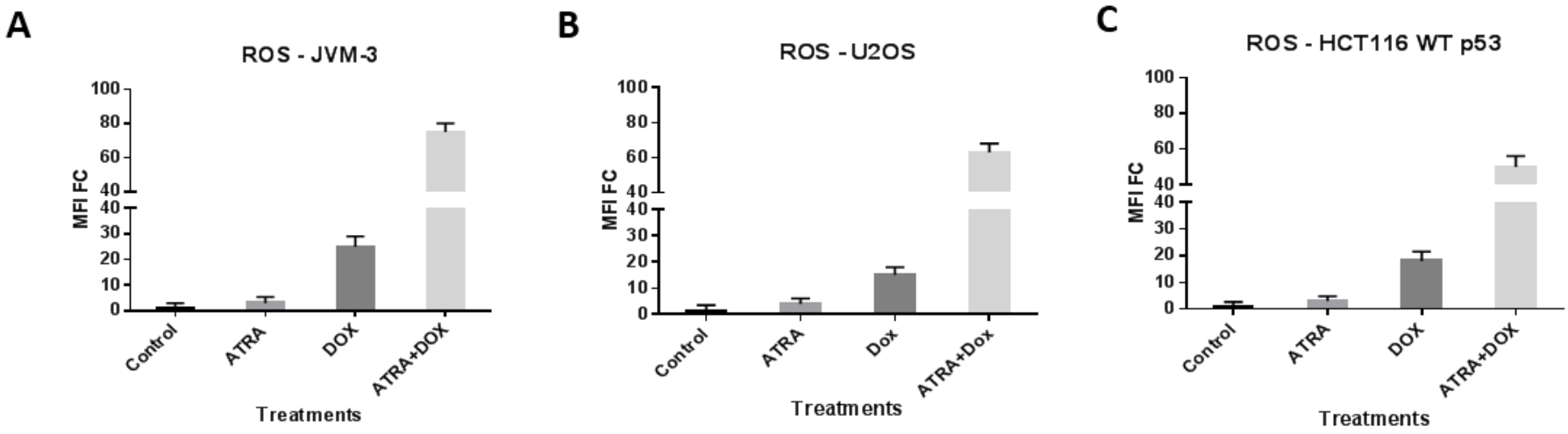

Figure 3. 29: **Measurements of reactive oxygen species MFI fold change in JVM-3 and U2OS cells (A, B & C).** The graphs show the levels of ROS produced in JVM-3 cells and U2OS cells after treatment with 1 µM of ATRA or 2 µM of Dox and with both ATRA and Dox of similar concentrations for a 24-hr incubation time. The results indicated a significant increase in mean fluorescence intensity of stimulated cells compared to ROS levels in cells treated with ATRA or Dox alone. Data are expressed as the fold change compared to control cells and as the mean ± SD of three independent experiments.

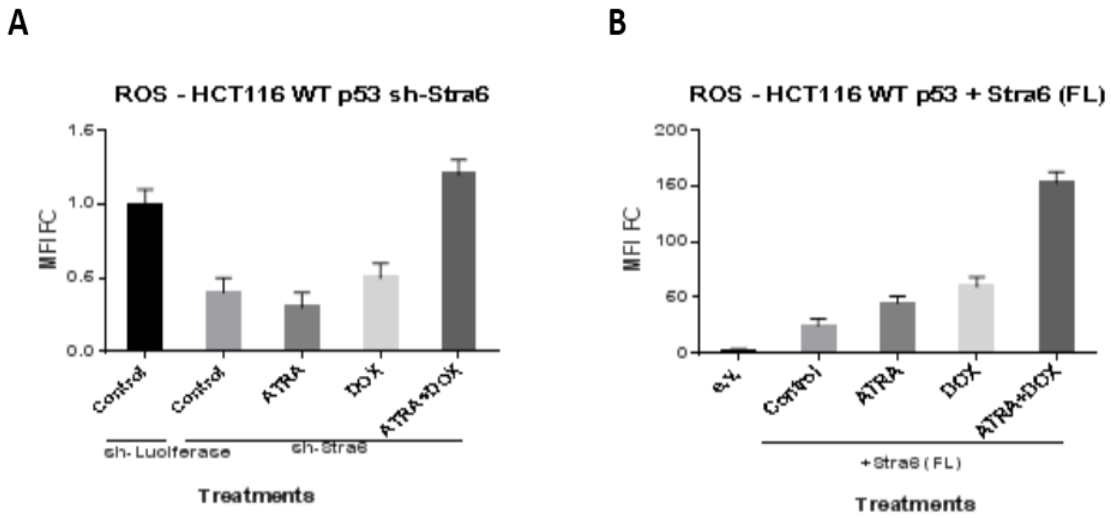

Figure 3. 30: **Stra6 induces ROS**. **(A)** This figure depicts ROS measurements in the HCT116 WT p53 sh-Stra6 model, which are accompanied by a reduction in MFI fold change. **(B)** HCT116 WT p53 after 4 µg of Stra6 (FL) transfection for 48 hrs with or without treatments indicate an increase in ROS production with an ATRA and Dox combined treatment approach. Data are expressed as the fold change compared to control cells and as the mean ± SD of three independent experiments**.**

3.5.3 The effect of ROS inhibitors on p53 levels

As this study has shown, higher ROS levels are associated with the induction of apoptosis in response to ATRA, dependent on activation of the p53-DNA damage response. Additionally, higher ROS levels correlated with the induction of Stra6, which consequently induces apoptotic response.

To extend these results, we tested whether Stra6 induction of ROS (Carrera et al., 2013) and the higher p53 protein levels associated with Stra6 transfection could be due to the fact that Stra6 induces p53 through ROS generation, as we hypothesized.

To test this hypothesis, the levels of intracellular ROS after cells were treated with Glutathione (GSH) or N-acetyl-L-cysteine (NAC), as shown in Figure 3.31A. MFI levels of ROS decreased in EJp53 cells cultured in the absence of tet and treated with ATRA or transfected with Stra6. In addition, ROS levels, as shown in Figure 3.31B, decreased in HCT116 WT p53 treated with GSH or NAC after a combined treatment of ATRA and Dox or transfection with Stra6. Both cell lines were compared to their respective control ROS levels with no GSH/NAC added, which demonstrated higher levels of ROS induction either by ATRA and tet removal or Dox or else by Stra6 transfection only (Figure 3.31). This suggest that Stra6 was responsible on ROS generation that was associated with p53 induced apoptosis.

p53 protein levels showed a significant reduction in p53 induced by Stra6 after cells were treated with GSH or NAC (Figure 3.32). This suggests that Stra6 possibly induces p53 through an ROS generation mechanism, as both GSH and NAC may reduce p53 to its basal level.

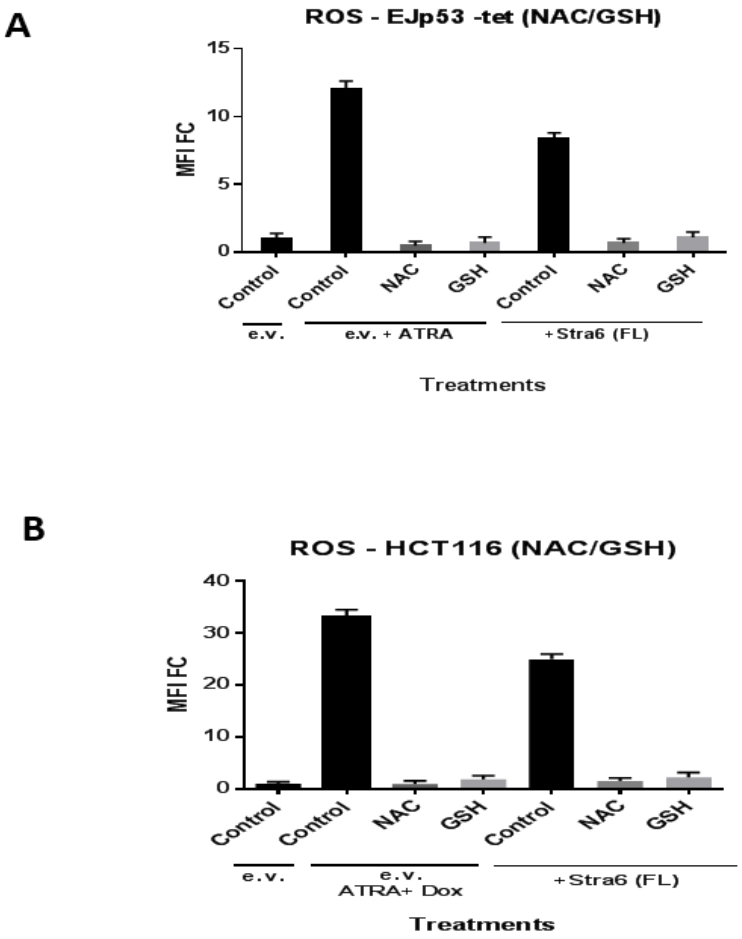

Figure 3. 31: Determining the influence of Stra6 on ROS generation using an ROS inhibitor (NAC/ GSH). (A) EJp53 cells were cultured without tet for two days to induce sufficient p53 expression. Cells were treated with 1 µM of ATRA in addition to an ROS inhibitor (NAC, 2 µM, 10 mM and GSH) for 24 hrs, or cells were transfected with an empty vector (e.v.), with Stra6 4 µg for 48 hrs alone or with an ROS inhibitor for 24 hrs. A significant depletion of ROS was observed after using ROS inhibitors, as expected. **(B)** Significant suppression of ROS was observed in HCT116 WT p53 cells. To induce p53 in HCT116 WT p53 cells, dox was used at a concentration of 2 µM for 24 hrs. Data are expressed as the fold change compared to the controls and as the mean ± SD of three independent experiments.

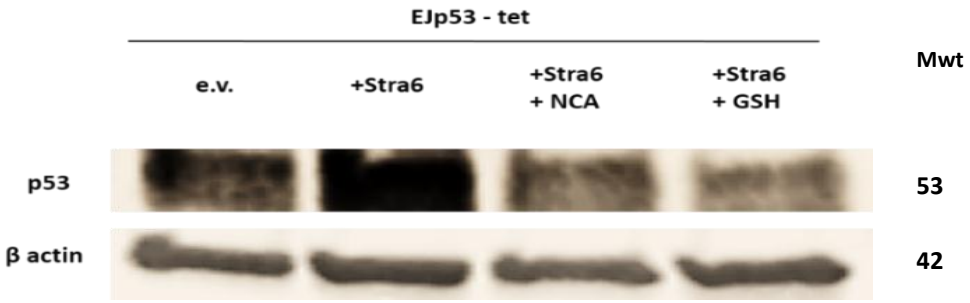

Figure 3. 32: **Stra6 induction of p53 operates through ROS production**. WB of EJp53 cells was conducted, and tet was removed from media for two days to induce a sufficient p53 expression. Cells were transfected with an empty vector (e.v.), with a Stra6 8 µg for 48 hrs alone or with an ROS inhibitor (NAC, 10 mM and GSH, 2 µM) for 24 hrs. A substantial reduction of p53 protein level was observed after using an ROS inhibitor. β-actin was used as a loading control. n=3

3.6 Discussion

Drug resistance is a major concern for cancer patients with recurrent relapses of leukaemia/lymphoma or tumours and it has been the main obstacle in achieving effective cancer treatment (Duesberg et al., 2007; Roberti et al., 2006). To overcome drug resistance, scientists have been examining the use of a combined treatment approach. For example, retinoic-acid based treatments in combination with anticancer drugs have been successful (Sun et al., 2015).

However, the involved signalling pathways and underlying mechanisms of this combined therapeutic regime were unclear. In general, the retinoic acid compounds, which can be either natural, such as ATRA, or synthetic, such as Fenretinide, have functions such as regulation of cell growth, differentiation and apoptosis. However, these effects are dependent on the concentration and exposure time (Hsu et al., 2000; Zhang et al., 2003; Okada et al., 2000). Moreover, retinoic acid can potentially treat and prevent cancers due to its antiproliferation and chemoprevention characteristics (Choi et al., 2003).

To provide molecular evidence of successful combined treatments of cancer cells pre-treated with ATRA as a sensitiser to DNA damaging agents (chemotherapy and radiation) the presented work was done. Because Stra6 is a retinoic acid responsive gene, its expression can be induced by retinoids and it has been shown to express and contribute to cell death after DNA damage (Carrera et al., 2013). Thus, the roles of Stra6 and p53 were investigated in the present study.

In most of these experiments, cells were cultured in four groups. The first group was the negative control with no treatment; the second group was treated with ATRA; the third group was treated with DNA damaging agents, including Dox or ionising radiation; and the forth group was a pre-treatment of ATRA followed by DNA damaging agents.

Concentrations of ATRA, Dox and gamma radiation were determined based on literature and recommendations from other users. We aimed to achieve a successful cell death (apoptosis) with minimal concentrations. The tested concentration of ATRA (1 μM) was a physiological concentration and did not induce cell cycle arrest or apoptosis, as these two cellular events require a higher concentration of ATRA (starting from 10 μM) to be induced (Huang et al., 2006; Mao et al., 2006; Mandegary & Mehrabani, 2010).

A Dox of 1.4 - 2 μM was the concentration of choice to be used in all our experiments, as this concentration had demonstrated its ability to elicit p53-induced apoptosis in cultured cell lines (Lüpertz et al., 2010). The applied radiation dose was 10 gray, as this dose and time can induce p53 apoptotic cell death in cultured cell lines based on previous studies (Allan & Fried, 1999; Vucic et al., 2006).

In our p53-inducible model, EJp53 cell lines that regulated by a tet off system, we have shown upregulation of Stra6 mRNA (Figure 3.1) and Stra6 protein levels (Figure 3.3) with a synergistic effect of ATRA treatment in response to p53 induction. Moreover, the p53 protein levels were accumulated and stabilised more with ATRA treatment compared to tet removal alone. Since we have observed previously that Stra6 is induced by p53 (Carrera et al., 2013), this strongly suggests that there was a positive feedback loop between the Stra6 and p53.

Previous studies have indicated that p53 induced Stra6 has no role on the regulation of downstream signalling pathway, such as RARα and RARβ mRNA levels (Carrera et al., 2013). The current study confirms these results, as shown in Figure 3.1. ATRA treatment regulated the mRNA levels of RARα and RARβ, as expected. However, the upregulated levels of these two retinoic acid receptors displayed different patterns that suggested different cellular functions. Figure 3.1 demonstrates that in ATRA treated cells the RARβ is

upregulated more than the RARα. RARβ has shown the tendency to support cell proliferation, differentiation and survival (Zhuang et al., 2003).

When p53 is induced and ATRA is applied, the RARα is upregulated more than the RARβ, which suggests that ATRA response to DNA damage drives cells in the opposite direction of cell proliferation towards more tendency of growth inhibition. This is consistent with previous experimental studies, which have shown that RARα plays an important role in cell-cycle arrest and growth inhibition (Boyle et al., 1999).

Similar results have been observed in HCT116, U2OS and JVM-3 cell lines, which demonstrated a clear, significant upregulation of Stra6 mRNA levels and a potentially synergistic effect of the combined treatments of ATRA and Dox (Figure 3.2). Moreover, RARβ mRNA levels were upregulated more after ATRA treatment than RARα mRNA levels, but RARα were upregulated more than RARβ mRNA levels after ATRA and DNA damage induction by Dox. This could determine the role of the ATRA pathway in enhancing DNA damaging signals.

Consistent with Stra6 mRNA levels, the Stra6 protein levels demonstrated a significant increase in the combined treatment of ATRA and DNA damaging agents, either by Dox or radiation, in cancer cell lines including HCT116, U2OS, MCF-7, PA-1, H460, KIS, D0HH2 and JVM-3, as shown in Figures 3.4, 3.5, 3.6, 3.7, 3.8, 3.9, 3.10, and 3.11, respectively.

Moreover, the p53 protein stability was significantly enhanced with more p53 protein accumulated in the cells after ATRA treatment (1 μM) with DNA damaging agents compared to p53 protein levels induced by DNA damaging agents alone. In line with this effect, a study done by Ablain et al. (2014) demonstrated that high levels of RA (100 mg) combined with arsenic trioxide stabilised p53 with an associated triggered increase in PML-RARα fusion protein degradation in PML. Moreover, the researchers suggested that p53 stabilisation was not affected by RA downstream signalling pathway when they conducted a p53 gene transcript analysis study (Ablain et al., 2014).

The cellular and molecular mechanisms involved in this treatment efficiency are still unclear. The current data suggest that both Stra6 and p53 may play an important role in cell death since ATRA alone did not induce the p53 protein (Figures 3.4-3.11), this indicates that its ability of inducing cell death is mediated by an enhancement of DNA damaging signals.

We further explored the effect of ATRA and DNA damaging agents on both cellular metabolism and morphological changes on EJp53 and JVM-3 cell lines. In Figure 3.12, cell viability was a direct screening method to test our hypothesis. ATRA showed a slight increase in cell viability compared to cells that received a combined treatment of ATRA followed by Dox within three days of continuous cell viability assessment. In addition, the combined treatments significantly reduced cell viability counts versus Dox treatment alone.

Previous studies have indicated that 1 µM of ATRA does not affect cell viability for 48 hours, whereas cell viability is reduced to 30% with a 10 µM concentration (Huang et al., 2006; Mandegary & Mehrabani, 2010). We observed that the combined treatment of ATRA and Dox caused a significant loss of viability of JVM3 cells compared to Dox alone. Of note, cell proliferation was enhanced significantly after ATRA treatment.

A study conducted by Mandegary & Mehrabani (2010) observed similar effects of ATRA treatment. However, cell proliferation was reduced significantly after an ATRA and Dox combined treatment compared to Dox treatment alone. This reduction in cellular metabolic activity could be associated with cell death or cell cycle arrest.

Consistent with this, cellular morphological changes were detected in characterised apoptotic cells with a higher degree of cell deterioration after ATRA treatment and p53 induction compared to p53 induction alone by tet removal or Dox in EJp53 and JVM-3 cells as shown in Figures 3.14 and 3.15, respectively.

On the contrary, EJp53 and JVM-3 have shown no more changes in cell morphology after ATRA treatment alone. A study indicated that 1 µM of ATRA after 72 hours induced cell differentiation in human myeloid leukaemia HL-60 cells (Huang et al., 2006).

We suggest that endogenous Stra6 may play different roles. First, in response to ATRA, based on study done by Berry et al. (2012), Stra6 facilitates cellular growth by tyrosine phosphorylation of the Stra6 receptors and JAK2/STAT5 signalling pathway activation, thus causing STAT5 translocation to the nucleus where downstream regulation and expression of target genes takes place, including regulation of cell differentiation and proliferation. Second, in response to ATRA treatment in the context of DNA damage-induced p53, Stra6 levels are highly upregulated and contribute to cell death. This suggests an involvement of Stra6 in another signalling pathway that would results in cell death induction.

The results of this study also show the ability of ATRA to determine cell fate decision by shifting the status of cell from cell cycle arrest to cell death response in the presence of p53 activation. Thus, ATRA could be used to sensitise cancer cells to DNA damage and thus enhance cell death induction. This was confirmed through Annexin V staining and FACS analysis, which determined that a combined treatment approach of ATRA and Dox significantly enhances apoptotic cell death after DNA damage using Dox compared to apoptotic cell death induction of Dox alone (Figures 3.17-3.21).

Many previous studies have indicated that combination therapy with ATRA and DNA damage agents provides better outcomes for cancer therapy than monotherapy (Gianni et al., 1998; Mandegary & Mehrabani, 2010; Jiang et al., 2011), which is consistent with our results. The novelty of our data lies on the fact that we propose that these sensitizing effects of retinoids may be mediated by Stra6, which we show is induced by retinoids and has a pro-apoptotic function in the context of the p53 pathway.

Though the study verified that cancer cells treated with 1 µM of ATRA are not able to induce cell death or cell cycle arrest and that the p53 protein level was not upregulated after ATRA treatment alone, the mechanisms behind this process were still unknown. Thus, we aimed to determine the underlying factors that upregulate the activity and stability of p53 protein levels towards enhanced apoptotic cell death after combined treatments of ATRA and DNA damaging agents compared to the p53 protein levels after treatments with DNA damaging agents alone. After confirming the efficiency of the shStra6 cell lines their readiness for use in further experiments (Figure 3.22 A and B), we observed that DNA damage-induced p53 protein levels are significantly depleted in cells that lack Stra6 after a combined treatment of ATRA and p53 induction by Dox or tet removal, as shown in (Figures 3.22 C and D). Also, there was a slight depletion in the levels of p53 protein after Dox or tet removal in HCT116-shStra6 and EJp53-shStra6 cells, respectively, which This supports the hypothesis of a positive feedback-loop between p53 and Stra6 after DNA damage.

Thus, our results demonstrated that retinoids mediate the upregulation and stabilisation of p53 after DNA damage and that this is dependent on Stra6, and this effect stems from Stra6 only, as it is considered a retinoic acid responsive gene. Moreover, this result suggests that the observed p53 upregulation with combined treatment is not dependent on the downstream retinoic acid signalling pathways since the RARs have no influence on p53 stabilisation. If the RARs have an influence on p53 protein upregulation, the levels of p53 protein should not be depleted even in Stra6 knock down cells.

More importantly, the slight depletion of p53 protein levels in cells induce p53 after DNA damage without ATRA treatment in sh-Stra6 cell lines (3.22 C and D) indicates that the increase in induction of p53 protein stability is exclusively maintained with Stra6 gene expression.

Ablain et al. (2014) showed that induction of p53 in cells from APL mice treated with retinoic acid in medium to high doses (10 – 100 mg, respectively) can induce p53 activation and stabilisation that leads to PML-RARα degradation, which determines the p53 stability, particularly as Trp53 transcripts are unaffected by retinoic acid treatments (Ablain et al., 2014). Moreover, similar studies have suggested that retinoid-induced apoptosis in numerous cancer cells appeared to be induced by an unknown mechanism independent of retinoic acid receptors activation and mediated by the intrinsic apoptotic cell death — mainly through association with mitochondrial cell death (Hail et al., 2006).

It has been well known that p53 activation can accumulate in cells through post-translational modifications (PTM) with small changes in protein abundance. This fact generated the possibility of Stra6 being significantly engaged in p53 stabilisation. To our knowledge, this is the first study that has stated the importance of ATRA and DNA damaging agents in increasing the stability of p53 protein and restoring its activity to overcome anticancer drug resistance — mainly through the expression of Stra6.

Previous studies have considered the molecular basis that could explain why the combined treatment of retinoids and DNA damaging agents can be effective in treating cancer. For example, ATRA and Arsenic trioxide in low concentrations were previously used effectively in the treatment of APL (Ablain et al., 2014), but its underlying mechanism was still elusive. Some scientists have suggested that this therapeutic efficacy in APL might be because of Arsenic-trioxide-induced PML-RARα degradation, but this is not the only reason behind a successful combination therapy, because HL-60 cells have not shown t (15;17) rearrangement and have not expressed the PML-RARα fusion protein, but still show the same effect (Andre et al., 1996; Huang et al., 2006). The results of this study indicate that Stra6 could be the mechanism behind the success of the combined treatment of ATRA and DNA damaging agents in p53 wild type cells.

The results of this study also demonstrate a synergistic effect of combined treatments regarding Stra6 upregulation at mRNA (Figures 3.1 and 3.2) and protein levels (Figures 3.3- 3.11). We first determined that the combined treatment of ATRA and DNA damaging agents produces more significant Stra6 mRNA and protein levels than mono therapy.

In a previous report, we showed that p53 was needed to induce Stra6 after DNA damage (Carrera et al., 2013). Our current results demonstrate that Stra6 can be induced by retinoids or DNA damaging agents by independent mechanisms. For example, Stra6 expression was observed after ATRA but not Dox treatment in $p53^{-/-}$ treated cells.

This study suggests Stra6 as an important factor in whether cancer cells undergo cell cycle arrest or apoptosis in response to DNA damage and retinoid treatment. Cells that lack p53 or Stra6 tended to be arrested compared to their counterpart wild type cells after ATRA and DNA damage response. The results demonstrated that both Stra6 and p53 are important in facilitating the induction of apoptotic cell death after a combined therapy of ATRA and DNA damage agents. Generally, our results indicate an over reduction in apoptotic cell death regardless of if cells lack p53 or Stra6 genes when compared to their counterpart WT cells that possess p53 or Stra6 genes. Consistently, previous reports have indicated that endogenous Stra6 knocked down by shRNA or siRNA cells converted to be more resistant to Dox (2 µM)- or Fenretinide (15 µM)-induced apoptotic cell death. (Carrera et al., 2013; Mittal et al., 2014).

Moreover, Chen et al. (2012) showed that siRNA against endogenous Stra6 decreased the levels of active caspase-3. Similar results show reduced levels of cleaved PARP and cleaved caspase-9 when Stra6 is silenced (Chen et al., 2012; Mittal et al., 2014). Taken together, previous reports support the results of this study.

The results of this study suggest that Stra6 induces p53 independent of DNA damage response, as shown in Figure 3.26, and Stra6 can induce p53 with a more potent expression level and stability compared to p53 protein level induced after DNA damage response with Dox or tet removal in HCT116 and EJp53 cells, respectively.

Previous studies showed that the p53-induced Stra6 after DNA damage was independent of retinoic acids' downstream signalling pathway (Carrera et al., 2013). Additionally, our results provide a clear explanation of cells transfected with Stra6 without using any DNA damaging agents do not show any upregulation of RARα and RARβ, suggesting that Stra6 has another principle function in addition to be a cellular receptor for retinol uptake. Moreover, these results correlate with our previous results regarding investigation of the observed relationship between the Stra6 and p53 positive feedback loop after combined treatment of ATRA and DNA damaging agents.

The results of the current study confirm that Stra6 is capable of inducing apoptosis given its observed ability to induce p53 protein and regulate its activity and stability. Our results suggest that Stra6 has its own apoptotic function dependent on p53, as Stra6 has no influence to enhance the induction of apoptotic cell death in cells that lack TP53. Furthermore, Stra6 itself has shown apoptotic cell death percentages like those cells treated with Dox after DNA damage as observed in Figure 3.21.

In a previous study conducted on renal dysfunction and diabetic patients by Chen et al. (2012), it was proposed that Stra6 induces apoptosis because of an increased ratio of apo-RBP4 to holo-RBP4. The referred term apo-RBP indicates when no retinol is present and holo-RBP indicates that retinol binds to RBP.

This ratio affects Stra6 signalling and activates a JAK2/STAT5 signalling cascade which in turn up-regulates adenylate cyclase 6 (AC6) and cAMP,

therefore enhancing the signalling cascade of JNK1/p38 and resulting in CRBP-I/RARα suppression and apoptosis induction (Chen et al., 2012).

We show that Stra6 as an important factor in increasing the caspase-3 cleavage with Dox dependent on WT p53. Other studies have indicated that siRNA against endogenous Stra6 would decrease the levels of active caspase-3, cleaved PARP and cleaved caspase-9 (Chen et al., 2012; Mittal et al., 2014).

Moreover, the combined treatment of ATRA and DNA damaging agents have similarly shown enhancement of pro-apoptotic and apoptotic protein levels of Bax and cleaved caspase-9, respectively, which supports the hypothesis that Stra6 enhances the apoptotic cascade.

As a further step, we determined the effects of ATRA and DNA damage on ROS generation Higher levels of ROS have been suggested as crucial factors in determining the cell fate decision between cell cycle arrest and apoptosis after the cell reaches a maximum threshold of oxidative damage (Macip et al., 2003).

Our results show that ATRA induces amounts of ROS, which does not correlate at any molecular levels to induce apoptosis. However, ATRA plus DNA damage shows higher ROS levels due to the induction of Stra6. The mechanisms by which Stra6 induces ROS remain to be elucidated.

The obtained results established the importance of endogenous Stra6 to mediate ROS generation after cells were treated with Dox or a combined treatment of ATRA and Dox based on the observed results regarding the HCT116 WT p53 sh-Stra6 model was demonstrated a robust overall reduction in MFI fold change of ROS generation compared to the result of HCT116 WT p53 that possess Stra6, as shown in Figure 3.29C.

A previous report indicated that cells that lack Stra6 show less induced oxidative damage to their DNA in response to doxorubicin (Carrera et al., 2013). Our results are consistent with this finding. In this study, cells lacked

Stra6 were more resistant to induce cell death and ended with cell cycle arrest. We propose that this is because these cells lack the Stra6-p53 positive feedback loop after ATRA and Dox combined treatments.

This study has shown for the first time to our knowledge that Stra6 induces p53 independent of DNA damage and has identified ROS generation as the mechanism by which Stra6 induces p53.

Overall, our conclusion is that Stra6 induces apoptotic cell death depending on p53 and demonstrates an additive apoptotic effect. More interestingly, the apoptotic features of Stra6 suggests that upregulation of Stra6 in combination with other anticancer treatments such as chemotherapy or radiotherapy could be therapeutically relevant. This could minimise the side effects of traditional cancer therapies, thus providing a better option for helping cancer patients in their treatment.

4 Study of the biological functions of Stra6

4.1 Introduction

There is much still to be known about Stra6 protein—both regarding its role in cell signalling and its structure. Their interacting partners have also not been extensively studied. This chapter provides the first step to understanding the biological function of Stra6 based on protein interaction studies to describe and identify Stra6 interacting proteins.

We aimed to investigate how and under what conditions Stra6 protein might interact with other proteins. We also aimed to investigate the functional consequences of these interactions in the context of different treatments—particularly DNA damage and cellular stress. We focused on the two most common methods that are used for protein-protein interactions (PPI) analysis: co-immunoprecipitation and the pull-down assay.

4.2 Protein-protein interacting partners for Stra6

An important step in characterising protein function is to determine which proteins interact with the studied protein. We reasoned that this would facilitate identifying the related biological signalling pathways of Stra6. In this section, we propose protein-protein interacting partners for Stra6 that may bind directly or indirectly. We used a database search for proteins of already known functions that were involved in cellular processes and cell signalling pathways that may be implicated with the Stra6's biological functions.

In Figure 4.1A, we first performed a pull-down assay with GFP antibody to pull-down GFP as a negative control of the experiment, which is presented in Figure 4.1. HCT116 (p53 $^{+}/^{+}$) cells were transfected with 13 µg of GFP. After 48-hrs, cell lysates were used for pull-down, and the IP product was subsequently sent for mass-spectrometry analysis as a negative control. The data obtained was used as a background to eliminate any other proteins that

may be falsely interacting with Stra6 when compared to the obtained mass-spectrometry data of the Stra6-GFP and/or Stra6 pull-down assay.

In these experiments, three wells were loaded with different sample preparations. The first lane contained the input (INP), which was 10% of protein lysate—no antibody or beads were added; this was known as the control IP. The second lane contained the negative control (N), made with anti-IgG, the non-specific antibody, which matched the class of the antibody that was used for pull-down. This sample preparation consisted of the protein lysate plus the beads and anti-IgG in purpose to eliminate false positive results of non-specific binding. This was known as the control antibody. The third lane, known as IP, was the anti-GFP antibody or with the anti-Stra6 antibody. This sample preparation consisted of the corresponding antibody to pull-down the protein of interest (Stra6) plus the protein lysate and beads. Samples were run on 10% SDS-PAGE and were stained with instant Commasiee blue.

In Figure 4.1B and 4.1C, the pull-down assays used a GFP antibody to pull-down the Stra6 tagged with GFP in the C-terminus of the protein as well as a Stra6 antibody to pull-down the Stra6 protein. HCT116 (p53 $^{+}/^{+}$) cells were divided into four groups. All groups were transfected with 13 µg of either Stra6-GFP or Stra6. After 24-hrs, the first group of cells was used as a control with no treatment received, the second group was treated with 1 µM of ATRA, the third group was treated with 2 µM of Dox, and the last group was treated with a combined treatment of ATRA and Dox, 1 and 2 µM, respectively. After 48-hrs, cells were collected and cell lysates were used for pull-down. The results with presented in 4.1B and 4.1C showed different IP product sizes of approximately 53 kDa as well as lower molecular band sizes of 25 and 20 kDa (especially following Dox and the combined treatment of ATRA and Dox). We hypothesised that these lower band sizes could be due to the fact that Stra6 undergoes cleavage, specifically within the C-terminus domain of the protein. This hypothesis was supported by previous results obtained in the lab, which

also suggested the presence of a smaller form of Stra6 in certain conditions (data not shown).

These 53 kDa bands are strong in ATRA/Dox-treated samples; the 25 and 20 kDa products are moderate in Dox/ATRA- and Dox-treated samples. The bands were cut and analysed to determine their identity using Peptide Mass Fingerprinting (PMF) by mass spectrometry analysis (performed by PNACLE).

In addition, the Stra6-GFP pull-down with the anti-GFP antibody (IP) in Figure 4.1B indicated a band of about 73 kDa. The expected size of the GFP-tagged Stra6 construct is approximately 100 kDa. However, the Stra6 IP in Figure 4.1C indicated the correct molecular size of untagged Stra6, which is about 73 kDa. In general, the pull-down and tagged pull-down assays were more successful using Stra6 than Stra6-GFP (Figure 4.1).

After we validated the IP samples of Stra6 and Stra6-GFP pull-down in Figure 4.1B and 4.1C, we run the same samples for 5 minutes on a 10% agarose gel and stained it with instant Coomassie blue. The purpose was to analyse them with LC-MS/MS, as this approach will provide us with extensive information about possible interacting protein binding partners for Stra6 (Figure 4.2).

The LC-MS/MS analysis data of the Stra6 pull-down, which is provided in Table 4.1, shows the possible PPI partners for Stra6 following different treatment protocols. The purpose was to investigate the influence of retinoids or DNA damage on PPI responses and better understand the Stra6 biological functions in each situation.

The LC-MS/MS data identified a series of proteins that have a role in cell signalling pathways and in regulating cellular processes, such as apoptosis (see the discussion section for more detail on these proteins). These proteins that are involved with Stra6 as possible interacting proteins have been identified on Uniprot, Swissprot and NCBI databases. In addition, the identified proteins have been analysed in the database of Wiki-Pi (http://severus.dbmi.pitt.edu/wiki-pi) to understand PPI and to help to

determine functions. This is because protein interactions can result in novel functions that would not adhere if the protein is presented alone.

The observed bands of approximately 20, 25 and 53 kDa in Figure 4.1 were analysed by PMF by mass-spectrometry analysis. We determined the identity of these bands/proteins as shown in Table 4.2 and 4.3 (see the discussion section for more detail on these proteins).

Furthermore, the PPI for Stra6 shows a noticeable difference in the proteins reported from the LC-MS/MS data of the Stra6 pull-down when it came to the type of treatment received. In Table 4.4, we provided the major differences between the PPI partners for Stra6 depending on the treatment of ATRA versus Dox. In other words, this difference in proteins that probably bind Stra6, may suggest the influence of retinoids-signalling pathway or the DNA damage response and be an important factor in shaping the function of Stra6 in each situation (Table 4.4).

We have identified from the LC-MS/MS data a list of the most interesting proteins to further confirm the physical interactions between Stra6 and these selected proteins. The list is provided in Table 4.5 and includes Lamin A/C (LMNA), Heterogenous Nuclear Ribonucleoprotein-K (hnRNPK), High Mobility Group Protein B1 (HMGB1) and Peroxiredoxin-6 (PRX-6) (Table 4.5).

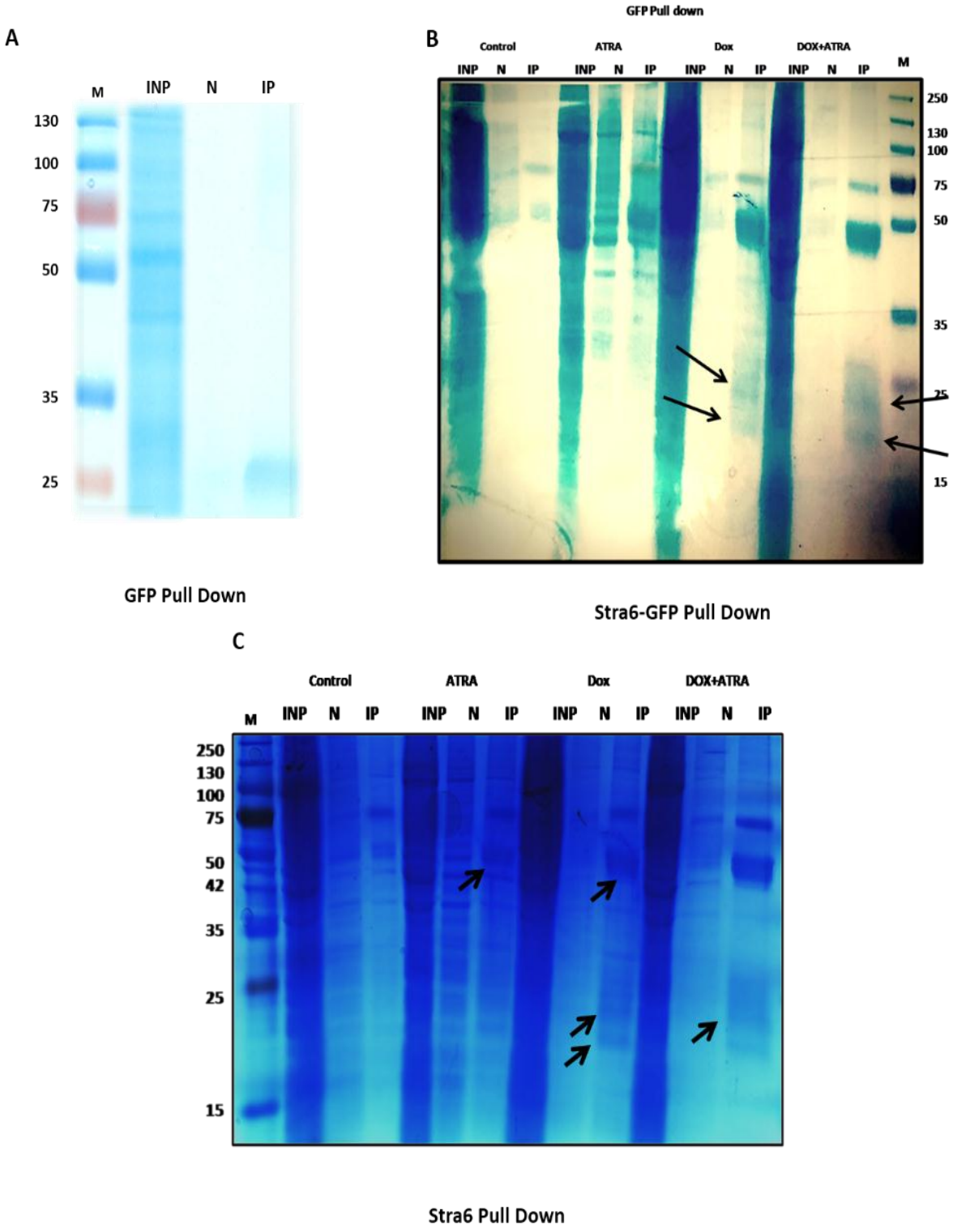

Figure 4.1: **Pull-down and tagged pull-down samples run on SDS-PAGE.** HCT116 WT p53 cells transfected with GFP as negative control **(A)**, Stra6 tagged GFP 13 µg **(B)** or with Stra6 transfection 13 µg **(C)** then pulled down with anti-GFP antibody (A & B) or anti-Stra6 antibody **(C).** Samples treated with 1 µM ATRA, 2 µM Dox and a combined treatment of ATRA and Dox at the same concentrations for 24-hrs **(B & C).** Three wells were loaded with different sample preparations: input (INP) 10% of sample, negative control made with anti-IgG (N), and IP made with anti-GFP or with anti- Stra6 (IP). Samples run on 10% SDS-PAGE and stained with instant Coomassie blue stain. The obtained results with IP samples in **(B & C**) showed different IP product sizes (Black arrow), these bands were analysed using Peptide Mass Fingerprinting (PMF).

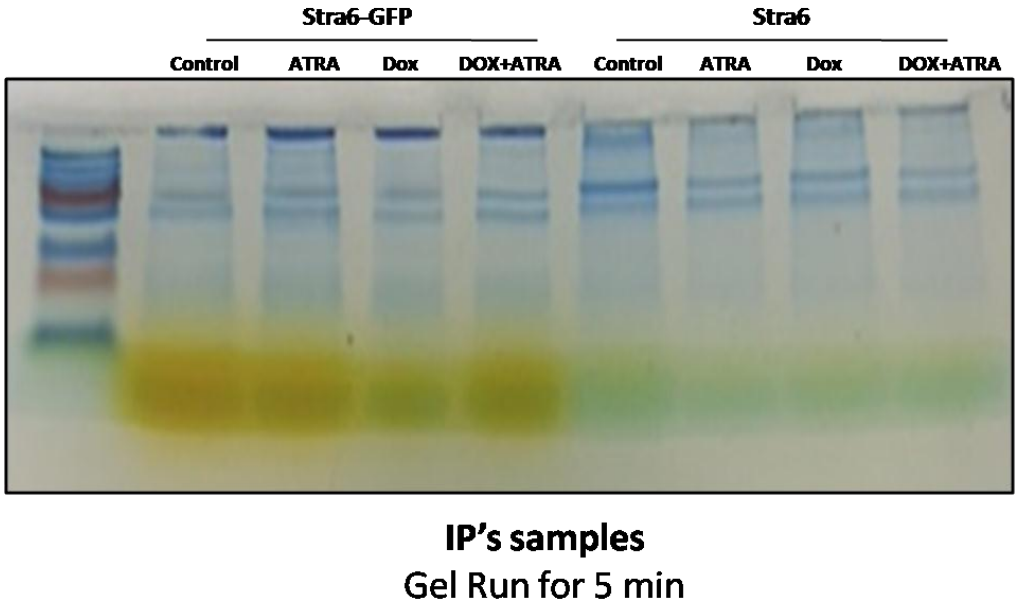

Figure 4.2: Pull-down of IP products to purify proteins that bind to Stra6 by LC-MS/MS analysis. Sample preparation done on HCT116 WT p53 cells transfected with 13 µg of Stra6 tagged GFP or with Stra6 transfection and pulled down with anti-GFP antibody or anti-Stra6 antibody, both transfected models treated with 1 µM ATRA, 2 µM Dox and a combined treatment of ATRA and Dox at the same concentrations for 24-hrs. IP's samples run on 10% SDS-PAGE for 5 minutes and stained with instant Coomassie blue stain.

Size (KDa)	Stra6	Stra6 (ATRA)	Stra6 (Dox)	Stra6 (ATRA + Dox)	Biological process
73	Stra6	Stra6	Stra6	Stra6	RBP receptor, Cell signalling receptors, Apoptosis
43	Alpha- Centractin (Arp1)	Alpha-Centractin (Arp1)	Alpha-Centractin (Arp1)	Alpha -Centractin (Arp1)	G2/M transition of mitotic cell cycle
107	Serine/Threonine Protein Kinase	X	Serine/Threonine Protein Kinase	Serine/Threonine Protein Kinase	Cell fate decision
29	60 S Ribosomal Protein S7 (RPS7)	X	60 S Ribosomal Protein S7 (RPS7)	60 S Ribosomal Protein S7 (RPS7)	Inhibit the MDM2 E3 ligase activity towards degradation of p53 tumor suppressor protein
25	40 S Ribosomal Protein S3 (RPS3)	X	40 S Ribosomal Protein S3 (RPS3)	40 S Ribosomal Protein S3 (RPS3)	Bind to p53, MDM2, hnRNPK and RPL9
25	Peroxiredoxin-6 (Prx-6)	X	Peroxiredoxin-6 (PRX-6)	Peroxiredoxin-6 (PRX-6)	Response to ROS and oxidative stress, bind to (Nuclear receptor RARα, Caspase 10, Caspase8, SUMO4, and PPARD)
18	60 S Ribosomal Protein L26 (RPL26)	X	60 S Ribosomal Protein L26 (RPL26)	60 S Ribosomal Protein L26 (RPL26)	Apoptosis
25	High Mobility Group Protein B1 (HMGB1)	X	High Mobility Group Protein B1 (HMGB1)	High Mobility Group Protein B1 (HMGB1)	Apoptosis, bind to p53, Caspase 3 and CDK1
33	Nucleophosmin (NPM)	X	Nucleophosmin (NPM)	Nucleophosmin (NPM)	In relation with ARF, p53 and MDM2 regulation
70	lamin A/C	X	lamin A/C	lamin A/C	Help proteins translocate to nucleus, apoptosis

Size (KDa)	Stra6	Stra6 (ATRA)	Stra6 (Dox)	Stra6 (ATRA + Dox)	Biological process
51	Heterogenous Nuclear Ribonucleoprotein-K (hnRNPK)	X	Heterogenous Nuclear Ribonucleoprotein-K (hnRNPK)	Heterogenous Nuclear Ribonucleoprotein-K (hnRNPK)	Apoptosis, DNA Damage response, p53
77	Nucleolin (NCL)	X	Nucleolin (NCL)	Nucleolin (NCL)	Apoptosis, bind to p53
87	Nucleolar RNA Helicase 2 (DDX21)	X	Nucleolar RNA Helicase 2 (DDX21)	Nucleolar RNA Helicase 2 (DDX21)	Cofactor for Jun, required to phosphorylate Jun
14	Histone H2A Type 1-B	X	Histone H2A Type 1-B	Histone H2A Type 1-B	Downregulation and inhibition of cell proliferation
14	Histone H2B Type 1-D	X	Histone H2B Type 1-D	Histone H2B Type 1-D	Apoptosis
31	Enoyl- CoA Hydratase Mitochondrial (ECHS1)	Enoyl-CoA Hydratase Mitochondrial (ECHS1)	Enoyl- CoA Hydratase Mitochondrial (ECHS1)	Enoyl- CoA Hydratase Mitochondrial (ECHS1)	Bind to Calpain large subunit (which binds to TP53, BID, HNRNPD), protein import to nucleus, negatively regulates STAT3 signaling
73	Caprin	X	Caprin	Caprin	G1/S cell cycle, protein synthesis inhibition
76	Splicing factor Proline and Glutamine Rich OS (PSF)	X	Splicing factor Proline and Glutamine Rich OS (PSF)	Splicing factor Proline and Glutamine Rich OS (PSF)	Post-transcriptional processing of mRNAs
285	Spectrin α/ β Chain, non-Erythrocytic	X	Spectrin α/ β Chain, non-Erythrocytic	Spectrin α/ β Chain, non-Erythrocytic	upregulated in response to cellular damage and heat stress

Table 4.1: Mass-spectrometry (LC-MS/MS) analysis of possible protein-protein interacting partners for Stra6 following different treatment protocols.

Size(KDa)	Stra6 (Dox) Approx. 25 KDa	Stra6 (Dox) Approx. 20 KDa	Stra6 (ATRA + Dox) Approx. 25 KDa	Biological process
22	X	Preoxiredoxine-1 (PRX1)	Preoxiredoxine-1 (PRX1)	Response to ROS
24	Preoxiredoxine-2 (PRX2)	X	Preoxiredoxine-2 (PRX2)	Response to oxidative stress, bind to BAD
24	60 Ribosomal Protein L13a (RPL13a)	X	60 Ribosomal Protein L13a (RPL13a)	Negative regulation of translation, induces cell growth arrest in G2/M and apoptosis
29	14-3-3 Protein Epsilon (YWHAE)	X	14-3-3 Protein Epsilon (YWHAE)	Apoptosis, JNK activation, bind to BAD and Caspase 3
25	High Mobility Group Protein B1 (HMGB1)	X	High Mobility Group Protein B1 (HMGB1)	Apoptosis, bind to p53, Caspase 3 and CDK1
25	X	40 S Ribosomal Protein S3 (RPS3)	40 S Ribosomal Protein S3 (RPS3)	Bind to p53, MDM2, hnRNPK and RPL9
25	Peroxiredoxin-6 (PRX-6)	X	Peroxiredoxin-6 (PRX-6)	Response to ROS and oxidative stress bind to (Nuclear receptor RARα, Caspase 10, Caspase8, SUMO4 and PPARD)
28	X	X	Proteosome Subunit α type 5 and 7	Proteasome-dependent degradation during apoptosis
31	Enoyl- CoA Hydratase Mitochondrial (ECHS1)	X	Enoyl- CoA Hydratase Mitochondrial (ECHS1)	Bind to Calpain large subunit (which binds to TP53, BID, HNRNPD), protein import to nucleus, negatively regulates STAT3 signaling

Size(KDa)	Stra6 (Dox) Approx. 25 KDa	Stra6 (Dox) Approx. 20 KDa	Stra6 (ATRA + Dox) Approx. 25 KDa	Biological process
20/25	Stra6	Stra6	Stra6	Apoptosis
29	X	X	Calpain (CAPNS1)	Apoptosis, binds to CDK4, NDRG1, PPARGC1A which bind to (RXRA, TP53, CDK6 and NCL)
28	X	X	B- Cell Receptor Associated Protein31 (BAP31)	Binds to Caspase 8, caspase 9 and Caspase 3.
29	X	X	Eukaryotic Translation Initiation Factor 4 Subunit E (eIF4E)	Cytokines mediated signalling pathway
28	X	X	Electron Transfer Flavoprotein, β Polypeptide (ETFB)	Transfers the electrons to the main mitoch. respiratory chain, bind to ETFA and Amyloid precursor protein (APP) which bind to c-Jun

Table 4.2: Peptide Mass Fingerprinting (PMF) analysis of specific IP products band sizes approximately (20 and 25 kDa) to determine possible protein-protein interacting partners for Stra6 following different treatment protocols.

Size(KDa)	Stra6 (ATRA) Approx. 53 KDa	Stra6 (Dox) Approx. 53 KDa	Biological process
51	RUVB-Like Protein 2 (RUVBL2)	RUVB-Like Protein 2 (RUVBL2)	Mediated growth arrest and apoptosis
47	α-Enolase (ENO1)	α-Enolase (ENO1)	Negative regulation of cell growth, response to stress, bind to HDAC1, (SUMO-4: regulation of apoptotic process)
51	X	Heterogenous Nuclear Ribonucleoprotein-K (hnRNPK)	Apoptosis, DNA Damage response, p53
59	X	Eukaryotic Translation Initiation Factor 2 Subunit 3 (eIF2S3)	Regulation of protein synthesis, bind to METAP2, (NDRG1: DNA damage response by p53)
95	Elongation Factor 2 (eEF2)	X	PTM of proteins and protein kinase binding, bind to p53, CDKN2A and NDRG1
77	X	Nucleolin	Apoptosis, bind to p53
48	Elongation Factor 1-α (eEF1A)	X	Protein kinase binding and interact with peroxiredoxin I in response to oxidative stress.
64	X	Ubiquitin-Like Modifier Activity Enzyme-1	Ubiquitin activating enzyme Activity
49	X	Heterogenous Nuclear Ribonucleoprotein-H1 (HNRNPH1)	stimulate pre-mRNA cleavage and polyadenylation
55	Drebrin Like Protein (DBNL)/HIP-55	X	Direct mechanism to inhibit HPK1 activity (HPK1 activate JNK regulating cellular stress response)

Size(KDa)	Stra6 (ATRA) Approx. 53 KDa	Stra6 (Dox) Approx. 53 KDa	Biological process
121	X	ATP- Citrate Synthase (ACLY)	Primary enzyme for cytosolic acetyl-CoA synthesis
91	X	Heterogenous Nuclear Ribonucleoprotein-U (HNRNPU)	Contributes to stabilize the kinetochore-microtubule interaction during mitosis, bind to NDRG1 and Caspase 3
53	X	Pyruvate Kinase (PKM)	Regulation of glycolysis, response to stress, bind to MDM2, NDRG1, CDK4 and CDKN1
58	X	Leucine-rich pentatricopeptide repeat containing (LRPPRC)	Play a role in mitoch. encoded cytochrome C oxidase stability, regulation of ROS and response to oxidative stress, bind to HNRPA1, FOXO1

Table 4.3: Peptide mass fingerprinting (PMF) analysis of specific IP products band sizes of approximately (53 kDa) to determine possible protein-protein interacting partners for Stra6 following different treatment protocols.

(ATRA)	(Dox)
MAP/Microtubule affinity kinase-3 (MARK3)	Lamin A/C
Drebrin Like Protein (DBNL)/HIP-55	Caprin
E3 ubiquitin-protein ligase TRIM21	Heterogenous Nuclear Ribonucleoprotein-K (hnRNPK)
Co-activator of PPAR Gamma Like Protein	60 S Ribosomal Protein (RPL13a) / (RPS7)
Hornerin (HRNR)	Histone H2A / Histone H2B
Eukaryotic Translation Initiation Factor 4 Subunit E (eIF4E)	Nucleolar RNA Helicase 2 (DDX21)
Elongation Factor 2 (eEF2)	Nucleophosmin (NPM)
Elongation Factor 1-α (eEF1A)	Nucleolin (NCL)

Table 4.4: The differences between the protein-protein interactions partners for Stra6 depends on the treatment (ATRA Vs Dox).

Protein Name	Recommended to test first	Biological process
Lamin A/C (LMNA)	√	Help proteins translocate to nucleus, apoptosis
Nucleophosmin (NPM)		In relation with p53, MDM2, ARF
Heterogenous Nuclear Ribonucleoprotein-K (hnRNPK)	√	Apoptosis, DNA Damage response, p53
Nucleolar RNA Helicase 2 (DDX21)		Cofactor for Jun, required to phosphorylate Jun
Spectrin Alpha Chain, non-Erythrocytic		Apoptosis, bind to Caspase 3
Nucleolin (NCL)		Apoptosis, bind to p53
High Mobility Group Protein B1 (HMGB1)	√	Apoptosis, bind to p53 and Caspase 3
Peroxiredoxin-6 (PRX-6)	√	Response to ROS and oxidative stress, bind to (Nuclear receptor RARα, Caspase 7, Caspase8, SUMO4, and PPARD)
Calpain (CAPNS1)		Apoptosis, binds to CDK4, NDRG1, PPARGC1A which bind to (RXRA, TP53, CDK6 and NCL)
Enoyl- CoA Hydratase Mitochondrial (ECHS1)		Bind to Calpain large subunit (which binds to TP53, BID, HNRNPD), protein import to nucleus, negatively regulates STAT3 signaling

Table 4.5: List of most interesting Stra6 binding protein for follow-up experiments.

4.3 Characterization of potential Stra6 binding partners

Based on the mass spectrometry of potential PPIs for Stra6, we selected four proteins to be tested to determine whether they are interacting with and bind to Stra6 protein. To address this, Co-immunoprecipitation (Co-IP) was performed with HCT116 ($p53^{+}/^{+}$) cells. The cells were transfected with Stra6; after 24-hrs, cells were exposed to a combined treatment of 1 µM ATRA and 2 µM Dox for 24 hrs. After that, a cell lysate was used for IP using anti-Stra6. This was followed by a Western blot analysis to visualize the physical interaction between Stra6 and HMGB1, hnRNPK, Peroxiredoxin6 and Lamin A/C proteins by using anti-HMGB1, anti-hnRNPK, anti-Peroxiredoxin6 and anti-Lamin A/C antibodies, respectively. Three wells were loaded with different sample preparations. The negative control was made with anti-IgG (N), input 10% of protein lysate (INP) and IP made with anti-Stra6 (IP).

Figure 4.3 shows the physical interaction between Stra6 and HMGB1 (Figure 4.3A), Stra6 and hnRNPK (Figure 4.3B), Stra6 and Peroxiredoxin6 (Figure 4.3C), and Stra6 and Lamin A/C (Figure 4.3D). These results suggest that these proteins support the function of the Stra6 in induced cell death (apoptosis) or in stress responses. However, this is subject to further verification (Figure 4.3).

In Figure 4.4, we further investigated the potential interactions of HMGB1, hnRNPK, Peroxiredoxin6 and Lamin A/C with Stra6. The experiment was done in reverse to the experiment in Figure 4.3. In this experiment, the HMGB1, hnRNPK, Peroxiredoxin6 and Lamin A/C were explored by pull-down in HCT116 ($p53^{+}/^{+}$) cells. The cells were transfected with Stra6; after 24-hrs, cells were treated with 1 µM ATRA and 2 µM Dox or treated with 2 µM of Dox for only for 24 hrs. A Western blot analysis followed to visualise the interaction of HMGB1, hnRNPK, Peroxiredoxin6 and Lamin A/C (IP products) with Stra6 using the Stra6 antibody to detect it. The results support the physical interaction of the pulled down proteins with Stra6; this suggested that these proteins are Stra6's protein binding partners.

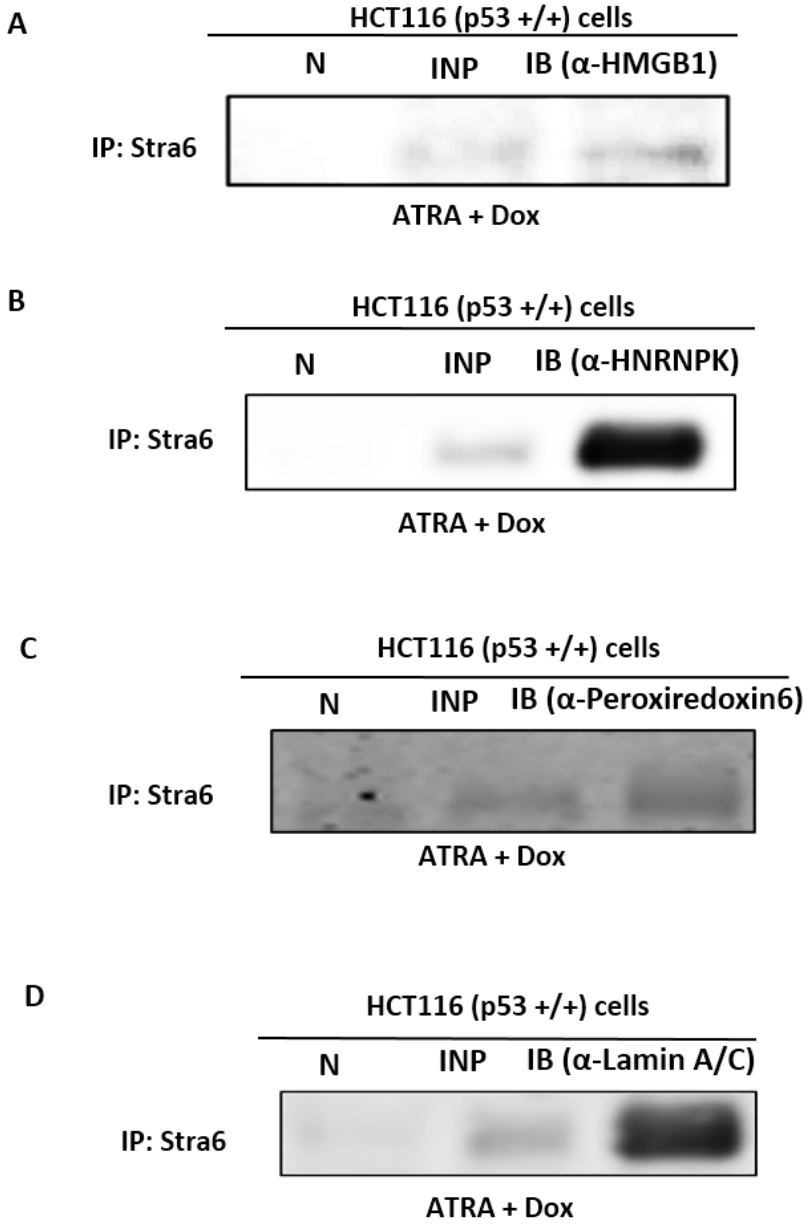

Figure 4.3: Co-immunoprecipitations indicate interaction of Stra6 with other proteins. The figure represents immunoprecipitation (IP) of Stra6 followed by Western blot using anti-HMGB1, anti-hnRNPK, anti-Peroxiredoxin6 and anti-Lamin A/C antibodies to detect HMGB1, hnRNPK, Peroxiredoxin6 and Lamin A/C proteins in figure A, B, C and D respectively. (N: immunoprecipitation with anti-IgG negative control, INP: 10% input, IB: immunoblot with anti-target protein of interest on Stra6 pulled down IP product).

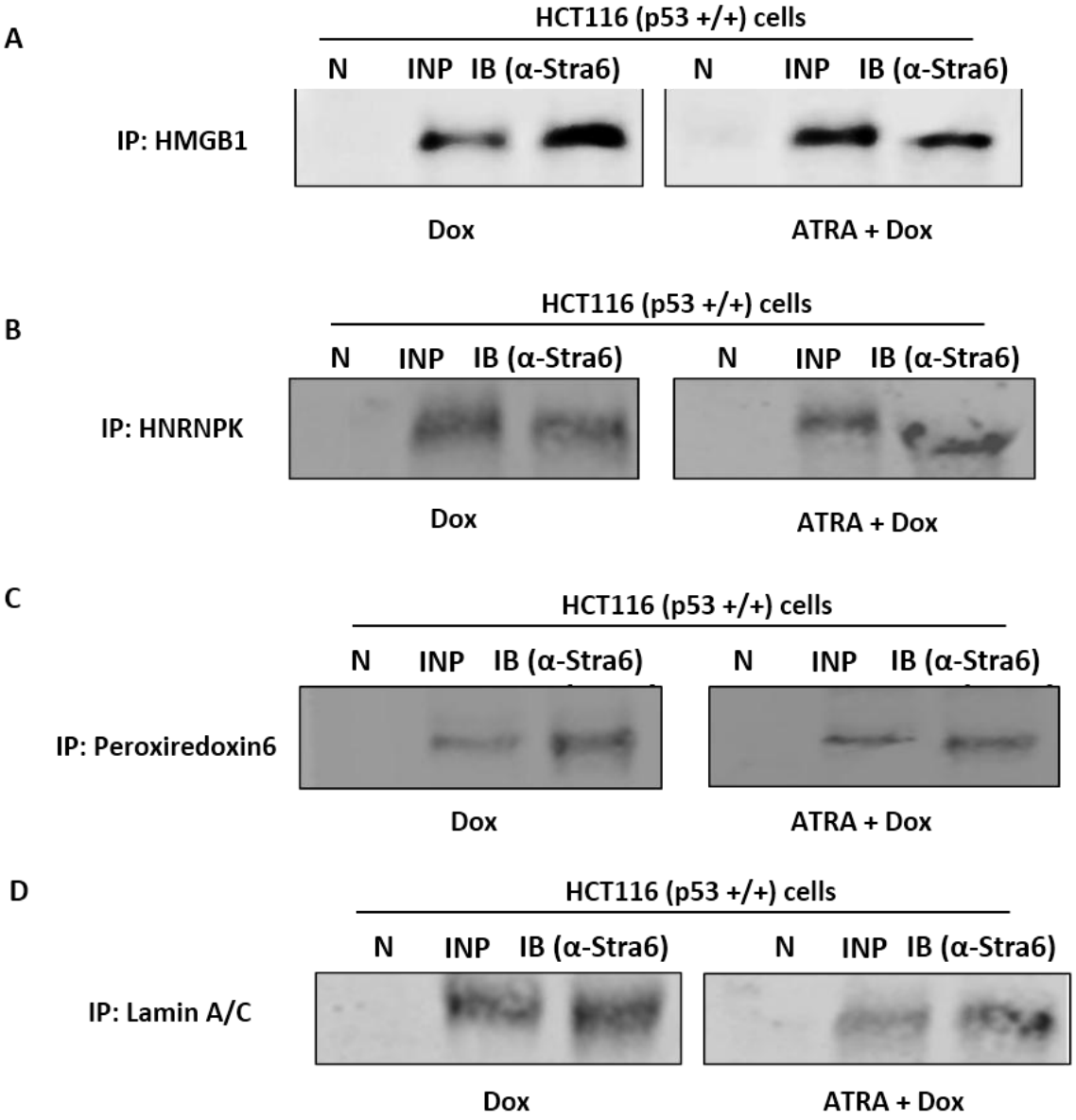

Figure 4.4: Co-immunoprecipitation show interaction between HMGB1, hnRNPK, Peroxiredoxin6 and Lamin A/C with Stra6. The figure represents immunoprecipitation (IP) of HMGB1, hnRNPK, Peroxiredoxin6 and Lamin A/C in figure A, B, C and D respectively, followed by Western blot using anti-Stra6 antibody (N: immunoprecipitation with anti-IgG negative control, INP: 10% input, IB: immunoblot with anti-Stra6 antibody on different pulled down IP product).

4.4 Study of protein levels of the potential binding partners of Stra6

We next investigated the interaction between Stra6 and the proteins described in section 4.3, including HMGB1, hnRNPK, Peroxiredoxin6 and Lamin A/C. In addition, the Jun N-terminal Kinase (JNK) signalling pathway in Figure 4.4 was investigated based on the identified PPI for Stra6, where some of these proteins were predicted to be involved in the JNK pathway.

A Western blot was performed with HCT116 ($p53^{+}/^{+}$) cells transfected with Stra6 to determine the protein levels of HMGB1, hnRNPK, Peroxiredoxin6, Lamin A/C, JNK and P-JNK related to the endogenous and exogenous Stra6 levels in the context of DNA damage. Also, we used HCT116 ($p53^{+}/^{+}$) cells transfected with 13 µg of Stra6 for 24-hrs followed by 1 µM of ATRA, 2 µM of Dox or the combined ATRA and Dox treatment for 24-hrs. As shown in Figure 4.5, the endogenous levels of Stra6 in response to DNA damage (Dox) correspond to an upregulation in the protein levels of Lamin-A, peroxiredoxine-6, HMBGB1 and hnRNPK but not in Lamin-C. The combined ATRA and Dox treatment with the endogenous levels of Stra6 showed similar results to the treatment of Dox but with the added upregulation in Lamin-C protein levels.

In cells transfected with Stra6, the levels of Lamin-A were upregulated more than Lamin-C in the control and ATRA treatment cells. However, Lamin-C was upregulated more than Lamin-A in response to DNA damage and the combined ATRA and Dox treatment.

In addition, there was very slight upregulation of hnRNPK, peroxiredoxine-6 and HMBGB1 proteins in the ATRA treatment. However, in control cells and cells treated with Dox and the combined ATRA and Dox, higher levels of these proteins were detected. These results together show induction of the potential binding partners of Stra6 in response to stimuli that can induce Stra6 itself. Thus, the data support the potential relationship between Stra6 and them. More experiments will need to be performed to further explore these

relationships but, unfortunately, there was no time to start this new phase of the project.

Induction of P-JNK was detected in cells treated with combined ATRA and Dox, but not in control cells and Dox treatment. In Stra6 transfected cells, cells treated with Dox or combined ATRA and Dox showed higher levels of P-JNK activation. However, Stra6 transfected cells treated with ATRA showed very slight levels of P-JNK activation (Figure 4.5). The obtained results are consistent with the hypothesis that Stra6 may engage the JNK signalling pathway in the induction of apoptosis.

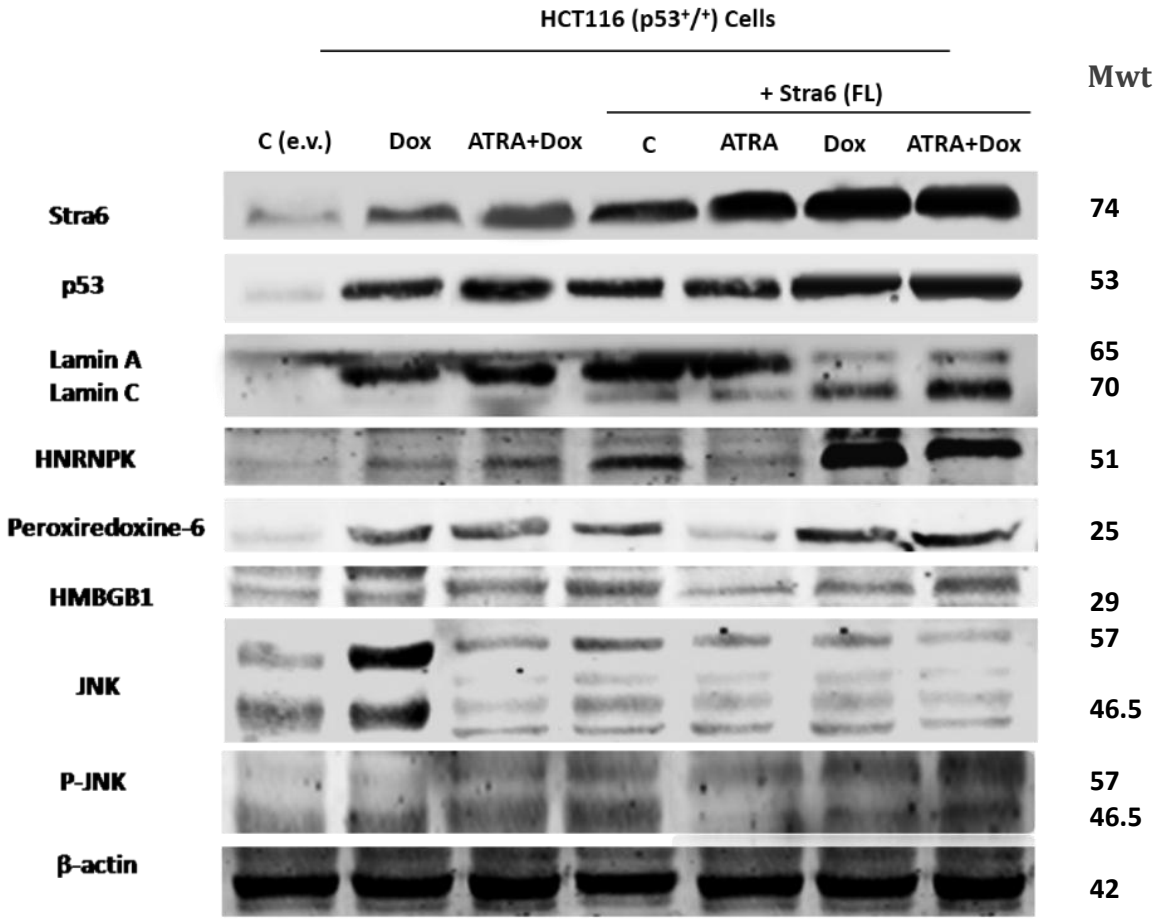

Figure 4.5: Protein levels of potential Stra6 binding partners and JNK signalling pathway. HCT116 WT p53 cells, treated with Dox or transfected with 13 µg followed by ATRA 1 µM, Dox 2 µM or combined ATRA and Dox treatment for 24-hrs. Stra6, p53, Lamin A/C, hnRNPK, Peroxiredoxine-6, HMBGB1, JNK and P-JNK proteins were detected with specific antibodies. C (e.v.) = empty vector. Mwt= Molecular weight in kDa.

4.5 Structural insights into Stra6: A prediction study

Using the Stra6 pull-down of IP products in Figure 4.2, Stra6 peptides were identified by LC-MS/MS analysis, which confirmed that the pulled down protein was indeed Stra6.

The mass spectrometry identified different Stra6 peptides. As shown in Figure 4.6, their expression depends on the stimuli received. We hypothesised that Stra6 could be cleaved in the C-terminus region of the protein, as previously suggested by Figure 4.1 whereas the bands in the sizes of 20 and 25 kDa were observed after the cells were treated with Dox or combined ATRA and Dox. Using the information in Figure 4.6B, we recognised that the peptide belongs to the C-terminus domain (AATLDPGYYTYR) in Stra6 transfected cells with no treatment, in cells treated with Dox and the combined ATRA and Dox treatment, but not with the ATRA treatment alone. Moreover, in all treatments a peptide of GAALDLSPLHR was detected, which is a Holo-RBP domain. Additionally, in Figure 4.6C, a peptide was only recognised in the presence of ATRA (QLWPDCVR), and it was related to the N-terminus domain of Stra6 protein (Figure 4.6).

We next aimed to investigate the potential phosphorylation sites of Stra6 with advanced bioinformatics software tools, using the NetPhos 2.0 software. Protein phosphorylation is a post-translational modification (PTM) that has an important role in regulating cell signalling, cell cycles and apoptosis in addition to many other cellular processes. As shown in Figure 4.7, NetPhos 2.0 predicted several Tyrosine, Threonine, or Serine phosphorylation sites in Stra6 protein. Phosphorylation prediction and mass spectrometry data show peptides of Stra6 that may undergo tyrosine and threonine phosphorylation mainly in the C-terminus domain and a serine phosphorylation in the extracellular helical part where Holo-RBP binds.

The NetPhos 2.0 phosphorylation software predicted that the C-terminus of Stra6 is a likely site for phosphorylation to take place. As shown in Figure 4.8,

we propose a model for Stra6 primary phosphorylation sites that would contribute to a Stra6 signalling pathway. We suggest that Stra6 may be cleaved at the C-terminus as a consequence of PTM of tyrosine and threonine. This would possibly recruit JNK/P-JNK upon DNA damage or in the absence of DNA damage, which is response dependent to p53 (Figure 4.8).

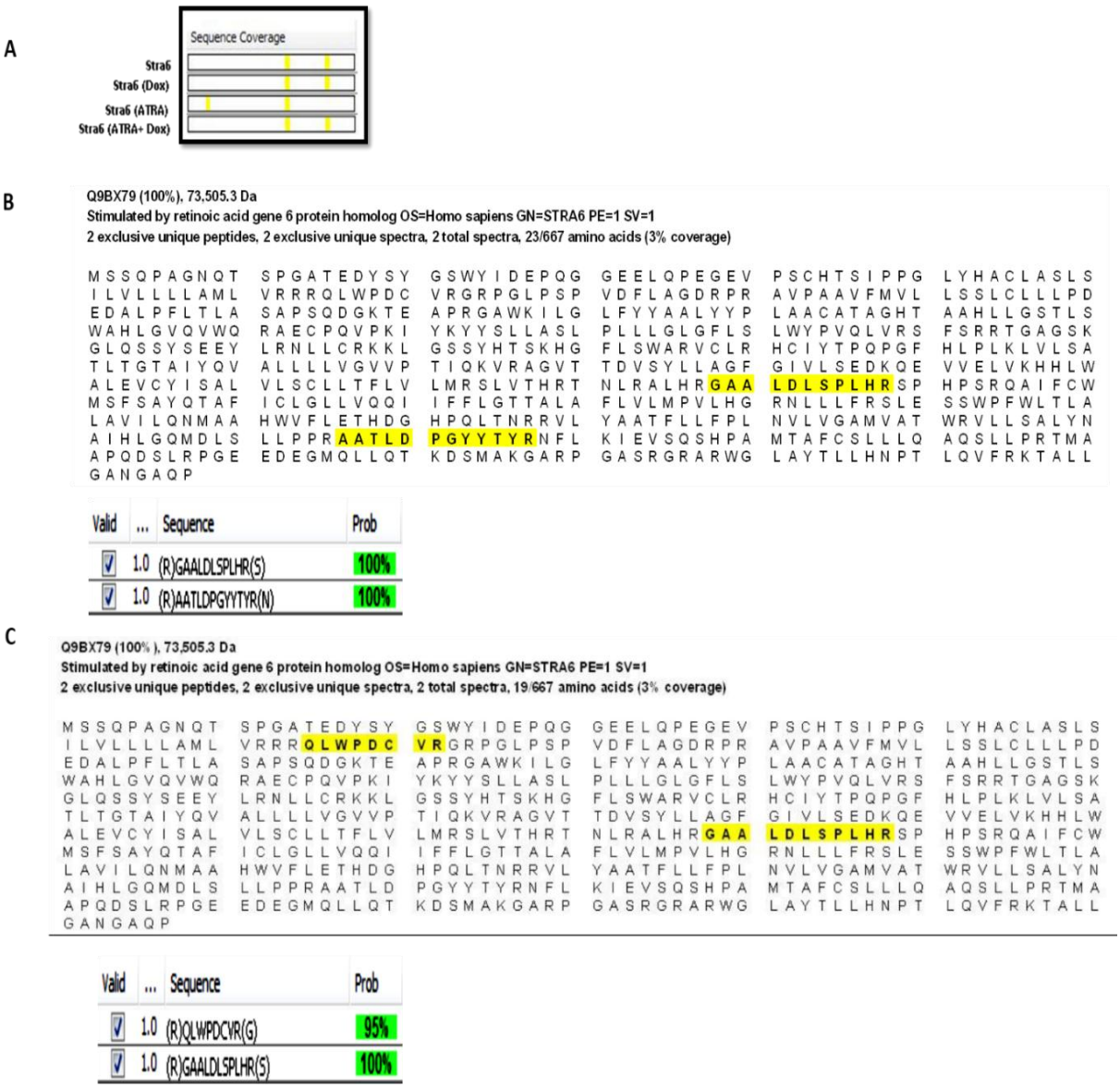

Figure 4.6: Stra6 peptides identified by LC-MS/MS analysis. (A) A representative graph of Stra6 sequence coverage based on tryptic peptides identified by LC-MS/MS, ranging from the left site (N-terminus) to the right site of the protein (C-terminus). **(B)** Yellow highlight show identified peptides from Stra6 protein of sample treated with Dox, ATRA and Dox or as control with no treatment. **(C)** Yellow highlight show identified peptides from Stra6 protein of sample treated with ATRA.

A

Stimulated by retinoic acid gene 6 protein homolog (Stra6) 667 Sequence

```
MSSQPAGNQTSPGATEDYSYGSWYIDEPQGGEELQPEGEVPSCHTSIPPGLYHACLASLSILVLLLLAMLVRRRQLWPDC 80
VRGRPGLPSPVDFLAGDRPRAVPAAVFMVLLSSLCLLLPDEDALPFLTLASAPSQDGKTEAPRGAWKILGLFYYAALYYP160
LAACATAGHTAAHLLGSTLSWAHLGVQVWQRAECPQVPKIYKYYSLLASLPLLLGLGFLSLWYPVQLVRSFSRRTGAGSK240
GLQSSYSEEYLRNLLCRKKLGSSYHTSKHGFLSWARVCLRHCIYTPQPGFHLPLKLVLSATLTGTAIYQVALLLLVGVVP320
TIQKVRAGVTTDVSYLLAGFGIVLSEDKQEVVELVKHHLWALEVCYISALVLSCLLTFLVLMRSLVTHRTNLRALHRGAA400
LDLSPLHRSPHPSRQAIFCWMSFSAYQTAFICLGLLVQQIIFFLGTTALAFLVLMPVLHGRNLLLFRSLESSWPFWLTLA480
LAVILQNMAAHWVFLETHDGHPQLTNRRVLYAATFLLFPLNVLVGAMVATWRVLLSALYNAIHLGQMDLSLLPPRAATLD560
PGYYTYRNFLKIEVSQSHPAMTAFCSLLLQAQSLLPRTMAAPQDSLRPGEEDEGMQLLQTKDSMAKGARPGASRGRARWG640
LAYTLLHNPTLQVFRKTALLGANGAQP                                                        720
```

```
.........S......YSY.S.Y.....................................................  80
........S.....................................................................  160
.....................................................................S....S.  240
...SS.S..Y...........SS.....................................................320
.........T.....................................................S.....400
........S.....................................................S.....480
.......................T.......................T.................T..Y..560
.Y..T.........Y.............................S...................S....Y...640
.........................                                                    720
```

B

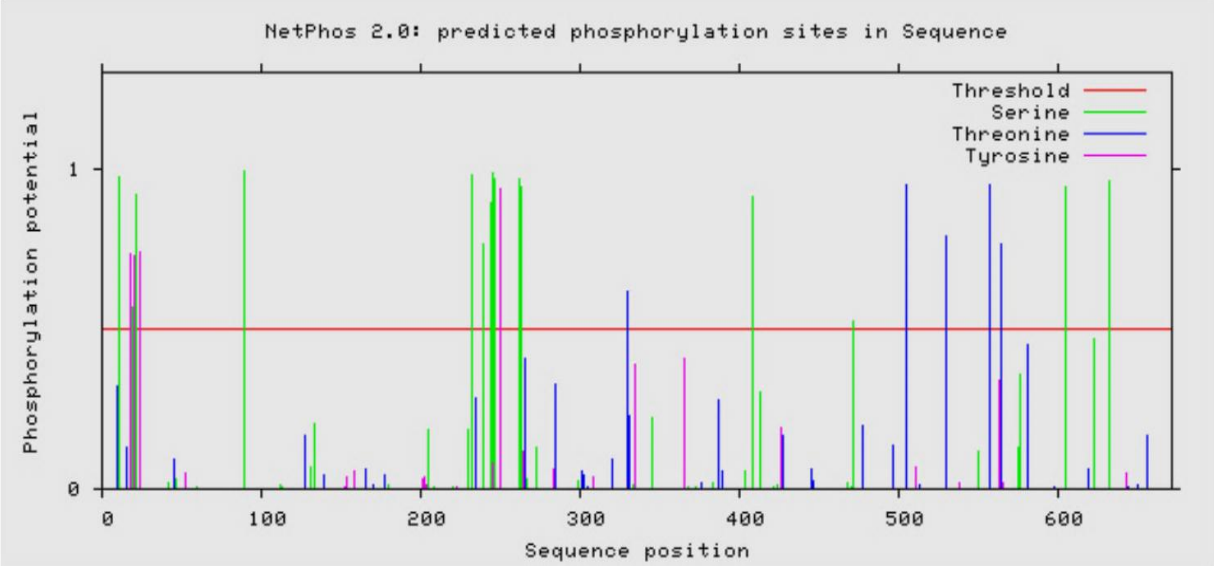

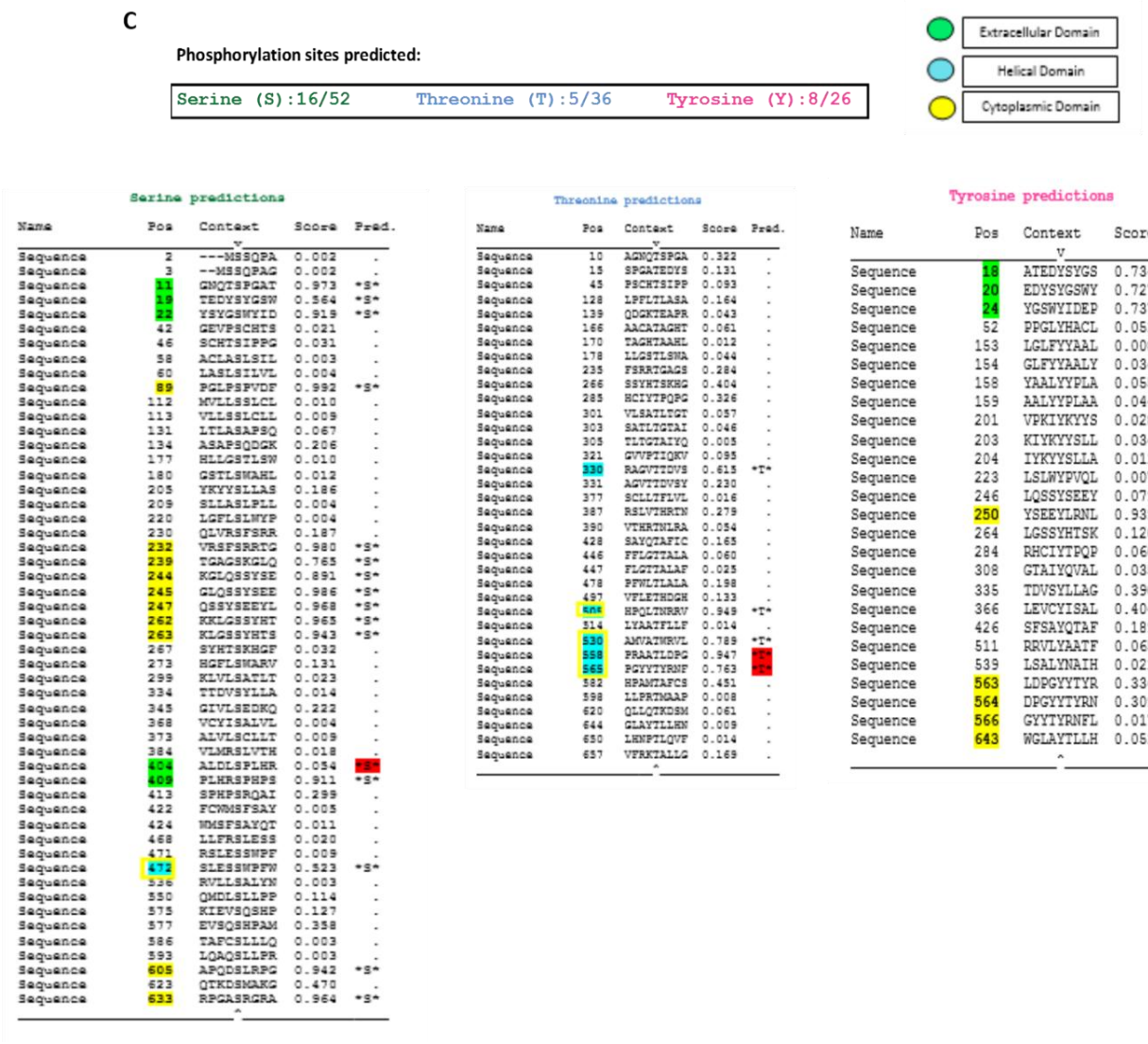

Figure 4.7: A prediction study of phosphorylation sites for Stra6. The NetPhos 2.0 software predicted Tyrosine, Threonine, or Serine phosphorylation sites in Stra6 protein. **(A)** amino acid sequence of Stra6. **(B)** Representative graph shows predicted phosphorylation site in the sequence. **(C)** Tables of Serine, Threonine and Tyrosine phosphorylation predictions with the corresponding peptides that show an exact amino acid number. The different colour code highlight and indicate whether the predicted phosphorylation site is within extracellular domain (green), helical domain (blue) and cytoplasmic domain (yellow). Red highlights show the correlation between these predicted phosphorylation sites in this figure and the obtained results of mass spec that show Stra6 identified peptides that contain Serine, Threonine, and Tyrosine residues.

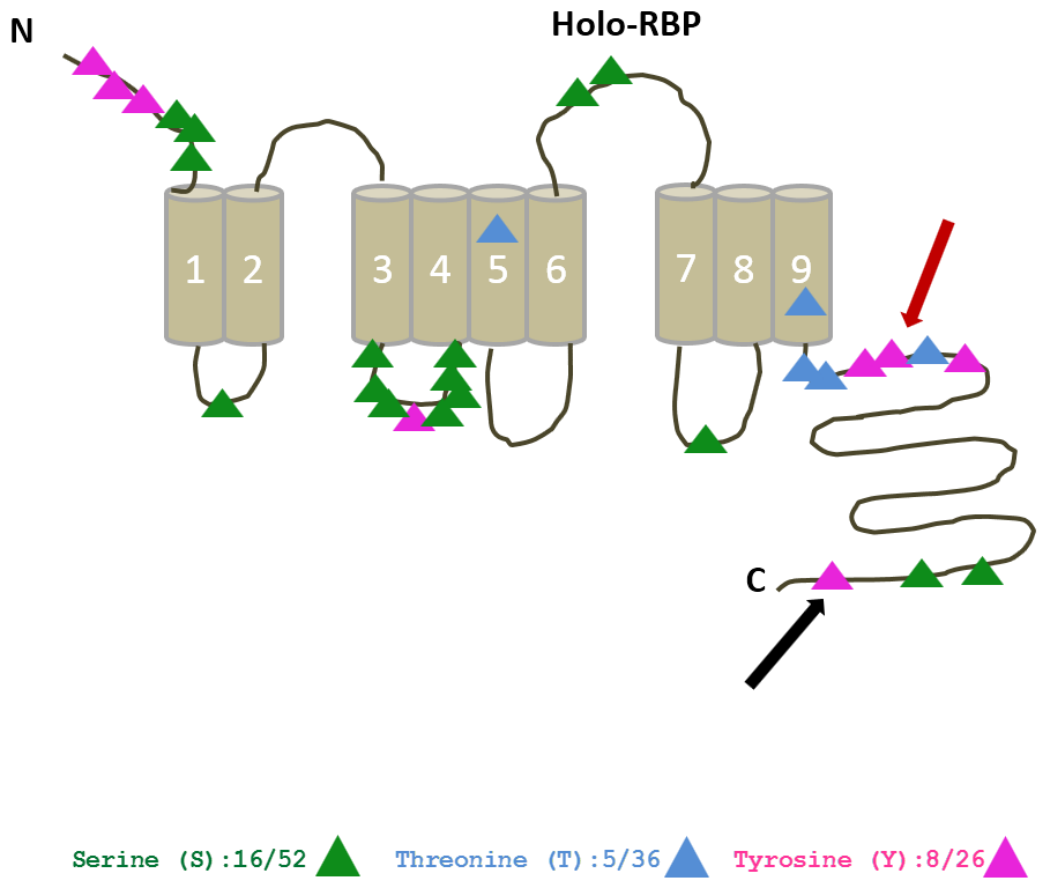

Figure 4.8: A proposed model of Stra6-primary phosphorylation sites that would contributes into Stra6 signalling pathway. Based on data from LC-MS/MS and NetPhos 2.0 phosphorylation prediction software we propose that the C-terminus of Stra6 is a likely site for phosphorylation to take place. The black arrow indicates the known fact upon retinol binds to RBP and transport to cells via Stra6 then Stat5 is recruited to the phosphorylate-tyrosine residue of Stra6, which is activated by JAK2, and after that Stat5 translocates to the nucleus, where it induces the expression of target genes (Berry, C. et al., 2012). The red arrow indicates the approximate suggested cleavage site of Stra6 within the C-terminus based on prediction analysis done by NetPhos software that showed PTMs in addition to the corresponding cleaved peptide of Stra6 protein at C - terminus domain within 25-15 kDa.

4.6 Discussion

Stra6's has a well-known function as a retinol binding protein (RBP) receptor and facilitating vitamin A transport into the cell. Here, we aimed to further characterise the Stra6 biological function in the context of DNA damage.

We have repeatedly observed Stra6 bands of approximately 53, 25 and 20 kDa-specifically. Considering that the full length Stra6 protein as around 75 kDa, it is likely that these are cleavage products. Stra6 is a cell surface receptor with 19 distinguishing domains (Kawaguchi et al., 2008), which make the protein difficult to be internalised from the cell surface and to bind other nuclear proteins. Thus, any potential nuclear functions (like interacting with p53) could be better explained by a cleaved form that does not have the transmembrane domains.

The pull-down assay using a Stra6 antibody to be shown an IP product size of approximately 75 kDa, in addition to an IP product size of 53 kDa and lower molecular band sizes of 25 and 20 kDa, especially following Dox and the combined treatment of ATRA and Dox. These 53, 25 and 20 kDa bands were cut and analysed to determine their identity by using Peptide Mass Fingerprinting (PMF) by mass spectrometry analysis. Thus, we hypothesized that Stra6 gets cleaved into a larger form (53 kDa) and a smaller form, that perhaps undergoes further cleavage or some PTMs that could account for the two different ~20kDa bands.

The C-terminus of Stra6 could be cleaved and translocated into the nucleus in response to DNA damage. This is supported by the fact that the mass spec screen identified nuclear proteins as potential binding partners for Stra6.

The LC-MS/MS data (Table 4.1, 4.2 and 4.3) shows numerous important proteins, co-factors, proteases and enzymes. These could be found within different cell compartments, such as the cell membrane, cytosol, mitochondria, ER or the nucleus, and they have a role in cell signalling pathways and in regulating cellular processes, such as apoptosis. These

identified proteins may be implicated in Stra6's biological function in response to DNA damage.

The first step to accept any mass spectrometry data is the existence of the pulled down protein of interest that has been tested. This indicates a successful pull-down experiment. The mass spectrometry result has identified that the Stra6 (pulled down) protein (Uniprot: Q9BX79) served the function of being the transporter of vitamin A and the RBP receptor.

Alpha-Centractin (Arp1) is a protein associated with the spindle assembly and chromosome segregation at the metaphase to anaphase transition; it is involved in the G2/M transition of the mitotic cell cycle. Overexpression of Arp1 in cells would disturb microtuble organization throughout mitosis and interphase (Hamada et al., 2004; Clark and Meyer, 1999). However, there is no clue how could Stra6 and Arp1 could interact to support Stra6 in its function towards apoptosis.

The Serine/Threonine protein kinase identified in the mass spectrometry data without specified any name for Serine/Threonine protein kinase. It has an influence on cell fate decision. The kinases of this family have been proposed to play a role in apoptosis, such as the mitogen-activated protein kinase (MAPK) family, particularly p38, Mitogen-activated protein kinase (MAPK) and c-Jun N-terminal kinase (JNK) and cyclic AMP-dependent protein kinase (Timothy et al., 2000). Chen et al. (2012), proposed that Stra6 induces apoptosis because of an increased ratio of apo-RBP4 to holo-RBP4. The referred term apo-RBP indicates when no retinol is present, and holo-RBP indicates that retinol binds to RBP. This ratio affects Stra6 signalling and activates a JAK2/STAT5 signalling cascade, which up-regulates adenylate cyclase 6 (AC6) and cAMP, enhancing the signalling cascade of JNK1/p38 and resulting in CRBP-I/RARα suppression and apoptosis induction (Chen et al., 2012).

Members of the peroxidases family (Prx) are present in the mass spectrometry data analysis—for instance, Peroxiredoxin-6 (Prx-6), Peroxiredoxin-2 (Prx-2) and Peroxiredoxin-1 (Prx-1). In the NH2 terminal domain, all Prx enzymes' families have a conserved cysteine residue that serves as the main oxidation site for hydrogen peroxide (H_2O_2). However, Prx 1, 2, 3, and 6 hold a further conserved cysteine residue in the COOH terminal domain (Chang et al., 2002). Theses Prx enzymes reduce reactive oxygen species (ROS) and oxidative stress (Fatma et al., 2008). However, there are some contradictory reports regarding the role of Prx-6, as it displayed dual biological functions. Prx-6 is a bifunctional catalytic enzyme that has peroxidase and phospholipase A-2 (PLA-2) activities; the function of the PLA-2 of Prx-6 is largely unidentified. Kim et al. (2011) reported a novel function for the PLA-2 that regulates TNF-induced apoptosis via the release of arachidonic acid (AA) and the production of interleukin-1β (IL-1β), which prevents tumorigenesis (Kim et al., 2011). The endogenous and overexpression levels of Prx-6 protected retinal ganglion cells (RGCs) from glutamate. In contrast, the overexpression of Prx-6 in the tumour cells of squamous cell carcinomas speeded up mechanism of malignant development of the same tumours (Rolfs et al., 2013).

Prx-1 and Prx-2 are cytosolic enzymes that respond to oxidative stress and ROS; they have an important role as cellular antioxidant mechanisms (Peskin et al., 2007). Prx-1 and Prx-2 both are phosphorylated by several cyclin-dependent kinases (CDKs); for example, Cdc2 was activated during the G2-M transition phase. Phosphorylation mediated by Cdc2 of these two Prxs resulted in their inactivation and accumulation of H_2O_2 within the cells. H_2O_2 accumulation stimulated Cdc25C inactivation, thus stopping the positive feedback loop between Cdc25C and Cdc2. Moreover, studies have found that high levels of H_2O_2 accumulation might have a role in Cdc25C activity inhibition in the G2-M transition phase of mitosis; this could prevent cell cycle progression. In addition, studies have demonstrated a cell cycle arrest via

$p21^{cip1}$ upregulation and cyclin D downregulation in response to sub-lethal levels of H_2O_2 (Barnouin et al., 2002; Chang et al., 2002). These observations supported our view of the possible role of the peroxidases family in response to ROS and oxidative stress.

The activation of High Mobility Group Protein B1 (HMGB1) is based on a reactive oxygen species (ROS)-dependent mechanism or calcium release. Researchers have found that transcription factors, such as p53, mediate the upregulation of HMGB1 expression (Yusein-Myashkova et al., 2016). In addition, HMGB1 overexpression is involved with apoptotic cell death in breast cancer cell lines treated with anti-cancer drugs or radiation (Sohun and Shen, 2016). We think this protein HMGB1 could be one of the possible protein binding partner for Stra6 by evaluating HMGB1 biological role and nature of induction, which correlates with Stra6-induced p53.

Histone H2B Type 1-D and Histone H2A Type 1-B were identified in the mass spectrometry data. Histone modifications play important roles in gene expression and chromatin regulation. Some studies correlate the involvement of histone H2B phosphorylation at serine 14 with cells that undergo apoptosis. Moreover, this was suggested to be significant for apoptotic chromatin condensation (Cheung et al., 2003; Zhang et al., 2004). Histone H2A Type 1-B's main biological function is to downregulate and inhibit cell proliferation. The phosphorylation of H2AS1, has been found to be associated with chromatin transcription inhibition (Kim et al., 2013).

Some ribosomal proteins were identified in the mass spectrometry data, such as 60 S Ribosomal Protein L26 (RPL26), 60 S Ribosomal Protein S7 (RPS7), 60 S Ribosomal Protein L13a (RPL13a) and 40 S Ribosomal Protein S3 (RPS3). Ribosomal proteins have discrete additional-ribosomal functions in apoptosis, DNA repair and transcription.

Ribosomal proteins are recognised for participating in additional functions to their known roles in ribosome assembly and protein translation. Several lines

of evidence have shown that ribosomal proteins are involved in regulating the transcription and activation of significant and important proteins, including c-Myc, NF-κB and nuclear receptors, and to trigger a p53 pathway activation in response to ribosomal stress (Lindström, 2009; Zhou et al., 2015). For instance, RPL26 and RPS7 were found to be involved in apoptosis by binding to MDM2, which would lead to E3 ligase activity inhibition and prevent p53 tumour suppressor degradation (Zhang et al., 2003; Khanna et al., 2003; He et al., 2007). Additionally, RPL26 promoted the translation of p53 mRNA after DNA damage via the process of binding to the p53 mRNA 5' untranslated region (5'UTR), which resulted in the more efficient translation of p53 protein (Takagi et al., 2005). A study revealed RPL13a's mechanism regarding its function as a negative regulator of translation, in which RPL13a was targeting the eukaryotic translation initiation factor 4 (eIF4G) by mRNA-bound produced transcript-specific translational suppression (Mazumder et al., 2003). Furthermore, studies have shown the association of RPL13a with cell growth arrest in the G2-M transition phase of mitosis and apoptosis (Chen et al., 1999). A good example of ribosomal protein that can directly regulate and control the gene transcription mechanism is RPS3. Because the KH-domain that RPS3 possessed facilitated DNA/RNA binding (Wan et al., 2007), many other proteins have the KH-domain, such as the first identified human protein with KH-domain, which is the heterogeneous nuclear ribonucleoprotein K (hnRNPK). RPS3 was implicated in the mechanism of caspase-dependent apoptosis induction (Jang et al., 2004). These observations support our view of a possible role of these ribosomal proteins in response to p53 tumour suppressor protein stabilisation and activation, which could be mediated by Stra6. In the results presented in Chapter 3, we determined the existence of a positive feedback loop between Stra6 and p53 protein, which resulted in p53 stabilisation. These ribosomal proteins were identified in the mass spectrometry data as possible Stra6 protein binding partners. They might be suggested to play a role in the observed p53 protein activation and stabilisation. This might be further analysed in future studies to correlate

these ribosomal proteins that are associated with p53 activation in response to Stra6 induction in the context of DNA damage and cellular stress.

Heterogeneous nuclear ribonucleoproteins (hnRNPs) are complexes of RNA and protein found in the nucleus during gene transcription and subsequent post-transcriptional modification of the newly synthesized RNA (pre-mRNA). From mass spectrometry data, three hnRNPs were identified: hnRNPK, hnRNPH1 and hnRNPU.

hnRNPK is mainly present in the nucleus and sometimes in the cytoplasm because of its K nuclear shuttling domain (KNS), which facilitates its transport between the nucleus and the cytoplasm. hnRNPK participated in many different cellular functions, such as protein transcription, pre-mRNA splicing and chromatin remodelling (Matunis et al., 1992; Bomsztyk et al., 2004). Recently, proteomics studies have identified hnRNPK to be associated to the response to DNA damage via the process of ATM-dependent phosphorylation of hnRNPK (Moumen et al., 2005). Moreover, hnRNPK has been identified as a p53 target for MDM2 regulation, and hnRNPK has been recognised to be a p53 transcriptional cofactor in response to DNA damage (Moumen et al., 2005; Enge et al., 2009). Studies have indicated that ATM-dependent hnRNPK phosphorylation is essential for hnRNPK stabilization (Moumen et al., 2013). Pelisch et al. (2012) found that DNA damage stimulated hnRNPK sumoylation, and this PTM was necessary for the expression and activation of p53 target genes (Pelisch et al., 2012).

hnRNPH1 was found to stimulate pre-mRNA cleavage, polyadenylation and alternative splicing. hnRNPH1 is upregulated in some cancers, such as pancreatic adenocarcinoma, hepatocellular carcinoma, gastric carcinoma and colon cancer. Sun et al. (2016) recently found that oesophageal squamous cell carcinoma has high expression levels of both hnRNPH1 mRNA and protein. Thus, it was related to tumour cells' poor differentiation status (Sun et al., 2016).

hnRNPU is an abundant nuclear protein. Ma et al. (2011) recently identified hnRNPU as a microtubule-associated protein (Ma et al., 2011). Moreover, a recent study has determined that hnRNPU, during mitotic cell division, is localised at the mitotic spindles. Indeed, the hnRNPU participated in the process of maintaining the stability of the kinetochore-microtubule interaction (Chun et al., 2016).

The most relevant hnRNPs found in our mass spectrometry data is the hnRNPK. We suggest that hnRNPK might be implicated within a Stra6-p53-apoptotic pathway as this protein was one of the possible protein binding partners for Stra6 as it has been recognised to be a p53 transcriptional cofactor in response to DNA damage and activation of p53 target genes that could have resulted in apoptosis, as we hypothesized.

Eukaryotic Translation Initiation Factor 4 (eIF4E) an Eukaryotic Translation Initiation Factor 2 (eIF2) both regulate protein translation and synthesis in response to DNA damage and other cellular stresses, such as apoptosis and nutrient deficiency (Kimball, 1999). eIF4E and eIF2 phosphorylation is enhanced by several protein kinases; this includes both the p38 mitogen-activated protein kinase (MAPK) and Erk signalling pathways (Wek et al., 2006).

Nucleophosmin (NPM1) is an important nucleolar protein that has shown a function as a tumour suppressor. NPM1 has participated in various cellular events, such as mRNA transport, chromatin remodelling, ribosome biogenesis and apoptosis (Grisendi et al., 2006; Sherr, 2006). Some researchers have reported a direct association of NPM1 with p53 (Colombo et al., 2002). Other researchers have also associated NPM1 with the tumour suppressor function of p53 by binding directly with MDM2 in a p14 Arf independent manner to act as an inhibitor of MDM2 and thus prevent p53 degradation (Kurki et al., 2004). An example of the regulatory mechanism of NPM1 in apoptosis is that both p14 Arf and NPM1 form a heterodimer in the nucleoli, thus permitting

MDM2 to bind to p53 for subsequent ubiquitination and degradation. Once the cell has been under stress and the DNA damage response started, both p14 Arf and NPM1 are dissociated and translocated to the nucleus to bind MDM2 and form MDM2-NPM1 and MDM2-p14 Arf complexes. This series of cellular events stabilise p53 and promote p53 to induce cell cycle arrest or apoptosis (Box et al., 2016). Overall, we hypothesise that this protein NPM1 could be involved in possible Stra6-NPM-p53 complex.

Nucleolin (NCL) is a nucleolus protein that has a role in ribosome assembly and biogenesis. Additionally, it has the role of providing a platform for PPI due to the nature of the NCL structure that is comprised of many structural domains (Ginisty et al., 1999). Cellular stress and DNA damage stimulated the process of translocation of NCL, allowing for NCL-p53 complex initiation and leading to a direct interaction between these two proteins. An *in-vivo* study revealed that the initiation of the NCL-p53 complex was dependent on the regulatory C-terminal domain of the p53 protein and was not dependent on p53 transactivation (Daniely et al., 2002).

All the previous studies regarding NPM1 and NCL proteins have strongly suggested that these two proteins are important proteins related to Stra6 in response to p53 stabilisation and could help explain the Stra6-mediated increase in p53 protein levels that we have observed.

Lamin A/C is considered to be one of the nuclear lamins' main components. Generally, lamins have an important role in controlling the structural organisation of the proteins involved in the nuclear membrane (Hozak et al., 1995). Moreover, lamins provide a foundation stage for the protein binding and chromatin remodelling as well as regulating the activity of some of the proteins involved in cell signalling, such as retinoblastoma (Rb)/E2F and mitogen activating protein kinase (MAPK) pathways (Gonzalez et al., 2008; Dittmer and Misteli, 2011). Previous studies have determined the role of lamin in controlling gene expression and cell cycle regulation (Vlcek et al.,

2007; Heessen et al., 2007). For instance, lamin A overexpression levels resulted in preventing cell proliferation (Gonzalez et al., 2008; He et al., 2015). In addition, Slee et al. (2000) have implicated caspase-6 as the primary caspase dependent for lamin A/C cleavage in apoptosis (Slee et al., 2000). We hypothesized that when Stra6 is cleaved and translocated to the nucleus it binds Lamin A/C that resulted in further cellular process towards apoptosis.

Caprin is cytoplasmic phosphoprotein necessary for maintaining normal cell progression and for controlling the G1-S phase of the cell cycle. Wang et al. (2005) established gene analysis studies that have shown the effect of cells that did not possess Caprin, with the G1-S phase delays in cell cycle progression (Wang et al., 2005). Caprin overexpression mediated protein synthesis inhibition via its ability to phosphorylate eukaryotic translation initiation factor 2 α (eIF-2 α) that binds mRNA (Solomon et al., 2007). We think it might be Stra6 binds Caprin is to inhibit cell cycle progression, as further experiments are necessary to define this hypothesis.

Drebrin-like (DBNL) protein, also known as HIP-55 (HPK1-interacting protein of 55 kDa), is a multidomain adaptor protein. This protein has been found to be vital in the immune response. HIP-55 facilitated tumorigenesis by inducing inhibition of the tumour suppressor activity of the hematopoietic progenitor kinase 1 (HPK1) (Li et al., 2014). Schulze et al. (2002) determined that HPK1 supported the apoptosis of T lymphocytes. HPK1 overexpression enhanced apoptosis through ROS generation. Moreover, HPK-1 expression was correlated with JNK activation and thus might participate in the HPK1-mediated apoptosis (Schulze et al., 2002).

14-3-3 protein epsilon (YWHAE) ,as it was described by mass spectometry data, it has a high phospho-serine and phospho-threonine binding activity that promotes and facilitates its interaction with different classes of cellular proteins. These include transcription factors, cell signalling cascades and apoptotic proteins. For example, several lines of evidence have shown that

JNK, in response to cellular stress, can disturb 14-3-3 interactions by its action of phosphorylation—either on the 14-3-3 proteins or on the 14-3-3 proteins' binding partners. In the apoptotic cellular events, JNK controls this mechanism when the 14-3-3 proteins undergo phosphorylation and release their ligands.

B-Cell Receptor Associated Protein 31 (BAP31) is a highly-expressed membrane protein with great abundance in the endoplasmic reticulum (ER), which could be found as homo or hetero dimers. BAP31 was found to serve as the possible modulator of apoptosis, and it was considered to be a caspase-8 substrate (Breckenridge et al., 2002). Nguyen et al. (2000) found that the cleavage of BAP31 was implicated with the cytoplasmic apoptotic activity linked with cellular fragmentation and membrane blebbing during apoptosis (Nguyen et al., 2000). We thought all of the above could be an explained reason for why Stra6 binds BAP31.

α-Enolase (ENO1) is also recognised as 2-phospho-D-glycerate hydrolase, which is found all over the cells from the cell surface to nucleus with more tendency for ENO1 expression found in the cytoplasm. In the glycolytic pathway, this metalloenzyme catalyses 2-phosphoglyceric acid and converts it to phosphoenolpyruvic acid (Pancholi and Fischetti, 1998; Ji et al., 2016). Many proteomic studies have associated ENO1 with the mechanism of stress response increase; this is because the recorded levels of ENO1 protein were dramatically different before and after the onset of stress (Young and Elliott, 1989). Sawhney et al. (2015) recently determined that mouse tumour cells model containing p53 isoform Δ133p53α have shown an upregulation of ENO1 protein expression. Therefore, these results have determined that the association between the p53 and ENO1 expression in inflammatory response induction and ENO1 was the main player in increasing the inflammatory response (Sawhney et al., 2015).

Enoyl-CoA Hydratase Mitochondrial (ECHS1) is localised within the mitochondrial matrix and is responsible for the catalysation process of the

mitochondrial fatty acid β-oxidation—especially when the cells have low levels of energy and glucose (Janben et al., 1997). Recently, ECHS1 has been recognised as the negative regulator of the STAT3 signalling cascade because ECHS1 was identified as the associated protein for STAT3. Moreover, a study determined ECHS1's capability to control STAT3 pro-oncogenic target genes, such as BCL-2 and Cyclin D1 (Chang et al., 2013). These observations could be a conceivable explanation for being possible protein binding partners for Stra6 and participating in shaping Stra6's biological function in apoptosis induction, which is dependent on p53 and mediated through JNK activation. This needs to be investigated in further studies.

RUVB-Like Protein 2 (RUVBL2) is also recognised as TIP49b with ATPase activity, and it is allocated within chromatin remodelling complexes. Later studies have found that cells lacking RUVBL2 have shown cell growth reduction, increased caspase-3 activity, and activation of pro-apoptotic genes, including BAK and BAX, in addition to a significant apoptotic cell death. Conversely, RUVBL2 has shown an oncogenic function when overexpressed, promoting tumour cell growth and increasing cell resistance towards apoptosis (Rousseau et al., 2007). Stra6 binds RUVBL2 could be as a negative regulator to supress RUVBL2 expression which will help in apoptosis.

Calpain is one of the well-known cysteine proteases involved in apoptotic cell death. Calpain is a calcium-dependent cysteine protease and is found all over the cytosol of cells. It has a biological role that is involved in the regulatory mechanism of many transcription factors and cell cycle-regulating factors, such as c-Jun, NF-κB and c-Fos. In-vitro studies have determined that p53 undergoes proteolytic cleavage by calpain (Kubbutat et al., 1997; Debiasi et al., 1999). A recent study by Sobhan et al. (2013) identified that both calpain and ROS facilitated Bax activation (Sobhan et al., 2013). We hypothesized that Calpain could be also cleaved Stra6 as well as when ROS generated from Stra6 binds to Calpain to upregulate Bax which result in apoptosis.

Leucine-rich pentatricopeptide repeat containing (LRPPRC) is found in the mitochondria. It plays an important role in the regulation process of mitochondrial mRNA stability, in the stimulation of mtDNA transcription and in cytochrome c oxidase stabilisation (Xu et al., 2004; Harmel et al., 2013).

The PPI data for Stra6 show an obvious difference in the proteins reported depending on the type of treatment received.). Most of the identified proteins appear in all different treatments, except for the ATRA treatment. In Table 4.4, we summarised the differences of proteins involved in the ATRA treatment versus the DNA damage response of cells treated with Dox. It might be suggested that both the PPI for Stra6 and the degree of received stimuli are important factors that participate in shaping the biological function of Stra6. For instance, Berry et al. (2012 and 2014) have called Stra6 a 'cytokine signalling transporter'(Berry et al., 2012; Berry et al., 2014). We propose that these observations are dependent on the control of specific factors, such as the ratio between Stra6 protein expressed to the amount of ATRA received. We agreed with Chen et al.'s (2012) that Stra6 induces apoptosis; that study also proposed the possible mechanism related to the increased ratio of apo-RBP4 to holo-RBP4. This ratio affects Stra6 signalling and activates a JAK2/STAT5 signalling cascade, which upregulates adenylate cyclase 6 (AC6) and cAMP. Therefore, it enhances the signalling cascade of JNK1/p38 and results in CRBP-I/RARα suppression and apoptosis induction (Chen et al., 2012). A recent report from our lab by Carrera et al. (2013) showed that Stra6 participated in apoptosis induction and as a new member in the p53 signalling pathway. This was in response to DNA damage, although this study did not reveal the underlying mechanism that engaged Stra6 in cell death. Taken together, we believe that Stra6 has a dual regulatory function in the context of retinoids or in the context of DNA damage. The PPIs and protein binding partners for Stra6 have a great influence on defining Stra6's role in cell fate decisions.

As the data produced by mass spectrometry was within a large scale of identified proteins, we selected some of these proteins for further varication and confirmation, examining the physical interactions between Stra6 and these selected proteins. We have made a list in Table 4.5 of the most interesting proteins that would be Stra6's possible binding partners based on their contribution in cell death and p53 DNA damage response. These include (LMNA) Lamin A/C, (hnRNPK) Heterogenous Nuclear Ribonucleoprotein-K, (HMGB1) High Mobility Group Protein B1 and (PRX-6) Peroxiredoxin-6 (Table 4.5).

Indeed, the obtained results in Figure 4.3 and Figure 4.4 showed the physical interaction between Stra6 and HMGB1 (Figure 4.3A and 4.4A), Stra6 and hnRNPK (Figure 4.3B and 4.4B), Stra6 and Peroxiredoxin-6 (Figure 4.3C and 4.4C), and Stra6 and Lamin A/C (Figure 4.3D and 4.4D). The author suggested that these proteins were Stra6's protein binding partners. Additionally, we suggest that many of the interacting proteins described contribute to the function of Stra6 to induce apoptosis. Therefore, these interactions play a critical role in the regulation of p53 at several levels, though this is subject to further verification.

In Figure 4.5, Western blot was performed to confirm whether Stra6 binds to HMGB1, hnRNPK, Peroxiredoxin-6 and Lamin A/C proteins to upregulate or downregulate them. It also confirmed whether these proteins would interact with Stra6 as a positive or negative regulator. Furthermore, the JNK signalling pathway was investigated in light of the mass spectrometry data that identified many PPIs for Stra6 that can cross talk with JNK-mediated apoptosis.

We found that the Western blot result (Figure 4.5) was consistent with the mass spectrometry data, suggesting that our mass spectrometry data are reliable. The endogenous Stra6 and overexpression of Stra6 in the presence or

absence of DNA damage have upregulated hnRNPK, HMGB1, Lamin A/C and Peroxiredoxin-6.

We propose that the molecular and cellular functions of the hnRNPK and HMGB1 proteins may play a causal role in apoptosis through ROS and DNA damage-dependent mechanism. hnRNPK has been found to be required for the expression and activation of the p53 target genes (Pelisch et al., 2012). In addition, HMGB1 was found to be implicated in apoptotic cell death mediated by p53 (Sohun and Shen, 2016). Moreover, we suggested that the lamin A/C upregulation is related to its role in cell cycle regulation and apoptosis since previous studies found that lamin A overexpression resulted in preventing cell proliferation (Gonzalez et al., 2008; He et al., 2015). Lamin A/C cleavage was also detected in apoptosis through the action of caspase-6 (Slee et al., 2000). More importantly, the obtained WB result suggested that Stra6 and possible protein binding partners for Stra6 induced apoptosis in response to DNA damage or in the absence of DNA damage dependent on p53 through the activation of the JNK signalling pathway that mediated apoptosis (Figure 4.5).

The results reported in Figure 4.6 have shown that mass spectrometry data identified a peptide (550-569) corresponding to the C-terminus domain of Stra6. We proposed that the represented region of Stra6 might be subjected to potential post-transnational modifications related to phosphorylation. Collectively, these results indicated that Stra6 may be cleaved and translocated to the nucleus to contribute to p53-dependent apoptosis (see next chapter).

Stra6 was not identified in previous studies in which Stra6 undergos PTM to regulate apoptosis. In Figure 4.7, The NetPhos 2.0 server predicts Tyrosine, Threonine, or Serine phosphorylation sites in Stra6 protein. Protein phosphorylation is a post-translational modification (PTM) performing an important role in regulating cell signalling, cell cycle and apoptosis in addition to many other cellular processes. Phosphorylation prediction data and mass

spectrometry data show peptides of Stra6 that may undergo phosphorylation in tyrosines and threonines mainly in the C-terminus domain and a serine phosphorylation in the extracellular helical part where Holo-RBP binds. For these reason, we postulate that Stra6 may regulate p53 expression through Stra6 C-terminus phosphorylation. This would potentially (our hypothesis) phosphorylate other protein binding partners for Stra6 that have a downstream effect on p53 stimulation in response to DNA damage or absence of DNA damage, triggering the p38/JNK signalling pathway mediated apoptosis.

Mass spectrometry data and NetPhos 2.0 phosphorylation prediction software analysis have shown that the C-terminus of Stra6 is a highly constitutive site for phosphorylation to occur. As shown in Figure 4.8, we suggest a model for Stra6 primary phosphorylation sites that would contribute to a Stra6 signalling pathway. We assumed that Stra6 could be cleaved within the C-terminus because of the possible PTM of tyrosine and threonine that founded in C-terminus region in addition to the biological functions of Stra6's protein binding partners and protein protein interactions that could have a role on this cleavage mechanism of Stra6 C-terminus. This would possibly later have recruited JNK signalling pathway upon DNA damage response in a p53-dependent manner towards apoptosis (Figure 4.8).

In summary, screening of PPIs for Stra6 could help in discovering proteins that contribute to apoptosis. This will also help in understanding Stra6's function. In addition, we propose that this screen could be used to outline ways to define the Stra6 signalling pathway. Although Stra6 appears to be implicated in p53-induced apoptosis, it is not clear what constitutes the upstream and downstream components of a signalling cascade that Stra6 might fit in, particularly in the context of a DNA damage response.

5 Investigation on the cellular localisation of Stra6

5.1 Introduction

This chapter focusses on the cellular localisation of the Stra6 protein considering different stimulations. The aim of this chapter is to further investigate the results that were presented in the past two chapters (Chapter 3 and Chapter 4). In Chapter 3, the results revealed a positive feedback loop between Stra6 and p53, which was mostly detected in cells that were treated with ATRA and Dox compared to Dox alone. These results made us curious about the mechanism by which a membrane protein, such as Stra6, may interact with a nuclear protein, such as p53. In addition, in chapter 4, mass spectrometry data and a co-Immunoprecipitation study revealed the association of nuclear and cytoplasmic proteins with Stra6 as its possible interacting binding partners. In this chapter, we investigated the localisation of Stra6, and the possibility of a translocation from cell membranes to nucleus after DNA damage, especially the cleaved C terminus domain of the Stra6 protein. Moreover, this hypothesis correlated with the observed biological function of Stra6 in apoptotic cell death, which could be related to Stra6-C-Term localisation within the nucleus. Cell fractionation as well as the confocal analysis of the cells were performed using HCT116 WT p53 after cells received different treatments, in order to study the cellular localisation of Stra6.

5.2 Cell fractionation to determine the subcellular localisation of Stra6

To confirm the localisation of the Stra6 protein, fractionation by a sucrose gradient of whole cell lysates of HCT116 $p53^{+/+}$ was performed. As shown in Figure 5.1, cells were transfected with an empty vector (e.v.) and treated with 2 µM of Dox for 48 hrs. Then, the cells were collected, and whole cell lysate was analysed on the sucrose gradient before centrifugation at 100,000 g for 18 hrs at 4 ^{o}C. After that, the cell lysate was separated into 24 fractions and was loaded onto a 10 % gel for Western blot analysis. The result determined the localisation of the Stra6 protein in the nuclear fraction, as the nuclear marker HDAC-1 was indicated. Therefore, this result suggested that the endogenous Sta6 protein after DNA damage response was in the nucleus, with a molecular size of 25 kDa, which represented the molecular size of the whole

intracellular C terminus domain of the Stra6 protein. However, there was also a detectable amount of the full size Stra6 protein within the cytosol fraction (Figure 5.1).

Next, this was compared to cells transfected with Stra6 (13 µg, 48 hrs) and no treatment added (Figure 5.2). The results determined that the exogenous Stra6 was detected within the cytosol, as shown by the cytosol marker MAPK. Na/K ATPase and HDAC1 are markers of plasma membrane and nucleus, respectively, and were used to make sure that no contamination occurred during fractionation (Figure 5.2).

Interestingly, Stra6 was mainly localised within the plasma membrane fraction after cells were transfected with Stra6 (13 µg, 48 hrs), and after the first 24 hrs of cell transfection, treated with 1 µM of ATRA for 24 hrs (Figure 5.3). Moreover, both the antibody for Stra6 C-Term and the Stra6 N-Term antibody found Stra6 predominately in the plasma membrane. MAPK and HDAC1 are markers of cytosol and nucleus, respectively, and were used to make sure that no contamination occurred during fractionation.

Finally, as shown in Figure 5.4, the HCT116 WT p53 was transfected with Stra6 (13 µg, 48 hrs), and after the first 24 hrs of cell transfection, the cells were treated with 2 µM of Dox for 24 hrs. The Stra6 protein was detected mainly in the nucleus, with molecular sizes of 25 and 15 kDa.).

Overall, Stra6 was not detected using the Stra6 N-Term antibody in the tested cells with endogenous and overexpressed Stra6 after DNA damage (Figure 5.1 and Figure 5.4, respectively). Moreover, the Stra6 N-Term antibody was not detected in cells overexpressing with Stra6, and those cells were not stimulated with DNA damage or retinoids (Figure 5.3). Of note, the Stra6 N-Term antibody was detected only in the cells that had the overexpressed Stra6 and had received retinoid treatment (ATRA).

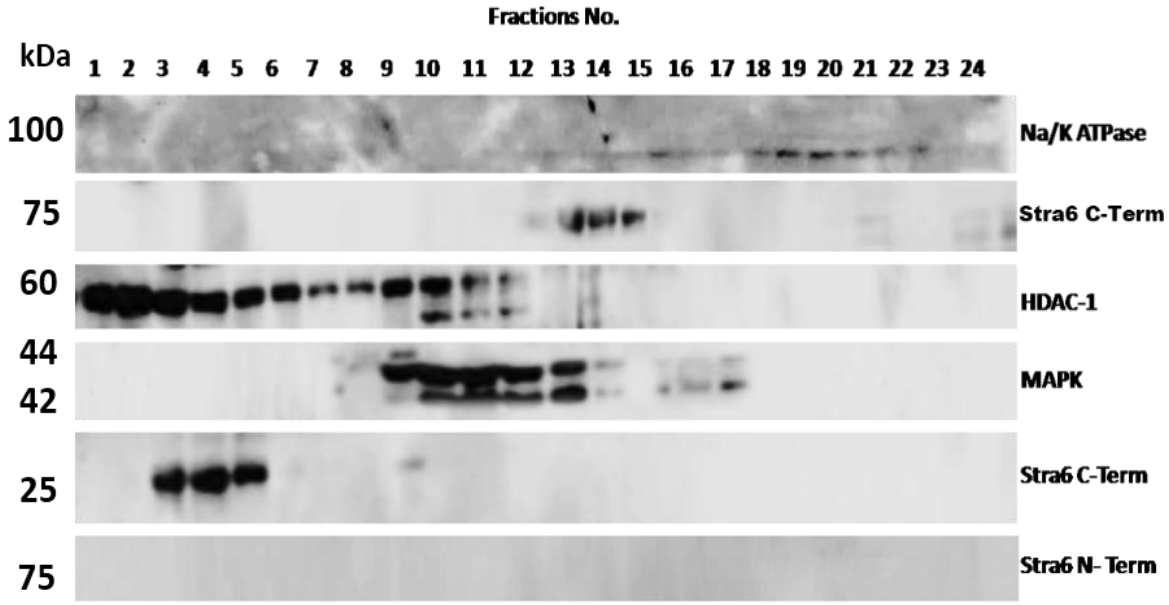

Figure 5.1: **Cell fractionation study to determine the subcellular localisation of Stra6 following Dox treatment in whole cell lysate of HCT116 WT p53**. Cells were transfected with empty vector (e.v.), and after 24 hrs, treated with 2 µl of Dox for 48 hrs. Cell lysate was loaded onto to a sucrose gradient before centrifugation at 100,000 g for 18 hrs at 4 ^{o}C. The yield was separated into 24 fractions and was loaded onto a 10 % gel for Western blot analysis. Na/K ATPase, HDAC-11 and MAPK were used as markers of plasma membrane, nucleus, and cytosol, respectively. Antibodies used to detect Stra6 were Stra6 C-Term and Stra6 N-Term. This experiment was done in duplicate**.**

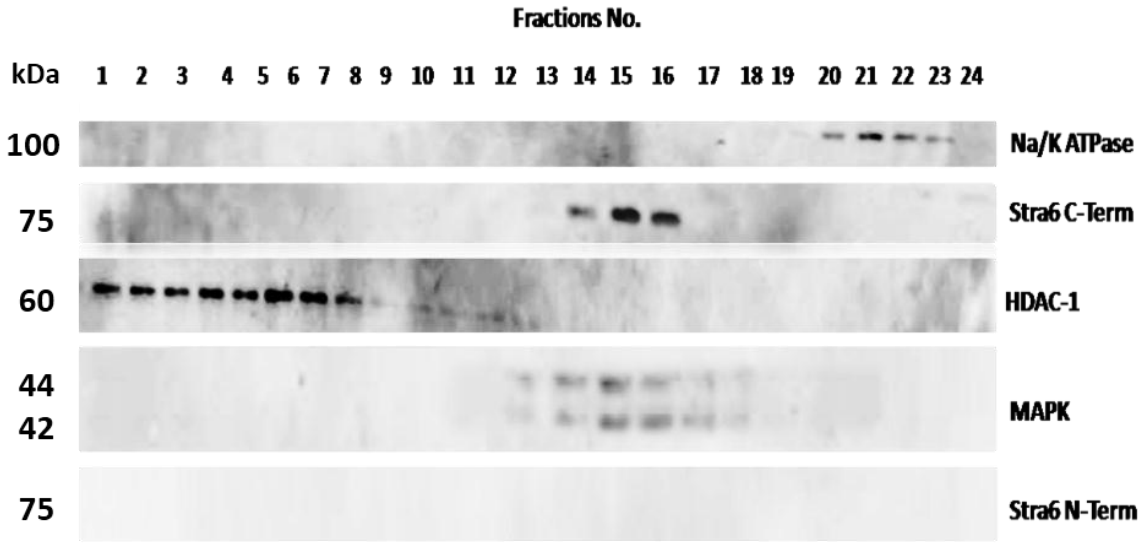

Figure 5.2: **Fractionation study to determine the subcellular localisation of Stra6 following Stra6 transfection in whole cell lysate of HCT116 WT p53**. Cells transfected with Stra6 (13 µg, 48 hrs). Cell lysate was applied to the sucrose gradient before centrifugation at 100,000 g for 18 hrs at 4 ^{o}C. The yield was separated into 24 fractions and was loaded onto a 10 % gel for Western blot analysis. Na/K ATPase, HDAC1 and MAPK are the markers of plasma membrane, nucleus, and cytosol, respectively. Antibodies used to detect Stra6 were Stra6 C-Term and Stra6 N-Term. Stra6 protein was detected mainly in the cytosol. This experiment was done in duplicate.

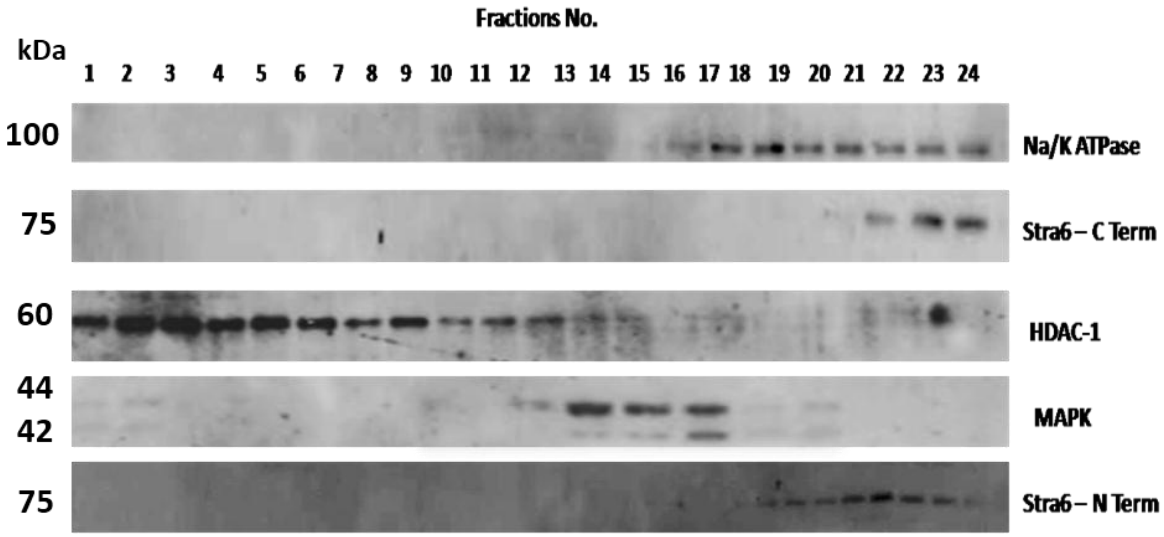

Figure 5.3: Fractionation study to determine the subcellular localisation of Stra6 following Stra6 transfection and ATRA treatment in whole cell lysate of HCT116 WT p53. Cells were transfected with Stra6 (13 µg, 48 hrs), and after the first 24 hrs of cell transfection, cells were treated with 1 µM of ATRA for 24 hrs. Cell lysate was applied to the sucrose gradient before centrifugation at 100,000 g for 18 hrs at 4 ^{o}C. The yield was separated into 24 fractions and was loaded onto a 10 % gel for Western blot analysis. Na/K ATPase, HDAC1 and MAPK are the markers of plasma membrane, nucleus, and cytosol, respectively. Antibodies used to detect Stra6 were Stra6 C-Term and Stra6 N-Term. Stra6 protein was detected mainly in the plasma membrane within both of the Stra6 antibodies that were used. This experiment was done in duplicate.

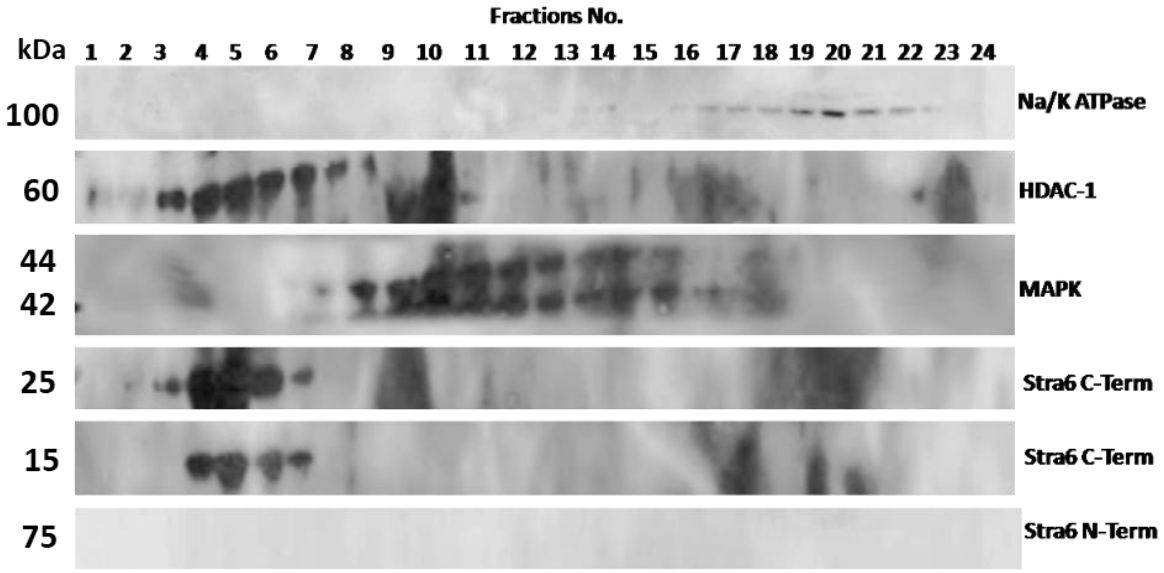

Figure 5.4: **Fractionation study to determine the subcellular localisation of Stra6 following Stra6 transfection and Dox treatment in whole cell lysate of HCT116 WT p53**. Cells were transfected with Stra6 (13 µg, 48 hrs), and after the first 24 hrs of cell transfection, cells were treated with 2 µM of Dox for 24 hours. Cell lysate was applied to the sucrose gradient before centrifugation at 100,000 g for 18 hrs at 4 ^{o}C. The yield was separated into 24 fractions and was loaded onto a 10 % gel for Western blot analysis. Na/K ATPase, HDAC1 and MAPK are the markers of plasma membrane, nucleus, and cytosol, respectively. Antibodies used to detect Stra6 were Stra6 C-Term and Stra6 N-Term. Stra6 protein was detected mainly in the nucleus with molecular sizes of 25 and 15 kDa. This experiment was done in duplicate.

5.3 Exploring the biological functions of the small fragment of Stra6 (Sm-C-term Stra6)

The results obtained from the pull-down assay with the Stra6 antibody and the mass spectrometry data in Chapter 4 determined protein bands of low molecular sizes of 25 and 20 kDa (Figure 4.1). It was later revealed that these smaller proteins were belonged to the Stra6 protein after the visualised bands were excised from the gel and analysed with the peptide mass fingerprinting (PMF) method.

To investigate the functions of the 25kDa fragment of Stra6 protein, it was cloned into expression vectors, as explained in Section 2.11.3.

Next, plasmid preparation and sequencing were performed to ensure that the correct nucleotide sequence was inserted in the vector and that the plasmids were ready to be used for experimental studies.

5.3.1 Role of Sm-C-Term Stra6 on p53 and the downstream apoptotic pathway

As shown previously in Chapter 3, Stra6 induced p53 independently of DNA damage (Figure 3.26); thus, we were interested in investigating p53 protein induction and stabilisation in addition to assessing pro-apoptotic gene caspases 3 as well as examining the apoptotic marker PARP after Stra6 transfection with the Sm-C-Term Stra6.

Therefore, a Western blot was conducted, and interestingly, as shown in Figure 5.5, the C terminus region of Stra6 was capable of conserving the biological function of the Stra6 gene by inducing p53 protein stability. Moreover, caspase 3, cleaved caspase 3, PARP and cleaved PARP were all upregulated in the HCT116 WT p53 cells treated with 1 µM of ATRA and/or 2 µM of Dox for 24 hrs after being transfected within the Sm-C-Term Stra6 plasmid for 48 hrs (Figure 5.5).

The transfection of Stra6 (Sm-C-Terminus) was compared with the endogenous levels of Stra6 after the combined treatment of ATRA and Dox (1 µM and 2 µM, respectively) for 24 hrs. The 15 kDa fragment of the Stra6 protein was detected mainly after the cells were treated with a DNA-damaging agent (Dox).

Still, endogenous levels of the Stra6 protein of a 75-kDa molecular size were detected because Stra6 induction by ATRA and Dox upregulated Stra6 induction, as expected.

5.3.2 The effect of Sm-C-Term Stra6 on inducing apoptotic cell death and ROS generation

Stra6 was found to induce p53 independently of DNA damage, and Stra6 overexpression was found to induce apoptotic cell death depending on p53, showing additive apoptotic cell death after a combined treatment of ATRA and Dox (Chapter 3; Figure 3.27). Thus, we wanted to test whether Sm-C-Term Stra6 could also induce apoptotic cell death and conserve the biological function of Stra6.

To determine this, Annexin V staining and FACS analysis was conducted on HCT116 WT p53 ($p53^{+/+}$) and U2OS WT p53 ($p53^{+/+}$) cells after cells were transfected with 4 μg of Sm-C-Term Stra6. The cells were treated with 1 μM of ATRA, treated with 2 μM of Dox or received a combined treatment of ATRA and Dox of similar concentrations (1 μM and 2 μM, respectively) for 24 hrs, 48 h after transfection.

As shown in Figure 5.6, 5.7 and 5.8, Sm-C-Term Stra6 showed an apoptotic cell death percentage that was greater than that after using DNA damage (Dox) alone. Overall, this confirms that the Stra6 overexpression of Sm-C-term induces apoptotic cell death and shows additive apoptotic cell death after a combined treatment of ATRA and Dox, particularly when compared to cells that have Stra6 overexpression (Figure 5.6 and Figure 5.8). The percentages of positive apoptotic cells for HCT116 WT p53 and U2OS WT p53 are presented as fold change in Figure 5.7 and Figure 5.9, respectively.

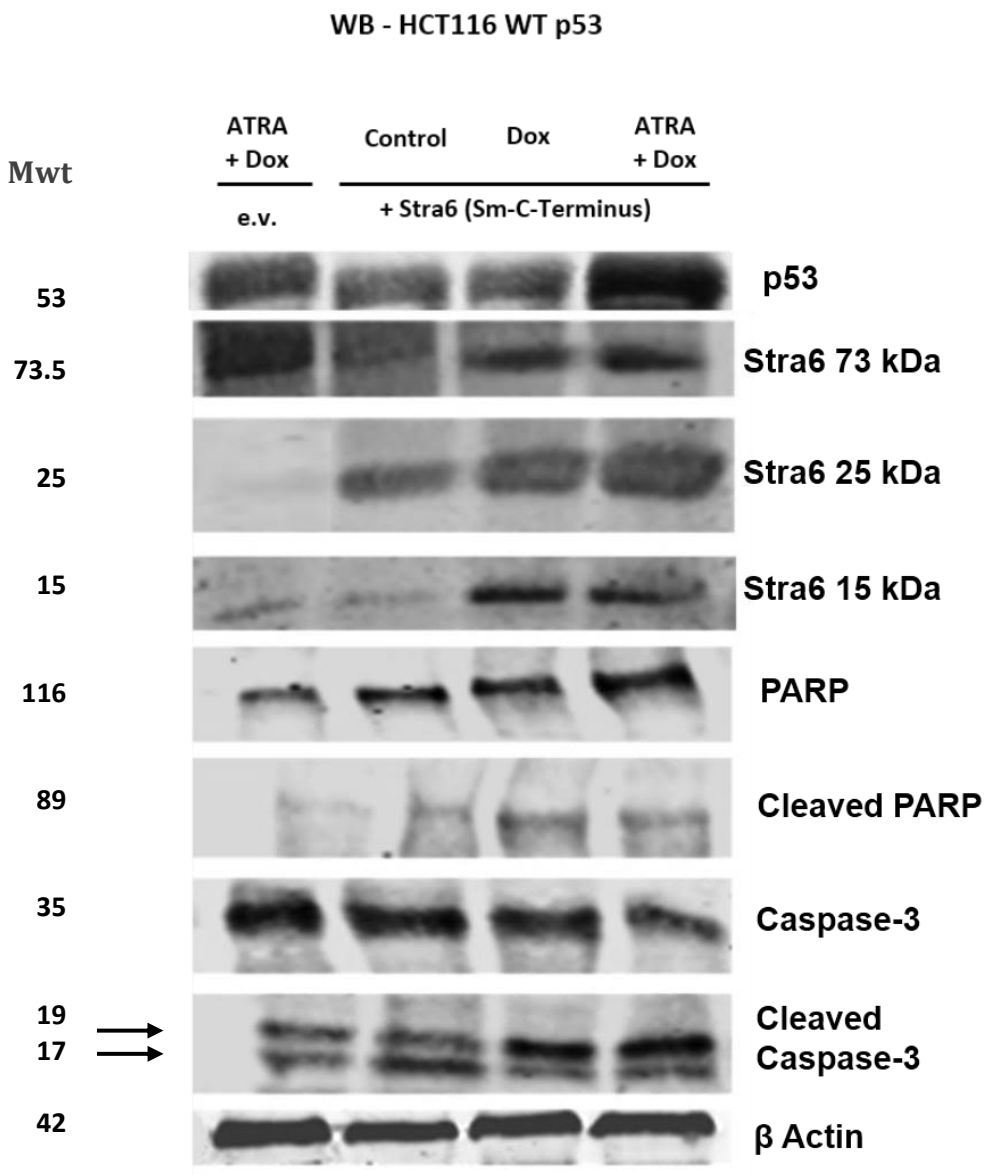

Figure 5.5: **The effect of Sm-C-Term Stra6 on p53 protein and other apoptotic markers.** HCT116 WT p53 cells with or without the adding of Dox (2 µM), treated with 1 µM of ATRA for 24 hrs and transfected with Sm-C-Term Stra6 (8 µg, 48 hrs). Here, Stra6 (Sm-C-Terminus) induced p53 and upregulated some of the investigated apoptotic proteins involved in p53 induced apoptosis. β-actin was used as a loading control. e.v. = empty vector. Mwt= Molecular weight in kDa.

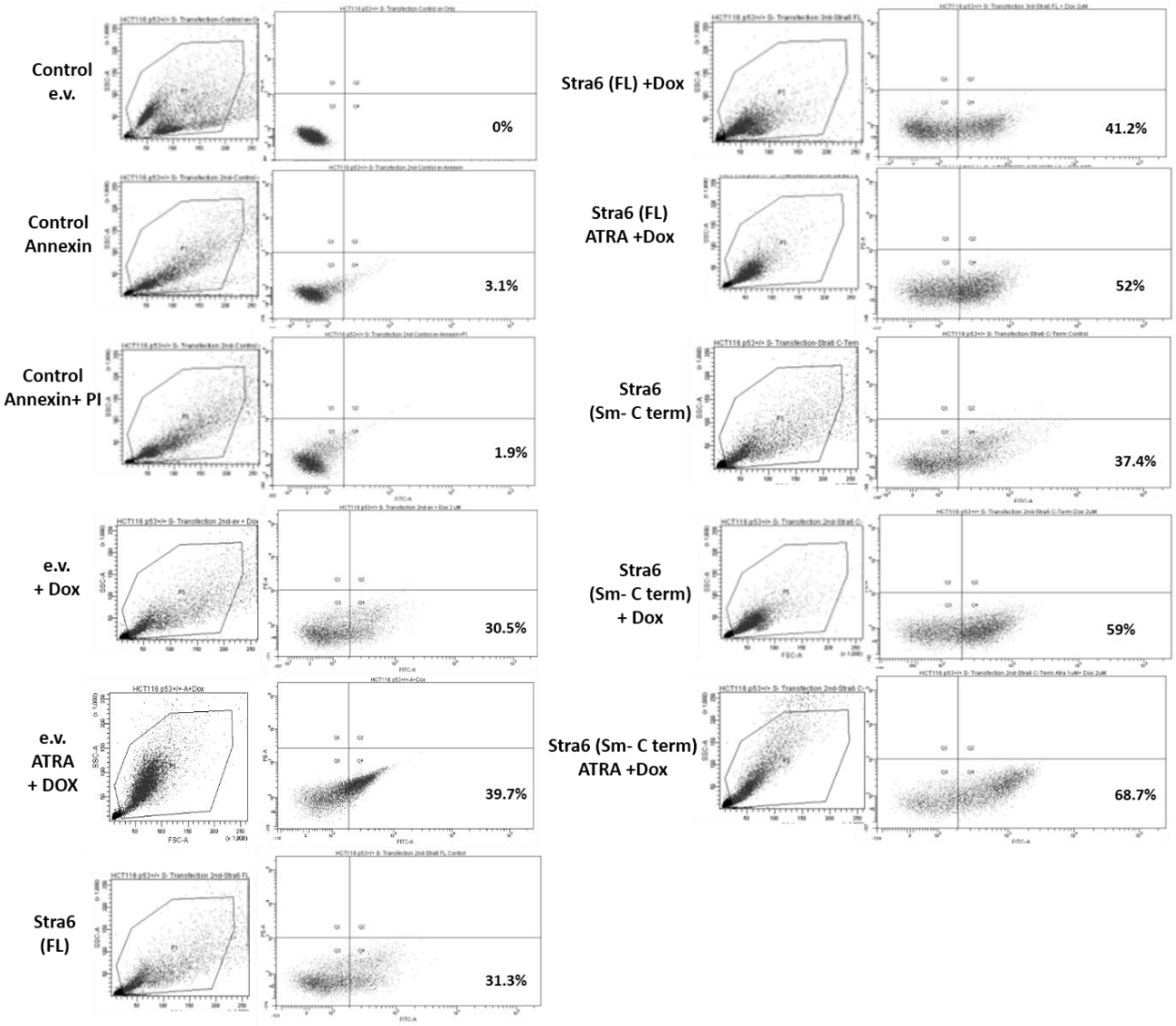

Figure 5.6: Stra6 small fragment (Sm-C-term) induces apoptotic cell death in HCT116 cells. Apoptosis was assessed using Annexin V staining and FACS analysis in HCT116 WT p53 cells. Cells were treated with 1 µM of ATRA, 2 µM of Dox or received a combined treatment of ATRA and Dox of similar concentrations (1 µM and 2 µM, respectively) for 24 hrs after transfection with 4 µg of Stra6 (FL/ Sm-C-term) for 48 hrs. e.v. = empty vector.

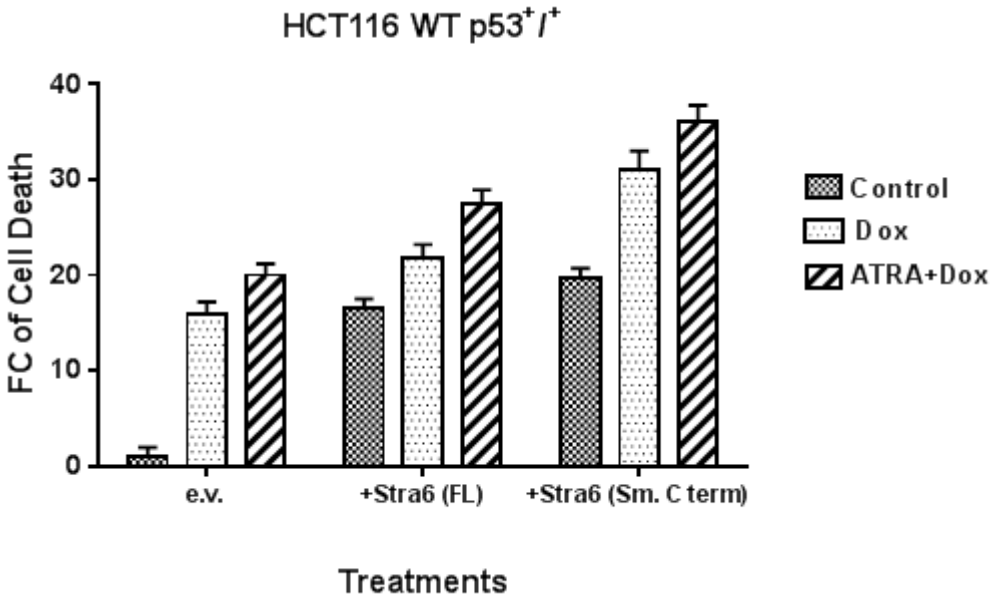

Figure 5.7: **HCT116 WT p53 fold changes in percentages of positive apoptotic cells**. Fold changes expressed as the mean ± SD of three independent experiments.

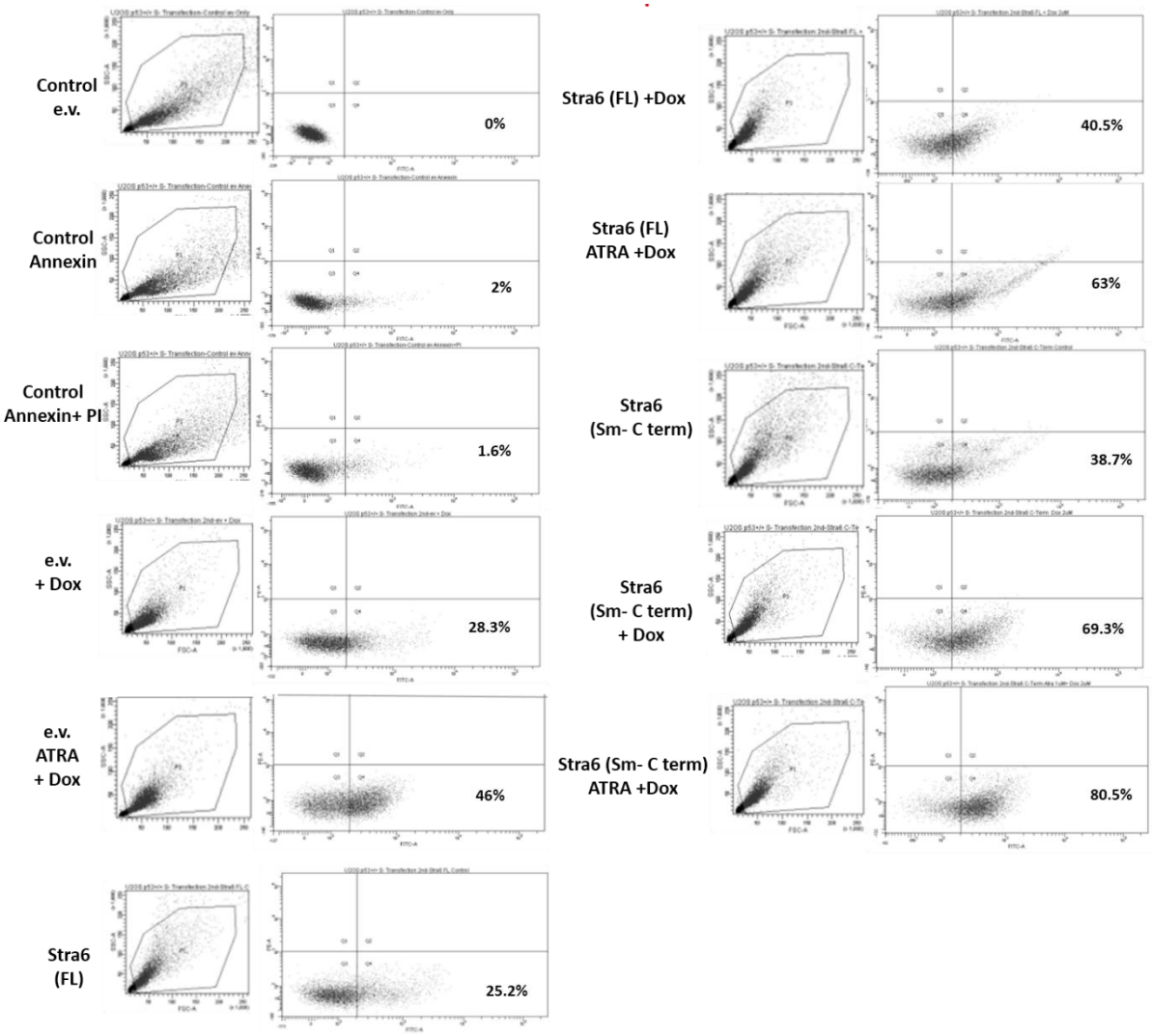

Figure 5.8: **Stra6 small fragment Sm-C-Term Stra6 induces apoptotic cell death in U2OS cells.** Apoptosis was assessed using Annexin V staining and FACS analysis in U2OS WT p53 cells. Split cells were treated with 1 µM of ATRA, were treated with 2 µM of Dox or received a combined treatment of ATRA and Dox of similar concentrations (1 µM and 2 µM, respectively) for 24 hrs after transfection with 4 µg of Stra6 (FL/ Sm-C-term) for 48 hrs**.** e.v. = empty vector.

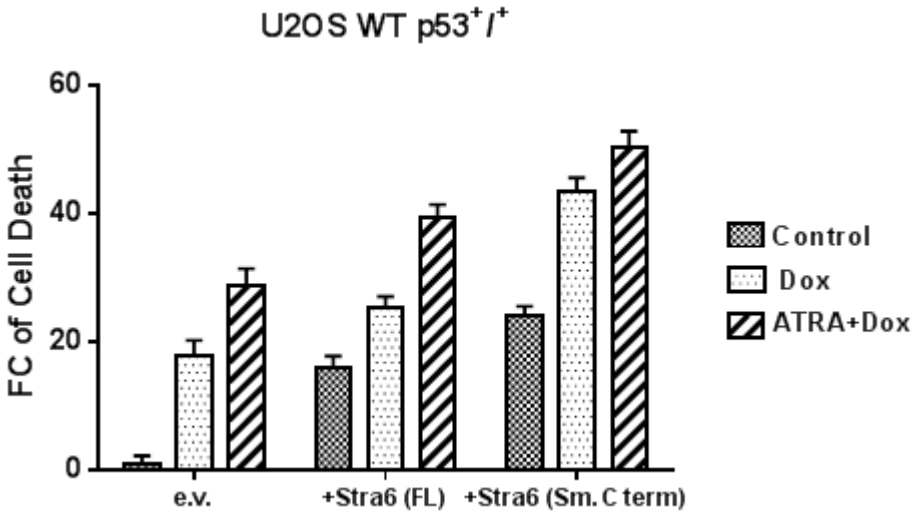

Figure 5.9: U2OS WT p53 fold changes of positive apoptotic cells. Fold changes expressed as the mean ± SD of three independent experiments. e.v. = empty vector.

We next assessed Stra6's role towards ROS generation by measuring changes in intracellular ROS levels. We had previously shown that full length Stra6 induces ROS accumulation inside the cells (Carrera et al., 2013). We aimed to examine whether Sm-C-Term Stra6 could also induce ROS.

As shown in Figure 5.10, we measured ROS in HCT116 WT p53 cells after the cells were transfected with (Sm-C-Term Stra6; 4 µg, 48 hrs) or an e.v. as a control. The results showed an increase in the mean fluorescence intensity in cells transfected with Sm-C Term Stra6.

Of note, Sm-C-Term Stra6 showed much higher apoptotic cell death percentages and ROS levels than did Stra6 itself as we observed this results over our obtainable results in chapter 3.

5.4 Explore the possible cleavage of Stra6

Our hypothesis is that, after DNA damage, Stra6 gets cleaved and a smaller C-Terminal fragment of ~25 kDa translocates into the nucleus, where it enhances p53 apoptotic functions. We explored the proteases that could potentially play a role in Stra6 cleavage using the MEROPS - the peptidase database (http://merops.sanger.ac.uk). This work was done in collaboration with Dr Jordi Villà (Universitat de Vic, Spain). The MEROPS database is based on a cohesive source of information that helps finding out whether or not a cleavage site could be biologically relevant in the light of cell signalling pathways and on the basis that such a cleavage site is probably conserved (Rawlings et al., 2016).

One interesting result revealed from the MEROPS database presented in (Table 5.1), is the identification of caspase-3, which could be cleaving Stra6 after the apoptotic pathway is engaged.

However, these data are considered to be only an initial result. Further confirmatory experiments are needed to define Stra6's cleavage sites and the proteases involved in such a process as well as to characterise their impacts on the Stra6 biological function towards apoptosis.

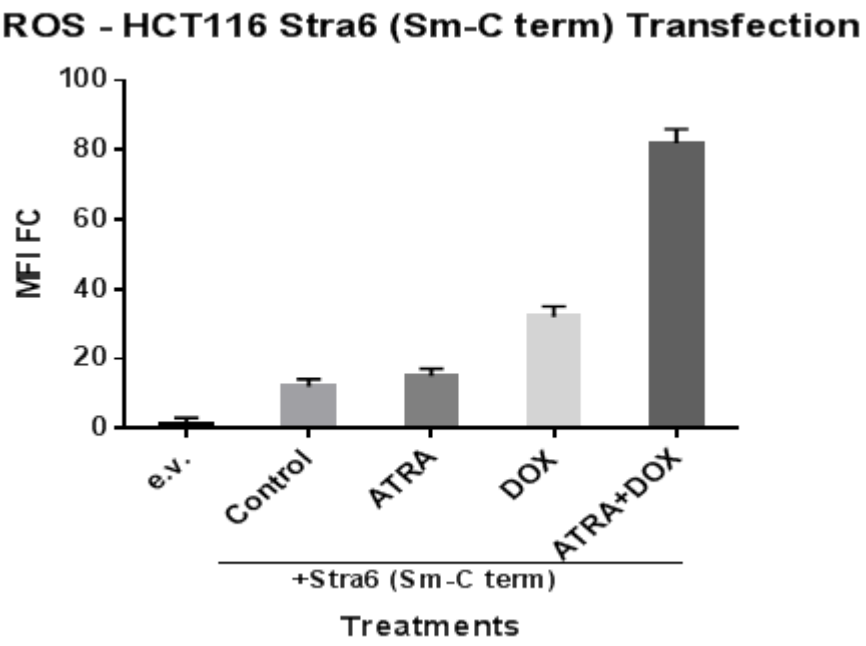

Figure 5.10: **Measurements of ROS represented by mean fluorescence intensity fold changes in HCT116 WT p53 cells**. The graphs show the levels of ROS produced in HCT116 WT p53 cells after cells were transfected with (Sm-C-Term Stra6; 4 µg, 48 hrs) or e.v. as a control. The results indicated an increase in the mean fluorescence intensity. Data are expressed as the fold changes compared to the control cells and as the mean ± SD of three independent experiments. e.v. = empty vector.

Motif	Weight-1 kDa	Weight-2 kDa	Cut-Position	Protease name
FLSWARVC	29.94	43.54	270	mucorpepsin
FLSWARVC	29.94	43.54	270	phytepsin
SWARVCLR	30.17	43.32	272	coagulation factor G
SWARVCLR	30.17	43.32	272	furin
VCLRHCIY	30.64	42.85	276	archealysin
VCLRHCIY	30.64	42.85	276	furin
VCLRHCIY	30.64	42.85	276	prostasin
LPLKLVLS	32.37	41.11	291	papain
VLSATLTG	32.86	40.63	296	mucorpepsin
VLSATLTG	32.86	40.63	296	phytepsin
LLLVGVVP	34.53	38.96	312	archaean proteasome
QKVRAGVT	35.61	37.88	322	furin
KVRAGVTT	35.68	37.81	323	elastase-1
VTTDVSYL	**36.15**	**37.33**	**328**	**caspase-3**
VSYLLAGF	36.61	36.87	332	rhizopuspepsin
SYLLAGFG	36.73	36.76	333	scytalidoglutamic peptidase
YLLAGFGI	36.8	36.69	334	elastase-1
LAGFGIVL	37	36.48	336	adenain
GIVLSEDK	37.38	36.1	340	dipeptidyl-peptidase III
VLSEDKQE	37.6	35.89	342	mucorpepsin
VLSEDKQE	37.6	35.89	342	phytepsin
LSEDKQEV	**37.71**	**35.77**	**343**	**caspase-3**
VTHRTNLR	40.81	32.68	370	mucorpepsin
VTHRTNLR	40.81	32.68	370	phytepsin
TNLRALHR	41.89	31.59	379	furin
TNLRALHR	41.89	31.59	379	PCSK5 peptidase
TNLRALHR	42.59	30.9	385	furin
TNLRALHR	43.07	30.41	389	archealysin
ALHRGAAL	43.07	30.41	389	furin
HRGAALDL	43.07	30.41	389	Kallikrein-1

Table 5.1: Possible proteases cleavage of Stra6. A list of predictable proteases and their expected cleavage sites at Stra6 protein using MEROPS - the peptidase database analysis**.**

5.5 Explore the cellular localisation of Stra6 by Immunofluorescence

After validating Sm-C-Term Stra6 functions, we studied its localisation following different cell stimuli, using immunofluorescence analysis and confocal imaging in HCT116 WT p53 cells.

Our results presented in the previous two chapters provide a rationale for how Stra6 can exert different biological functions depending on its localization.

As shown in Figure 5.11, HCT116 $p53^{+}/^{+}$ cells treated with 1 µM of ATRA and/or 2 µM of Dox for 48 hrs showed that non-stimulated cells had very low endogenous levels of Stra6. ATRA treatment localised Stra6 mainly within the cell membrane as expected. On the contrary, the DNA damage response to Dox treatment showed that Stra6 was distributed equally within the cytosol and nucleus. However, in cells stimulated with the combined ATRA and Dox treatment, we can observe that Stra6 is mostly located within the nucleus.

Figure 5.12 provides a negative control to the experiments described above, using anti-Rabbit IgG-DyLight-488 antibody only with no Stra6's primary antibody. The result confirms the quality of the used secondary antibody in avoiding non-specific binding activity.

Next, cells were co-transfected with 0.4 µg of both Stra6-C-EGFP and Stra6-N-mCherry plasmids. The main aim of this experiment was to study Stra6 localisation under different treatment conditions (1 µM of ATRA and/or 2 µM of Dox for 24 hrs). The C terminus tagged version of Stra6 included both the full length and the shorter forms, while the N terminus tagged was on full length version. As shown in Figure 5.13, we observed that Stra6 appears at different localisations within the cell according to the received stimulus. ATRA treatment resulted in Stra6 localisation within the cell membrane as anticipated. However, Stra6 was mostly in the nuclear membrane after DNA damage. In addition, the combined ATRA and Dox treatment showed accumulation of Stra6 mainly within the nucleus. In the cells that were not stimulated,

Stra6 was found to be predominantly in the cytosol with a small amount of Stra6 expressed on the plasma cell membrane. Of note, the Stra6 tagged with mCherry at the N terminus was detected only on the cells treated with ATRA, and not with other stimulated or not-stimulated cells, for reasons that are not fully understood.

Last, as shown in Figure 5.14, HCT116 $p53^{+}/^{+}$ cells were transfected with Sm-C-Term Stra6 tagged EGFP; 0.4 µg, 48 hrs), and after the first 24 hrs, the cells were treated with 1 µM of ATRA and/or 2 µM of Dox for 24 hrs. We observed that Sm-C-Term Stra6 tagged EGFP appears mainly localised within the nucleus regardless of the stimuli.

In non-stimulated cells, Sm-C-Term Stra6 was found to be localised within the nucleus, with low amounts in the cytosol. ATRA treatment resulted in Stra6 localisation mainly around the nucleus. Following DNA damage, Stra6 was found within the nucleus. Moreover, the combined ATRA and Dox treatment provoked Stra6 accumulation predominantly inside the nucleus.

Of note, these results correlated with the results obtained via a fractionation study to determine the subcellular localisation of Stra6.

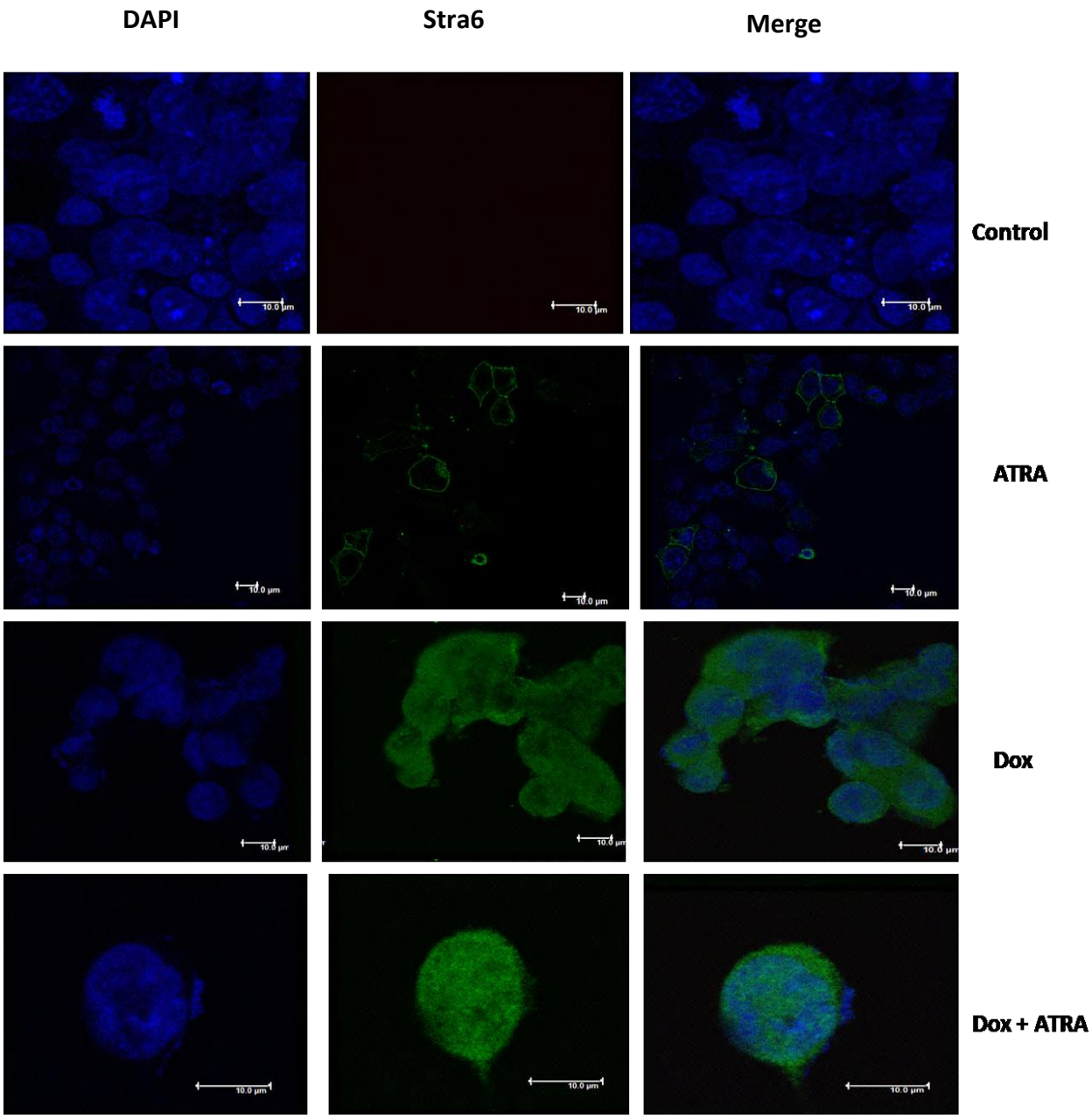

Figure 5.11: **Immunofluorescence analysis of endogenous Stra6 subcellular localisation in HCT116 WT p53 cells following different cell stimulations**. Representative immunofluorescence confocal analysis in HCT116 $p53^{+}/^{+}$–stimulated cells treated with 1 µM of ATRA and/or 2 µM of Dox for 48 hrs. Displaying Stra6 (green), which means green fluorescence indicates Stra6 protein labelled with anti-Stra6 (C-term) antibody in addition to anti-Rabbit IgG-DyLight-488–conjugated secondary antibody. The nucleus (blue) stained with DAPI. 'Merge' shows the overlapped images. The objective power used was 63x. The results shown are representative of the analysis done on duplicate of two different samples.

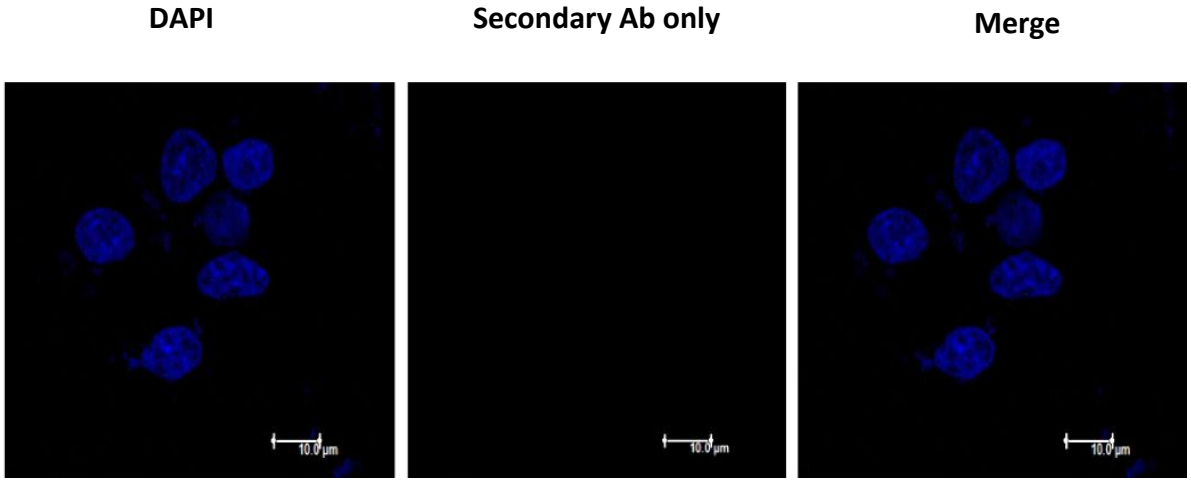

Figure 5.12: **Negative control of endogenous Stra6 testing with the addition of anti-Rabbit IgG-DyLight-488 antibody alone**. Representative immunofluorescence confocal analysis in HCT116 $p53^{+}/^{+}$ stimulated cells treated with 2 µM of Dox for 48 hrs. The anti-Stra6 (C-term) antibody was not added, to be able to confirm that the used antibody was not inducing non-specific binding. Scale bar= 10 µm.

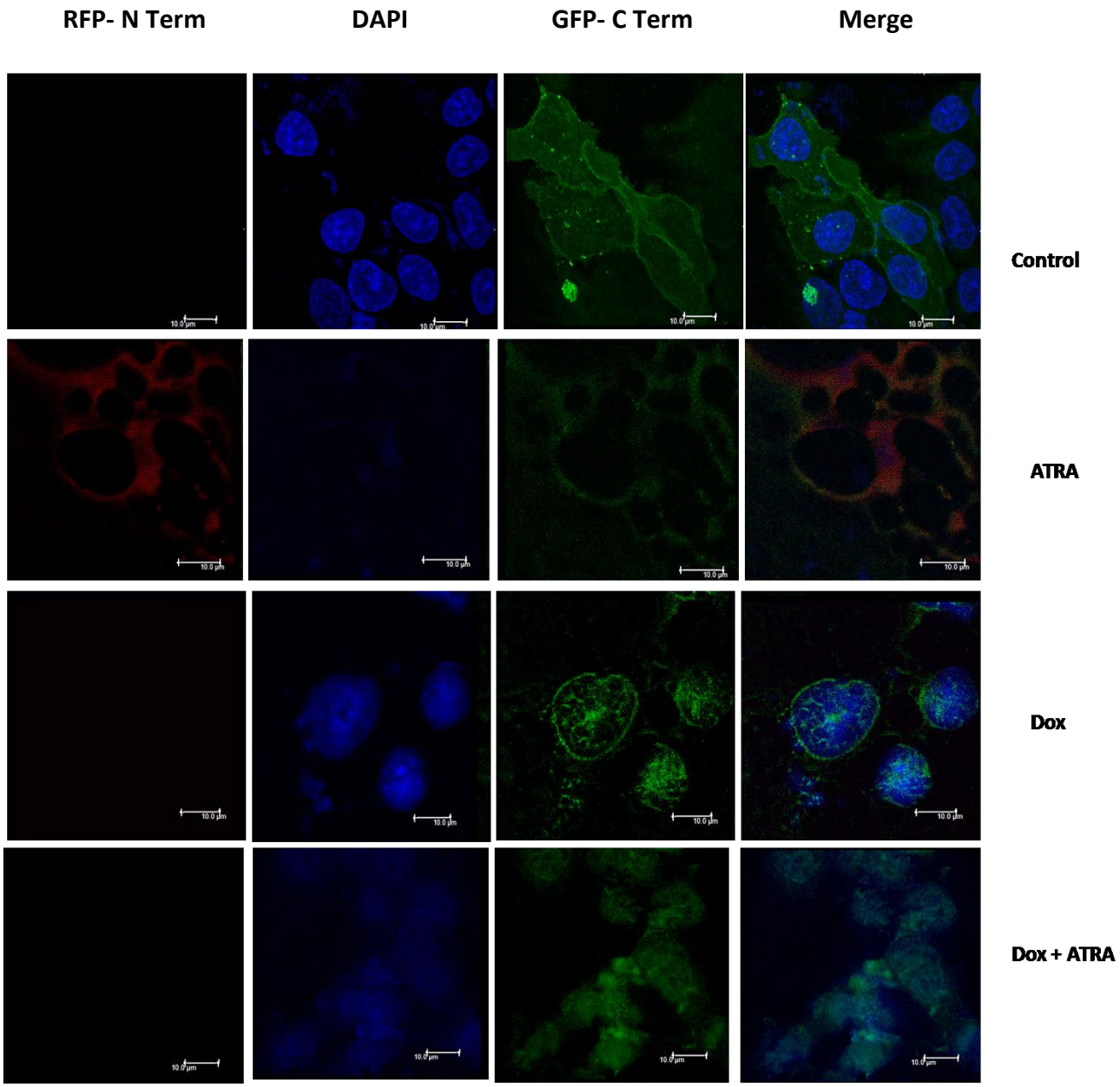

Figure 5.13: **Intracellular localisation of Stra6-C-EGFP/ Stra6-N-mCherry following different cell stimulations in HCT116 WT p53 cells.** Representative immunofluorescence confocal analysis in HCT116 $p53^{+}/^{+}$ cells transfected with 0.4 µg of Stra6 for 48 hrs and after the first 24 hrs cells treated with 1 µM of ATRA and/or 2 µM of Dox for 24 hrs. Stimulated cells displaying Stra6 tagged with either EGFP or mCherry) at C and N terminus, respectively, and the nucleus displaying (blue) stained with DAPI. 'Merge' shows the overlapped images. The objective power used was 63 x. The results shown are representative of the analysis done on duplicate of two different samples. Scale bar= 10 µm.

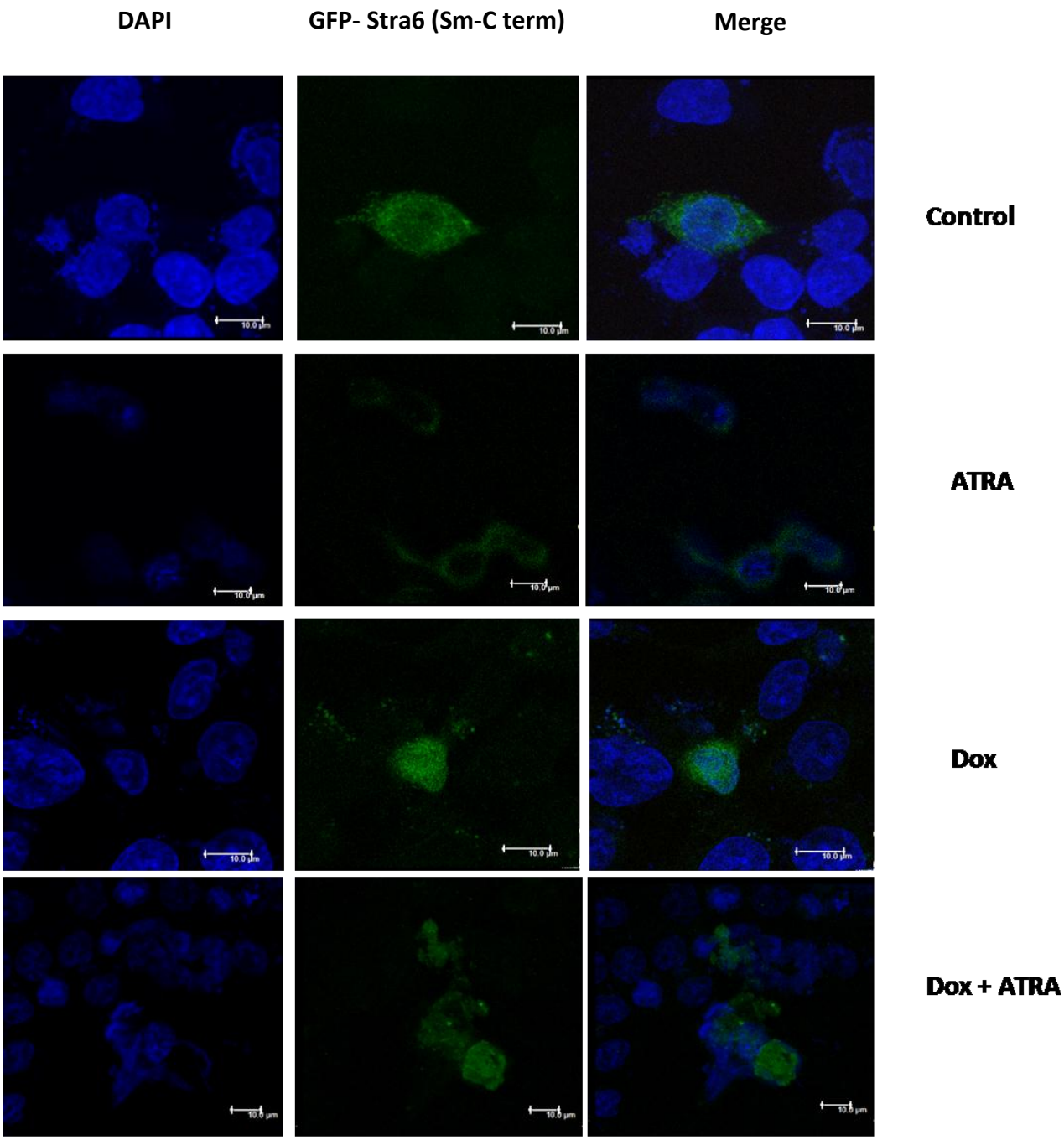

Figure 5.14: **Immunofluorescence analysis of Stra6 small fragment (Sm-C-Term Stra6) tagged with EGFP of its intracellular localisation following different cell stimulations in HCT116 WT p53 cells**. Representative immunofluorescence confocal analysis in HCT116 $p53^{+}/^{+}$ cells were transfected with Stra6 (Sm-C-term; 0.4 µg, 48 hrs), and after the first 24 hrs, cells were treated with 1 µM of ATRA and/or 2 µM of Dox for 24 hrs. The nucleus was stained with DAPI. 'Merge' shows the overlapped images. The objective power used was 63x. The results shown are representative of the analysis done on duplicate of two different samples. Scale bar= 10 µm.

5.6 Discussion

Our research on Stra6 subcellular localisation in cancer cells that received different treatments revealed that the Stra6 has at least three different cellular localisations—either on the cell membrane, in the cytosol or within the nuclear complex. —These localisations are fundamentally dependent on the type of stimulus the cell received.

Fractionation studies were done first assessing the endogenous Stra6 cellular localisation in response to DNA damage, followed by evaluating the overexpressed Stra6 towards DNA damage or ATRA treatment.

Endogenous Stra6 after a DNA damage was found to be in the nucleus, with a detected molecular size of 25 kDa. This result suggested that Stra6, which normally has a molecular size of 73.5 kDa, was cleaved to a smaller part to be re-localised from the cell membrane to the nucleus. However, there was a detectable amount of the endogenous Stra6 protein within the cytosol, and that could suggest that not all stra6 is cleaved upon stimulation (Figure 5.1).

Regarding the overexpression of Stra6 in cells where no treatment was added, we observed (Figure 5.2) that Stra6 was detected only in the cytosol. On the other hand, when the cells received ATRA, Stra6 was detected in the plasma cell membrane (Figure 5.3). This suggests that Stra6 has its own specified function to be achieved at a specified cellular localisation. For instance, Stra6 has always been identified as an RBP receptor that facilitates retinol uptake, and to serve this function, Stra6 needs to be localised on the plasma cell membrane (Berry et al., 2012; Breen et al., 2015).

Therefore, we could relate the observed biological function of Stra6 to the fact that Stra6 induces p53 independently of DNA damage (results presented in Chapter 3). We can do this by suggesting somehow that transcriptional modification was involved in the context of these two proteins Stra6 and p53 towards apoptotic cell death.

As described in the past report, p53 cytoplasmic immunoreactivity increased, which preceded Bax activation and caspase-3 cleavage (Geng et al., 2010). Also, the same authors found that the cytoplasmic p53 also showed colocalisation with

nucleophosmin (NPM), a nuclear chaperone protein previously implicated in cell death, and it was one of the proteins that has been identified from our mass spectrometry analysis data as a possible protein binding partner for Stra6 (results presented in Chapter 4). As we hypothesized that could be a link of how could Stra6 induces p53 induction towards cell death through NPM.

Still, Stra6 protein was detected primarily in the nucleus with molecular sizes of 25 and 15 kDa (Figure 5.4). Most remarkably, the 15-kDa fragment of Stra6 that was detected in the nucleus typically represented the molecular size of the C terminus domain of the Stra6 protein.

Furthermore, these data were in line with our previous data that showed that both 20- and 25-kDa fragments belonged to Stra6 by mass spectrometry analysis.

Generally, Stra6 cytosolic and nuclear fragments on non-stimulated cells and Dox-stimulated cells, respectively, have been detected by using the Stra6 antibody that recognised the C terminal domain. However, using the Stra6 antibody to detect the N term of the Stra6 protein was not possible most of the times, and this could be due to experimental and technical issues. However, after ATRA treatment, Stra6 was detected on the plasma cell membrane using the N term antibody. In addition, this could be related to the protein nature, involving cleavage and protein folding, which would restrict the epitope of the N term antibody from binding to Stra6 at the N terminus domain.

We have confirmed from our results of the Western blot analysis in Figure 5.5 that Sm-C-Term Stra6 induces p53 independent of DNA damage as well as increases apoptotic proteins, such as caspase-3 cleavage and apoptotic marker PARP cleavage, with or without Dox-induced DNA damage dependent on WT p53. Furthermore, the combined treatment of ATRA and DNA damaging agents have shown the enhancement of the cleavage of PARP and cleaved caspase-3. The observed result supports the hypothesis that Stra6 enhances the apoptotic cascade, particularly the C terminus of the Stra6 domain. In addition, endogenous levels of Stra6 were upregulated in proportion to the degree of stimulus received, especially when combined ATRA and Dox was added after

p53 was induced. This continued to support our hypothesis about the initiation of a positive feedback loop between Stra6 and p53. However, in this experiment, we transfected only the cells with Sm-C-Term Stra6 and we still can recognise the increased induction of Stra6 (endogenous and overexpressed) along with an increase in p53 protein stabilisation.

The 15 kDa form of Stra6 was detected mainly in the presence of DNA damage, suggesting that the 25 kDa of transfected Stra6 could undergo another cleavage to induce a smaller fragment of the protein. Both 25- and 15-kDa Stra6 were together or individually translocated into the nucleus, which suggested the association of Stra6 and p53 in starting the apoptotic cellular events.

Also, the obtained data from MEROPS identified caspase-3 as a predictable protease that would participate in Stra6 protein cleavage.

Accordingly, the results confirmed that Stra6 (Sm-C-term) can induce apoptotic cell death. We propose that Stra6 (Sm-C-term) has apoptotic function, probably dependent on p53. Moreover, Stra6 (Sm-C-term) determines an apoptotic effect that might be related to the fact that not all Stra6 undergoes cleavage.

In addition, we established the involvement of Sm-C-Term Stra6 in mediating ROS generation. The mechanisms by which Stra6 induces ROS are still not understood.

Stra6 has a known role as a cell surface receptor for RBP and its localisation on the plasma cell membrane serves this function in the context of being an important member of the retinoid signalling pathway. The confocal images showed that Stra6 has a membrane localisation following ATRA treatment in the endogenous Stra6 and Stra6 overexpression model. However, upon DNA damage, Stra6's showed different cellular localisations, especially in the area of the nucleus.

Overall, the changes of Stra6 subcellular localisation are likely a consequence of many issues, the biological function under certain conditions, the interacting binding partners, post transcriptional modification and other factors that all cooperate in shaping Stra6's role and facilitate the cross-talk between the retinoid signalling pathway and p53 apoptotic pathway.

6 Overview, Conclusion and Summary

6.1 Overview

The work presented in this thesis has brought further insight into the biological role that Stra6 plays in p53-induced apoptosis, in addition to its role as a retinol-RBP receptor or as a member of other signalling pathways. We also provided molecular evidence of a potentially successful combination treatment for cancer, based on using retinoids as sensitizers to DNA-damaging agents, which would depend on Stra6 expression. As Stra6 is a retinoic acid responsive gene, its expression can be induced by ATRA and other retinoids, and it has been shown to contribute to cell death following DNA damage (Carrera et al., 2013). Exploiting these two features of Stra6 may result in improved antineoplastic therapies.

We found that endogenous Stra6 mRNA and protein levels were upregulated in response to retinoid treatment and DNA damage, observing a significant marked increase in Stra6 induction when both ATRA and DNA-damaging agents were used. Moreover, p53 protein levels were also increased after Stra6 upregulation, with high stability and apoptotic-inducing activity in following cell sensitisation with ATRA, and stimulation with DNA-damaging agents, showing that Stra6 can help drive tumour cells to apoptosis. Thus, our results showed that retinoids can enhance the upregulation and stabilisation of p53 after DNA damage, and that this is dependent on Stra6**.** However, both Stra6 and Tp53 were important in achieving maximum cell death, as was observed by the identification of a positive feedback loop between Stra6 and p53.

Of note, overexpression of Stra6 showed that this molecule can induce p53 independently of DNA damage, thus stimulating downstream apoptotic and proapoptotic proteins, such as caspase-3 and caspase-9, as well as PARP cleavages. More interestingly, we observed differences in retinoid stimulation of Stra6 in several cancer cell lines.

According to whether it was endogenously expressed or overexpressed, as the latter has shown the obvious characteristic of being an apoptotic protein, rather than functioning only as a retinol-RBP cell surface receptor. The novelty of our data lies in the fact that we propose that these sensitising effects of retinoids may be mediated by Stra6, which we have shown is induced by retinoids and has a pro-apoptotic function in the context of the p53 pathway.

Overexpression of Stra6 in cancer cell lines that were sensitised with ATRA and stimulated with DNA-damaging agents showed an accumulation of ROS, which we propose would result in enhanced cell death. The mechanisms by which Stra6 induces ROS remain to be elucidated. Treatment of these cells with ROS inhibitors (NAC and GSH) showed that Stra6 induced p53 through ROS generation, and the possibility of an existing cooperation between binding partners still remains. We explored this possibility in order to identify potential binding partners for Stra6, as there is much still to elucidate about its mechanisms of action, both regarding its role in cell signalling and its apoptotic characteristics. These interacting partners were identified by carrying out a pull-down assay that was analysed by mass spectrometry and confirmed by co-IP.

These data identified important nuclear and cytosolic proteins, many of which have been related to apoptosis, such as NPM (Box et al., 2016), NCL (Daniely et al., 2002) and HMGB1 (Sohun and Shen, 2016). Moreover, DNA damage stimulates hnRNPK SUMOylation, and this PTM was necessary for the expression and activation of p53 target genes that triggered apoptosis (Pelisch et al., 2012).

The pull-down assay of Stra6 protein in cells stimulated by ATRA and/or Dox showed bands of low molecular weight, specifically 25 and 20 kDa, that were related to the Stra6 sequence, as identified by peptide mass fingerprinting. This led to the hypothesis that Stra6 is somehow cleaved at its C-terminal domain in response to cellular stress and DNA damage. We assumed that

Stra6 could be cleaved within the C-terminus in response to the PTM of tyrosine and threonine in that region, on the basis of our primary data using a phosphorylation prediction software programme. However, this area of research requires further study.

We observed that the truncated forms of Stra6 could be translocated from the plasma cell membrane to the cytosol in the absence of DNA damage, and then relocated within the nucleus in response to Dox. Furthermore, this small fragment of Stra6, which represented the C-terminus domain of the molecule, was capable of generating ROS and inducing p53-dependent apoptotic cell death, and it also enhanced the downstream cascade of the p53 signalling pathway.

The presence of a 15 kDa form of Stra6 detected in the presence or absence of DNA damage suggests that the 25 kDa of transfected Stra6 may undergo another cleavage to produce smaller fragment of the protein. Both 25 and 15 kDa Stra6 were present in the nucleus, which is indicative of the fact that the association of Stra6 and p53 cooperate in the pro-apoptotic cellular events that eventually occur.

To sum up, our experimental studies have provided strong evidence of the fact that Stra6 is involved in sensitising tumour cells to DNA-damaging agents and functions as an apoptotic protein in a p53-dependent manner.

The changes of subcellular localisation of Stra6 would be important to define its biological function, the selection of interacting protein-binding partners, PTM and other factors, which would all cooperate in shaping the biological role of Stra6 to address the corresponding stimuli and facilitate the existing cross-talks between the retinoid signalling pathway and the p53 apoptotic signalling pathway. Most importantly, the apoptotic features of Stra6 suggest that its upregulation in combination with other anticancer treatments, such as chemotherapy or radiotherapy, could be therapeutically promising. Given the fact that retinoids have minimal side effects, when compared to classic

chemotherapy, they could be used as adjuvants to induce Stra6 and minimise the side effects of traditional cancer therapies, providing a better option for helping people receiving cancer treatment.

Finally, below is a proposed model (Figure 6.1) of the most likely ways in which Stra6 participates in inducing apoptotic cell death, whereby the increased oxidative stress and DNA damage is dependent on TP53, and the resulting levels of oxidative DNA damage and ROS generation initiate the upregulation of p53. Furthermore, these p53 levels would increase induction of Stra6 levels, meaning that Stra6 induces p53 expression in a positive feedback loop, with a greater tendency of ROS production to fully trigger an apoptotic cell death response through the stimulation of p53-dependent pro-apoptotic and apoptotic proteins in cooperation with the binding protein partners of Stra6.

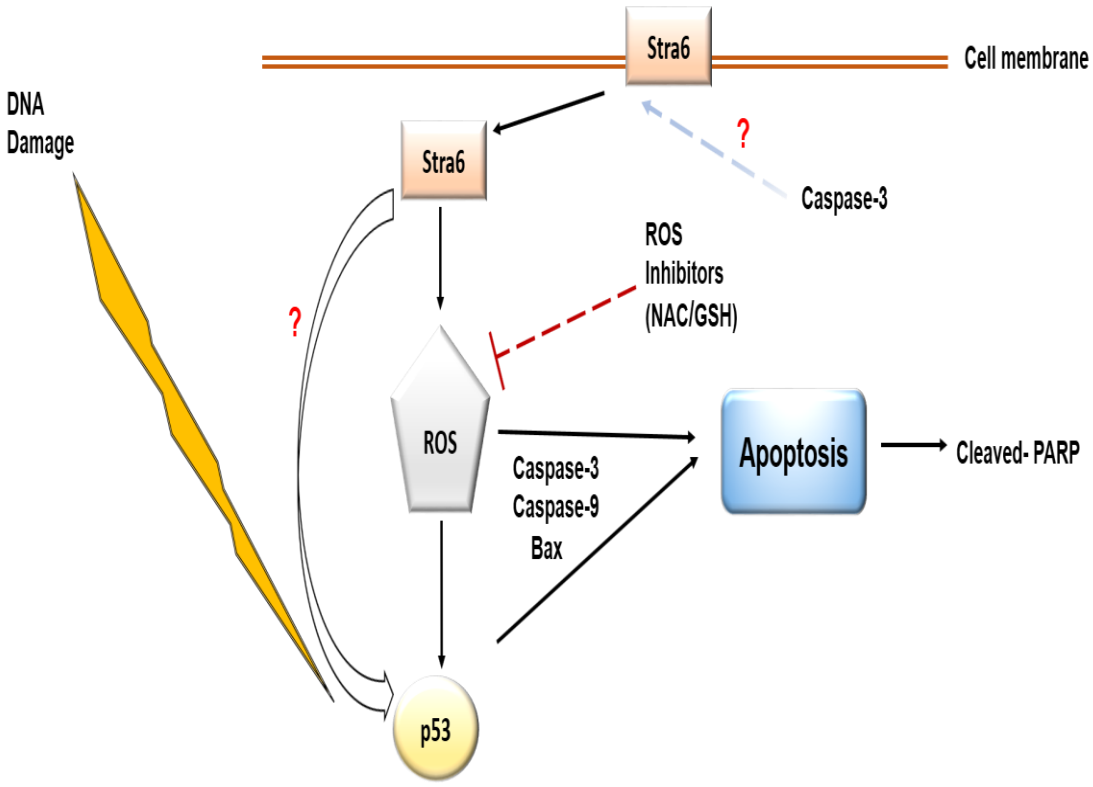

Figure 6. 1: **A summary of a proposed model of the role of Stra6 in a p53-dependent apoptosis.** It has been shown that p53 induces Stra6 in the context of the response to DNA damage and in a p53 dependent manner, (Carrera et al., 2013). Here, we prposes Stra6 induces p53 independent of DNA damage through ROS generation and initiates a Stra6-p53 positive feedback loop that would trigger an apoptotic cell death response via the stimulation of p53-dependent pro-apoptotic and apoptotic proteins, in cooperation with the binding-protein partners of Stra6 represented on the diagram by (?). Moreover, Caspase-3 could be associated with Stra6 cleavage process and its could be facilitate Stra6 translocation from cell membrane to be inside the cell**.**

6.2 Summary

- p53 upregulates Stra6 and Stra6 upregulates p53 thus suggesting a positive feedback loop.

- Stra6 can induce p53 independent of DNA damage.

- Stra6 induced p53 mainly through a ROS generation mechanism.

- Stra6 induction sensitizes cells to DNA-damaging agents.

- Several Stra6 binding protein partners are involved in apoptosis.

- Stra6 could be cleaved to smaller fragments at its C-terminus domain in response to DNA damage, resulting in truncated forms of 25 and 20–15 kDa molecular sizes.

- The Stra6 C-terminus truncated version of the protein has tumour suppressor characteristics, thus suggesting that this domain of the Stra6 protein has conserved an apoptotic function.

- Fractionation and immunofluorescence studies showed Stra6 cytosolic and nuclear localisation in the absence or presence of DNA damage, respectively. Therefore, Stra6 function may depend on its subcellular localisation and the stimulus that induces it.

6.3 Outcomes and future studies

The experiments conducted in the present study suggest that Stra6 expression can be a predictive marker of tumour sensitivity to DNA damaging agents and that vitamin A, through Stra6, could be useful as adjuvants. The presence of Stra6 should enhance the apoptotic effect of DNA-damaging agents. Moreover, of all the tested cancer cell lines that responded to a combination of retinoid and DNA-damaging agents, it was shown that those cell lines would particularly benefit from this approach following upregulation of Stra6 levels after retinoid treatment leads to an increased sensitivity to chemotherapy/radiotherapy. Determining the induction of Stra6 in different cancers in response to retinoids should allow us to predict which would be more sensitive to a retinoid pre-treatment.

Furthermore, our results have provided novel understandings regarding the Stra6 mechanism of tumour suppression, which had not been previously well defined. In addition, the data we obtained regarding Stra6 and its binding-protein partners, as well as its localisation, were used to propose a new hypothesis relating to the mechanism of action of Stra6. All of these outcomes provide evidence that vitamin A is a possible chemopreventive agent and/or an adjuvant, via Stra6 in a p53-dependent manner. Additional studies are necessary to further examine Stra6 as a potential new member of the apoptotic signalling pathway and as playing a role in tumour suppression.

One suggested area of further study is to confirm the clinical relevance of the abovementioned outcomes and apply these findings *in vivo* by using mouse models of tumour development in order to test the possibility that a basal increase in Stra6 from chronic dietary supplementation with vitamin A would sensitize cancer cells to DNA damaging agents. Thus, it would help in characterising the adjuvant effects of retinoids via Stra6-expressing tumours that would be treated with DNA-damaging agents. An alternative would be to take a wider approach to the study of proteins that bind Stra6 by using a yeast

two-hybrid system and the Human Kidney MATCHMAKER cDNA library (Clontech) or to use the tandem affinity purification method.

PTM is another area of Stra6 research that requires further investigation in order to identify at what residue, and by which proteases, Stra6 undergoes PTM and cleavage in the context of the response to DNA damage; the PTM of Stra6 by ATRA would be used as a control.

Bibliography

1. Ablain, J. et al., 2014. Activation of a promyelocytic leukemia-tumor protein 53 axis underlies acute promyelocytic leukemia cure. *Nature medicine*, 20(2), pp.167–74.

2. Abdelalim, E.M. and Tooyama, I., 2014. Knockdown of p53 suppresses Nanog expression in embryonic stem cells. *Biochemical and biophysical research communications*, 443(2), pp.652-657.

3. Alapatt, P. et al., 2013. Liver Retinol transporter and receptor for serum retinol-binding protein (RBP4)., 288(2), pp.1250–1265.

4. Alarcon-Vargas, D. and Ronai, Z.E., 2002. p53–Mdm2—the affair that never ends. *Carcinogenesis*, 23(4), pp.541-547.

5. Allan, L.A. & Fried, M., 1999. p53-dependent apoptosis or growth arrest induced by di erent forms of radiation in U2OS cells: p21 WAF1 / CIP1 repression in UV induced apoptosis.

6. Allenby, G. et al., 1993. Retinoic acid receptors and retinoid X receptors: interactions with endogenous retinoic acids. *Proceedings of the National Academy of Sciences*, 90(1), pp.30–34.

7. Allenby, G. et al., 1994. Binding of 9-cis-retinoic acid and all-trans-retinoic acid to retinoic acid receptors alpha, beta, and gamma. Retinoic acid receptor gamma binds all-trans-retinoic acid preferentially over 9-cis-retinoic acid. *J. Biol. Chem*., 269, pp.16689–95.

8. Altucci, L. and Gronemeyer, H., 2001. The promise of retinoids to fight against cancer. *Nature Reviews Cancer*, 1(3), pp.181-193.

9. Anzano, M.A. et al., 1994. Prevention of breast cancer in the rat with 9- cis - retinoic acid as a single agent and in combination with tamoxifen. *Cancer Research*, 54, pp.4614–4617.

10. Appella, E. & Anderson, C.W., 2001. Post-translational modifications and activation of p53 by genotoxic stresses. *European Journal of Biochemistry*, 268(10), pp.2764–2772.

11. Bai, L. and Zhu, W.G., 2006. p53: structure, function and therapeutic applications. *J Cancer Mol*, 2(4), pp.141-153.

12. Baker, S.J., Fearon, E.R., Nigro, J.M., Hamilton, S.R. and Preisinger, A.C., 1989. Chromosome 17 deletions an p53 gene mutations in colorectal carcinomas. *Science*, 244(4901), p.217-221.

13. Barnouin, K. et al., 2002. H2O2 induces a transient multi-phase cell cycle arrest in mouse fibroblasts through modulating cyclin D and p21Cip1 expression. *Journal of Biological Chemistry*, 277(16), pp.13761–13770.

14. Baybutt, R.C., Hu, L. and Molteni, A., 2000. Vitamin A deficiency injures lung and liver parenchyma and impairs function of rat type II pneumocytes. *The Journal of nutrition*, 130(5), pp.159-1165.

15. Bellovino, D., Morimoto, T., Tosetti, F. and Gaetani, S., 1996. Retinol binding protein and transthyretin are secreted as a complex formed in the endoplasmic reticulum in HepG2 human hepatocarcinoma cells. *Experimental cell research*, 222(1), pp.77-83.

16. Bender, D.A., 2003. Nutritional biochemistry of the vitamins. *Cambridge university press*.

17. Bensaad, K. et al., 2006. TIGAR, a p53-inducible regulator of glycolysis and apoptosis. *Cell*, *126*(1), pp.107-120.

18. Benson, M.J., Pino-Lagos, K., Rosemblatt, M. and Noelle, R.J., 2007. All-trans retinoic acid mediates enhanced T reg cell growth, differentiation, and gut homing in the face of high levels of co-stimulation. *Journal of Experimental Medicine*, 204(8), pp.1765-1774.

19. Berry, D.C. & Noy, N., 2012. Signaling by vitamin A and retinol-binding protein in regulation of insulin responses and lipid homeostasis. *Biochimica et biophysica acta*, 1821(1), pp.168–76.

20. Berry, D.C. et al., 2011. Signaling by vitamin A and retinol-binding protein regulates gene expression to inhibit insulin responses.

21. Berry, D.C. et al., 2012. Cross talk between signaling and vitamin A transport by the retinol-binding protein receptor STRA6. *Molecular and cellular biology*, 32(15), pp.3164–75.

22. Berry, D.C. et al., 2012. Transthyretin Blocks Retinol Uptake and Cell Signaling by the Holo-Retinol-Binding Protein Receptor STRA6. *Molecular and Cellular Biology*, 32(19), pp.3851–3859.

23. Berry, D.C. et al., 2013. The STRA6 receptor is essential for retinol-binding

protein induced insulin resistance but not for maintaining vitamin a homeostasis in tissues other than the eye. *Journal of Biological Chemistry*, 288(34), pp.24528–24539.

24. Berry, D.C., Levi, L. & Noy, N., 2014. Holo-retinol-binding protein and its receptor STRA6 drive oncogenic transformation.

25. Bhat, M.K. and Cama, H.R., 1979. Gonadal cell surface receptor for plasma retinol-binding protein A method for its radioassay and studies on its level during spermatogenesis. *Biochimica et Biophysica Acta (BBA)-General Subjects*, *587*(2), pp.273-281.

26. Bieging, K.T., Mello, S.S. & Attardi, L.D., 2014. Unravelling mechanisms of p53-mediated tumour suppression. *Nature reviews. Cancer*, 14(5), pp.359–70.

27. Blaner, W.S. and Olson, J.A., 1994. Retinol and retinoic acid metabolism. *The retinoids: Biology, chemistry, and medicine*, *2*, pp.229-256.

28. Blom, N., Gammeltoft, S. and Brunak, S., 1999. Sequence and structure-based prediction of eukaryotic protein phosphorylation sites. *Journal of molecular biology*, *294*(5), pp.1351-1362.

29. Blomhoff, R. and Blomhoff, H.K., 2006. Overview of retinoid metabolism and function. *Journal of neurobiology*, *66*(7), pp.606-630.

30. Bocchia, M., Xu, Q., Wesley, U., Xu, Y., Korontsvit, T., Loganzo, F., Albino, A.P. and Scheinberg, D.A., 1997. Modulation of p53, WAF1/p21 and BCL-2 expression during retinoic acid-induced differentiation of NB4 promyelocytic cells. *Leukemia research*, *21*(5), pp.439-447.

31. Bok, D. and Heller, J., 1976. Transport of retinol from the blood to the retina: an autoradiographic study of the pigment epithelial cell surface receptor for plasma retinol-binding protein. *Experimental eye research*, *22*(5), pp.395-402.

32. Bomsztyk, K., Denisenko, O. and Ostrowski, J., 2004. hnRNP K: one protein multiple processes. *Bioessays*, *26*(6), pp.629-638.

33. Bonet, M.L., Ribot, J. and Palou, A., 2012. Lipid metabolism in mammalian tissues and its control by retinoic acid. *Biochimica et Biophysica Acta (BBA)-Molecular and Cell Biology of Lipids*, *1821*(1), pp.177-189.

34. Boonstra, J. and Post, J.A., 2004. Molecular events associated with reactive oxygen species and cell cycle progression in mammalian cells. *Gene*, *337*, pp.1-13.

35. Bouillet, P., Oulad-Abdelghani, M., Vicaire, S., Garnier, J.M., Schuhbaur, B., Dollé, P. and Chambon, P., 1995. Efficient cloning of cDNAs of retinoic acid-responsive genes in P19 embryonal carcinoma cells and characterization of a novel mouse gene, Stra1 (mouse LERK-2/Eplg2). *Developmental biology*, *170*(2), pp.420-433.

36. Bouillet, P., Sapin, V., Chazaud, C., Messaddeq, N., Décimo, D., Dollé, P. and Chambon, P., 1997. Developmental expression pattern of Stra6, a retinoic acid-responsive gene encoding a new type of membrane protein. *Mechanisms of development*, *63*(2), pp.173-186.

37. Box, J.K. et al., 2016. Nucleophosmin : from structure and function to disease development. *BMC Molecular Biology*, pp.1–12.

38. Boyle, J.O. et al., 1999. Cyclin D1 proteolysis: a retinoid chemoprevention signal in normal, immortalized, and transformed human bronchial epithelial cells. *Journal of the National Cancer Institute*, 91, pp.373–379.

39. Breckenridge, D.G. et al., 2002. the BAP31 complex at the endoplasmic reticulum. *Apoptosis*.

40. Breems-de Ridder, M.C., Löwenberg, B. and Jansen, J.H., 2000. Retinoic acid receptor fusion proteins: friend or foe. *Molecular and cellular endocrinology*, *165*(1), pp.1-6.

41. Breen, C.J. et al., 2015. Production of functional human vitamin a transporter/RBP receptor (STRA6) for structure determination. *PLoS ONE*, 10(3), pp.1–18.

42. Calo, E., Flynn, R.A., Martin, L., Spitale, R.C., Chang, H.Y. and Wysocka, J., 2015. RNA helicase DDX21 coordinates transcription and ribosomal RNA processing. *Nature*, *518*(7538), pp.249-253.

43. Cantorna, M.T., Nashold, F.E. & Hayes, C.E., 1994. In vitamin A deficiency multiple mechanisms establish a regulatory T helper cell imbalance with excess Th1 and insufficient Th2 function. *Journal of immunology*, 152(4), pp.1515–1522.

44. Carrera, S. et al., 2013. Stra6, a retinoic acid-responsive gene, participates in p53-induced apoptosis after DNA damage. *Cell death and differentiation*, 20(7), pp.910–9.

45. Chambon, P., 1996. A decade of molecular biology of retinoic acid receptors. *The*

FASEB Journal, *10*(9), pp.940-954.

46. Chang, T.S. et al., 2002. Regulation of peroxiredoxin I activity by Cdc2-mediated phosphorylation. *Journal of Biological Chemistry*, 277(28), pp.25370–25376.

47. Chang, Y. et al., 2013. ECHS1 interacts with STAT3 and negatively regulates STAT3 signaling. *FEBS Letters*, 587(6), pp.607–613.

48. Chassaing, N. et al., 2009. Phenotypic spectrum of STRA6 mutations: From matthew-wood syndrome to non-lethal anophthalmia. *Human Mutation*, 30(5), pp.673-81.

49. Chen, C.H. et al., 2012. Increased unbound retinol-binding protein 4 concentration induces apoptosis through receptor-mediated signaling. *Journal of Biological Chemistry*, 287(13), pp.9694–9707.

50. Chen, C.-H. et al., 2016. Electronegative low density lipoprotein induces renal apoptosis and fibrosis: STRA6 signaling involved. *Journal of Lipid Research*, 57(8), pp.1435–1446.

51. Chen, D., Zhang, Z., Li, M., Wang, W., Li, Y., Rayburn, E.R., Hill, D.L., Wang, H. and Zhang, R., 2007. Ribosomal protein S7 as a novel modulator of p53–MDM2 interaction: binding to MDM2, stabilization of p53 protein, and activation of p53 function. *Oncogene*, 26(35), pp.5029-5037.

52. Chen, F. et al., 2007. Inhibition of Tgfβ signaling by endogenous retinoic acid is essential for primary lung bud induction. *Development*, 134(16), pp.2969–2979.

53. Chen, F.W. and Ioannou, Y.A., 1999. Ribosomal proteins in cell proliferation and apoptosis. *International reviews of immunology*, *18*(5-6), pp.429-448.

54. Chen, Y. et al., 2016. Structure of the STRA6 receptor for retinol uptake. *Science*, 353(6302), pp.8266.

55. Cheung, W.L. et al., 2003. Apoptotic phosphorylation of histone H2B is mediated by mammalian sterile twenty kinase. *Cell*, 113(4), pp.507–517.

56. Chicheportiche, Y., Bourdon, P.R., Xu, H., Hsu, Y.M., Scott, H., Hession, C., Garcia, I. and Browning, J.L., 1997. TWEAK, a new secreted ligand in the tumor necrosis factor family that weakly induces apoptosis. *Journal of Biological Chemistry*, *272*(51), pp.32401-32410.

57. Chipuk, J.E., Kuwana, T., Bouchier-Hayes, L., Droin, N.M., Newmeyer, D.D., Schuler, M. and Green, D.R., 2004. Direct activation of Bax by p53 mediates

mitochondrial membrane permeabilization and apoptosis. *Science*, *303*(5660), pp.1010-1014.

58. Chivot, M., 2005. Retinoid therapy for acne. *American journal of clinical dermatology*, *6*(1), pp.13-19.

59. Cho, Y., Gorina, S., Jeffrey, P.D. and Pavletich, N.P., 1994. Crystal structure of a p53 tumor suppressor-DNA complex: understanding tumorigenic mutations. *Science-AAAS-Weekly Paper Edition*, *265*(5170), pp.346-355.

60. Choi, Y., Kim, S.Y., Kim, S.H., Yang, J., Park, K. and Byun, Y., 2003. Inhibition of tumor growth by biodegradable microspheres containing all-trans-retinoic acid in a human head-and-neck cancer xenograft. *International journal of cancer*, 107(1), pp.145-148.

61. Chomienne, C., Fenaux, P. and Degos, L., 1996. Retinoid differentiation therapy in promyelocytic leukemia. *The FASEB Journal*, 10(9), pp.1025-1030.

62. Choy, L. and Derynck, R., 2003. Transforming growth factor-β inhibits adipocyte differentiation by Smad3 interacting with CCAAT/enhancer-binding protein (C/EBP) and repressing C/EBP transactivation function. *Journal of Biological Chemistry*, 278(11), pp.9609-9619.

63. Chun, Y., Kim, R. & Lee, S., 2016. Centromere protein (CENP)-W interacts with heterogeneous nuclear ribonucleoprotein (hnRNP) U and may contribute to kinetochore-microtubule attachment in mitotic cells. *PLoS ONE*, 11(2), pp.1–16.

64. Clark, I.B. and Meyer, D.I., 1999. Overexpression of normal and mutant Arp1alpha (centractin) differentially affects microtubule organization during mitosis and interphase. *J Cell Sci*, 112(20), pp.3507-3518.

65. Clore, G.M., Ernst, J., Clubb, R., Omichinski, J.G., Kennedy, W.P., Sakaguchi, K., Appella, E. and Gronenborn, A.M., 1995. Refined solution structure of the oligomerization domain of the tumor suppressor p53. *Nature structural biology*, *2*(4), pp.321-333.

66. Colombo, E., Marine, J.C., Danovi, D., Falini, B. and Pelicci, P.G., 2002. Nucleophosmin regulates the stability and transcriptional activity of p53. *Nature cell biology*, 4(7), pp.529-533.

67. Cory, S. and Adams, J.M., 2002. The Bcl2 family: regulators of the cellular life-or-death switch. *Nature Reviews Cancer*, *2*(9), pp.647-656.

68. Cotarla, I., Ren, S., Zhang, Y., Gehan, E., Singh, B. and Furth, P.A., 2004. Stat5a is

tyrosine phosphorylated and nuclear localized in a high proportion of human breast cancers. *International journal of cancer*, 108(5), pp.665-671.

69. Coyle, K.M., 2013. The International Open Access Special Issue Title: Signal transduction-Cancer Handling Editor. , (January 2014).

70. Creek, K.E., St. Hilaire, P. and Hodam, J.R., 1993. A comparison of the uptake, metabolism and biologic effects of retinol delivered to human keratinocytes either free or bound to serum retinol-binding protein. *JOURNAL OF NUTRITION-BALTIMORE AND SPRINGFIELD THEN BETHESDA-*, 123, pp.356-356.

71. Croquet, V., Pilette, C., Lespine, A., Vuillemin, E., Rousselet, M.C., Oberti, F., Saint André, J.P., Periquet, B., François, S., Ifrah, N. and Calès, P., 2000. Hepatic hyper-vitaminosis A: importance of retinyl ester level determination. *European journal of gastroenterology & hepatology*, 12(3), pp.361-hyhen.

72. Cross, T.G., Scheel-Toellner, D., Henriquez, N.V., Deacon, E., Salmon, M. and Lord, J.M., 2000. Serine/threonine protein kinases and apoptosis. *Experimental cell research*, 256(1), pp.34-41.

73. Dai, C. and Gu, W., 2010. p53 post-translational modification: deregulated in tumorigenesis. *Trends in molecular medicine*, 16(11), pp.528-536.

74. Daniely, Y., Dimitrova, D.D. & Borowiec, J.A., 2002. Stress-Dependent Nucleolin Mobilization Mediated by p53-Nucleolin Complex Formation. , 22(16), pp.6014–6022.

75. de Thé, H. and Chen, Z., 2010. Acute promyelocytic leukaemia: novel insights into the mechanisms of cure. *Nature Reviews Cancer*, *10*(11), pp.775-783.

76. De, U., 1996. The PML and PML / RAR a Domains: From Autoimmunity to Molecular Oncology and from Retinoic Acid to Arsenic 1., 260(229), pp.253–260.

77. Debiasi, R.L. et al., 1999. Reovirus-induced apoptosis is preceded by increased cellular calpain activity and is blocked by calpain inhibitors. *Journal of virology*, 73(1), pp.695–701.

78. Delage, B., Groubet, R., Pallet, V., Bairras, C., Higueret, P. and Cassand, P., 2004. Vitamin A prevents high fat diet-induced ACF development and modifies the pattern of expression of peroxisome proliferator and retinoic acid receptor m-RNA. *Nutrition and cancer*, 48(1), pp.28-36.

79. DeLeo, A.B., Jay, G., Appella, E., Dubois, G.C., Law, L.W. and Old, L.J., 1979. Detection of a transformation-related antigen in chemically induced sarcomas

and other transformed cells of the mouse. *Proceedings of the National Academy of Sciences*, 76(5), pp.2420-2424.

80. Dippold, W.G., Jay, G., DeLeo, A.B., Khoury, G. and Old, L.J., 1981. p53 transformation related protein: detection by monoclonal antibody in mouse and human cells. *Proceedings of the National Academy of Sciences*, 78(3), pp.1695-1699.

81. Dittmer, T. & Misteli, T., 2011. The lamin protein family. *Genome Biology*, 12(5), p.222.

82. Dollé, P., 2009. Developmental expression of retinoic acid receptors (RARs). *Nucl Recept Signal*, 7, p.e006.

83. Donehower, L.A. and Harvey, M., 1992. Mice deficient for p53 are developmentally normal but susceptible to spontaneous tumours. *Nature*, 356(6366), p.215.

84. Duesberg, P., Li, R., Sachs, R., Fabarius, A., Upender, M.B. and Hehlmann, R., 2007. Cancer drug resistance: the central role of the karyotype. *Drug Resistance Updates*, 10(1), pp.51-58.

85. Edwards, S.J., Hananeia, L., Eccles, M.R., Zhang, Y.F. and Braithwaite, A.W., 2003. The proline-rich region of mouse p53 influences transactivation and apoptosis but is largely dispensable for these functions. *Oncogene*, 22(29), pp.4517-4523.

86. Eliyahu, D., Michalovitz, D., Eliyahu, S., Pinhasi-Kimhi, O. and Oren, M., 1989. Wild-type p53 can inhibit oncogene-mediated focus formation. *Proceedings of the National Academy of Sciences*, 86(22), pp.8763-8767.

87. Elmore, S., 2007. Apoptosis: a review of programmed cell death. *Toxicologic pathology*, 35(4), pp.495-516.

88. Enge, M., Bao, W., Hedström, E., Jackson, S.P., Moumen, A. and Selivanova, G., 2009. MDM2-dependent downregulation of p21 and hnRNP K provides a switch between apoptosis and growth arrest induced by pharmacologically activated p53. *Cancer cell*, 15(3), pp.171-183.

89. Espinosa, J.M. and Emerson, B.M., 2001. Transcriptional regulation by p53 through intrinsic DNA/chromatin binding and site-directed cofactor recruitment. *Molecular cell*, 8(1), pp.57-69.

90. Faria, T.N. et al., 1999. The targeted disruption of both alleles of RARβ2 in F9 cells results in the loss of retinoic acid-associated growth arrest. Journal of Biological Chemistry, 274(38), pp.26783–26788.

91. Fatma, N., Kubo, E., Sen, M., Agarwal, N., Thoreson, W.B., Camras, C.B. and Singh, D.P., 2008. Peroxiredoxin 6 delivery attenuates TNF-α-and glutamate-induced retinal ganglion cell death by limiting ROS levels and maintaining Ca 2+ homeostasis. *Brain research*, 1233, pp.63-78.

92. Fazi, F., Zardo, G., Gelmetti, V., Travaglini, L., Ciolfi, A., Di Croce, L., Rosa, A., Bozzoni, I., Grignani, F., Lo-Coco, F. and Pelicci, P.G., 2007. Heterochromatic gene repression of the retinoic acid pathway in acute myeloid leukemia. *Blood*, 109(10), pp.4432-4440.

93. Feng, Z., Zhang, H., Levine, A.J. and Jin, S., 2005. The coordinate regulation of the p53 and mTOR pathways in cells. *Proceedings of the National Academy of Sciences of the United States of America*, 102(23), pp.8204-8209.

94. Fernandez-Fernandez, M.R. and Sot, B., 2011. The relevance of protein–protein interactions for p53 function: the CPE contribution. *Protein Engineering, Design and Selection*, 24(1-2), pp.41-51.

95. Fierce, Y., de Morais Vieira, M., Piantedosi, R., Wyss, A., Blaner, W.S. and Paik, J., 2008. In vitro and in vivo characterization of retinoid synthesis from β-carotene. *Archives of biochemistry and biophysics*, 472(2), pp.126-138.

96. Fiorella, P.D., Giguere, V. and Napoli, J.L., 1993. Expression of cellular retinoic acid-binding protein (type II) in Escherichia coli. Characterization and comparison to cellular retinoic acid-binding protein (type I). *Journal of Biological Chemistry*, 268(29), pp.21545-21552.

97. Freed-Pastor, W.A. and Prives, C., 2012. Mutant p53: one name, many proteins. *Genes & development*, 26(12), pp.1268-1286.

98. Freemantle, S.J., Spinella, M.J. & Dmitrovsky, E., 2003. Retinoids in cancer therapy and chemoprevention: promise meets resistance. *Oncogene*, 22(47), pp.7305–15.

99. Fujimoto, K., Hosotani, R., Wada, M., Lee, J.U., Koshiba, T., Miyamoto, Y., Tsuji, S., Nakajima, S. and Imamura, M., 1999. Induction of cell-cycle arrest and apoptosis by a novel retinobenzoic-acid derivative, TAC-101, in human pancreatic-cancer cells. *International Journal of Cancer*, 81(4), pp.637-644.

100. Fuster, G., Almendro, V., Fontes-Oliveira, C.C., Toledo, M., Costelli, P., Busquets,

S., López-Soriano, F.J. and Argilés, J.M., 2011. Interleukin-15 affects differentiation and apoptosis in adipocytes: implications in obesity. *Lipids*, 46(11), pp.1033-1042.

101. Geng, Y. et al., 2010. Cytoplasmic p53 and activated Bax regulate p53-dependent, transcription-independent neural precursor cell apoptosis. *The journal of histochemistry and cytochemistry : official journal of the Histochemistry Society*, 58(3), pp.265–75.

102. Giannì, M., Koken, M.H., Chelbi-Alix, M.K., Benoit, G., Lanotte, M. and Chen, Z., 1998. Combined arsenic and retinoic acid treatment enhances differentiation and apoptosis in arsenic-resistant NB4 cells. *Blood*, 91(11), pp.4300-4310.

103. Gillespie, R.F. and Gudas, L.J., 2007. Retinoic acid receptor isotype specificity in F9 teratocarcinoma stem cells results from the differential recruitment of coregulators to retinoic acid response elements. *Journal of Biological Chemistry*, 282(46), pp.33421-33434.

104. Ginisty, H. et al., 1999. Structure and functions of nucleolin. *Journal of Cell Science*, 112, pp.761–72.

105. González, J.M., Navarro-Puche, A., Casar, B., Crespo, P. and Andrés, V., 2008. Fast regulation of AP-1 activity through interaction of lamin A/C, ERK1/2, and c-Fos at the nuclear envelope. *The Journal of cell biology*, 183(4), pp.653-666.

106. Gown, A.M. and Willingham, M.C., 2002. Improved detection of apoptotic cells in archival paraffin sections: immunohistochemistry using antibodies to cleaved caspase 3. *Journal of Histochemistry & Cytochemistry*, *50*(4), pp.449-454.

107. Gratas, C., Menot, M.L., Dresch, C. and Chomienne, C., 1993. Retinoid acid supports granulocytic but not erythroid differentiation of myeloid progenitors in normal bone marrow cells. *Leukemia*, 7(8), pp.1156-1162.

108. Green, D.R. and Kroemer, G., 2009. Cytoplasmic functions of the tumor suppressor p53. *Nature*, 458(7242), p.1127.

109. Grisendi, S., Mecucci, C., Falini, B. and Pandolfi, P.P., 2006. Nucleophosmin and cancer. *Nature reviews. Cancer*, 6(7), p.493.

110. Gu, W. and Roeder, R.G., 1997. Activation of p53 sequence-specific DNA binding by acetylation of the p53 C-terminal domain. *Cell*, 90(4), pp.595-606.

111. Gudas, L.J. and Wagner, J.A., 2011. Retinoids regulate stem cell differentiation. *Journal of cellular physiology*, 226(2), pp.322-330.

112. Guo, X., Knudsen, B.S., Peehl, D.M., Ruiz, A., Bok, D., Rando, R.R., Rhim, J.S., Nanus, D.M. and Gudas, L.J., 2002. Retinol metabolism and lecithin: retinol acyltransferase levels are reduced in cultured human prostate cancer cells and tissue specimens. *Cancer research*, 62(6), pp.1654-1661.

113. Guo, X., Nanus, D.M., Ruiz, A., Rando, R.R., Bok, D. and Gudas, L.J., 2001. Reduced levels of retinyl esters and vitamin A in human renal cancers. *Cancer research*, 61(6), pp.2774-2781.

114. Gupta, S., 2003. Molecular signaling in death receptor and mitochondrial pathways of apoptosis (Review). *International journal of oncology*, 22(1), pp.15-20.

115. Gupta, V. & Bamezai, R.N.K., 2010. Human pyruvate kinase M2: A multifunctional protein. *Protein Science*, 19(11), pp.2031–2044.

116. Hagen, E., Myhre, A.M., Smeland, S., Halvorsen, B., Norum, K.R. and Blomhoff, R., 1999. Uptake of vitamin A in macrophages from physiologic transport proteins: role of retinol-binding protein and chylomicron remnants. *The Journal of nutritional biochemistry*, 10(6), pp.345-352.

117. Hail, N., Kim, H.J. & Lotan, R., 2006. Mechanisms of fenretinide-induced apoptosis. *Apoptosis : an international journal on programmed cell death*, 11(10), pp.1677–94.

118. Hamada, K. et al., 2004. Increased expression of the genes for mitotic spindle assembly and chromosome segregation in both lung and pancreatic carcinomas. Cancer Genomics and Proteomics, 1(3), pp.231–240.

119. Harmel, J. et al., 2013. The leucine-rich pentatricopeptide repeat-containing protein (LRPPRC) does not activate transcription in mammalian mitochondria. *Journal of Biological Chemistry*, 288(22), pp.15510–15519.

120. Harrison, E.H. and Hussain, M.M., 2001. Mechanisms involved in the intestinal digestion and absorption of dietary vitamin A. *The Journal of nutrition*, *131*(5), pp.1405-1408.

121. Hayes, J.D. and McLELLAN, L.I., 1999. Glutathione and glutathione-dependent enzymes represent a co-ordinately regulated defence against oxidative stress. *Free radical research*, 31(4), pp.273-300.

122. Heessen, S. and Fornerod, M., 2007. The inner nuclear envelope as a transcription factor resting place. *EMBO reports*, 8(10), pp.914-919.

123. Herr, F.M., Wardlaw, S.A., Kakkad, B., Albrecht, A., Quick, T.C. and Ong, D.E., 1993. Intestinal vitamin A metabolism: coordinate distribution of enzymes and CRBP (II). *Journal of lipid research*, 34(9), pp.1545-1554.

124. Heyman, R.A., Mangelsdorf, D.J., Dyck, J.A., Stein, R.B., Eichele, G., Evans, R.M. and Thaller, C., 1992. 9-cis retinoic acid is a high affinity ligand for the retinoid X receptor. *Cell*, 68(2), pp.397-406.

125. Hix, L.M., Lockwood, S.F. and Bertram, J.S., 2004. Bioactive carotenoids: potent antioxidants and regulators of gene expression. *Redox Report*, 9(4), pp.181-191.

126. Holmström, T.H., Mialon, A., Kallio, M., Nymalm, Y., Mannermaa, L., Holm, T., Johansson, H., Black, E., Gillespie, D., Salminen, T.A. and Langel, Ü., 2008. c-Jun supports ribosomal RNA processing and nucleolar localization of RNA helicase DDX21. *Journal of Biological Chemistry*, 283(11), pp.7046-7053.

127. Hoque, M.O., Begum, S., Topaloglu, O., Jeronimo, C., Mambo, E., Westra, W.H., Califano, J.A. and Sidransky, D., 2004. Quantitative detection of promoter hypermethylation of multiple genes in the tumor, urine, and serum DNA of patients with renal cancer. *Cancer research*, 64(15), pp.5511-5517.

128. Hozák, P., Sasseville, A.M., Raymond, Y. and Cook, P.R., 1995. Lamin proteins form an internal nucleoskeleton as well as a peripheral lamina in human cells. *Journal of cell science*, 108(2), pp.635-644.

129. Hsu, S.L., Hsu, J.W., Liu, M.C., Chen, L.Y. and Chang, C.D., 2000. Retinoic acid-mediated G1 arrest is associated with induction of p27kip1 and inhibition of cyclin-dependent kinase 3 in human lung squamous carcinoma CH27 cells. *Experimental cell research*, *258*(2), pp.322-331.

130. IARC. IARC Handbooks of Cancer Prevention, Vol. 2, Carotenoids. International Agency for Research on Cancer; 1998.

131. IARC. IARC Handbooks of Cancer Prevention, Vol. 3, Vitamin A. International Agency for Research on Cancer; 1998.

132. Iavnilovitch, E. et al., 2004. Deregulation of Stat5 expression and activation causes mammary tumors in transgenic mice. *International Journal of Cancer*, 112(4), pp.607–619.

133. Idelchik, M.D.P.S., Begley, U., Begley, T.J. and Melendez, J.A., 2017, April. Mitochondrial ROS Control of Cancer. In *Seminars in Cancer Biology*. Academic Press.

134. Isken, A. et al., 2008. RBP4 disrupts vitamin A uptake homeostasis in a STRA6-deficient animal model for Matthew-Wood syndrome. *Cell metabolism*, 7(3), pp.258–68.

135. Jang, C.Y., Kim, H.D. & Kim, J., 2012. Ribosomal protein S3 interacts with TRADD to induce apoptosis through caspase dependent JNK activation. *Biochemical and Biophysical Research Communications*, 421(3), pp.474–478.

136. Janssen, U. et al., 1997. Human mitochondrial enoyl-CoA hydratase gene (ECHS1): structural organization and assignment to chromosome 10q26.2-q26.3. *Genomics*, 40(40), pp.470–475.

137. Jenkins, L.M.M. et al., 2012. p53 N-terminal phosphorylation: A defining layer of complex regulation. *Carcinogenesis*, 33(8), pp.1441–1449.

138. Ji, H. et al., 2016. Progress in the biological function of alpha-enolase. *Animal Nutrition*, 2(1), pp.12–17.

139. Jiang, D. et al., 2011. Full p53 transcriptional activation potential is dispensable for tumor suppression in diverse lineages. Proceedings of the National Academy of Sciences of the United States of America, 108(41), pp.17123–17128.

140. Junttila, M.R., and Evan, G.I., 2009. p53- a Jack of all trades but master of none. *Nat. Rev. Cancer* (9), pp.821–829.

141. Kamei, Y. et al., 1994. The prevention of adipose differentiation of 3T3-L1 cells caused by retinoic acid is elicited through retinoic acid receptor alpha. *Life Sci*. (55), pp.307–312.

142. Kato, Y., Egusa, C., Maeda, T. and Tsuboi, R., 2016. Combination of retinoid and histone deacetylase inhibitor produced an anti-tumor effect in cutaneous T-cell lymphoma by restoring tumor suppressor gene, retinoic acid receptorβ2, via histone acetylation. *Journal of dermatological science*, 81(1), pp.17-25.

143. Kawaguchi, R. & Sun, H., 2010. Retinoids H. Sun & G. H. Travis, eds. , 652(8).

144. Kawaguchi, R. et al., 2007. A membrane receptor for retinol binding protein mediates cellular uptake of vitamin A. *Science (New York, N.Y*, 315(5813), pp.820–825.

145. Kawaguchi, R. et al., 2008. An essential ligand-binding domain in the membrane receptor for retinol-binding protein revealed by large-scale mutagenesis and a human polymorphism. *Journal of Biological Chemistry*, 283(22), pp.15160–15168.

146. Kawaguchi, R. et al., 2012. STRA6-catalyzed vitamin A influx, efflux, and exchange. *The Journal of membrane biology*, 245(11), pp.731–45.

147. Kemp, C.J., Wheldon, T., and Balmain, A., 1994. p53-deficient mice are extremely susceptible to radiation-induced tumorigenesis. *Nat. Genet.* (8), pp.66–69.

Kim, S.Y., Chun, E. & Lee, K.-Y., 2011. Phospholipase A(2) of peroxiredoxin 6 has a critical role in tumor necrosis factor-induced apoptosis. *Cell death and differentiation*, 18(10), pp.1573–1583.

148. Kim, K., Kim, J.M., Kim, J.S., Choi, J., Lee, Y.S., Neamati, N., Song, J.S., Heo, K. and An, W., 2013. VprBP has intrinsic kinase activity targeting histone H2A and represses gene transcription. *Molecular cell*, 52(3), pp.459-467.

149. Kimball, S.R., 1999. Eukaryotic initiation factor eIF2. *International Journal of Biochemistry and Cell Biology*, 31(1), pp.25–29.

150. Kischkel, F.C., Hellbardt, S., Behrmann, I., Germer, M., Pawlita, M., Krammer, P.H. and Peter, M.E., 1995. Cytotoxicity-dependent APO-1 (Fas/CD95)-associated proteins form a death-inducing signaling complex (DISC) with the receptor. *The EMBO journal*, 14(22), p.5579.

151. Kobayashi, M., Kawashima, A., Mai, M. and Ooi, A., 1996. Analysis of chromosome 17p13 (p53 locus) alterations in gastric carcinoma cells by dual-color fluorescence in situ hybridization. *The American journal of pathology*, 149(5), pp.1575.

152. Krasinski, S.D., Russell, R.M., Otradovec, C.L., Sadowski, J.A., Hartz, S.C., Jacob, R.A. and McGandy, R.B., 1989. Relationship of vitamin A and vitamin E intake to fasting plasma retinol, retinol-binding protein, retinyl esters, carotene, alpha-tocopherol, and cholesterol among elderly people and young adults: increased plasma retinyl esters among vitamin A-supplement users. *The American journal of clinical nutrition*, 49(1), pp.112-120.

153. Kruse, J.P. and Gu, W., 2009. Modes of p53 regulation. *Cell*, *137*(4), pp.609-622.

154. Kruse, J.P. and Gu, W., 2009. MSL2 promotes Mdm2-independent cytoplasmic localization of p53. *Journal of Biological Chemistry*, *284*(5), pp.3250-3263.

155. Krust, A., Kastner, P.H., Petkovich, M., Zelent, A. and Chambon, P., 1989. A third human retinoic acid receptor, hRAR-gamma. *Proceedings of the National Academy of Sciences*, 86(14), pp.5310-5314.

156. Kryston, T.B., Georgiev, A.B., Pissis, P. and Georgakilas, A.G., 2011. Role of oxidative stress and DNA damage in human carcinogenesis. *Mutation Research/Fundamental and Molecular Mechanisms of Mutagenesis*, 711(1), pp.193-201.

157. Kubbutat, M.H. and Vousden, K.H., 1997. Proteolytic cleavage of human p53 by calpain: a potential regulator of protein stability. *Molecular and Cellular Biology*, *17*(1), pp.460-468.

158. Kurki, S., Peltonen, K., Latonen, L., Kiviharju, T.M., Ojala, P.M., Meek, D. and Laiho, M., 2004. Nucleolar protein NPM interacts with HDM2 and protects tumor suppressor protein p53 from HDM2-mediated degradation. *Cancer cell*, 5(5), pp.465-475.

159. Kyriakis, J.M. and Avruch, J., 2001. Mammalian mitogen-activated protein kinase signal transduction pathways activated by stress and inflammation. *Physiological reviews*, 81(2), pp.807-869.

160. Laine, A. and Ronai, Z.E., 2007. Regulation of p53 localization and transcription by the HECT domain E3 ligase WWP1. *Oncogene*, 26(10), pp.1477-1483.

161. Landeras-Bueno, S. et al., 2011. The splicing factor proline-glutamine rich (SFPQ/PSF) is involved in influenza virus transcription. PLoS Pathogens, 7(11).

162. Lane, Dp., 1992. Cancer - P53, Guardian of The Genome. *Nature,* 358(6381), pp.15-16.

163. Larsson, S.C., Mantzoros, C.S. and Wolk, A., 2007. Diabetes mellitus and risk of breast cancer: a meta-analysis. *International journal of cancer*, 121(4), pp.856-862.

164. Laursen, K.B. & Gudas, L.J., 2014. Crossing the barrier: STRA6 in epidermal differentiation. *The Journal of investigative dermatology*, 134(6), pp.1504–6.

165. Laursen, K.B. & Gudas, L.J., 2014. Crossing the barrier: STRA6 in epidermal differentiation. *The Journal of investigative dermatology*, 134(6), pp.1504–6.

166. Lee, S.C., Chan, J., Clement, M.V. and Pervaiz, S., 2006. Functional proteomics of resveratrol-induced colon cancer cell apoptosis: Caspase-6-mediated cleavage of lamin A is a major signaling loop. *Proteomics*, 6(8), pp.2386-2394.

167. Lejeune, D., Dumoutier, L., Constantinescu, S., Kruijer, W., Schuringa, J.J. and Renauld, J.C., 2002. Interleukin-22 (IL-22) activates the JAK/STAT, ERK, JNK, and p38 MAP kinase pathways in a rat hepatoma cell line Pathways that are shared

with and distinct from IL-10. *Journal of Biological Chemistry*, 277(37), pp.33676-33682.

168. Li, Z., Park, H.R., Shi, Z., Li, Z., Pham, C.D., Du, Y., Khuri, F.R., Zhang, Y., Han, Q. and Fu, H., 2014. Pro-oncogenic function of HIP-55/Drebrin-like (DBNL) through Ser269/Thr291-phospho-sensor motifs. *Oncotarget*, *5*(10), pp.3197-3209.

169. Liang, S.H. and Clarke, M.F., 2001. Regulation of p53 localization. *The FEBS Journal*, 268(10), pp.2779-2783.

170. Lidén, M. and Eriksson, U., 2006. Understanding retinol metabolism: structure and function of retinol dehydrogenases. *Journal of Biological Chemistry*, 281(19), pp.13001-13004.

171. Lin, X.-C. et al., 2014. Integrated analysis of long non-coding RNAs and mRNA expression profiles reveals the potential role of lncRNAs in gastric cancer pathogenesis. *International Journal of Oncology*, 45(2), pp.619–628.

172. Lindström, M.S., 2009. Emerging functions of ribosomal proteins in gene-specific transcription and translation. *Biochemical and Biophysical Research Communications*, 379(2), pp.167–170.

173. Liu, L. and Gudas, L.J., 2005. Disruption of the lecithin: retinol acyltransferase gene makes mice more susceptible to vitamin A deficiency. *Journal of Biological Chemistry*, 280(48), pp.40226-40234.

174. Long, J.S. & Ryan, K.M., 2012. New frontiers in promoting tumour cell death: targeting apoptosis, necroptosis and autophagy. *Oncogene*, 31(49), pp.5045–60.

175. Lotan, R., Neumann, G. and Lotan, D., 1981. Characterization of Retinoic Acid-Induced Alterations in the Proliferation and Differentiation of a Murine and a Human Melanoma Cell Line in Culture. *Annals of the New York Academy of Sciences*, 359(1), pp.150-170.

176. Lozano, G. and Zambetti, G.P., 2005. What have animal models taught us about the p53 pathway? *The Journal of pathology*, *205*(2), pp.206-220.

177. Lüpertz, R. et al., 2010. Dose- and time-dependent effects of doxorubicin on cytotoxicity, cell cycle and apoptotic cell death in human colon cancer cells. *Toxicology*, 271(3), pp.115–21.

178. MacDonald, P.N., Bok, D. and Ong, D.E., 1990. Localization of cellular retinol-binding protein and retinol-binding protein in cells comprising the blood-brain barrier of rat and human. *Proceedings of the National Academy of*

Sciences, 87(11), pp.4265-4269.

179. Macip, S., Igarashi, M., Berggren, P., Yu, J., Lee, S.W. and Aaronson, S.A., 2003. Influence of induced reactive oxygen species in p53-mediated cell fate decisions. *Molecular and cellular biology*, 23(23), pp.8576-8585.

180. Mandegary, A. and Mehrabani, M., 2010. Effects of arsenic trioxide, all-trans-retinoic acid and dexamethasone on NB4 cell line. *Daru: journal of Faculty of Pharmacy, Tehran University of Medical Sciences*, 18(4), p.303.

181. Mangelsdorf, D.J., Umesono, K., Kliewer, S.A., Borgmeyer, U., Ong, E.S. and Evans, R.M., 1991. A direct repeat in the cellular retinol-binding protein type II gene confers differential regulation by RXR and RAR. *Cell*, 66(3), pp.555-561.

182. Maraini, G.I.O.V.A.N.N.I. and Gozzoli, F.L.A.V.I.O., 1975. Binding of retinol to isolated retinal pigment epithelium in the presence and absence of retinol-binding protein. *Investigative Ophthalmology & Visual Science*, 14(10), pp.785-787.

183. Marks, P.A., Richon, V.M. and Rifkind, R.A., 2000. Histone deacetylase inhibitors: inducers of differentiation or apoptosis of transformed cells. *Journal of the National Cancer Institute*, 92(15), pp.1210-1216.

184. Marouco, D., Garabadgiu, A.V., Melino, G. and Barlev, N.A., 2013. Lysine-specific modifications of p53: a matter of life and death?. *Oncotarget*, 4(10), p.1556.

185. Marwarha, G. et al., 2014. The retinol esterifying enzyme LRAT supports cell signaling by retinol-binding protein and its receptor STRA6. *FASEB Journal*, 28(1), pp.26–34.

186. Matsumoto, M., Furihata, M. and Ohtsuki, Y., 2006. Posttranslational phosphorylation of mutant p53 protein in tumor development. *Medical molecular morphology*, 39(2), pp.79-87.

187. Matunis, M.J., Michael, W.M. and Dreyfuss, G., 1992. Characterization and primary structure of the poly (C)-binding heterogeneous nuclear ribonucleoprotein complex K protein. *Molecular and cellular biology*, 12(1), pp.164-171.

188. Mazumder, B., Sampath, P., Seshadri, V., Maitra, R.K., DiCorleto, P.E. and Fox, P.L., 2003. Regulated release of L13a from the 60S ribosomal subunit as a mechanism of transcript-specific translational control. *Cell*, 115(2), pp.187-198.

189. McKinney, K., Mattia, M., Gottifredi, V. and Prives, C., 2004. p53 linear diffusion

along DNA requires its C terminus. *Molecular cell*, 16(3), pp.413-424.

190. Meek, D.W., 2009. Tumour suppression by p53: a role for the DNA damage response?. *Nature Reviews Cancer*, 9(10), pp.714-723.

191. Michalak, E.M., Vandenberg, C.J., Delbridge, A.R., Wu, L., Scott, C.L., Adams, J.M. and Strasser, A., 2010. Apoptosis-promoted tumorigenesis: γ-irradiation-induced thymic lymphomagenesis requires Puma-driven leukocyte death. *Genes & Development*, 24(15), pp.1608-1613.

192. Mittal, N., Malpani, S., Dyson, M., Ono, M., Coon, J.S., Kim, J.J., Schink, J.C., Bulun, S.E. and Pavone, M.E., 2014. Fenretinide: a novel treatment for endometrial cancer. *PloS one*, *9*(10), p.e110410.

193. Moumen, A. et al., 2005. hnRNP K: an HDM2 target and transcriptional coactivator of p53 in response to DNA damage. *Cell*, 123(6), pp.1065–78.

194. Moumen, A., Magill, C., Dry, K. and Jackson, S.P., 2013. ATM-dependent phosphorylation of heterogeneous nuclear ribonucleoprotein K promotes p53 transcriptional activation in response to DNA damage. *Cell Cycle*, 12(4), pp.698-704.

195. Mucida, D., Park, Y., Kim, G., Turovskaya, O., Scott, I., Kronenberg, M. and Cheroutre, H., 2007. Reciprocal TH17 and regulatory T cell differentiation mediated by retinoic acid. *Science*, 317(5835), pp.256-260.

196. Muenzner, M. et al., 2013. Retinol-binding protein 4 and its membrane receptor STRA6 control adipogenesis by regulating cellular retinoid homeostasis and retinoic acid receptor α activity. *Molecular and cellular biology*, 33(20), pp.4068–82.

197. Muller, P.A., Caswell, P.T., Doyle, B., Iwanicki, M.P., Tan, E.H., Karim, S., Lukashchuk, N., Gillespie, D.A., Ludwig, R.L., Gosselin, P. and Cromer, A., 2009. Mutant p53 drives invasion by promoting integrin recycling. *Cell*, 139(7), pp.1327-1341.

198. Murray-Zmijewski, F., Slee, E.A. and Lu, X., 2008. A complex barcode underlies the heterogeneous response of p53 to stress. *Nature reviews Molecular cell biology*, 9(9), pp.702-712.

199. Muto, Y., Moriwaki, H. and Shiratori, Y., 1998. Prevention of second primary tumors by an acyclic retinoid, polyprenoic acid, in patients with hepatocellular carcinoma. *Digestion*, 59(Suppl. 2), pp.89-91.

200. Nair, A.K. et al., 2010. Case-control analysis of SNPs in GLUT4, RBP4 and STRA6: Association of SNPs in STRA6 with type 2 diabetes in a south indian population. *PLoS ONE*, 5(7), p.e11444.

201. Napoli, J.L., 1993. Biosynthesis and metabolism of retinoic acid: roles of CRBP and CRABP in retinoic acid: roles of CRBP and CRABP in retinoic acid homeostasis. *The Journal of nutrition*, 123(2 Suppl), pp.362-366.

202. Napoli, J.L., 1996. Retinoic acid biosynthesis and metabolism. *The FASEB Journal*, 10(9), pp.993-1001.

203. Naylor, H.M. and Newcomer, M.E., 1999. The Structure of Human Retinol-Binding Protein (RBP) with Its Carrier Protein Transthyretin Reveals an Interaction with the Carboxy Terminus of RBP†. *Biochemistry*, 38(9), pp.2647-2653.

204. Nguyen, M., Breckenridge, D.G., Ducret, A. and Shore, G.C., 2000. Caspase-Resistant BAP31 Inhibits Fas-Mediated Apoptotic Membrane Fragmentation and Release of Cytochrome cfrom Mitochondria. *Molecular and Cellular Biology*, 20(18), pp.6731-6740.

205. Noa, N.O.Y., 2000. Retinoid-binding proteins: mediators of retinoid action. *Biochemical Journal*, 348(3), pp.481-495.

206. Norbury, C.J. and Hickson, I.D., 2001. Cellular responses to DNA damage. *Annual review of pharmacology and toxicology*, 41(1), pp.367-401.

207. Noy, N., 2016. Vitamin A in regulation of insulin responsiveness: mini review. *Proceedings of the Nutrition Society*, 75(02), pp.212-215.

208. O'Brate, A. and Giannakakou, P., 2003. The importance of p53 location: nuclear or cytoplasmic zip code?. *Drug resistance updates*, *6*(6), pp.313-322.

209. Okada, Y., Shimazaki, T., Sobue, G. and Okano, H., 2004. Retinoic-acid-concentration-dependent acquisition of neural cell identity during in vitro differentiation of mouse embryonic stem cells. *Developmental biology*, 275(1), pp.124-142.

210. Oliner, J.D., Pietenpol, J.A., Thiagalingam, S., Gyuris, J., Kinzler, K.W. and Vogelstein, B., 1993. Oncoprotein MDM2 conceals the activation domain of tumour suppressor p53. *Nature*, 362(6423), p.857.

211. Olivier, M., Hollstein, M. and Hainaut, P., 2010. TP53 mutations in human cancers: origins, consequences, and clinical use. *Cold Spring Harbor perspectives*

in biology, 2(1), p.a001008.

212. Olson, J.A., 1996. Benefits and liabilities of vitamin A and carotenoids. *The Journal of nutrition*, 126(4S), p.1208S.

213. Ong, D.E., 1994. Cellular transport and metabolism of vitamin A: Roles of the cellular retinoid-binding proteins. *Nutrition reviews*, 52(2), pp.S24-S31.

214. Paiva, S.A. and Russell, R.M., 1999. β-Carotene and other carotenoids as antioxidants. *Journal of the American college of nutrition*, 18(5), pp.426-433.

215. Panariello, L., Quadro, L., Trematerra, S. and Colantuoni, V., 1996. Identification of a novel retinoic acid response element in the promoter region of the retinol-binding protein gene. *Journal of Biological Chemistry*, 271(41), pp.25524-25532.

216. Pancholi, V. and Fischetti, V.A., 1998. α-Enolase, a novel strong plasmin (ogen) binding protein on the surface of pathogenic streptococci. *Journal of Biological Chemistry*, 273(23), pp.14503-14515.

217. Park, D.S., Lee, H., Frank, P.G., Razani, B., Nguyen, A.V., Parlow, A.F., Russell, R.G., Hulit, J., Pestell, R.G. and Lisanti, M.P., 2002. Caveolin-1-deficient mice show accelerated mammary gland development during pregnancy, premature lactation, and hyperactivation of the Jak-2/STAT5a signaling cascade. *Molecular biology of the cell*, 13(10), pp.3416-3430.

218. Pelisch, F., Pozzi, B., Risso, G., Muñoz, M.J. and Srebrow, A., 2012. DNA damage-induced heterogeneous nuclear ribonucleoprotein K sumoylation regulates p53 transcriptional activation. *Journal of Biological Chemistry*, 287(36), pp.30789-30799.

219. Peskin, A. V. et al., 2007. The high reactivity of peroxiredoxin 2 with H2O2 is not reflected in its reaction with other oxidants and thiol reagents. *Journal of Biological Chemistry*, 282(16), pp.11885–11892.

220. Petkovich, M., Brand, N.J., Krust, A. and Chambon, P., 1987. A human retinoic acid receptor which belongs to the family of nuclear receptors. *Nature*, 330(6147), pp.444-450.

221. Polyak, K. et al., 1997. letters to nature A model for p53-induced apoptosis., 389, pp.300–305.

222. Quadro, L., Blaner, W.S., Salchow, D.J., Vogel, S., Piantedosi, R., Gouras, P., Freeman, S., Cosma, M.P., Colantuoni, V. and Gottesman, M.E., 1999. Impaired retinal function and vitamin A availability in mice lacking retinol-binding

protein. *The EMBO journal*, 18(17), pp.4633-4644.

223. Rajagopalan, S., Andreeva, A., Teufel, D.P., Freund, S.M. and Fersht, A.R., 2009. Interaction between the transactivation domain of p53 and PC4 exemplifies acidic activation domains as single-stranded DNA mimics. *Journal of Biological Chemistry*, 284(32), pp.21728-21737.

224. Rawlings, N.D., Barrett, A.J. and Finn, R., 2016. Twenty years of the MEROPS database of proteolytic enzymes, their substrates and inhibitors. *Nucleic acids research*, 44(D1), pp.D343-D350.

225. Repa, J.J., Hanson, K.K. and Clagett-Dame, M., 1993. All-trans-retinol is a ligand for the retinoic acid receptors. *Proceedings of the National Academy of Sciences*, 90(15), pp.7293-7297.

226. Resendes, K.K. and Rosmarin, A.G., 2006. GA-binding protein and p300 are essential components of a retinoic acid-induced enhanceosome in myeloid cells. *Molecular and cellular biology*, 26(8), pp.3060-3070.

227. Ritter, E., Elgeti, M. and Bartl, F.J., 2008. Activity switches of rhodopsin. *Photochemistry and photobiology*, 84(4), pp.911-920.

228. Roberti, A., Sala, D.L. and Cinti, C., 2006. Multiple genetic and epigenetic interacting mechanisms contribute to clonally selection of drug-resistant tumors: Current views and new therapeutic prospective. *Journal of cellular physiology*, 207(3), pp.571-581.

229. Roberts, A.B. and Sporn, M.B., 1984. The retinoids. *Cellular Biology and Biochemistry of Retinoids. Sporn MB, Roberts AB and Goodman DS (eds.) Academic Press, New York*, *2*.

230. Rolfs, F., Huber, M., Gruber, F., Böhm, F., Pfister, H.J., Bochkov, V.N., Tschachler, E., Dummer, R., Hohl, D., Schäfer, M. and Werner, S., 2013. Dual role of the antioxidant enzyme peroxiredoxin 6 in skin carcinogenesis. *Cancer research*, *73*(11), pp.3460-3469.

231. Ross, A.C. and Ternus, M.E., 1993. Vitamin A as a hormone: recent advances in understanding the actions of retinol, retinoic acid, and beta carotene. *Journal of the American Dietetic Association*, 93(11), pp.1285-1290.

232. Ross, S.A., McCaffery, P.J., Drager, U.C. and De Luca, L.M., 2000. Retinoids in embryonal development. *Physiological reviews*, 80(3), pp.1021-1054.

233. Rousseau, B., Ménard, L., Haurie, V., Taras, D., Blanc, J.F., Moreau-Gaudry, F.,

Metzler, P., Hugues, M., Boyault, S., Lemiere, S. and Canron, X., 2007. Overexpression and role of the ATPase and putative DNA helicase RuvB-like 2 in human hepatocellular carcinoma. *Hepatology*, 46(4), pp.1108-1118.

234. Ruiz, A. et al., 2012. Retinoid content, visual responses, and ocular morphology are compromised in the retinas of mice lacking the retinol-binding protein receptor, STRA6. *Investigative ophthalmology & visual science*, 53(6), pp.3027–3039.

235. Sablina, A.A., Budanov, A.V., Ilyinskaya, G.V., Agapova, L.S., Kravchenko, J.E. and Chumakov, P.M., 2005. The antioxidant function of the p53 tumor suppressor. *Nature medicine*, 11(12), pp.1306-1313.

236. Sakamuro, D., Sabbatini, P., White, E. and Prendergast, G.C., 1997. The polyproline region of p53 is required to activate apoptosis but not growth arrest. *Oncogene*, 15(8), pp.887-898.

237. Samokyszyn, V.M. and Marnett, L.J., 1990. Inhibition of liver microsomal lipid peroxidation by 13-cis-retinoic acid. *Free Radical Biology and Medicine*, 8(5), pp.491-496.

238. Sawhney, S., Hood, K., Shaw, A., Braithwaite, A.W., Stubbs, R., Hung, N.A., Royds, J.A. and Slatter, T.L., 2015. Alpha-Enolase Is Upregulated on the Cell Surface and Responds to Plasminogen Activation in Mice Expressing aΔ 133p53α Mimic. *PloS one*, 10(2), p.e0116270.

239. Schmitz, H.H., Poor, C.L., Wellman, R.B. and Erdman Jr, J.W., 1991. Concentrations of selected carotenoids and vitamin A in human liver, kidney and lung tissue. *J Nutr*, 121(10), pp.1613-1621.

240. Schulze-Luehrmann, J., Santner-Nanan, B., Jha, M.K., Schimpl, A., Avots, A. and Serfling, E., 2002. Hematopoietic progenitor kinase 1 supports apoptosis of T lymphocytes. *Blood*, *100*(3), pp.954-960.

241. Schwarz, E.J., Reginato, M.J., Shao, D., Krakow, S.L. and Lazar, M.A., 1997. Retinoic acid blocks adipogenesis by inhibiting C/EBPbeta-mediated transcription. *Molecular and cellular biology*, *17*(3), pp.1552-1561.

242. Scoumanne, A. and Chen, X., 2008. Protein methylation: a new regulator of the p53 tumor suppressor. *Histology and histopathology*, 23(9), p.1143.

243. Seewaldt, V.L., Johnson, B.S., Parker, M.B., Collins, S.J. and Swisshelm, K., 1995. Expression of retinoic acid receptor beta mediates retinoic acid-induced growth arrest and apoptosis in breast cancer cells. *Cell growth & differentiation: the*

molecular biology journal of the American Association for Cancer Research, 6(9), pp.1077-1088.

244. Sheren-Manoff, M., Shin, S.J., Su, D., Bok, D., Rando, R.R. and Gudas, L.J., 2006. Reduced lecithin: retinol acyltransferase expression in human breast cancer. *International journal of oncology*, *29*(5), p.1193.

245. Sherr, C.J., 2006. Divorcing ARF and p53: an unsettled case. *Nature reviews. Cancer*, 6(9), pp.663–73.

246. Shevchenko, A., Tomas, H., Havli, J., Olsen, J.V. and Mann, M., 2006. In-gel digestion for mass spectrometric characterization of proteins and proteomes. *Nature protocols*, *1*(6), pp.2856-2860.

247. Shieh, S.Y., Taya, Y. and Prives, C., 1999. DNA damage-inducible phosphorylation of p53 at N-terminal sites including a novel site, Ser20, requires tetramerization. *The EMBO journal*, *18*(7), pp.1815-1823.

248. Sieprath, T. et al., 2015. Sustained accumulation of prelamin A and depletion of lamin A/C both cause oxidative stress and mitochondrial dysfunction but induce different cell fates. *Nucleus (Austin, Tex.)*, 6(3), pp.236–46.

249. Sirchia, S.M., Ren, M., Pili, R., Sironi, E., Somenzi, G., Ghidoni, R., Toma, S., Nicolò, G. and Sacchi, N., 2002. Endogenous reactivation of the RARβ2 tumor suppressor gene epigenetically silenced in breast cancer. *Cancer research*, 62(9), pp.2455-2461.

250. Sivaprasadarao, A., Boudjelal, M. and Findlay, J.B., 1994. Solubilization and purification of the retinol-binding protein receptor from human placental membranes. *Biochemical Journal*, 302(1), pp.245-251.

251. Smeenk, L., Van Heeringen, S.J., Koeppel, M., Gilbert, B., Janssen-Megens, E., Stunnenberg, H.G. and Lohrum, M., 2011. Role of p53 serine 46 in p53 target gene regulation. *PloS one*, *6*(3), p.e17574.

252. Smeland, S., Bjerknes, T., Malaba, L., Eskild, W., Norum, K.R. and Blomhoff, R., 1995. Tissue distribution of the receptor for plasma retinol-binding protein. *Biochemical journal*, *305*(2), pp.419-424.

253. Sobhan, P.K. et al., 2013. Calpain and Reactive Oxygen Species Targets Bax for Mitochondrial Permeabilisation and Caspase Activation in Zerumbone Induced Apoptosis. *PLoS ONE*, 8(4).

254. Sohun, M. & Shen, H., 2016. The implication and potential applications of high-

mobility group box 1 protein in breast cancer. *Annals of translational medicine*, 4(11), p.217.

255. Solomon, S. et al., 2007. Distinct structural features of caprin-1 mediate its interaction with G3BP-1 and its induction of phosphorylation of eukaryotic translation initiation factor 2alpha, entry to cytoplasmic stress granules, and selective interaction with a subset of mRNAs. *Molecular and Cellular Biology*, 27(6), pp.2324–42.

256. Sonneveld, E., Van den Brink, C.E., Van der Leede, B.J.M., Schulkes, R.K.A., Petkovich, M., Van der Burg, B. and Van der Saag, P.T., 1998. Human retinoic acid (RA) 4-hydroxylase (CYP26) is highly specific for all-trans-RA and can be induced through RA receptors in human breast and colon carcinoma cells. *Cell Growth and Differentiation-Publication American Association for Cancer Research*, 9(8), pp.629-638.

257. Spike, B.T. and Wahl, G.M., 2011. P53, stem cells, and reprogramming tumor suppression beyond guarding the genome. *Genes & cancer*, 2(4), pp.404-419.

258. Stage, L. & Food, S., 2001. Dietary Reference Intakes: Vitamins Nutrient Adverse effects of excessive consumption Dietary Reference Intakes: Vitamins Folate., (1997).

259. Stähelin, H.B., Gey, K.F., Eichholzer, M., Lüdin, E., Bernasconi, F., Thumeysen, J. and Brubacher, G., 1991. Plasma antioxidant vitamins and subsequent cancer mortality in the 12-year follow-up of the prospective Basel Study. *American Journal of Epidemiology*, 133(8), pp.766-775.

260. Stephensen, C.B., 2001. Vitamin A, infection, and immune function. *Annual review of nutrition*, 21(1), pp.167-192.

261. Stephensen, C.B., Rasooly, R., Jiang, X., Ceddia, M.A., Weaver, C.T., Chandraratna, R.A. and Bucy, R.P., 2002. Vitamin A enhances in vitro Th2 development via retinoid X receptor pathway. *The Journal of Immunology*, 168(9), pp.4495-4503.

262. Stiewe, T., 2007. The p53 family in differentiation and tumorigenesis. *Nature Reviews Cancer*, 7(3), pp.165-167.

263. Sueoka, N., Lee, H.Y., Walsh, G.L., Hong, W.K. and Kurie, J.M., 1999. Posttranslational Mechanisms Contribute to the Suppression of Specific Cyclin. *Cancer research*, 59(15), pp.3838-3844.

264. Sugrue, M.M., Shin, D.Y., Lee, S.W. and Aaronson, S.A., 1997. Wild-type p53 triggers a rapid senescence program in human tumor cells lacking functional p53. *Proceedings of the National Academy of Sciences*, 94(18), pp.9648-9653.

265. Sun, R., Liu, Y., Li, S.Y., Shen, S., Du, X.J., Xu, C.F., Cao, Z.T., Bao, Y., Zhu, Y.H., Li, Y.P. and Yang, X.Z., 2015. Co-delivery of all-trans-retinoic acid and doxorubicin for cancer therapy with synergistic inhibition of cancer stem cells. *Biomaterials*, 37, pp.405-414.

266. Sun, Y.-L. et al., 2016. Protein and gene expression characteristics of heterogeneous nuclear ribonucleoprotein H1 in esophageal squamous cell carcinoma. *World Journal of Gastroenterology*, 22(32), p.7322.

267. Suzui, M., Shimizu, M., Masuda, M., Lim, J.T., Yoshimi, N. and Weinstein, I.B., 2004. Acyclic retinoid activates retinoic acid receptor β and induces transcriptional activation of p21CIP1 in HepG2 human hepatoma cells. *Molecular cancer therapeutics*, 3(3), pp.309-316.

268. Swift, M.E., Wallden, B., Wayner, E.A. and Swisshelm, K., 2006. Truncated RAR beta isoform enhances proliferation and retinoid resistance. *Journal of cellular physiology*, 209(3), pp.718-725.

269. Szeto, W. et al., 2001. Overexpression of the retinoic acid-responsive gene Stra6 in human cancers and its synergistic induction by Wnt-1 and retinoic acid. *Cancer Research*, 61(10), pp.4197–4205.

270. Takagi, M., Absalon, M.J., McLure, K.G. and Kastan, M.B., 2005. Regulation of p53 translation and induction after DNA damage by ribosomal protein L26 and nucleolin. *Cell*, 123(1), pp.49-63.

271. Tasdemir, E., Maiuri, M.C., Galluzzi, L., Vitale, I., Djavaheri-Mergny, M., D'amelio, M., Criollo, A., Morselli, E., Zhu, C., Harper, F. and Nannmark, U., 2008. Regulation of autophagy by cytoplasmic p53. *Nature cell biology*, *10*(6), pp.676-687.

272. Terra, R., Wang, X., Hu, Y., Charpentier, T., Lamarre, A., Zhong, M., Sun, H., Mao, J., Qi, S., Luo, H. and Wu, J., 2013. To investigate the necessity of STRA6 upregulation in T cells during T cell immune responses. *PloS one*, *8*(12), p.e82808.

273. Tian, W., Zhang, Z. and Cohen, D.M., 2000. MAPK signaling and the kidney. *American Journal of Physiology-Renal Physiology*, 279(4), pp.F593-F604.

274. Tocci, A., Parolini, I., Gabbianelli, M., Testa, U., Luchetti, L., Samoggia, P., Masella, B., Russo, G., Valtieri, M. and Peschle, C., 1996. Dual action of retinoic acid on human embryonic/fetal hematopoiesis: blockade of primitive progenitor proliferation and shift from multipotent/erythroid/monocytic to granulocytic differentiation program. *Blood*, 88(8), pp.2878-2888.

275. Tokarz, P., Piastowska-Ciesielska, A.W., Kaarniranta, K. and Blasiak, J., 2016. All-trans retinoic acid modulates DNA damage response and the expression of the VEGF-A and MKI67 genes in ARPE-19 cells subjected to oxidative stress. *International Journal of Molecular Sciences*, 17(6), p.898.

276. Toshiyuki, M. & Reed, J., 1995. Tumor suppressor p53 is a direct transcriptional activator of the human bax gene. *Cell*, 80, pp.293–299.

277. Travis, G.H., Golczak, M., Moise, A.R. and Palczewski, K., 2007. Diseases caused by defects in the visual cycle: retinoids as potential therapeutic agents. *Annu. Rev. Pharmacol. Toxicol.*, 47, pp.469-512.

278. Ukleja, A., Scolapio, J.S., McConnell, J.P., Spivey, J.R., Dickson, R.C., Nguyen, J.H. and O'brien, P.C., 2002. Nutritional assessment of serum and hepatic vitamin A levels in patients with cirrhosis. *Journal of Parenteral and Enteral Nutrition*, 26(3), pp.184-188.

279. Valko, M., Leibfritz, D., Moncol, J., Cronin, M.T., Mazur, M. and Telser, J., 2007. Free radicals and antioxidants in normal physiological functions and human disease. *The international journal of biochemistry & cell biology*, 39(1), pp.44-84.

280. Varani, J., Warner, R.L., Gharaee-Kermani, M., Phan, S.H., Kang, S., Chung, J., Wang, Z., Datta, S.C., Fisher, G.J. and Voorhees, J.J., 2000. Vitamin A Antagonizes Decreased Cell Growth and Elevated Collagen-Degrading Matrix Metalloproteinases and Stimulates Collagen Accumulation in Naturally Aged Human Skin 1. *Journal of Investigative Dermatology*, 114(3), pp.480-486.

281. Vigneron, A. and Vousden, K.H., 2010. p53, ROS and senescence in the control of aging. *Aging (Albany NY)*, 2(8), p.471.

282. Vlcek, S. and Foisner, R., 2007. Lamins and lamin-associated proteins in aging and disease. *Current opinion in cell biology*, 19(3), pp.298-304.

283. Vousden, K.H. and Prives, C., 2009. Blinded by the light: the growing complexity of p53. *Cell*, 137(3), pp.413-431.

284. Vousden, K.H. and Ryan, K.M., 2009. p53 and metabolism. *Nature Reviews Cancer*, *9*(10), pp.691-700.

285. Vousden, K.H., 2002. Activation of the p53 tumor suppressor protein. *Biochimica et Biophysica Acta (BBA)-Reviews on Cancer*, 1602(1), pp.47-59.

286. Vu, N.T., Park, M.A., Shultz, J.C., Goehe, R.W., Hoeferlin, L.A., Shultz, M.D., Smith, S.A., Lynch, K.W. and Chalfant, C.E., 2013. hnRNP U enhances caspase-9 splicing and is modulated by AKT-dependent phosphorylation of hnRNP L. *Journal of Biological Chemistry*, 288(12), pp.8575-8584.

287. Vucic, V., Isenovic, E.R., Adzic, M., Ruzdijic, S. and Radojcic, M.B., 2006. Effects of gamma-radiation on cell growth, cycle arrest, death, and superoxide dismutase expression by DU 145 human prostate cancer cells. *Brazilian journal of medical and biological research*, 39(2), pp.227-236.

288. Wagner, K.U. and Rui, H., 2008. Jak2/Stat5 signaling in mammogenesis, breast cancer initiation and progression. *Journal of mammary gland biology and neoplasia*, 13(1), pp.93-103.

289. Wajant, H., 2002. The Fas signaling pathway: more than a paradigm. *Science*, 296(5573), pp.1635-1636.

290. Wakai, K., Matsuo, K., Nagata, C., Mizoue, T., Tanaka, K., Tsuji, I., Sasazuki, S., Shimazu, T., Sawada, N., Inoue, M. and Tsugane, S., 2011. Lung cancer risk and consumption of vegetables and fruit: an evaluation based on a systematic review of epidemiological evidence from Japan. *Japanese journal of clinical oncology*, 41(5), pp.693-708.

291. Wan, F., Anderson, D.E., Barnitz, R.A., Snow, A., Bidere, N., Zheng, L., Hegde, V., Lam, L.T., Staudt, L.M., Levens, D. and Deutsch, W.A., 2007. Ribosomal protein S3: a KH domain subunit in NF-κB complexes that mediates selective gene regulation. *Cell*, 131(5), pp.927-939.

292. Wang, B., David, M.D. and Schrader, J.W., 2005. Absence of caprin-1 results in defects in cellular proliferation. *The Journal of Immunology*, 175(7), pp.4274-4282.

293. Wang, J., Steelman, C.K., Vincent, R., Richburg, D., Chang, T.S. and Shehata, B.M., 2010. Two case reports of anophthalmia and congenital heart disease: Adding a new dimension to this association. *Fetal and pediatric pathology*, 29(5), pp.291-298.

294. Wargovich, M.J., Jimenez, A., McKee, K., Steele, V.E., Velasco, M., Woods, J., Price, R., Gray, K. and Kelloff, G.J., 2000. Efficacy of potential chemopreventive agents on rat colon aberrant crypt formation and

progression. *Carcinogenesis*, 21(6), pp.1149-1155.

295. Weinberg, R.L., Veprintsev, D.B. and Fersht, A.R., 2004. Cooperative binding of tetrameric p53 to DNA. *Journal of molecular biology*, 341(5), pp.1145-1159.

296. Wek, R.C., Jiang, H.-Y. & Anthony, T.G., 2006. Coping with stress: eIF2 kinases and translational control. Biochemical Society transactions, 34(Pt 1), pp.7–11.

297. Westermarck, J. et al., 2002. The DEXD / H-box RNA helicase RHII / Gu is a co-factor for c-Jun-activated transcription, 21(3), pp.451–460.

298. Wolf, G., 1996. A history of vitamin A and retinoids. *The FASEB Journal*, 10(9), pp.1102-1107.

299. Wolf, G.E.O.R.G.E., 1984. Multiple functions of vitamin A. *Physiol Rev*, 64(3), pp.873-937.

300. Xu, F., Addis, J.B., Cameron, J.M. and Robinson, B.H., 2012. LRPPRC mutation suppresses cytochrome oxidase activity by altering mitochondrial RNA transcript stability in a mouse model. *Biochemical Journal*, 441(1), pp.275-283.

301. Xue, J.C., Schwarz, E.J., Chawla, A. and Lazar, M.A., 1996. Distinct stages in adipogenesis revealed by retinoid inhibition of differentiation after induction of PPARgamma. *Molecular and Cellular Biology*, 16(4), pp.1567-1575.

302. Yang, Q., Graham, T.E., Mody, N., Preitner, F., Peroni, O.D., Zabolotny, J.M., Kotani, K., Quadro, L. and Kahn, B.B., 2005. Serum retinol binding protein 4 contributes to insulin resistance in obesity and type 2 diabetes. *Nature*, 436(7049), pp.356-362.

303. Yang, Y., Bazhin, A.V., Werner, J. and Karakhanova, S., 2013. Reactive oxygen species in the immune system. *International reviews of immunology*, 32(3), pp.249-270.

304. Yoon, K.A., Nakamura, Y. and Arakawa, H., 2004. Identification of ALDH4 as a p53-inducible gene and its protective role in cellular stresses. *Journal of human genetics*, 49(3), pp.134-140.

305. Young, R.A. and Elliott, T.J., 1989. Stress proteins, infection, and immune surveillance. *Cell*, 59(1), pp.5-8.

306. Yuan, J., Luo, K., Zhang, L., Cheville, J.C. and Lou, Z., 2010. USP10 regulates p53 localization and stability by deubiquitinating p53. *Cell*, 140(3), pp.384-396.

307. Yusein-Myashkova, S., Stoykov, I., Gospodinov, A., Ugrinova, I. and Pasheva, E.,

2016. The repair capacity of lung cancer cell lines A549 and H1299 depends on HMGB1 expression level and the p53 status. *The Journal of Biochemistry*, 160(1), pp.37-47.

308. Zhang, H., Satyamoorthy, K., Herlyn, M. and Rosdahl, I., 2003. All-trans retinoic acid (atRA) differentially induces apoptosis in matched primary and metastatic melanoma cells–a speculation on damage effect of atRA via mitochondrial dysfunction and cell cycle redistribution. *Carcinogenesis*, 24(2), pp.185-191.

309. Zhang, J.W., Gu, J., Wang, Z.Y., Chen, S.J. and Chen, Z., 2000. Mechanisms ofall-trans retinoic acid-induced differentiation of acute promyelocytic leukemia cells. *Journal of biosciences*, 25(3), pp.275-284.

310. Zhang, Y. & Lu, H., 2009. Signaling to p53: ribosomal proteins find their way. *Cancer cell*, *16*(5), pp.369-377.

311. Zhang, Y., 2003. Transcriptional regulation by histone ubiquitination and deubiquitination. *Genes & development*, 17(22), pp.2733-2740.

312. Zhou, X. et al., 2015. Ribosomal proteins: Functions beyond the ribosome. *Journal of Molecular Cell Biology*, 7(2), pp.92–104.

313. Zhu, J. et al., 2000. Definition of the p53 functional domains necessary for inducing apoptosis. *Journal of Biological Chemistry*, 275(51), pp.39927–39934.

314. Zhu, W.Y., Jones, C.S., Kiss, A., Matsukuma, K., Amin, S. and De Luca, L.M., 1997. Retinoic acid inhibition of cell cycle progression in MCF-7 human breast cancer cells. *Experimental cell research*, 234(2), pp.293-299.

315. Zhuang, Y., Faria, T.N., Chambon, P. and Gudas, L.J., 2003. Identification and Characterization of Retinoic Acid Receptor β2 Target Genes in F9 Teratocarcinoma Cells1 1 NIH grant R01 CA43796 to LJG; a research grant from the American Institute for Cancer Research; and in part by a Cancer Pharmacology Training Grant (CA62948-08) (YZ). *Molecular cancer research*, 1(8), pp.619-630.

316. Ziouzenkova, O., Orasanu, G., Sukhova, G., Lau, E., Berger, J.P., Tang, G., Krinsky, N.I., Dolnikowski, G.G. and Plutzky, J., 2007. Asymmetric cleavage of β-carotene yields a transcriptional repressor of retinoid X receptor and peroxisome proliferator-activated receptor responses. *Molecular endocrinology*, 21(1), pp.77-88.

317. Zouboulis, C.C., 2001. Retinoids–which dermatological indications will benefit in the near future? *Skin Pharmacology and Physiology*, 14(5), pp.303-315.